Adaptive Predictor-Based Output Feedback Control of Unknown Multi-Input Multi-Output Systems: Theory and Application to Biomedical Inspired Problems

Chuong Hoang Nguyen

Dissertation submitted to the Faculty of the

Virginia Polytechnic Institute and State University

in partial fulfillment of the requirements for the degree of

Doctor of Philosophy

in

Mechanical Engineering

Alexander Leonessa, Chair

Andrew J. Kurdila

Alfred L. Wicks

Steve C. Southward

Nicole T. Abaid

May 6th, 2016

Blacksburg, Virginia

Keywords: Unknown system dynamics, non-model based control, model predictor, nonlinear MIMO systems, output feedback control, adaptive control.

Adaptive Predictor-Based Output Feedback Control of Unknown Multi-Input Multi-Output Systems: Theory and Application to Biomedical Inspired Problems

Chuong Hoang Nguyen

Abstract

Functional Electrical Stimulation (FES) is a technique that applies electrical currents to nervous tissue in order to actively induce muscle contraction. Recent research has shown that FES provides a promising treatment to restore functional tasks due to paralysis caused by spinal cord injury, head injury, and stroke, to mention a few. Therefore, the overarching goal of this research work is to develop FES controllers to enable patients with movement-disorder to control their limbs in a desired manner and, in particular, to aid Parkinson's patients to suppress hand tremor. In our effort to develop strategies for muscle stimulation control, we first implement a model-based control technique assuming that all the states are measurable. The Hill-type muscle model coupled with a simplified 2DoF model of the arm is used to study the performance of our proposed adaptive sliding mode controller for simulation purpose. However, in the more practical situations, human limb dynamics are extremely complicate and it is inadequate to use model based controllers, especially considering there are still technical limitations that allow *in vivo* measurements of muscle activity. To tackle these challenges, we have developed output feedback adaptive control approaches for a class of unknown multi-input multi-output systems. Such control strategies are first developed for linear systems, and then extended to the nonlinear case. The proposed controllers, supported by experimental results, require minimum knowledge of the system dynamics and avoid many restrictive assumptions typically found in the literature. Therefore, we expect that the results introduced in this dissertation can provide a solution for a wide class of nonlinear uncertain systems, with focus on practical issues such as partial state measurement and the presence of mismatched uncertainties.

Contents

List of Figures

List of Tables

Chapter 1

Introduction

1.1 Motivation and Current Methodologies for Parkinson's disease and Stroke patients

Pathological tremor is one of Parkinsons disease symptoms described as a rhythmical, oscillatory movement of body parts with abnormally high amplitudes and a broad band of frequencies. People suffering from this neurological disorder have serious difficulties in perform daily activities. For example, some simple movements such as writing, drinking from a cup of water, inserting a key or driving become formidable for these patients. Noticeably, according to a recent report ([7]) 15% of people older than fifty years suffer from this disorder and over 65% of them reported that they encounter severe difficulty in performing daily activities.

Currently, two common options for tremor treatment are drug therapy and surgery. Unfortunately, these treatments come with some limitations. Drugs often induce side effects, and show decreased effectiveness over years of use ([8]). Surgery with deep brain stimulation is one of the most advanced method, however it introduces some risks such as brain hemorrhage, seizures and other cognitive problems. Moreover, the price for treatment is extremely high. This motivates research in alternative means to compensate the tremor and provide a continuous health care outside the clinical environment.

Recently, some researchers have developed rehabilitation robotic exoskeleton equipment as an alternative for tremor suppression. However, many patients do hesitate to use these devices due to their bulky size and uncomfortable shapes, as illustrated in Fig. 1.1. Therefore, the possibility to develop a soft, noninvasive, wearable device that facilitates patients in daily activities becomes necessary and attractive to many researchers in the area of rehabilitation robotic.

(a)

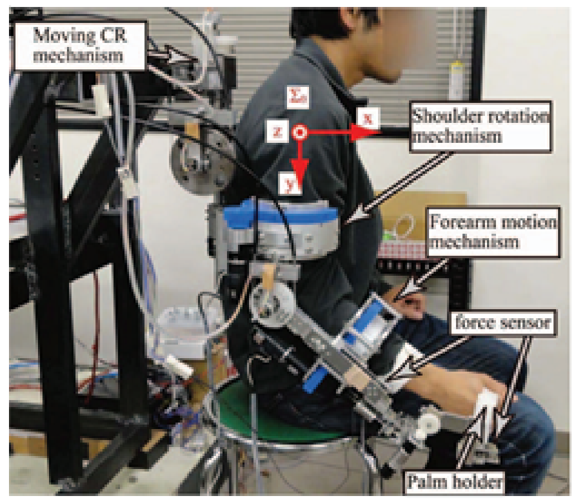

(b)

Figure 1.1: Examples of Rehabilitation Robotic Exoskeleton: (a) The device is developed by Consejo Superior de Investigaciones Cientficas, Madrid, Spain ([1]), (b) The device is developed by Dept. Advanced Technology Fusion, Saga University, Saga, Japan ([2])

Functional electrical stimulation (FES), which is primarily used to restore function in people with disabilities, offers a potential solution. FES uses several electrodes attached on patient skin to stimulate the muscles underneath and hence manipulating the body movements. Due to its small size and non-invasivity, FES is an elegant choice to develop a soft and wearable device to suppress tremor, as illustrated in Fig. 1.2. In fact, there are several on-going projects working in this area, such as ([3],[4], [9], [10]).

In order to achieve the desired movement, the approach follows through three steps: sense the movement, separate the actual tremor from the voluntary movement, and provide appropriate

(a) (b)

Figure 1.2: Examples of on-going project to develop a soft, wearable device for tremor suppression: (a) TremUNA project developed by a group of researchers from Serbia and Spain ([3]) (b). TREMOR project develop by a group of researchers from Spain ([4])

control commands to suppress the tremor by electrical stimulation. However, the current research, to our knowledge, focuses on the first two steps, while only using simple control strategies to drive the stimulations. The typical controllers found on recent publications ([3, 4, 10–14]) are open loop, PID, and fuzzy logic. These controllers are preferred because they are simple and do not require knowledge of the system dynamics. However, their performance relies greatly on how well their parameters are tuned, while the tuning process depends on trials and errors and varies from patient to patient.

These disadvantages motivate the development of more robust control algorithms. The challenges in developing a feedback controller are the complexity, uncertainty and highly nonlinear behavior of the human body. Moreover, many parameters of the system dynamics are unknown, not measurable, time variant and different from each patient. Therefore, designing a controller for *multi-input and multi-output (MIMO) systems with uncertain or even unknown dynamics and high relative degrees, in the absence of full state measurements as well as the lack of knowledge regarding the number of states,* is inevitably required. Furthermore, the application of such controller can extend to many other areas.

1.2 Adaptive Control for High Relative Degree Systems with Mismatched Uncertainties

Designing adaptive control for high relative degree systems with mismatched uncertainties is complicated because the control signal can not directly cancel the uncertainties. Backstepping control ([15]) provides a systematic and effective framework to handle the problem when the mismatched terms are known. Approaches utilizing backstepping control compute the virtual control signals to stabilize the system at each level. The virtual control signals are then differentiated and fed to the lower level. These steps are repeated until the physical control signals appear explicitly. Hence, the mismatch terms will be differentiated as many times as the relative degree. However, if the mismatched terms are unknown and estimated by adaptive laws, their derivatives are not available for feedback to the lower levels. Thus, designing adaptive control for high relative degree systems with mismatched uncertainties becomes very challenging and complicated. The standard approach is that the uncertainties are approximated by a finite combination of orthonormal basis functions, using neural network or fuzzy logics, with the set coefficients assumed to be unknown but constant ([16–23]). Then, the adaptive backstepping framework ([15]) is implemented to simultaneously design the adaptive laws and control signals at each level. However, for a system with a relative degree greater than 2, the original adaptive backstepping leads to very complicated adaptive laws and control structures, which is well known as ”explosion of the terms”. This drawback restricts the original adaptive backstepping to further practical applications. Yip et. al. ([24]) proposed dynamics surface control, a simplified version of adaptive backstepping. In [24–27], the virtual control signals are passed through a first order low-pass filter before being differentiated. In [28–30], the authors proposed a command filter adaptive backstepping approach, in which the virtual control signals are obtained by passing the stabilizing functions through a monotonic, odd, smooth function. The virtual control signals are then passed through a low pass filter before being differentiated. These adaptive backsteping-like approaches simplify the control structure by avoiding the analytical partial derivatives required in the original adaptive backstepping. However, high gain low pass filters must be used to obtain an acceptable tracking error, which leads to high magnitude control signals. Furthermore, as the relative degree of a system increases, the cascade structure of these low pass filters makes the controller more complicated and computationally expensive.

1.3 Output Feedback Control of Uncertain Systems

Output feedback control design for uncertain systems is a challenging task, essentially due to two different issues. First, common control techniques require full state feedback, while in practice only partial state information is available. To overcome this problem, most of the existing output feedback control strategies rely on the separation principle which tries to reconstruct the full state by using observer ([31], [32]) and then close the loop with such reconstructed state ([33]). However, designing observers for systems characterized by either parametric or structural uncertainties often presents many problems and several restrictive assumptions ([34],[35],[36]). Secondly, controllers are commonly derived leveraging some knowledge of the dynamics of the system. When the system model is uncertain or even unavailable, model-based control techniques are generally inadequate. While either one of the challenges has been addressed extensively in the literature, a few effective approaches can handle both simultaneously.

A number of results addressing the output feedback control problem for uncertain systems can be found in the literature, which can be classified into two approaches. The first approach extends the separation principle of the classical output feedback control using robust or adaptive techniques to deal with system uncertainty. For example, in [37] and [38], the authors develop a robust state feedback control algorithms based on the standard High Gain Observer. First, the controller is designed under the full state feedback assumption to obtain global uniform ultimate boundedness for the tracking error, despite of the parameter's uncertainty. Then, the results are extended to the case of output feedback control using the High Gain Observer, in which the peaking phenomenon is suppressed by using saturation function. Alternatively, if the system dynamics structure is uncertain, approximation techniques such as adaptive Neural Network or Fuzzy Logic are often combined with observer techniques to solve the problem. For example, in [39], the unknown nonlinear functions are first approximated by fuzzy logic systems, then a fuzzy adaptive observer is designed for state estimation as well as system identification. Combining this approach with backstepping design techniques, a fuzzy adaptive output feedback control is constructed recursively to obtain a semi-global uniform ultimate boundedness for all the signals while the tracking error is guaranteed to remain in a small neighborhood of origin.

Another attractive approach that has been extensively developed recently is the $\mathscr{L}_1$ adaptive control technique, which can achieve both fast adaptation and robustness. In [40], the authors provided an $\mathscr{L}_1$ adaptive control for a class of stable minimum phase SISO systems with relative degree 1 with uncertainties and disturbances satisfying a particular matching condition. In [41], the authors extended the results presented in [40] to a class of strictly positive real (SPR) systems, with unknown dimensions and relative degree less than or equal to 2. In [42], the authors relaxed the SPR requirement for a class of SISO systems with unknown relative degree. In [43], the authors extended the $\mathscr{L}_1$ adaptive control to a class of SISO minimum phase, unknown systems with known relative degree, which is matched by the reference system. In [44], the authors proposed $\mathscr{L}_1$ adaptive output feedback control augmentation of a Model Reference Controller (MRC) for a class of unknown SISO LTI system. By using the controller structure proposed in [45], the $\mathscr{L}_1$ adaptive control is applied to match the closed loop dynamics with that of the desired reference system, which is described by a strictly positive real (SPR) transfer function. However, because it relies on the matching condition of two SPR transfer functions, it is hard to apply the results to high relative degree systems. In general, the previous methods are restricted to SISO systems and are designed for systems with relative degree 1 or relative degree 2 in particular situations. In [46], the authors extended the results to MIMO systems and relaxed the SPR requirement. However, they required the number of control inputs be equal to the number of states, and all control inputs have relative degree 1. Deviating from $\mathscr{L}_1$ adaptive control scheme, in [47], the authors avoid the adaptive technique by proposing a controller which is based on a predictor capable of predicting the system output for any input. However, the prediction relies on derivatives estimation of the output, which is quite restrictive if the output is corrupted by noise, especially for high relative degree systems.

In light of this literature we believe there is the need of a control algorithm for unknown MIMO systems, with arbitrary relative degree and limited measurements available.

1.4 Contribution of the Dissertation

This dissertation presents new approaches to improve the standard designs in adaptive control theory, with a focus on output feedback adaptive control for high relative degree systems with unknown dynamics. The research application is devoted to controlling biomedical systems where an accurate dynamics model and full state measurement are unable to be obtained. This work will provide advanced control algorithms to develop rehabilitation devices using FES to restore limb's motion for Parkinson and stroke patients.

In Chapter 2, we introduce a new sliding mode control technique to handle the matched uncertainties of the dynamics systems. The presented control algorithm provides an improvement over other sliding mode control techniques ([48]), in particular by considering the overestimation problem of the sliding mode switching gain. In the standard approaches, a large constant switching gain is necessary to suppress the maximum uncertainties. However, this creates a large magnitude control signal, which also magnifies the control gain error, leading to large transient tracking error. We address this problem by making the switching gain adaptive and taking account for the singularity problem of the control gain. The proposed sliding mode control is then combined with a backstepping framework to study motion control of a human arm using muscle excitation signals. This chapter also illustrates the complexity and challenges in designing controllers for the musculotendon systems using model-based control techniques. Even if the system model is assumed to be accurate, full state estimation using observer-like techniques for complex nonlinear systems is still an ongoing problem with limited success. Hence, the challenges are addressed by our novel adaptive-output feedback control developed in the next chapters.

Chapter 3 establishes the first main contribution, which constitutes the foundation for the rest of the dissertation, by introducing the output feedback adaptive predictor-based control framework. In this chapter, we first consider the problem of controlling a general class of unknown MIMO linear systems using output feedback. The novel idea is that, in the circumstance that the system model is unknown and the state vector is unmeasured, reconstructing the model dynamics and observing the full state using this estimated model is ill established. Instead, we introduce an output predictor, capable of predicting the system outputs for any admissible inputs. Hence, designing an output tracking control for the unknown system is equivalent to constructing a full state tracking control for the predictor, whose dynamics are known. With this approach, the tracking task can be achieved by designing a tracking controller for a linear time varying system. In particular, the method proposed in [49] is adopted for the tracking task. Furthermore, in order to guarantee actuator amplitude and rate saturation constraints, the modified reference system method proposed in [50] is applied. The algorithm in Chapter 3 is then extended in Chapter 4 to control a class of nonlinear unknown dynamic systems. Simulation and experimental results obtained on a Quanser helicopter confirm the theoretical analysis.

The problem of obtaining the prediction's desired bounded error in the presence of time varying unknown uncertainties from Chapter 4 continues to be addressed in Chapter 5. Another major contribution of this chapter is to address the insufficiencies of the current approaches ([15], [24], [28], [51, 52]) in designing adaptive control for high relative degree system with unmatched uncertainties. Since the proposed controller structure avoids the recursive designs of the standard adaptive backstepping methods, its implementation remains simple regardless of the physical system's relative degree. Therefore, we can purposely increase the system's orders and relative degree by adding low pass filters in front of the control signals. Consequently, we can obtain a smooth control signal without complicating the controller structure. The proposed controller is applied to control the motion of human arm models to demonstrate its advantages over the approaches found in the literature. The results from Chapter 5 are extended to MIMO systems in Chapter 6, and further simulation and experimental results are reported to verify the theoretical analysis.

Chapter 2

Control Motion of A Human Arm: A Simulation Study

The following result was presented at the 2014 International Conference of Control, Dynamic Systems, and Robotics ([53]).

2.1 Introduction

This chapter presents a simulation study to control the motion of a human arm's using muscle excitations as inputs. Our simulation implements the musculoskeletal model Arm26 ([54]) provided in OpenSim which has 2 DOF and 6 muscles as actuators. First, in order to drive the limbs' motion to track a desired trajectory, we propose an Adaptive Sliding Mode Controller (ASMC) to compute the necessary driving moments at each joint. Since the system is over actuated, the Generalized Reduced Gradient (GRG) method is implemented to optimally distribute such moments to the corresponding forces for each muscle. Because the system has a cascade structure, a second Sliding Mode Control (SMC) within a backstepping algorithm framework is used to drive the muscle excitation so that each muscle can produce the needed force. The simulation shows that this controller can handle the mismatches between the mathematic model and physical body and bounded disturbances. This will establish a foundation for future work, in which we would like to use the FES to adjust the neural excitation so that we can cancel the tremor and stabilize the arm movement.

This chapter is organized as follows. Section 2.2 introduces the arm dynamics and the adaptive sliding mode controller to control the movement of the arm. Section 2.3 describes the algorithm to optimally distribute forces to each muscle. Section 2.4 presents the muscle dynamics and the back stepping controller to control the muscle contraction. Numerical simulation results are presented in Section 2.5. Finally, Section 2.6 concludes this chapter.

2.2 Body Dynamics and Adaptive Control

2.2.1 Dynamics model

We consider the case of controlling the joint flexion in the sagittal plane as illustrated in Fig 2.1, which shows both the right arm's skeleton model and the corresponding free body diagram.

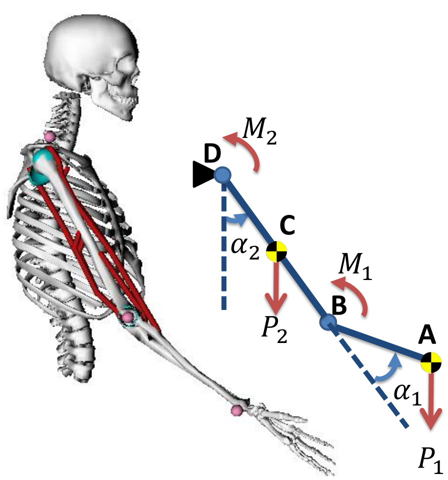

Figure 2.1: Arm Model

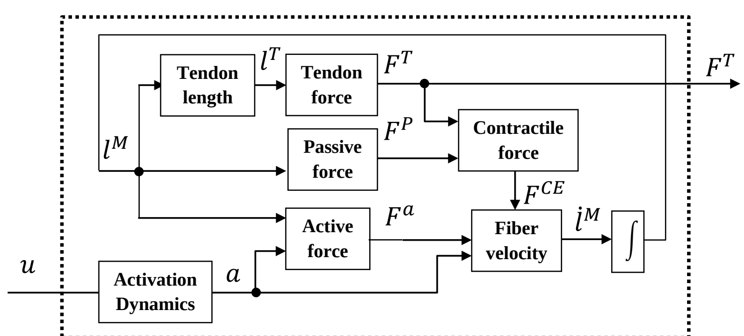

Figure 2.2: Muscle dynamics model

Let m_1, P_1, I_1 and m_2, P_2, I_2 be the mass, the gravity force, and the inertial moment at the mass center points A and C of the lower arm and the upper arm, respectively. M_1 and M_2 are the elbow and shoulder moments. Let (α_1, α_2) be the elbow and shoulder flexion. Applying the Newton laws to the 2-link segments model depicted in Fig 2.1, yields the following motion dynamics

$$\begin{bmatrix} z_1 & z_2(\alpha_2(t)) \\ z_3(\alpha_1(t)) & z_4(\alpha_1(t)) \end{bmatrix} \begin{bmatrix} \ddot{\alpha}_1(t) \\ \ddot{\alpha}_2(t) \end{bmatrix} = \begin{bmatrix} M_1(t) - Y_1(\alpha_1(t), \alpha_2(t), \dot{\alpha}_2(t)) \\ M_2(t) - M_1(t) - (Y_2(\alpha_1(t), \alpha_2(t), \dot{\alpha}_1(t), \dot{\alpha}_2(t)) \end{bmatrix},$$

where

$$\begin{aligned} &z_1 \triangleq I_1 + m_1 l_{AB}^2, && z_2(\alpha_1) \triangleq m_1 l_{AB} l_{BD} \cos\alpha_1 + m_1 l_{AB}^2, \\ &z_3(\alpha_1) \triangleq m_1 l_{AB} l_{BD} \cos\alpha_1, && z_4(\alpha_1) \triangleq I_2 + m_2 l_{CD}^2 + m_1 l_{BD}^2 + m_1 l_{AB} l_{BD} \cos\alpha_1, \\ &Y_1(\alpha_1, \alpha_2, \dot{\alpha}_2) \triangleq P_1 l_{AB} \sin(\alpha_1 + \alpha_2) + m_1 l_{AB} l_{BD} \sin\alpha_1 \dot{\alpha}_2^2, \\ &Y_2(\alpha_1, \alpha_2, \dot{\alpha}_1, \dot{\alpha}_2) \triangleq (P_1 l_{BD} + P_2 l_{CD}) \sin\alpha_2 - m_1 l_{AB} l_{BD} \sin\alpha_1 (\dot{\alpha}_1 + \dot{\alpha}_2)^2. \end{aligned}$$

Equ. (2.1) is rewritten as

$$\begin{bmatrix} \ddot{\alpha}_1(t) \\ \ddot{\alpha}_2(t) \end{bmatrix} = \frac{1}{z_1 z_4 - z_2 z_3} \left(\begin{bmatrix} -z_4 Y_1 + z_2 Y_2 \\ z_3 Y_1 - z_1 Y_2 \end{bmatrix} + \begin{bmatrix} z_2 + z_4 & -z_2 \\ -(z_1 + z_3) & z_1 \end{bmatrix} \begin{bmatrix} M_1(t) \\ M_2(t) \end{bmatrix} \right) \tag{2.1}$$

with the reduced notations $z_i \triangleq z_i(\alpha_1)$ and $Y_i \triangleq Y_i(\alpha_1, \alpha_2, \dot{\alpha}_1, \dot{\alpha}_2)$.

2.2.2 Adaptive Sliding Mode Controller (ASMC)

The dynamic model in (2.1) can be rewritten in a more general form

$$\ddot{x}(t) = f(x(t), \dot{x}(t)) + g(x(t), \dot{x}(t))u(t) + d(t), \tag{2.2}$$

where $x(t) \in \mathbb{R}^n$ is the state vector, $u(t) \in \mathbb{R}^n$ is the control input, $f(x(t), \dot{x}(t)) \in \mathbb{R}^n$, $g(x(t), \dot{x}(t)) \in \mathbb{R}^{n\times n}$ are function of $x(t)$ and $\dot{x}(t)$, and $d(t)$ is the unknown disturbance. The objective is to control this system to follow a desired trajectory $x_{\mathrm{d}}(t)$.

Due to the errors between the theretical model and the physical one, the plant dynamic can be rewritten as

$$\begin{aligned}\ddot{x}(t) &= f_{\mathrm{n}}(x(t),\dot{x}(t)) + g_{\mathrm{n}}(x(t),\dot{x}(t))u(t) + (\Delta f + \Delta g u + d)(t) \\ &= f_{\mathrm{n}}(x(t),\dot{x}(t)) + g_{\mathrm{n}}(x(t),\dot{x}(t))u(t) + \overline{d}(t),\end{aligned} \tag{2.3}$$

where $f_{\mathrm{n}}(\cdot)$ and $g_{\mathrm{n}}(\cdot)$ describe the nominal system with known estimated parameters, $\Delta f(t)$ and $\Delta g(t)$ are the unknown difference between the real and nominal systems and $\overline{d}(t) \triangleq (\Delta f(t) + \Delta g(t)u(t) + d(t))$ is the total uncertainty error and disturbance.

We introduce sliding mode variable

$$s(t) \triangleq \dot{e}(t) + Ce(t) \in \mathbb{R}^n, \tag{2.4}$$

where $e(t) \triangleq x(t) - x_{\mathrm{d}}(t)$ is the tracking error, and $C \in \mathbb{R}^{n\times n}, C > 0$. Differentiating the sliding mode variable defined in 2.4 yields

$$\dot{s}(t) = \ddot{e}(t) + C\dot{e}(t) = f_{\mathrm{n}}(x,\dot{x}) + g_{\mathrm{n}}(x,\dot{x})u(t) + \overline{d}(t) - \ddot{x}_{\mathrm{d}}(t) + C\dot{e}(t). \tag{2.5}$$

where the short notation $x = x(t)$ is used to simplify the notation.

According to Sliding Mode Control (SMC) ([55]), we introduce the following control input

$$u(t) = -g_{\mathrm{n}}^{-1}(x,\dot{x})(f_{\mathrm{n}}(x,\dot{x}) - \ddot{x}_{\mathrm{d}}(t) + C\dot{e}(t) + \mathrm{sgn}(s(t))k) \tag{2.6}$$

where $\mathrm{sgn}(s) \triangleq \mathrm{diag}([\mathrm{sgn}(s_1)...\mathrm{sgn}(s_n)])$ is the diagonal matrix and $k \triangleq [k_1...k_n]^{\mathrm{T}}$ with $k_i \geq |\overline{d}_{\max}|$, where $|\overline{d}_{\max}|$ is the maximum absolute value of $\overline{d}(t)$.

Differentiating the Lyapunov function

$$V(s) = \frac{1}{2}s(t)^{\mathrm{T}}s(t) \tag{2.7}$$

along the trajectory (2.5) and (2.6) yields

$$\begin{aligned}\dot{V}(t) &= s(t)^{\mathrm{T}}\dot{s}(t) = s^{\mathrm{T}}(t)(f_{\mathrm{n}}(x,\dot{x}) + g_{\mathrm{n}}(x,\dot{x})u(t) + \overline{d}(t) - \ddot{x}_{\mathrm{d}}(t) + C\dot{e}(t)) \\ &= -|s^{\mathrm{T}}(t)|k + s^{\mathrm{T}}(t)\overline{d}(t) \leq -|s^{\mathrm{T}}(t)|k + |s^{\mathrm{T}}(t)||\overline{d}_{\max}| \leq 0.\end{aligned} \tag{2.8}$$

which, according to LaSalle-Yoshizawa theorem, guarantees $s(t) \to 0$ as $t \to \infty$. However, note that $\overline{d}(t)$ depends on $\Delta g(t)u(t)$, which leads to the fact that $|\overline{d}_{\max}|$ can be magnified when $u(t)$ is large, and choosing a large constant $|\overline{d}_{\max}|$ can worsen the controller performance. Therefore, we modify the control law given above.

Theorem 2.2.1 *Consider the system (2.3), and a desired trajectory $x_{\mathrm{d}}(t) \in \mathscr{C}^2$. Assume that there exists $k^* \in \mathbb{R}^n$ and $K^* \in \mathbb{R}^{n\times n}$ such that*

$$k_i^* > |d_i(t) + \Delta f_i(t)|_{\max}, \qquad K_{ij}^* > |\Delta g_{ij}(t)|_{\max}, \qquad i,j = 1,...,n, \tag{2.9}$$

then the controller

$$u(t) \triangleq u_{s1}(t) + u_{s2}(t), \tag{2.10a}$$

$$u_{s1}(t) \triangleq -g_{\mathrm{n}}^{-1}(x,\dot{x})(f_{\mathrm{n}}(x,\dot{x}) - \ddot{x}_{\mathrm{d}}(t) + C\dot{e}(t) + \mathrm{sgn}(s(t))\hat{k}(t)), \tag{2.10b}$$

$$u_{s2}(t) \triangleq -g_{\mathrm{n}}^{-1}(x,\dot{x})\mathrm{sgn}(s(t))\hat{K}(t)|u(t)|, \tag{2.10c}$$

with the adaptive laws

$$\dot{\hat{k}}(t) = \mathrm{Proj}(\hat{k}(t), P_k|s(t)|), \tag{2.11a}$$

$$\dot{\hat{K}}(t) = \mathrm{Proj}(\hat{K}(t), P_K|s(t)||u^{\mathrm{T}}(t)|), \tag{2.11b}$$

where $P_k \in \mathbb{R}^{n\times n}, P_K > 0$ and $P_K \in \mathbb{R}^{n\times n}, P_K > 0$, guarantees that the closed loop system defined by (2.3),(2.10) and (2.11) is Lyapunov stable, and the tracking error $e(t) = x(t) - x_{\mathrm{d}}(t) \to 0$ as $t \to \infty$.

Proof *Substituting the controller defined in (2.10) into (2.5) to obtain*

$$\dot{s}(t) = -\mathrm{sgn}(s(t))\hat{k}(t) - \mathrm{sgn}(s(t))\hat{K}(t)|u(t)| + (d(t) + \Delta f(t)) + \Delta g(t)u(t). \tag{2.12}$$

Differentiating the Lyapunov function

$$V_{\mathrm{a}}(t) = \frac{1}{2}s(t)^{\mathrm{T}}s(t) + \frac{1}{2}(k(t) - k^*)^{\mathrm{T}}P_{\alpha}^{-1}(k(t) - k^*)^{\mathrm{T}} + \frac{1}{2}\mathrm{tr}[(\hat{K}(t) - K^*)^{\mathrm{T}}P_{\beta}^{-1}(\hat{K}(t) - K^*)], \tag{2.13}$$

along the trajectory of (2.12) and substituting the update laws (2.11) yield

$$\begin{aligned}\dot{V}_{\mathrm{a}}(t) &= s^{\mathrm{T}}(t)\dot{s}(t) + (\hat{k}(t)-k^{*})^{\mathrm{T}}P_{\alpha}^{-1}\dot{\hat{k}}(t) + \mathrm{tr}[(\hat{K}(t)-K^{*})^{\mathrm{T}}P_{\beta}^{-1}\dot{\hat{K}}(t)] \\ &= -|s^{\mathrm{T}}(t)|\hat{k}(t) - |s^{\mathrm{T}}(t)|\hat{K}(t)|u(t)| + s^{\mathrm{T}}(t)(d(t)+\Delta f(t)) + s^{\mathrm{T}}(t)\Delta g(t)u(t) \\ &\quad + (\hat{k}(t)-k^{*})|s^{\mathrm{T}}(t)| + \mathrm{tr}[(\hat{K}(t)-K^{*})^{\mathrm{T}}|u(t)||s^{\mathrm{T}}(t)|]. \end{aligned} \tag{2.14}$$

Using the property that $\mathrm{tr}[X^{\mathrm{T}}Y] = \mathrm{tr}[YX^{\mathrm{T}}] = \mathrm{tr}[Y^{\mathrm{T}}X] = Y^{\mathrm{T}}X$ *if* $Y^{\mathrm{T}}X \in \mathbb{R}$ *yields*

$$\begin{aligned}\mathrm{tr}\left[(\hat{K}(t)-K^{*})^{\mathrm{T}}|s(t)||u^{\mathrm{T}}(t)|\right] &= \mathrm{tr}\left[(|s(t)|u^{\mathrm{T}}(t)|)^{\mathrm{T}}|(\hat{K}(t)-K^{*})\right] = \mathrm{tr}\left[|u(t)||s^{\mathrm{T}}(t)||(\hat{K}(t)-K^{*})\right] \\ &= |s^{\mathrm{T}}(t)|(\hat{K}(t)-K^{*})^{\mathrm{T}}|u(t)|. \end{aligned} \tag{2.15}$$

Substituting (2.15) into (2.14) to obtain

$$\begin{aligned}\dot{V}_{\mathrm{a}}(t) &=_{\mathrm{s}}^{\mathrm{T}} (t)(d(t)+\Delta f(t)) - k^{*}|s^{\mathrm{T}}(t)| + s^{\mathrm{T}}(t)\Delta g(t)u(t) - |s^{\mathrm{T}}(t)|K^{*}|u(t)| \\ &\leq -\left(k^{*} - |d(t)+\Delta f(t)|\right)|s^{\mathrm{T}}(t)| - |s^{\mathrm{T}}(t)|(K^{*} - |\Delta g(t)|)|u(t)| \\ &= -\sum_{i=1}^{n}\left(k_i^{*} - |d_i(t)+\Delta f_i(t)|\right)|s_i| - \sum_{i=1}^{n}\sum_{j=1}^{n}\left(K_{ij}^{*} - |\Delta g_{ij}(t)|\right)|s_i u_j| \leq 0. \end{aligned} \tag{2.16}$$

where we used the definition of k_i^{*}, K_{ij}^{*} *in (2.9). According to the Lasalle-Yoshizawa theorem, all signals remain bounded and* $s(t) \to 0$ *as* $t \to 0$, *so that* $e(t) \to 0$ *as* $t \to 0$. □

Remark 2.2.1 *It follows from ((2.10)) that the controller* $u(t)$ *can be rewritten as*

$$u(t) = -(g_n(x,\dot{x}) + \mathrm{sgn}(s(t))\hat{K}(t)\mathrm{sgn}(u(t)))^{-1}(f_n(x,\dot{x}) - \ddot{x}_{\mathrm{d}}(t) + C\dot{e}(t) + \mathrm{sgn}(s(t))\hat{k}(t)). \tag{2.17}$$

Comparing (2.17) to the conventional SMC, the proposed ASMC adds the gain K, to account for the uncertainty in estimating system control gain ($\Delta g(x,\dot{x})u(t)$*) which can be magnified when the control* $u(t)$ *is large. Note that, when* $u^{\mathrm{T}}(t)s(t)$ *converges to zero, then the ASMC controller converges to the conventional SMC controller.*

Furthermore, $\hat{K}(t)$ *provides an easy way to handle the case of a singular* $g_{\mathrm{n}}(x,\dot{x})$, *which would cause the standard SMC to become unbounded. Also note that in (2.17),* $u(t)$ *depends on* $\mathrm{sgn}(u(t))$. *Therefore, in practical implementation, the previous value of* $u(t)$ *can be used to predict* $\mathrm{sgn}(u(t))$, *and compute new $u(t)$. Finally, the* $\text{sgn}(s(t))$ *can be replaced by the saturate function* $\text{Sat}(s(t), \varepsilon > 0)$ *to avoid the chattering problem of SMC ([31]).*

2.2.3 Simulation Results

This section presents the simulation results to control the 2-link segments model (2.1) by applying the proposed controller (2.17). The simulation was conducted in MATLAB/Simulink 2014b. MATLAB ODE3 solver is used for integration. The physical parameters to simulate the arm model and the nominal parameters for the controller are given in Tab.2.1.

Table 2.1: Arm model simulation parameters

Model	m_1	I_1	l_{AB}	m_2	I_2	l_{BD}	l_{CD}
Physical	1.53	0.02	0.14	1.87	0.013	0.29	0.18
Nominal	1.8	0.022	0.16	2	0.015	0.31	0.20

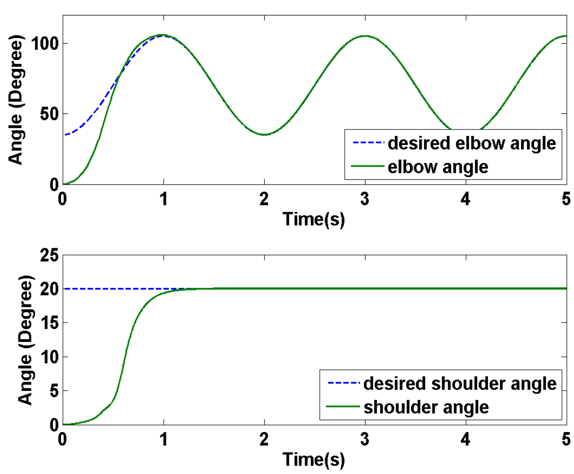

Figure 2.3: Tracking performance

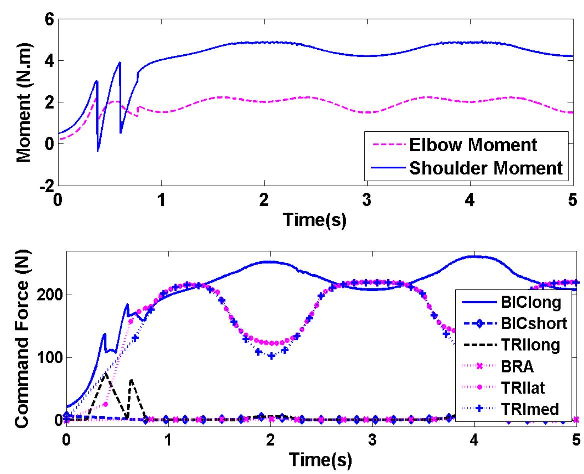

Figure 2.4: Control moments and optimal force distribution

The controller parameters are chosen as $C = \text{diag}([7\ \ 7])$, $P_\alpha = 100$, $P_\beta = 100$, $\varepsilon = 1^\circ$. The system response and control inputs are shown in Fig. (2.3) and (2.4). Figure (2.3) shows that the system output converges to the desired output after $1.5s$ dispite the differences in paramters of the physical and nominal systems.

2.3 Optimal Force Distribution

In the Arm26 body model, 6 muscles *BIClong, BICshort, TRIlong, BRA, TRIlat, TRImed* (with respective index $i = 1,\dots,6$) contribute to the moment M_1, and 3 of them (*BIClong, BICshort, TRIlong*) also contribute to the moment M_2. In order to compute the muscle forces, the criterion that the muscles should produce the least possible forces with minimal change rate to generate the necessary moment is selected. The problem is formulated as minimizing the following cost function

$$f(F) = \frac{1}{2}F^{\mathrm{T}}W_1F + \frac{1}{2}(F - F_{\Delta t})^{\mathrm{T}}W_2(F - F_{\Delta t}),$$

with $F \triangleq [F_1,...,F_6]^{\mathrm{T}} \in \mathbb{R}^n,\ n = 6$, satisfying the constraints

$$\sum_{i=1}^{6} r_i^1 F_i = M_1, \quad \sum_{i=1}^{3} r_i^2 F_i = M_2, \ \ F_i^{\min} \le F_i \le F_i^{\max}, \tag{2.18}$$

where F_i is the force produced by the muscle i, and $F_{\Delta t} \triangleq F(t - \Delta t)$. $W_1 > 0,\ W_2 > 0$ are weight matrices, r_i^1 and r_i^2 are the moment arms of the muscle i at the elbow and the shoulder, respectively. The constraints in (2.18) can be rewritten as

$$\begin{bmatrix} r_1^1 & r_2^1 & r_3^1 & r_4^1 & r_5^1 & r_6^1 \\ r_1^2 & r_2^2 & r_3^2 & 0 & 0 & 0 \end{bmatrix} F = \begin{bmatrix} M_1 \\ M_2 \end{bmatrix} \Rightarrow AF = b, \tag{2.19}$$

with obvious definitions for $A \in \mathbb{R}^{m \times n}$ and $b \in \mathbb{R}^m$, $m = 2$ is the number of the equality constraints.

The Generalized Reduced Gradient iterative procedure ([56]) is applied to solve the optimization problem as follows. The vector F can be partitioned as

$$F = [F_{\mathrm{B}}^{\mathrm{T}}, F_{\mathrm{N}}^{\mathrm{T}}]^{\mathrm{T}}, \quad F_{\mathrm{B}} \in \mathbb{R}^m,\ F_{\mathrm{N}} \in \mathbb{R}^{n-m}.$$

where F_{B} and F_{N} are the basic vector and nonbasic vector, respectively. Let B and N be partitions of A corresponding to the vectors F_{B} and F_{N}. Hence, (2.19) can be rewritten as

$$[B \mid N] \begin{bmatrix} F_{\mathrm{B}} \\ F_{\mathrm{N}} \end{bmatrix} = b \Rightarrow BF_{\mathrm{B}} + NF_{\mathrm{N}} = b. \tag{2.20}$$

The vector F can be reordered so that F_{B} can be chosen such that $F_i^{\min} < F_{\mathrm{B}i} < F_i^{\max}$ and the matrix B is nonsingular. Next, assume that at each iteration step, F changes by a small variation $\delta = [\delta_{\mathrm{B}}^{\mathrm{T}}, \delta_{\mathrm{N}}^{\mathrm{T}}]^{\mathrm{T}}$ while still satisfying the constraint (2.20), which yields

$$B(F_{\mathrm{B}} + \delta_{\mathrm{B}}) + N(F_{\mathrm{N}} + \delta_{\mathrm{N}}) = b \Rightarrow \delta_{\mathrm{B}} = -B^{-1}N\delta_{\mathrm{N}}. \tag{2.21}$$

Let $\nabla f(F) \triangleq [\nabla_{\mathrm{B}} f^{\mathrm{T}}, \nabla_{\mathrm{N}} f^{\mathrm{T}}]^{\mathrm{T}}$ be the gradient vector of $f(F)$ with two components $\nabla_{\mathrm{B}} f, \nabla_{\mathrm{N}} f$ corresponding to the vectors F_{B} and F_{N}. It follows from (2.21) that the change of f caused by the variation δ is

$$\Delta f = \nabla f^{\mathrm{T}}(F)\delta = \nabla_{\mathrm{B}} f^{\mathrm{T}}(F)\delta_{\mathrm{B}} + \nabla_{\mathrm{N}} f^{\mathrm{T}}(F)\delta_{\mathrm{N}} = (\nabla_{\mathrm{N}} f^{\mathrm{T}}(F) - \nabla_{\mathrm{B}} f^{\mathrm{T}}(F)B^{-1}N)\delta_{\mathrm{N}} = \gamma_{\mathrm{N}}^{\mathrm{T}}\delta_{\mathrm{N}}, \tag{2.22}$$

where $\gamma_{\mathrm{N}}^{\mathrm{T}} \triangleq \nabla_{\mathrm{N}} f^{\mathrm{T}}(F) - \nabla_{\mathrm{B}} f^{\mathrm{T}}(F)B^{-1}N$. Hence, the value of the cost function f is reduced if the variation δ_{N} is chosen so that $\Delta f < 0$.

Let $[\delta_{\mathrm{B}}^{\mathrm{T}}\ \delta_{\mathrm{N}}^{\mathrm{T}}]^{\mathrm{T}} = \alpha\Gamma$, where $\Gamma \triangleq [\Gamma_{\mathrm{B}}^{\mathrm{T}}\ \Gamma_{\mathrm{N}}^{\mathrm{T}}]^{\mathrm{T}}$ is the reduced gradient direction vector, and α is the optimal step size. It follows from (2.21) and (2.22) that Γ can be chosen as.

$$\Gamma_{\mathrm{B}} = -B^{-1}N\Gamma_{\mathrm{N}}, \qquad \Gamma_{\mathrm{N}i} = \begin{cases} 0, & \text{if} \quad (\Gamma_{\mathrm{N}i} = F_i \min,\ \gamma_{\mathrm{N}i} > 0), \\ 0, & \text{if} \quad (\Gamma_{\mathrm{N}i} = F_i \max,\ \gamma_{\mathrm{N}i} < 0), \\ -\gamma_{\mathrm{N}i}, & \text{otherwise}, \end{cases}$$

After Γ is determined, the optimal step α can be found as

$$\alpha = \operatorname{argmin} f(F + \alpha\Gamma), \quad 0 \le \alpha \le \alpha \max, \tag{2.23}$$

$$\alpha \max = \sup\{\alpha \mid F \min \le F + \alpha\Gamma \le F \max\}. \tag{2.24}$$

Suppose F_k and Γ_k are the force and the direction vector at the iteration step k, respectively. The maximum step size $\alpha_k^{\max}$ can be obtained by solving the linear inequality (2.24), and the optimal step size α_k is obtained by solving $\partial f(F,\alpha,\Gamma)/\partial\alpha = 0$ as following ([56])

$$\alpha_k = \min\left\{\alpha_k^{\max}, -\frac{F_k^{\mathrm{T}} W_1 \Gamma_k + (F_k - F_{\Delta t})^{\mathrm{T}} W_2 \Gamma_k}{\Gamma_k^{\mathrm{T}} (W_1 + W_2) \Gamma_k}\right\}.$$

The iteration will repeat with $F_k + \alpha_k \Gamma_k \mapsto F$ by finding the direction vector Γ and the step size α until $||\Gamma_{\mathrm{N}}|| = 0$ or $||F_{k+1} - F_k|| < \varepsilon_F$, where ε_F is the chosen tolerance, or until there is no arrangement of F_B such that B is nonsingular.

Fig. (2.4) illustrates the simulation results for the required moments obtained in Section 2.2. The muscle maximum forces are taken from the default values of the Arm26 model, and given below.

Muscles	BIClong	BICshort	TRIlong	BRA	TRIlat	TRImed
$F^{\max}(N)$	624.3	435.56	798.52	987.26	624.3	624.3

The algorithm converges in less than 5 iterations on average, with a tolerance $\varepsilon_F = 1N$.

2.4 Control Muscle

2.4.1 Muscle Dynamics Model

This section summarizes the Thelen muscle model ([57,58]), whose block diagram is shown in Fig. 2.2. All muscles share the same block structures and formulas, but differ in four properties: the maximum isometric force F_0^{M}, the optimal fiber length l_0^{M}, the tendon slack length l_s^{T}, and the pennation angle at the optimal fiber length α_0. Table 2.2 shows other parameters that are similar across all muscles in the model. The interested reader can find more details in [58].

Tendon length The relationship between the tendon length $l_T(t)$ and the muscle length l^{M} is given by $l_T = l^{\mathrm{MT}} - l^{\mathrm{M}} \cos\alpha$, where $l^{\mathrm{MT}} \triangleq l^{\mathrm{MT}}(\alpha_1, \alpha_2)$ is the muscle tendon length and α is the

Table 2.2: Muscle model parameters

$\varepsilon_0^{\mathrm{M}}$	k_{toe}	$\varepsilon_0^{\mathrm{T}}$	k_{lin}	$\varepsilon_{\mathrm{toe}}^{\mathrm{T}}$	$\overline{F}_{\mathrm{toe}}^{\mathrm{T}}$	k_{P}	γ	A_f	$\overline{F}_{\mathrm{len}}^{\mathrm{M}}$
0.6	3	0.033	$1.712/\varepsilon_0^{\mathrm{T}}$	$10.609\varepsilon_0^{\mathrm{T}}$	1/3	4	0.5	0.3	1.8

pennation angle

$$\alpha = \begin{cases} 0, \quad l^{\mathrm{M}}(t) = 0 \quad \text{or} \quad w/l^{\mathrm{M}}(t) \le 0, \\ \sin^{-1}(w/l^{\mathrm{M}}(t)), \quad 0 < w/l^{\mathrm{M}}(t) < 1, \\ \pi/2, \quad w/l^{\mathrm{M}}(t) \ge 1, \end{cases} \quad \text{with} \quad w = l_0^{\mathrm{M}} \sin \alpha_0. \tag{2.25}$$

where l^{MT} is the muscle tendon length which depends on the elbow and shoulder angles and α is the pennation angle.

Tendon Force The tendon force $F_T(t)$ is governed by the tendon length l_T as $F_T(t) = F_0^{\mathrm{M}} \overline{F}_T(\varepsilon_T)$, where

$$\overline{F}_T(\varepsilon_T) = \frac{1+\varepsilon_T}{1000} + \begin{cases} k_{\mathrm{lin}}(\varepsilon^{\mathrm{T}} - \varepsilon_{\mathrm{toe}}^{\mathrm{T}}) + \overline{F}_{\mathrm{toe}}^{\mathrm{T}}, \quad \varepsilon_T > \varepsilon_{\mathrm{toe}}^{\mathrm{T}}, \\ \overline{F}_{\mathrm{toe}}^{\mathrm{T}} \dfrac{e^{k_{\mathrm{toe}} \varepsilon^{\mathrm{T}} / \varepsilon_{\mathrm{toe}}^{\mathrm{T}}} - 1}{e^{k_{\mathrm{toe}}} - 1}, \quad 0 < \varepsilon^{\mathrm{T}} \le \varepsilon_{\mathrm{toe}}^{\mathrm{T}}, \\ 0, \quad \varepsilon^{\mathrm{T}} \le 0, \end{cases} \quad \text{with} \quad \varepsilon^{\mathrm{T}} = l^{\mathrm{T}}/l_{\mathrm{s}}^{\mathrm{T}} - 1. \tag{2.26}$$

Passive Force The passive force F_{P} is controlled by the muscle length l^{M} as $F_{\mathrm{P}} = F_o^m \overline{F}_{\mathrm{P}}(\bar{l}^{\mathrm{M}})$, where $\bar{l}^{\mathrm{M}} = l^{\mathrm{M}}/l_0^{\mathrm{M}}$ is the normalized muscle length, and

$$\overline{F}_{\mathrm{P}}(\bar{l}^{\mathrm{M}}) = \begin{cases} 1 + \frac{k_{\mathrm{P}}}{\varepsilon_0^{\mathrm{M}}}(\bar{l}^{\mathrm{M}} - (1+\varepsilon_0^{\mathrm{M}})), \quad \text{if} \quad \bar{l}^{\mathrm{M}} > (1+\varepsilon_0^{\mathrm{M}}), \\ \dfrac{e^{k_{\mathrm{P}}(\bar{l}^{\mathrm{M}}-1)/\varepsilon_0^{\mathrm{M}}}}{e^{k_{\mathrm{P}}}}, \quad \text{if} \quad \bar{l}^{\mathrm{M}} \le (1+\varepsilon_0^{\mathrm{M}}). \end{cases} \tag{2.27}$$

Active Force The active force F_{a} is controlled by the muscle activation a and the normalized muscle length $\bar{l}^{\mathrm{M}}$

$$F_{\mathrm{a}} = a F_0^{\mathrm{M}} e^{-(\bar{l}^{\mathrm{M}}-1)^2}. \tag{2.28}$$

Contractile force The force in the contractile element F_{CE} is calculated from tendon force F_T and passive force F_P as follows

$$F_{\mathrm{CE}} = \frac{F_T}{\cos\alpha} - F_{\mathrm{P}}. \tag{2.29}$$

Fiber Velocity The fiber velocity $\dot{l}^{\mathrm{M}}$ is calculated as $\dot{l}^{\mathrm{M}} = (5+5a)l_0^{\mathrm{M}}\bar{\dot{l}}^{\mathrm{M}}$, where $\bar{\dot{l}}^{\mathrm{M}}$ is the normalized contraction velocity

$$\bar{\dot{l}}^{\mathrm{M}} = \Psi_1(l^{\mathrm{M}}, a) = \begin{cases} \dfrac{F_{\mathrm{CE}}}{\varepsilon}\left(\dfrac{\varepsilon - F_{\mathrm{a}}}{F_{\mathrm{a}} + \frac{\varepsilon}{A_f} + \xi} + \dfrac{F_{\mathrm{a}}}{F_{\mathrm{a}} + \xi}\right) - \dfrac{F_{\mathrm{a}}}{F_{\mathrm{a}} + \xi}, & \text{if} \quad F_{\mathrm{CE}} < 0, \\ \dfrac{F_{\mathrm{CE}} - F_{\mathrm{a}}}{F_{\mathrm{a}} + \frac{F_{\mathrm{CE}}}{A_f} + \xi}, & \text{if} \quad 0 \le F_{\mathrm{CE}} < F_{\mathrm{a}}, \\ \dfrac{F_{\mathrm{CE}} - F_{\mathrm{a}}}{\frac{1}{\overline{F}^{\mathrm{M}}_{\mathrm{len}} - 1}(2 + \frac{2}{A_f})(F_{\mathrm{a}}\overline{F}^{\mathrm{M}}_{\mathrm{len}} - F_{\mathrm{CE}}) + \xi}, & \text{if} \quad F_{\mathrm{a}} \le F_{\mathrm{CE}} < 0.95F_{\mathrm{a}}\overline{F}^{\mathrm{M}}_{\mathrm{len}}, \\ f_{v0} + \dfrac{F_{\mathrm{CE}} - 0.95F_{\mathrm{a}}\overline{F}^{\mathrm{M}}_{\mathrm{len}}}{F_{\mathrm{a}}\overline{F}^{\mathrm{M}}_{\mathrm{len}}}(f_{v1} - f_{v0}), & \text{if} \quad 0.95F_{\mathrm{a}}\overline{F}^{\mathrm{M}}_{\mathrm{len}} \le F_{\mathrm{CE}}, \end{cases} \tag{2.30}$$

where

$$f_{v0} = \frac{0.95F_{\mathrm{a}}\overline{F}^{\mathrm{M}}_{\mathrm{len}} - F_{\mathrm{a}}}{\frac{1}{\overline{F}^{\mathrm{M}}_{\mathrm{len}} - 1}(2 + \frac{2}{A_f})0.05(F_{\mathrm{a}}\overline{F}^{\mathrm{M}}_{\mathrm{len}}) + \xi}, \quad f_{v1} = \frac{(0.95+\varepsilon)F_{\mathrm{a}}\overline{F}^{\mathrm{M}}_{\mathrm{len}} - F_{\mathrm{a}}}{\frac{1}{\overline{F}^{\mathrm{M}}_{\mathrm{len}} - 1}(2 + \frac{2}{A_f})(0.05 - \varepsilon)(F_{\mathrm{a}}\overline{F}^{\mathrm{M}}_{\mathrm{len}}) + \xi}. \tag{2.31}$$

Activation dynamics The activation dynamics a is modeled as the first order lowpass filter of the excitation signal u, with $T_{\mathrm{act}} = 0.01$ and $T_{\mathrm{dact}} = 0.04$ are the activate time and the deactivate time, respectively. Hence, the activation dynamics can be rewritten as

$$\dot{a} = \Psi_2(a, u) = \begin{cases} (u - a)/T_{\mathrm{act}} & \text{if} \quad u > a, \\ (u - a)/T_{\mathrm{dact}} & \text{if} \quad u \le a. \end{cases} \tag{2.32}$$

2.4.2 Muscle Control

The entire system dynamics has a cascade form and can be summarized as follows

$$\ddot{x}(t) = f(x(t), \dot{x}(t)) + g(x(t), \dot{x}(t))u(t), \tag{2.33a}$$

$$\dot{l}_i^{\mathrm{M}} = \Psi_1({l^{\mathrm{M}}}_i, a_i), \tag{2.33b}$$

$$\dot{a}_i = \Psi_2(a_i, u_i), \qquad i = 1, \ldots, 6, \tag{2.33c}$$

where (2.33a) is the arm dynamics defined in Section (2) and (3) with $x(t) = [\alpha_1(t)\ \alpha_2(t)]^{\mathrm{T}}$ are the joint angles, and $u(t) = [\sum_{i=1}^{6} r_i^{(1)}(x)F_i(l_i^{\mathrm{M}}(x))\ \ \sum_{i=1}^{6} r_i^{(2)}(x)F_i(l_i^{\mathrm{M}}(x))]^{\mathrm{T}}$ is the control moment.

The backstepping algorithm ([31]) can be applied to control this system . First, suppose that the set of desired forces $\{F_{\mathrm{d}i} = F_i(l_{\mathrm{d}i}^{\mathrm{M}}), \quad i = 1, ..., 6\}$ is available after solving the optimal force distribution step as described in section (2) and (3), and also suppose that their time derivative $\dot{F}_{\mathrm{d}}$ is available. Then, the desired muscle length $l_{\mathrm{d}}^{\mathrm{M}}$ and its time derivative $\dot{l}_{\mathrm{d}}^{\mathrm{M}}$ can be computed using the Eq. (2.25) and (2.26).

Back-Stepping Level 1 Let $u_{\mathrm{d}}(t) = \left[\begin{array}{cc} \sum_{i=1}^{6} r_i^{(1)}(x)F_{\mathrm{d}i} & \sum_{i=1}^{6} r_i^{(2)}(x)F_{\mathrm{d}i} \end{array}\right]^{\mathrm{T}}$ be the desired joint moment that stabilize the Lyapunov function $V_1(t) = \frac{1}{2}s^{\mathrm{T}}(t)s(t)$, such that

$$\dot{V}_1(t) = s^{\mathrm{T}}(t)(f_{\mathrm{n}}(x, \dot{x}) + g_{\mathrm{n}}(x, \dot{x})u_{\mathrm{d}}(t) + \bar{d}(t) - \ddot{x}_{\mathrm{d}}(t) + C\dot{e}(t)) \leq 0, \tag{2.34}$$

where $F_{\mathrm{d}i} = F_i(l_{\mathrm{d}i}^{\mathrm{M}}), \quad i = \{1, ..., 6\}$ is the solution computed following the procedure described in Section 2.2 and Section 2.3.

Back-Stepping Level 2 Let ${e_{l^{\mathrm{M}}}}_i \triangleq l_i^{\mathrm{M}} - l_{\mathrm{d}i}^{\mathrm{M}}$ be the error between the actual muscle length l_i^{M} and the desired muscle length $l_{\mathrm{d}i}^{\mathrm{M}}$. The control moment $u(t)$ can be rewritten in term of the desired $u_d(t)$ and the error ${e_{l^{\mathrm{M}}}}_i(t)$ as

$$u(t) = u_{\mathrm{d}}(t) + \begin{bmatrix} \sum_{i=1}^{6} r_i^{(1)}(x)\nabla F_i(l_{\mathrm{d}i}^{\mathrm{M}}){e_{l^{\mathrm{M}}}}_i(t) \\ \sum_{i=1}^{6} r_i^{(2)}(x)\nabla F_i(l_{\mathrm{d}i}^{\mathrm{M}}){e_{l^{\mathrm{M}}}}_i(t) \end{bmatrix}, \qquad \nabla F_i(l_{\mathrm{d}}^{\mathrm{M}}) \triangleq \frac{F_i(l_i^{\mathrm{M}}) - F_i(l_{\mathrm{d}i}^{\mathrm{M}})}{{e_{l^{\mathrm{M}}}}_i(t)}. \tag{2.35}$$

Differentiating the Lyapunov function

$$V_2(t) = \frac{1}{2}s^{\mathrm{T}}(t)s(t) + \frac{1}{2}\sum_{i=1}^{6} {e_{l_i^{\mathrm{M}}}}^2(t),$$

along the trajectories (2.34) and (2.35) yields

$$\dot{V}_2(t) = s^{\mathrm{T}}(t)(f_{\mathrm{n}}(x,\dot{x}) + g_{\mathrm{n}}(x,\dot{x})u(t) + \bar{d}(t) - \ddot{x}_{\mathrm{d}} + c\dot{e}) + \sum_{i=1}^{6} e_{l_i^{\mathrm{M}}}(\Psi_1(a_i) - \dot{l}_{\mathrm{d}}^{\mathrm{M}})$$
$$= \dot{V}_1(t) + \sum_{i=1}^{6} e_{l_i^{\mathrm{M}}}(\Psi_1(a_i) - \dot{l}_{\mathrm{d}}^{\mathrm{M}} + s^{\mathrm{T}} g_{\mathrm{n}} r_i \nabla F_i(l_{\mathrm{d}i}^{\mathrm{M}})), \tag{2.36}$$

where $r_i(x) \triangleq [r_i^{(1)}(x) \;\; r_i^{(1)}(x)]^{\mathrm{T}}$. Therefore, the control activation $a_{\mathrm{d}i}(t)$ is chosen as follow so that $\dot{V}_2(t) \leq 0$

$$a_{\mathrm{d}i}(t) = \Psi_1^{-1}(-k_{a_i}\mathrm{sgn}(e_{l_i^{\mathrm{M}}}(t)) + \dot{l}_{\mathrm{d}i}^{\mathrm{M}} - s^{\mathrm{T}}(t) g_{\mathrm{n}}(x,\dot{x}) r_i \nabla F_i(l_{\mathrm{d}i}^{\mathrm{M}})), \tag{2.37}$$

where k_{a_i} is the chosen control gain. (2.37) can be approximated by a quadratic equation in term of $a_{\mathrm{d}i}$ and solved analytically.

Back-Stepping Level 3 Suppose $a_{\mathrm{d}i}(t)$ is available after solving (2.37), let $e_{\mathrm{a}i}(t) \triangleq a_i(t) - a_{\mathrm{d}i}(t)$ be the error between the actual activation $a_i(t)$ and the desired activation $a_{\mathrm{d}i}(t)$. The muscle contraction velocity are rewritten

$$\Psi_1(a_i) = \Psi_1(a_{\mathrm{d}i}) + \nabla\Psi_1(a_{\mathrm{d}i})e_{\mathrm{a}i}, \qquad \nabla\Psi_1(a_{\mathrm{d}i}) = \frac{\Psi_1(a_i) - \Psi_1(a_{\mathrm{d}i})}{e_{\mathrm{a}i}(t)}. \tag{2.38}$$

Differentiating the Lyapunov function

$$V_3(t) = \frac{1}{2}s^{\mathrm{T}}(t)s(t) + \frac{1}{2}\sum_{i=1}^{6} e_{l_i^{\mathrm{M}}}^2(t) + \frac{1}{2}\sum_{i=1}^{6} e_{a_i}^2(t),$$

along the trajectory (2.36) and (2.38) yields

$$\dot{V}_3(t) = \dot{V}_1(t) + \sum_{i=1}^{6} e_{l_i^{\mathrm{M}}}(t)(\Psi_1(a_i) - \dot{l}_{\mathrm{d}i}^{\mathrm{M}}(t) + s^{\mathrm{T}}(t) g_{\mathrm{n}}(x,\dot{x}) r_i(x) \nabla F_i(l_{\mathrm{d}i}^{\mathrm{M}})) + \sum_{i=1}^{6} e_{ai}(t)(\Psi_2(u_i) - \dot{a}_{\mathrm{d_i}}(t))$$
$$= \dot{V}_2(t) + \sum_{i=1}^{6} e_{ai}(t)(\Psi_2(u_i) - \dot{a}_{\mathrm{d}i}(t) + e_{l^{\mathrm{M}}i}(t)\nabla\Psi_1(a_{\mathrm{d}i})),$$

then the excitation control signal $u_i(t)$ is chosen such that $\dot{V}_3(t) \leq 0$, as

$$u_i(t) = \Psi_2^{-1}(-k_{u_i}\mathrm{sgn}(e_{a_i}(t)) + \dot{a}_{\mathrm{d_i}}(t) - e_{l_i^{\mathrm{M}}}(t)\nabla\Psi_1(a_{\mathrm{d}i}(t))) = \begin{cases} T_{\mathrm{act}}(a_i + z_i) & \text{if} \quad z_i > 0, \\ T_{\mathrm{dact}}(a_i + z_i) & \text{if} \quad z_i \leq 0, \end{cases}$$

where

$$z_i(t) \triangleq -k_{u_i}\mathrm{sgn}(e_{a_i}(t)) + \dot{a}_{\mathrm{d_i}}(t) - e_{l_i^{\mathrm{M}}}(t)\nabla\Psi_1(a_{\mathrm{d}i}(t)).$$

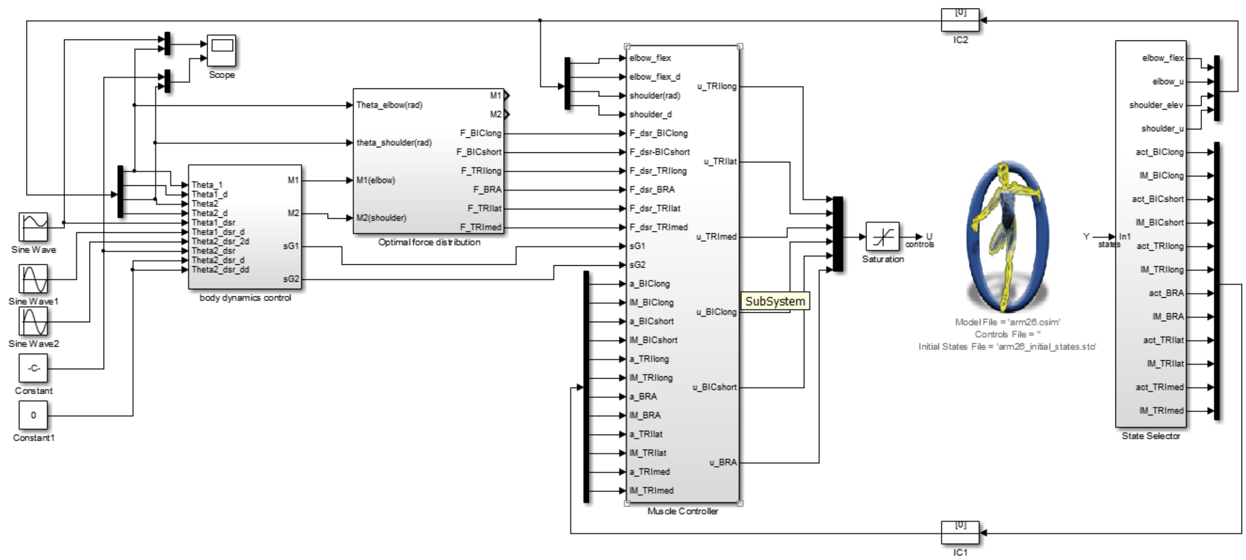

Figure 2.5: Simulation Interface

2.5 Simulation Results

The simulation was conducted by using the interface between OpenSim and Simulink ([59]), as described in Fig 2.5. The simulation parameters are given in Tab.1 and Tab.2, with the following initial states

- $l^{\mathrm{M}}(0) = [0.1138 \;\; 0.1138 \;\; 0.0858 \;\; 0.134 \;\; 0.1321 \;\; 0.1157]^{\mathrm{T}}$,
- $a_i(0) = 0, \; i = 1, \ldots, 6$
- $\alpha_j(0) = \dot{\alpha}_i(0) = \ddot{\alpha}_i(0) = 0, \; j = 1, 2.$

Figure 2.6 shows that the responses converge to the reference trajectories after 2s with the chosen parameters $C = [3 \;\; 11]$, $\alpha = 0.5$, $\beta = 0.02$. Fig. 2.8 shows the required moments and muscle forces, respectively. The required muscle length, muscle activation and muscle excitation are shown in Figure 2.9 and Fig. 2.10.

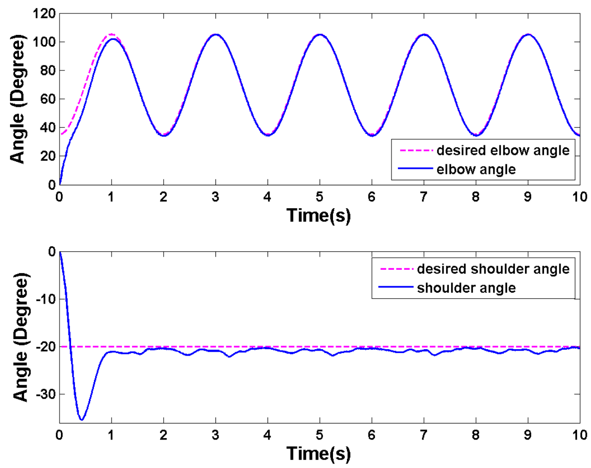

Figure 2.6: System output using the control gain $C = \mathrm{diag}([3\ 11])$, $P_\alpha = 2,\ \beta = 50$.

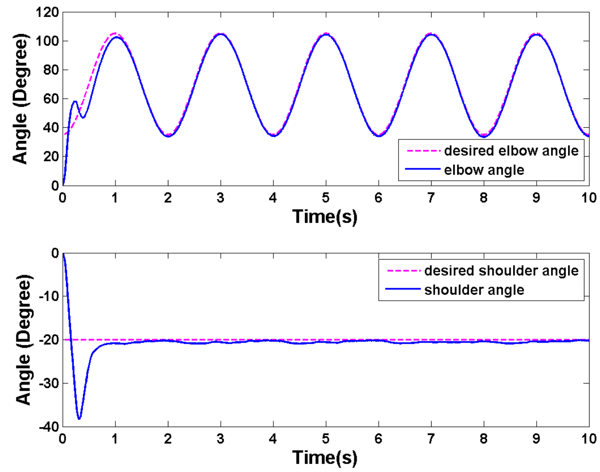

Figure 2.7: System output using the control gain $C = \mathrm{diag}([4\ 40])$, $\alpha = 2,\ \beta = 50$.

The tracking error depends on the chosen boundary of saturate function. In this example, the error boundary is 1°, and the maximum error reported is 1.5° at the shoulder. This is because the muscles BIClong, BICshort, TRIlong contributes to both the shoulder and elbow moments.This leads to the slight vibration at the shoulder angle to achieve the small error at elbow angle. Moreover, the gain can be adjusted to reduce the error. Figure 2.7 shows the system response when the control parameters are chosen as $C = \mathrm{diag}([4\ \ 40])$, $\alpha = 0.5$, $\beta = 0.02$ and the saturate boundary is 0.1°. The maximum settling error is 0.9° at the shoulder and 1° at the elbow.

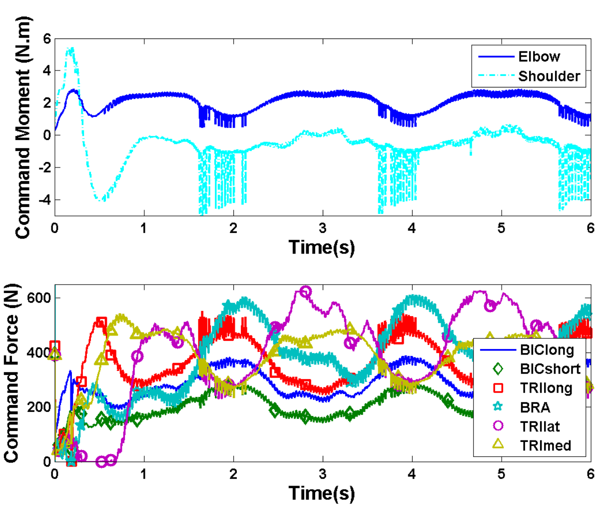

Figure 2.8: Requires moments and optimal forces

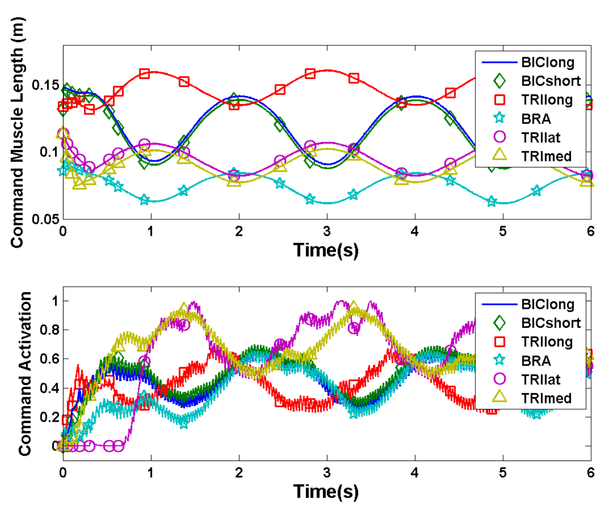

Figure 2.9: Muscle length and activation response

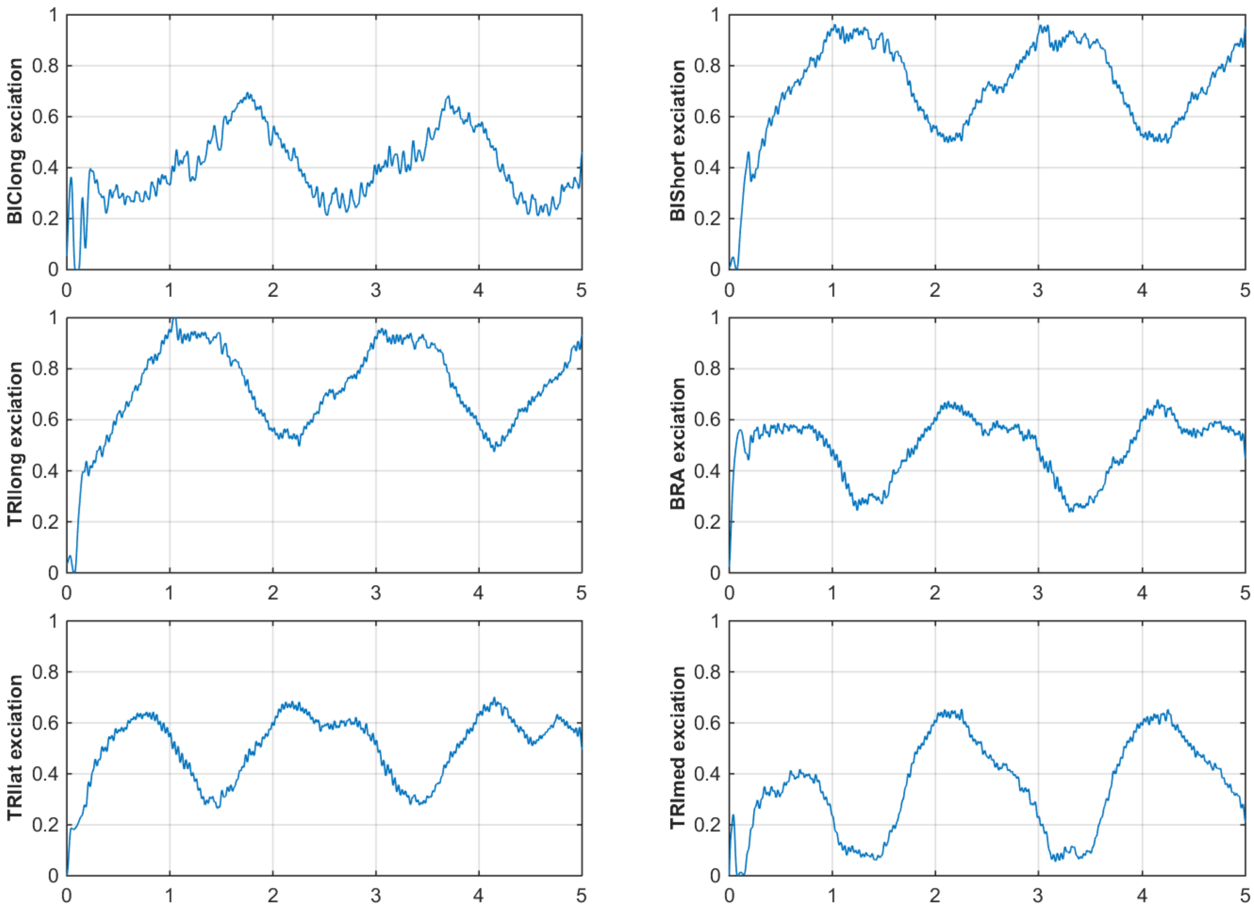

Figure 2.10: Muscles excitation

2.6 Conclusion

In this chapter, we proposed an adaptive controller to control the arm movement and validate its performance through a simulation study. First, we proposed an ASMC to derive the driving moments. Secondly, we implemented the Generalized Reduced Gradient method to optimally distribute forces to each muscle. Finally, we used another SMC to drive the activation and excitation. Because the model dynamics had a cascade form, the backstepping technique was implemented to compute the muscle excitations. The simulation study showed that our controller can handle the parametric uncertainties. Comparing to the Computed Muscle Control toolbox provided in OpenSim which uses the PID controller, the proposed method does not require heavy effort in tuning process. One drawback of this controller is that it requires full state knowledge including muscle length and activations for feedback purpose. This shortcoming will be addressed with a novel output feedback approach which will be described in the next chapters.

Chapter 3

Adaptive Predictor-Based Output Feedback Control for a Class of Unknown MIMO Linear Systems

The following result was presented at the 2014 ASME Dynamcis System and Control Conference ([60] and [61]) and object of an article submitted to International Journal of Adaptive Control and Signal Processing.

3.1 Introduction

In this chapter, the problem of characterizing adaptive output feedback control laws for a general class of unknown MIMO linear systems is considered. The controller proposed in this chapter is built upon the strategy introduced in [47], but avoids using the output derivatives and it is applicable to minimum phase MIMO systems with any relative degrees. The key idea is that, in the circumstance that the system model is unknown and the state vector is unmeasured, it is not necessary to construct the model dynamics and attempt to estimate the full state if the output (i.e. the measurements) is all we need to control. Instead, we introduce an output predictor, capable of predicting the system output using the history of the system input and output stored in autoregressive filtered vectors. Hence, designing an output tracking control for the unknown system is equivalent to constructing a tracking control for the predictor, which is a virtual system whose dynamics and state are known. With this approach, the tracking task can be achieved by designing a tracking controller for a linear time varying system, using one of many approaches existing in the literature. In particular, the method proposed in [49] is adopted for the tracking task. Furthermore, in order to guarantee actuator amplitude and rate saturation constraints, the modified reference system method proposed in [50] is applied. Ultimately, it is shown that the plant output, the predictor output and the reference system output simultaneously converge to the desired trajectory. Exponential stability of the prediction error and uniformly ultimate boundedness of the tracking error are proved using the Lyapunov's direct method.

This chapter is organized as follows. Section 3.2 establishes the mathematical background and the problem formulation. In Section 3.3, the novel output predictor is derived. Design of the control algorithm for the predictor is then presented in Section 3.4. In addition, the actuator amplitude and rate saturation constraints are also analyzed in this section. Furthermore, Section 3.5 summarizes the framework to implement the algorithm. Section 3.6 provides two numerical simulations for both linear and nonlinear systems to illustrate the algorithm's efficacy, and Section 3.7 provides the experimental results in implementing the algorithm on a helicopter. Finally, Section 3.8 concludes the chapter.

3.2 Mathematical Preliminaries

In this section, we establish definitions, notations and assumptions used later in the paper.

Definition 3.2.1 *([62]) For a signal $\xi(t) \in \mathbb{R}^n$, $t > 0$, the $\mathscr{L}_\infty$ norm is defined as*

$$\|\xi\|_{\mathscr{L}_\infty} = \max_{i=1,\dots,n} (\sup_{\tau \geq 0} |\xi_i(\tau)|),$$

where ξ_i is the i^{th} component of ξ.

Definition 3.2.2 *([62]) The $\mathscr{L}_1$ gain of a stable proper SISO system $H(s)$ is defined as $\|H(s)\|_{\mathscr{L}_1} = \int_0^\infty |h(t)|\mathrm{d}t$, where $h(t)$ is the impulse response of $H(s)$.*

Definition 3.2.3 *([62]) For a stable proper system $H(s)$ with m input, n output, its $\mathscr{L}_1$ gain is defined as*

$$\|H(s)\|_{\mathscr{L}_1} = \max_{i=1,\dots,n}\left(\sum_{j=1}^{m}\|H_{ij}(s)\|_{\mathscr{L}_1}\right),$$

where $H_{ij}(s)$ is the i^{th} row, j^{th} column element of $H(s)$.

Lemma 3.2.1 *([62]) For a stable proper MIMO system $H(s)$ with input $r(t) \in \mathbb{R}^m$ and output $x(t) \in \mathbb{R}^n$, the following holds $\|x(t)\|_{\mathscr{L}_\infty} \leq \|H(s)\|_{\mathscr{L}_1}\|r(t)\|_{\mathscr{L}_\infty}, t \geq 0$.*

Definition 3.2.4 *([63]) If $A \in \mathbb{C}^{m\times n}$, then the pseudo-inverse $A^\dagger$ is the unique matrix in $\mathbb{C}^{m\times n}$ such that*

$$AA^\dagger A = A, \quad A^\dagger AA^\dagger = A^\dagger, \quad (AA^\dagger)^* = AA^\dagger, \quad (A^\dagger A)^* = A^\dagger A.$$

where $(\cdot)^*$ denotes the conjugate transpose.

Definition 3.2.5 *([31]) The Lie derivative of a function $\phi(x) \in \mathbb{R}$, $x \in \mathbb{R}^n$ along the flow of a vector field $p(x) \in \mathbb{R}^n$ is defined as*

$$L_p\phi(x) \triangleq \frac{\partial\phi(x)}{\partial x}p(x).$$

Definition 3.2.6 *([31]) Consider the following n^{th}-order nonlinear SISO system $\mathscr{G}_{\text{NL}}$*

$$\dot{x}(t) = f(x(t)) + g(x(t))u(t), \quad x(0) = x_0, \quad t \geq 0, \tag{3.1a}$$

$$y(t) = h(x(t)), \tag{3.1b}$$

with $x(t) \in \mathbb{R}^n$, $f : \mathbb{R}^n \to \mathbb{R}^n$, $g : \mathbb{R}^n \to \mathbb{R}^n$, $h : \mathbb{R}^n \to \mathbb{R}$. $\mathscr{G}_{\text{NL}}$ has relative degree $0 < r < n$ in a region $\mathscr{D} \subseteq \mathbb{R}^n$ if $L_g\psi_i(x(t)) = 0$ and $L_g\psi_r(x(t)) \neq 0$, $x(t) \in \mathscr{D}$, $t \geq 0$, where $\psi_1(x(t)) \triangleq h(x(t))$

and $\psi_{i+1}(x(t)) \triangleq L_f \psi_i(x(t)),\ i = 1,\ldots,r-1$. *In short, the relative degree of a given system is the number of times one must differentiate the output* $y(t)$ *before the input* $u(t)$ *appears explicitly.*

Consider the following linear time invariant (LTI) MIMO system $\mathscr{G}_{\mathrm{L}}$

$$\dot{x}(t) = Ax(t) + Bu(t), \quad x(0) = x_0, \quad t \geq 0, \tag{3.2a}$$

$$y(t) = Cx(t), \tag{3.2b}$$

where $x(t) \in \mathbb{R}^n$ is the state vector, $y(t) \in \mathbb{R}^p$ is the output, $u(t) \in \mathbb{R}^m$ is the control input, and the matrices $A \in \mathbb{R}^{n\times n}$, $B = [b_1 \ldots b_m] \in \mathbb{R}^{n\times m}$ where $b_j \in \mathbb{R}^n,\ j = 1\ldots m$, and $C = [c_1 \ldots c_p]^{\mathrm{T}} \in \mathbb{R}^{p\times n}$ where $c_i \in \mathbb{R}^n,\ i = 1\ldots p$, are defined accordingly. The matrices $A,\ B,\ C$ are unknown and r_{ij} is the known relative degree of the input $u_j(t)$ with respect to the output $y_i(t)$.

The control objective is to design an adaptive controller to ensure that, for a given bounded reference input $r(t) \in \mathbb{R}^p$, $y(t)$ tracks the output $y_{\mathrm{m}}(t)$ of the following desired system

$$\dot{y}_{\mathrm{m}}(t) = A_{\mathrm{m}} y_{\mathrm{m}}(t) + B_{\mathrm{m}} r(t), \quad t \geq 0. \tag{3.3}$$

where $A_{\mathrm{m}} \in \mathbb{R}^{p\times p}$ is a stable matrix, and B_{m} is a full rank matrix.

Lemma 3.2.2 *Consider the LTI MIMO system* $\mathscr{G}_{\mathrm{L}}$ *defined in (3.2). The* i^{th} *output of the system* $\mathscr{G}_{\mathrm{L}}$ *can be represented in the Laplace domain by the following transfer function*

$$y_i(s) = G_i(s)u(s) = \frac{\sum_{j=1}^{m} N_{ij}(s)u_j(s)}{D(s)}, \tag{3.4}$$

where $s \in \mathbb{C}$ *denotes the Laplace variable and* $G_i(s) \triangleq c_i^{\mathrm{T}}(sI_n - A)^{-1}B$ *is the transfer function relative to the output* $y_i(t)$. *Accordingly,*

$$D(s) = s^n + \alpha_{n-1}s^{n-1} + \ldots + \alpha_1 s + \alpha_0 = \det(sI_n - A) \tag{3.5}$$

$$N_{ij}(s) = \beta_{ij}^{(n-r_{ij})} s^{n-r_{ij}} + \ldots + \beta_{ij}^{(1)} s + \beta_{ij}^{(0)} = c_i^{\mathrm{T}} A_{\mathrm{a}}(s) b_j, \tag{3.6}$$

represent the denominator and numerator's components of the transfer function $G_i(s)$*, respectively,* *where $A_{\mathrm{a}}(s)$ denotes the adjunct matrix of $(sI_n - A)$. Then, the system output can be obtained as*

$$y(t) = \omega_y^{\mathrm{T}}(t)\alpha + \beta^{\mathrm{T}}\omega_u(t), \quad t \geq 0, \tag{3.7}$$

where $\alpha \in \mathbb{R}^n$ and $\beta \in \mathbb{R}^{nm\times p}$ are defined as

$$\alpha \triangleq \begin{bmatrix} \alpha_0 - \lambda_0 & \dots & \alpha_{n-1} - \lambda_{n-1} \end{bmatrix}^{\mathrm{T}}, \tag{3.8a}$$

$$\beta \triangleq \begin{bmatrix} \beta_{11} & \cdots & \beta_{p1} \\ \vdots & \ddots & \vdots \\ \beta_{1m} & \cdots & \beta_{pm} \end{bmatrix}, \qquad \beta_{ij} \triangleq \begin{bmatrix} \beta_{ij}^{(0)} & \dots & \beta_{ij}^{(n-r_{ij})} & 0_{r_{ij}-1}^{\mathrm{T}} \end{bmatrix}^{\mathrm{T}} \in \mathbb{R}^n, \tag{3.8b}$$

and $\omega_y(t) \in \mathbb{R}^{n\times p}$ and $\omega_u(t) \in \mathbb{R}^{nm}$ are defined as

$$\omega_y(t) \triangleq [\omega_{y_1}(t) \cdots \omega_{y_p}(t)], \qquad \omega_u(t) \triangleq [\omega_{u1}^{\mathrm{T}}(t) \cdots \omega_{um}^{\mathrm{T}}(t)]^{\mathrm{T}}, \tag{3.9a}$$

where $\omega_{y_i} \in \mathbb{R}^n$, $\omega_{uj} \in \mathbb{R}^n$ are the regression vectors obtained as follows

$$\dot{\omega}_{y_i}(t) = A_{\mathrm{f}}\omega_{y_i}(t) - B_{\mathrm{f}}y_i(t), \qquad \omega_{y_i}(0) = \omega_{y_{i0}}, \; t \geq 0, \tag{3.10a}$$

$$\dot{\omega}_{u_j}(t) = A_{\mathrm{f}}\omega_{u_j}(t) + B_{\mathrm{f}}u_j(t), \qquad \omega_{u_j}(0) = \omega_{u_{i0}}, \; t \geq 0, \tag{3.10b}$$

where $i = 1, \dots, p$ and $j = 1, \dots, m$, and

$$A_{\mathrm{f}} \triangleq \begin{bmatrix} 0_{n-1} & I_{(n-1)} \\ -\lambda_0 \quad \dots & -\lambda_{n-1} \end{bmatrix} \in \mathbb{R}^{n\times n}, \qquad B_{\mathrm{f}} \triangleq \begin{bmatrix} 0_{n-1} \\ 1 \end{bmatrix} \in \mathbb{R}^n, \tag{3.11}$$

such that $\Lambda(s) \triangleq \det(sI_n - A_{\mathrm{f}}) = s^n + \lambda_{n-1}s^{n-1} + \dots + \lambda_1 s + \lambda_0$ is a n^{th} order, Hurwitz polynomial.

Proof *Consider the single output transfer function defined in (3.4). By multiplying both sides of (3.4) by $D(s)/\Lambda(s)$, it follows*

$$\frac{D(s)}{\Lambda(s)}y_i(s) = \frac{\sum_{j=1}^m N_{ij}(s)u_j(s)}{\Lambda(s)},$$

which implies

$$y_i(s) = -\frac{D(s) - \Lambda(s)}{\Lambda(s)}y_i(s) + \frac{\sum_{j=1}^m N_{ij}(s)u_j(s)}{\Lambda(s)} = \omega_{y_i}^{\mathrm{T}}(s)\alpha + \sum_{j=1}^m \beta_{ij}^{\mathrm{T}}\omega_{u_j}(s), \tag{3.12}$$

where α and β_{ij} are defined in (3.8) , and

$$\omega_{y_i}(s) = -(sI_n - A_{\mathrm{f}})^{-1}B_{\mathrm{f}}y_i(s) = -\left[\frac{y_i(s)}{\Lambda(s)}, \cdots, \frac{s^{n-1}y_i(s)}{\Lambda(s)}\right]^{\mathrm{T}},$$
$$\omega_{u_j}(s) = (sI_n - A_{\mathrm{f}})^{-1}B_{\mathrm{f}}u_j(s) = \left[\frac{u_j(s)}{\Lambda(s)}, \cdots, \frac{s^{n-1}u_j(s)}{\Lambda(s)}\right]^{\mathrm{T}},$$

which are the Laplace transform of $\omega_{y_i}(t)$ and $\omega_{u_j}(t)$ defined in (3.10), respectively. Hence, it follows from (3.12) that the output of the system can be obtained by

$$y(t) = \begin{bmatrix} \omega_{y_1}^{\mathrm{T}}(t) \\ \vdots \\ \omega_{y_p}^{\mathrm{T}}(t) \end{bmatrix} \alpha + \begin{bmatrix} \beta_{11}^{\mathrm{T}} & \cdots & \beta_{1m}^{\mathrm{T}} \\ \vdots & \ddots & \vdots \\ \beta_{p1}^{\mathrm{T}} & \cdots & \beta_{pm}^{\mathrm{T}} \end{bmatrix} \begin{bmatrix} \omega_{u_1}(t) \\ \vdots \\ \omega_{u_m}(t) \end{bmatrix}$$

which proves (3.7) and concludes the proof. □

Lemma 3.2.3 *(Theorem (4.12) [31]) Let $x = 0$ be the exponentially stable equilibrium point of the linear time varying system $\dot{x}(t) = A(t)x(t)$. Suppose $A(t) \in \mathbb{R}^{n\times n}$ is continuous and bounded. Let $Q(t) \in \mathbb{R}^{n\times n}$ be a $\mathscr{C}^0$ matrix such that*

$$Q(t) > c_3 I > 0, \quad Q(t) = Q^{\mathrm{T}}(t).$$

Then, there exits a $\mathscr{C}^1$ matrix $P(t) \in \mathbb{R}^{n\times n}$ that satisfies

$$0 < c_1 I \leq P(t) \leq c_2 I, \quad P(t) = P^{\mathrm{T}}(t),$$
$$-\dot{P}(t) = P(t)A(t) + A^{\mathrm{T}}(t)P(t) + Q(t), \quad t \geq 0.$$

and $V(t,x) = x^{\mathrm{T}}(t)P(t)x(t)$ is a Lyapunov function for the system that satisfies

$$c_1\|x\|_2^2 \leq V(t,x) \leq c_2\|x\|_2^2,$$
$$\dot{V}(t,x) = -x^{\mathrm{T}}Q(t)x \leq -c_3\|x\|_2^2.$$

Lemma 3.2.4 *([49]) Consider the LTV system*

$$\dot{x}(t) = A(t)x(t) + B(t)u(t), \tag{3.14}$$

where $x(t) \in \mathbb{R}^n$, $u(t) \in \mathbb{R}^m$, and $A(t) \in \mathbb{R}^{n\times n}$, $B(t) \in \mathbb{R}^{n\times m}$, and consider the transformation *matrices*

$$T(x) \triangleq I_n - 2x(t)x^\dagger(t) \in \mathbb{R}^{n\times n},$$
$$A_T(x,t) \triangleq -T(x)A(t)T(x) \in \mathbb{R}^{n\times n}, \quad B_T(x,t) \triangleq T(x)B(t) \in \mathbb{R}^{n\times m}.$$

where the time dependence of the state $x(t)$ is not explicitly shown in order to simplify the notation. Let $R(t) : [t_0,\infty) \to \mathbb{R}^{m\times m}$, $R(t) > 0$ and $Q(t) : [t_0,\infty) \to \mathbb{R}^{n_a\times n_a}$, $Q(t) > 0$ be design bounded matrices. Assume that the following state dependent Riccati differential equation

$$\dot{P}(t) = -P(t)A_T(x,t) - A_T^{\mathrm{T}}(x,t)P(t) + Q(t) - \varepsilon(t)P(t)B_T(x,t)R^{-1}(t)B_T^{\mathrm{T}}(x,t)P(t), \tag{3.15}$$

with $P(t_0) = P_0 > 0$ admits solution $P(t) > 0$ over $[t_0,\infty)$, and $R(t)$, $Q(t)$ and $\varepsilon(t) > 0$ satisfies

$$Q(t) + (2-\varepsilon(t))P(t)B_T(x,t)R^{-1}(t)B_T^{\mathrm{T}}(z,t)P(t) > \sigma I_{n_a}, \tag{3.16}$$

where $\sigma > 0$. If $(A(t),B(t))$ is uniformly controllable, then $(A_T(t),B_T(t))$ is also uniformly controllable and $P(t)$ is uniformly bounded. Furthermore, the feedback control

$$u(t) = K_f(t)x(t), \quad K_f(t) = R^{-1}B_T^{\mathrm{T}}(x,t)P(t), \tag{3.17}$$

guarantees that the closed-loop system (3.14) and (3.17) is globally exponentially stable.

3.3 Predictor Design

In this section, we will obtain the output predictor, capable of predicting the system output using the history of the system input and output stored in autoregressive vectors. For the statement of the following theorems, we define the following notation

$$A_u \triangleq I_m \otimes A_f \in \mathbb{R}^{nm\times nm}, \quad B_u \triangleq I_m \otimes B_f \in \mathbb{R}^{nm\times m}, \tag{3.18}$$

where A_f, B_f are defined in (3.11), and

$$\eta_y(t) \triangleq (A_f + k_p I_n)\omega_y(t) - B_f y^{\mathrm{T}}(t) \in \mathbb{R}^{n\times p}, \tag{3.19}$$

$$\eta_u(t) \triangleq (A_u + k_p I_{nm})\omega_u(t) + B_u u(t) \in \mathbb{R}^{nm}. \tag{3.20}$$

Theorem 3.3.1 *Consider the system $\mathscr{G}_{\mathrm{L}}$ defined in (3.2) which has input $u(t) \in \mathbb{R}^m$, output $y(t) \in \mathbb{R}^p$, and the regression vectors $\omega_y(t)$ and $\omega_u(t)$ defined in (3.9). Let $k_{\mathrm{p}} > 0$ and introduce the tuning matrices $\Gamma \in \mathbb{R}^{p\times p}$, $\Gamma > 0$, $P_\alpha \in \mathbb{R}^{n\times n}$, $P_\alpha > 0$, $P_\beta \in \mathbb{R}^{nm\times nm}$, $P_\beta > 0$. Then, the output predictor*

$$\dot{y}_{\mathrm{p}}(t) = -k_{\mathrm{p}} y_{\mathrm{p}}(t) + \eta_y^{\mathrm{T}}(t)\hat{\alpha}(t) + \hat{\beta}^{\mathrm{T}}(t)\eta_u(t), \qquad y_{\mathrm{p}}(0) = y_{\mathrm{p}0},\ t \geq 0, \tag{3.21}$$

with $\hat{\alpha}(t) \in \mathbb{R}^n$, and $\hat{\beta}(t) \in \mathbb{R}^{nm\times p}$ obtained from the adaptive law

$$\dot{\hat{\alpha}}(t) = P_\alpha\big(\eta_y(t)\Gamma^{\mathrm{T}} e_{\mathrm{p}}(t) + \sigma(t)\omega_y(t)\varepsilon(t)\big), \quad \hat{\alpha}(0) = \hat{\alpha}_0,\ \ t \geq 0, \tag{3.22a}$$

$$\dot{\hat{\beta}}(t) = P_\beta\big(\eta_u(t)e_{\mathrm{p}}^{\mathrm{T}}(t)\Gamma + \sigma(t)\omega_u(t)\varepsilon^{\mathrm{T}}(t)\big), \quad \hat{\beta}(0) = \hat{\beta}_0,\ \ t \geq 0, \tag{3.22b}$$

where $e_{\mathrm{p}}(t) \triangleq y(t) - y_{\mathrm{p}}(t)$ is the prediction error, $\sigma(t) \in \mathscr{C}^0$, $\sigma(t) \geq 0$ is a bounded function, and

$$\varepsilon(t) \triangleq y(t) - \omega_y^{\mathrm{T}}(t)\hat{\alpha}(t) - \hat{\beta}^{\mathrm{T}}(t)\omega_u(t), \tag{3.23}$$

guarantees that the system defined by (3.21) - (3.22) is Lyapunov stable, and the prediction error $e_{\mathrm{p}}(t) \to 0$ and $\varepsilon(t) \to 0$ as $t \to \infty$.

Proof *It follows from Lemma (3.2.2) that any n^{th} order MIMO system can be represented by*

$$y(t) = \omega_y^{\mathrm{T}}(t)\alpha + \beta^{\mathrm{T}}\omega_u(t). \tag{3.24}$$

Taking the time derivative of (3.24) yields

$$\begin{aligned}
\dot{y}(t) &= \left(\omega_y^{\mathrm{T}}(t)A_{\mathrm{f}}^{\mathrm{T}} - y(t)B_{\mathrm{f}}^{\mathrm{T}}\right)\alpha + \beta^{\mathrm{T}}(A_u\omega_u(t) + B_u u(t)) \\
&= -k_{\mathrm{p}}y(t) + \left(\omega_y^{\mathrm{T}}(t)(A_{\mathrm{f}}^{\mathrm{T}} + k_{\mathrm{p}}I_n) - y(t)B_{\mathrm{f}}^{\mathrm{T}}\right)\alpha + \beta^{\mathrm{T}}\left((A_u + k_{\mathrm{p}}I_{nm})\omega_u(t) + B_u u(t)\right) \\
&= -k_{\mathrm{p}}y(t) + \eta_y^{\mathrm{T}}(t)\alpha + \beta^{\mathrm{T}}\eta_u(t),
\end{aligned} \tag{3.25}$$

where $\eta_y(t)$ and $\eta_u(t)$ are defined in (3.19) and (3.20), respectively.

It follows from (3.25) and (3.21) that the prediction error dynamics is obtained as

$$\dot{e}_{\mathrm{p}}(t) = -k_{\mathrm{p}}e_{\mathrm{p}}(t) + \eta_y^{\mathrm{T}}(t)\tilde{\alpha}(t) + \tilde{\beta}^{\mathrm{T}}(t)\eta_u(t), \quad e_{\mathrm{p}}(0) = e_{\mathrm{p}0},\ t \geq 0, \tag{3.26}$$

where $\tilde{\alpha}(t) \triangleq \alpha - \hat{\alpha}(t) \in \mathbb{R}^n$ and $\tilde{\beta}(t) \triangleq \beta - \hat{\beta}(t) \in \mathbb{R}^{nm\times p}$. Now, differentiating the Lyapunov function candidate

$$V(e_{\mathrm{p}},\tilde{\alpha},\tilde{\beta}) = \frac{1}{2}e_{\mathrm{p}}^{\mathrm{T}}(t)\Gamma e_{\mathrm{p}}(t) + \frac{1}{2}\tilde{\alpha}^{\mathrm{T}}(t)P_{\alpha}^{-1}\tilde{\alpha}(t) + \frac{1}{2}\mathrm{tr}[\tilde{\beta}^{\mathrm{T}}(t)P_{\beta}^{-1}\tilde{\beta}(t)], \tag{3.27}$$

along the error dynamics trajectories given by (3.26) and substituting the update laws (3.22), yields

$$\begin{aligned}\dot{V}(t) &= -k_{\mathrm{p}}e_{\mathrm{p}}^{\mathrm{T}}(t)\Gamma e_{\mathrm{p}}(t) + e_{\mathrm{p}}^{\mathrm{T}}(t)\Gamma\eta_y^{\mathrm{T}}(t)\tilde{\alpha}(t) + e_{\mathrm{p}}^{\mathrm{T}}(t)\Gamma\tilde{\beta}^{\mathrm{T}}(t)\eta_u(t) - \tilde{\alpha}^{\mathrm{T}}(t)P_{\alpha}^{-1}\dot{\hat{\alpha}}(t) - \mathrm{tr}[\tilde{\beta}^{\mathrm{T}}(t)P_{\beta}^{-1}\dot{\hat{\beta}}(t)]\\ &= -k_{\mathrm{p}}e_{\mathrm{p}}^{\mathrm{T}}(t)\Gamma e_{\mathrm{p}}(t) + \tilde{\alpha}^{\mathrm{T}}(t)\big(\eta_y(t)\Gamma^{\mathrm{T}}e_{\mathrm{p}}(t) - P_{\alpha}^{-1}\dot{\hat{\alpha}}(t)\big) + \mathrm{tr}[\tilde{\beta}^{\mathrm{T}}(t)(\eta_u(t)e_{\mathrm{p}}^{\mathrm{T}}(t)\Gamma - P_{\beta}^{-1}\dot{\hat{\beta}}(t))]\\ &= -k_{\mathrm{p}}e_{\mathrm{p}}^{\mathrm{T}}(t)\Gamma e_{\mathrm{p}}(t) - \sigma(t)\tilde{\alpha}^{\mathrm{T}}(t)\omega_y(t)\varepsilon(t) - \mathrm{tr}[\sigma(t)\tilde{\beta}^{\mathrm{T}}(t)\omega_u(t)\varepsilon^{\mathrm{T}}(t)].\end{aligned} \tag{3.28}$$

Using the fact that if $x\in\mathbb{R}$ then $x = x^{\mathrm{T}}$ yields

$$\sigma(t)\tilde{\alpha}^{\mathrm{T}}(t)\omega_y(t)\varepsilon(t) = \sigma(t)\varepsilon^{\mathrm{T}}(t)\omega_y^{\mathrm{T}}(t)\tilde{\alpha}(t). \tag{3.29}$$

and the fact that if $X\in\mathbb{R}^{1\times n}$ and $Y\in\mathbb{R}^{1\times n}$ then $\mathrm{tr}[X^{\mathrm{T}}Y] = \mathrm{tr}[YX^{\mathrm{T}}] = YX^{\mathrm{T}}$ *yields*

$$\mathrm{tr}[\sigma(t)\tilde{\beta}^{\mathrm{T}}(t)\omega_u(t)\varepsilon^{\mathrm{T}}(t)] = \sigma(t)\varepsilon^{\mathrm{T}}(t)\tilde{\beta}^{\mathrm{T}}(t)\omega_u(t). \tag{3.30}$$

Substituting (3.24) into (3.23), we rewrite $\varepsilon(t)$ as

$$\varepsilon(t) = \omega_y^{\mathrm{T}}(t)\tilde{\alpha}(t) + \tilde{\beta}^{\mathrm{T}}(t)\omega_u(t). \tag{3.31}$$

Finally, substituting (3.29), (3.30) and (3.31) into (3.28) yields

$$\begin{aligned}\dot{V}(t) &= -k_{\mathrm{p}}e_{\mathrm{p}}^{\mathrm{T}}(t)\Gamma e_{\mathrm{p}}(t) - \sigma(t)\varepsilon^{\mathrm{T}}(t)(\omega_y^{\mathrm{T}}(t)\tilde{\alpha}(t) + \tilde{\beta}^{\mathrm{T}}(t)\omega_u(t))\\ &= -k_{\mathrm{p}}e_{\mathrm{p}}^{\mathrm{T}}(t)\Gamma e_{\mathrm{p}}(t) - \sigma(t)\varepsilon^{\mathrm{T}}(t)\varepsilon(t) \le 0.\end{aligned} \tag{3.32}$$

Hence, the dynamic system given by (3.26) and (3.22) is Lyapunov stable and, by the LaSalle-Yoshizawa theorem, $\lim_{t\to\infty}\dot{V}(t) = 0$*, and hence,* $e_{\mathrm{p}}(t)\to 0$ *and* $\varepsilon(t)\to 0$ *as* $t\to 0$*, which concludes the proof.* □

Corollary 3.3.1 *Consider the system $\mathscr{G}_{\mathrm{L}}$ defined in (3.2) which has input $u(t)\in\mathbb{R}^m$, output $y(t)\in\mathbb{R}^p$, and the regression vectors $\omega_y(t)$, $\omega_u(t)$ defined in (3.9). Let $k_{\mathrm{p}} > 0$ and introduce the tuning matrices $\Gamma\in\mathbb{R}^{p\times p}$, $\Gamma > 0$, $P_\alpha\in\mathbb{R}^{n\times n}$, $P_\alpha > 0$, $P_\beta\in\mathbb{R}^{nm\times nm}$, $P_\beta > 0$. Then, the output predictor*

$$\dot{y}_{\mathrm{p}}(t) = -k_{\mathrm{p}}y_{\mathrm{p}}(t) + \eta_y^{\mathrm{T}}(t)\hat{\alpha}(t) + \hat{\beta}^{\mathrm{T}}(t)\eta_u(t), \quad y_{\mathrm{p}}(0) = y_{\mathrm{p}0},\ t\ge 0, \tag{3.33}$$

with $\hat{\alpha}(t) \in \mathbb{R}^n$, *and* $\hat{\beta}(t) \in \mathbb{R}^{nm\times p}$ *obtained from the adaptive law*

$$\dot{\hat{\alpha}}(t) = P_\alpha\left(\eta_y(t)\Gamma^{\mathrm{T}} e_{\mathrm{p}}(t) + \int_{t-T}^{t} \sigma(t,\tau)\omega_y(\tau)\varepsilon(t,\tau)\mathrm{d}\tau\right), \quad \hat{\alpha}(0) = \hat{\alpha}_0, \ t \geq T \geq 0, \tag{3.34a}$$

$$\dot{\hat{\beta}}(t) = P_\beta\left(\eta_u(t)e_{\mathrm{p}}^{\mathrm{T}}(t)\Gamma + \int_{t-T}^{t} \sigma(t,\tau)\omega_u(\tau)\varepsilon^{\mathrm{T}}(t,\tau)\mathrm{d}\tau\right), \quad \hat{\beta}(0) = \hat{\beta}_0, \ t \geq T \geq 0, \tag{3.34b}$$

where $e_{\mathrm{p}}(t) \triangleq y(t) - y_{\mathrm{p}}(t)$ *is the prediction error,* $\sigma(t,\tau) \in \mathscr{C}^0, \ \sigma(t,\tau) \geq 0$ *is a bounded function, and*

$$\varepsilon(t,\tau) = y(\tau) - \omega_y^{\mathrm{T}}(\tau)\hat{\alpha}(t) - \hat{\beta}^{\mathrm{T}}(t)\omega_u(\tau), \quad t-T \leq \tau \leq t, \ t \geq 0, \tag{3.35}$$

guarantees that that the system defined by (3.33) - (3.34) is Lyapunov stable, the prediction error $e_{\mathrm{p}}(t) \to 0$ *as* $t \to \infty$, *and*

$$\lim_{t\to\infty} \int_{t-T}^{t} \sigma(t,\tau)\varepsilon^{\mathrm{T}}(t,\tau)\varepsilon(t,\tau)\mathrm{d}\tau = 0. \tag{3.36}$$

Proof *Similar to the proof of Theorem 3.3.1, differentiating the Lyapunov function candidate* $V(e_{\mathrm{p}}, \tilde{\alpha}, \tilde{\beta})$ *defined in (3.27) along the error dynamics trajectories given by (3.26) and substituting the update law (3.34), yields*

$$\begin{aligned}\dot{V}(t) &= -k_{\mathrm{p}} e_{\mathrm{p}}^{\mathrm{T}}(t)\Gamma e_{\mathrm{p}}(t) - \tilde{\alpha}^{\mathrm{T}}(t)\int_{t-T}^{t}\sigma(t,\tau)\omega_y(\tau)\varepsilon(t,\tau)\mathrm{d}\tau - \mathrm{tr}\left[\tilde{\beta}^{\mathrm{T}}(t)\int_{t-T}^{t}\sigma(t,\tau)\omega_u(\tau)\varepsilon^{\mathrm{T}}(t,\tau)\mathrm{d}\tau\right]\\ &= -k_{\mathrm{p}} e_{\mathrm{p}}^{\mathrm{T}}(t)\Gamma e_{\mathrm{p}}(t) - \int_{t-T}^{t}\sigma(t,\tau)\tilde{\alpha}^{\mathrm{T}}(t)\omega_y(\tau)\varepsilon(t,\tau)\mathrm{d}\tau - \mathrm{tr}\left[\int_{t-T}^{t}\sigma(t,\tau)\tilde{\beta}^{\mathrm{T}}(t)\omega_u(\tau)\varepsilon^{\mathrm{T}}(t,\tau)\mathrm{d}\tau\right].\end{aligned} \tag{3.37}$$

where the second equality observing that $\tilde{\alpha}^{\mathrm{T}}(t)$ *and* $\tilde{\beta}^{\mathrm{T}}(t)$ *are independent of* τ. *Similar to (3.29), (3.30) and (3.31), the following properties hold*

$$\int_{t-\tau}^{t}\sigma(t,\tau)\tilde{\alpha}^{\mathrm{T}}(t)\omega_y(\tau)\varepsilon(t,\tau)\mathrm{d}\tau = \int_{t-\tau}^{t}\sigma(t,\tau)\varepsilon^{\mathrm{T}}(t,\tau)\omega_y^{\mathrm{T}}(\tau)\tilde{\alpha}(t)\mathrm{d}\tau, \tag{3.38a}$$

$$\mathrm{tr}\left[\int_{t-T}^{t}\sigma(t,\tau)\tilde{\beta}^{\mathrm{T}}(t)\omega_u(\tau)\varepsilon^{\mathrm{T}}(t,\tau)\mathrm{d}\tau\right] = \int_{t-T}^{t}\sigma(t,\tau)\varepsilon^{\mathrm{T}}(t,\tau)\tilde{\beta}^{\mathrm{T}}(t)\omega_u(\tau)\mathrm{d}\tau, \tag{3.38b}$$

$$\varepsilon(t,\tau) = \omega_y^{\mathrm{T}}(\tau)\tilde{\alpha}(t) + \tilde{\beta}^{\mathrm{T}}(t)\omega_u(\tau). \tag{3.38c}$$

Hence, substituting (3.38) into (3.37) yields

$$\begin{aligned}\dot{V}(t) &= -k_{\mathrm{p}}e_{\mathrm{p}}^{\mathrm{T}}(t)\Gamma e_{\mathrm{p}}(t) - \int_{t-T}^{t}\sigma(t,\tau)\varepsilon^{\mathrm{T}}(t,\tau)(\omega_y^{\mathrm{T}}(\tau)\tilde{\alpha}(t) + \tilde{\beta}^{\mathrm{T}}(t)\omega_u(\tau))\mathrm{d}\tau \\ &= -k_{\mathrm{p}}e_{\mathrm{p}}^{\mathrm{T}}(t)\Gamma e_{\mathrm{p}}(t) - \int_{t-T}^{t}\sigma(t,\tau)\varepsilon^{\mathrm{T}}(t,\tau)\varepsilon(t,\tau)\mathrm{d}\tau \le 0.\end{aligned}$$

Hence, the dynamic system given by (3.26) and (3.34) is Lyapunov stable, and, by the LaSalle-Yoshizawa theorem, $\lim_{t\to\infty}\dot{V}(t) = 0$*, and hence,* $e_{\mathrm{p}}(t) \to 0$ *as* $t \to 0$*, and proves (3.36), which concludes the proof.* □

Remark 3.3.1 *In order to compute the adaptive law (3.34) efficiently, notice that*

$$\begin{aligned}\omega_y(\tau)\varepsilon(t,\tau) &= \omega_y(\tau)\big(y(\tau) - \omega_y^{\mathrm{T}}(\tau)\hat{\alpha}(t) - \hat{\beta}^{\mathrm{T}}(t)\omega_u(\tau)\big) \\ &= \omega_y(\tau)y(\tau) - \omega_y(\tau)\omega_y^{\mathrm{T}}(\tau)\hat{\alpha}(t) - (\omega_u^{\mathrm{T}}(\tau)\otimes\omega_y(\tau))\mathrm{vec}(\hat{\beta}^{\mathrm{T}}(t)),\end{aligned} \tag{3.39}$$

by using the property $\mathrm{vec}(AXB) = (B^{\mathrm{T}}\otimes A)\mathrm{vec}(X)$ *([64]) we obtain*

$$\omega_y(\tau)\hat{\beta}^{\mathrm{T}}(t)\omega_u(\tau) = \mathrm{vec}(\omega_y(\tau)\hat{\beta}^{\mathrm{T}}(t)\omega_u(\tau)) = (\omega_u^{\mathrm{T}}(\tau)\otimes\omega_y(\tau))\mathrm{vec}(\hat{\beta}^{\mathrm{T}}(t)).$$

Similarly, we have

$$\begin{aligned}\omega_u(\tau)\varepsilon^{\mathrm{T}}(t,\tau) &= \omega_u(\tau)\big(y^{\mathrm{T}}(\tau) - (\omega_y^{\mathrm{T}}(\tau)\hat{\alpha}(t))^{\mathrm{T}} - \omega_u^{\mathrm{T}}(\tau)\hat{\beta}(t)\big) \\ &= \omega_u(\tau)y^{\mathrm{T}}(\tau) - \omega_u(\tau)\omega_u^{\mathrm{T}}(\tau)\hat{\beta}(t) - (\omega_u(\tau)\omega_y^{\mathrm{T}}(\tau))\hat{\alpha}(t),\end{aligned} \tag{3.40}$$

where $(\omega_y^{\mathrm{T}}(\tau)\hat{\alpha}(t)) = \hat{\alpha}(t)^{\mathrm{T}}\omega_y(\tau)$*. Substituing (3.39) and (3.40) into (3.34), we rewrite the adaptive law as*

$$\dot{\hat{\alpha}}(t) = P_\alpha\big(\eta_y(t)\Gamma^{\mathrm{T}}e_{\mathrm{p}}(t) + D_\alpha(t) - H_\alpha(t)\mathrm{vec}(\hat{\beta}^{\mathrm{T}}(t)) - \Omega_\alpha(t)\hat{\alpha}(t)\big), \quad \alpha(0) = \alpha_0, \tag{3.41a}$$

$$\dot{\hat{\beta}}(t) = P_\beta\big(\eta_u(t)e_{\mathrm{p}}^{\mathrm{T}}(t)\Gamma + D_\beta(t) - H_\beta(t)\hat{\alpha}(t) - \Omega_\beta(t)\hat{\beta}(t)\big), \quad \beta(0) = \beta_0,\ t \ge 0, \tag{3.41b}$$

where $D_\alpha(t) \in \mathbb{R}^n$*,* $D_\beta(t) \in \mathbb{R}^{nm\times p}$*,* $H_\alpha(t) \in \mathbb{R}^{n\times nmp}$*,* $H_\beta(t) \in \mathbb{R}^{nm\times np}$*,* $\Omega_\alpha(t) \in \mathbb{R}^{n\times n}$*, and* $\Omega_\beta(t) \in \mathbb{R}^{nm\times nm}$ *are defined as,*

$$\begin{aligned}D_\alpha(t) &\triangleq \int_{t-T}^{t}\sigma(t,\tau)\omega_y(\tau)y(\tau)\mathrm{d}\tau, & D_\beta(t) &\triangleq \int_{t-T}^{t}\sigma(t,\tau)\omega_u(\tau)y^{\mathrm{T}}(\tau)\mathrm{d}\tau, \\ \Omega_\alpha(t) &\triangleq \int_{t-T}^{t}\sigma(t,\tau)\omega_y(\tau)\omega_y^{\mathrm{T}}(\tau)\mathrm{d}\tau, & \Omega_\beta(t) &\triangleq \int_{t-T}^{t}\sigma(t,\tau)\omega_u(\tau)\omega_u^{\mathrm{T}}(\tau)\mathrm{d}\tau,\end{aligned}$$

$$H_\alpha(t) \triangleq \int_{t-T}^{t} \sigma(t,\tau)\omega_u^{\mathrm{T}}(\tau) \otimes \omega_y(\tau)\mathrm{d}\tau, \qquad H_\beta(t) \triangleq \int_{t-T}^{t} \sigma(t,\tau)\omega_u(\tau)\omega_y^{\mathrm{T}}(\tau)\mathrm{d}\tau.$$

Note that since $\Omega_\alpha(t) \geq 0$ and $\Omega_\beta(t) \geq 0$, $-\Omega_\alpha(t)\hat{\alpha}(t)$ and $-\Omega_\beta(t)\hat{\beta}(t)$ play a role of damping components that attenuate the high frequency content contained in the adaptive law (3.41), which allows us to use high gain adaptation P_α, P_β and still guarantee robustness.

Remark 3.3.2 *The projection operator should be applied to all adaptive laws (3.22) or (3.34), to ensure the boundedness of the estimated signals $\hat{\alpha}(t)$, $\hat{\beta}(t)$. Furthermore, $\hat{\beta}_{ij}(t)$ needs to satisfy the topological equivalence of the input $u_j(t)$ with respect to the output $y_i(t)$, such that*

$$\hat{\beta}_{ij}(t) \triangleq \begin{bmatrix} \hat{\beta}_{ij}^{(0)}(t) & \ldots & \hat{\beta}_{ij}^{(n-r)}(t) & 0_{r_{ij}-1}^{\mathrm{T}} \end{bmatrix}^{\mathrm{T}} \in \mathbb{R}^n.$$

which can also be enforced using the projection operator.

Remark 3.3.3 *If $\sigma(\tau)$ is chosen as*

$$\sigma(\tau) \triangleq \begin{cases} 0, & \text{if } \|\omega_y\|^2 + \|\omega_y\|^2 = 0; \\ \dfrac{\kappa_1 e^{-\kappa_2(t-\tau)}}{\|\omega_y(\tau)\|^2 + \|\omega_u(\tau)\|^2}, \quad \kappa_1 \geq 0, \kappa_2 \geq 0, & \text{otherwise,} \end{cases} \tag{3.42}$$

it follows from (3.23), (3.36) and (3.42) that

$$J(\varepsilon) = \int_{t-T}^{t} \kappa_1 e^{-\kappa_2(t-\tau)} \frac{\|y(\tau) - \omega_y^{\mathrm{T}}(\tau)\hat{\alpha}(t) - \hat{\beta}^{\mathrm{T}}(t)\omega_u(\tau)\|^2}{\|\omega_y(\tau)\|^2 + \|\omega_u(\tau)\|^2}\mathrm{d}\tau,$$

which is the cost function to estimate α and β using the least square with forgetting factor method. According to Corollary 3.3.1, $J(\varepsilon)$ converges to 0 as $t \to \infty$.

3.4 Controller Design

In this section, we will rewrite the predictor in the form of linear time varying (LTV) system, and extend the control design framework in [10] to control this LTV system.

3.4.1 Controller using Forward Riccati Differential Equation

It follows from (3.20) and (3.21) that the predictor dynamics can be obtained as

$$\begin{aligned}\dot{y}_{\mathrm{p}}(t) &= -k_{\mathrm{p}}y_{\mathrm{p}}(t) + \eta_y^{\mathrm{T}}(t)\hat{\alpha}(t) + \hat{\beta}^{\mathrm{T}}(t)(A_u + k_{\mathrm{p}}I_{nm})\omega_u(t) + \hat{\beta}^{\mathrm{T}}(t)B_u u(t) \\ &= -k_{\mathrm{p}}y_{\mathrm{p}}(t) + \eta_y^{\mathrm{T}}(t)\hat{\alpha}(t) + C_u(t)\omega_u(t) + D_u(t)u(t),\end{aligned} \tag{3.43}$$

where

$$C_u(t) \triangleq \hat{\beta}^{\mathrm{T}}(t)(A_u + k_{\mathrm{p}}I_{nm}) \in \mathbb{R}^{p\times nm}, \;\; D_u(t) \triangleq \hat{\beta}^{\mathrm{T}}(t)B_u \in \mathbb{R}^{p\times m}.$$

Note that if the control inputs $u_j(t),\ j = 1,\ldots,m$, have relative degree $r_{ij} \geq 2$ then $D_u(t) = 0_{p\times m}$. Now, consider the desired reference system defined in (3.3) and let $e_{\mathrm{r}}(t) \triangleq y_{\mathrm{p}}(t) - y_{\mathrm{m}}(t)$ be the tracking error between the predictor and the reference system. It follows from (3.3) and (3.43) that

$$\begin{aligned}\dot{e}_{\mathrm{r}}(t) &= -k_{\mathrm{p}}(y_{\mathrm{p}}(t) - y_{\mathrm{m}}(t)) + \eta_y^{\mathrm{T}}(t)\hat{\alpha}(t) + C_u(t)\omega_u(t) + D_u(t)u(t) - (A_{\mathrm{m}} + k_{\mathrm{p}}I_p)y_{\mathrm{m}}(t) - B_{\mathrm{m}}r(t) \\ &= -(k_{\mathrm{p}}I_p + K_{\mathrm{r}})e_{\mathrm{r}}(t) + C_u(t)\omega_u(t) + D_u(t)u(t) - \varphi_{\mathrm{d}}(t),\end{aligned} \tag{3.44}$$

where $K_{\mathrm{r}} \in \mathbb{R}^{p\times p}, K_{\mathrm{r}} > 0$ and

$$\varphi_{\mathrm{d}}(t) \triangleq -K_{\mathrm{r}}e_{\mathrm{r}}(t) - \eta_y^{\mathrm{T}}(t)\hat{\alpha}(t) + (A_{\mathrm{m}} + k_{\mathrm{p}}I_p)y_{\mathrm{m}}(t) + B_{\mathrm{m}}r(t). \tag{3.45}$$

The problem of driving $e_{\mathrm{r}}(t)$ to the origin therefore reduces to design a full state feedback controller such that the following linear system

$$\dot{\omega}_u(t) = A_u\omega_u(t) + B_u u(t), \tag{3.46a}$$

$$\varphi(t) = C_u(t)\omega_u(t) + D_u(t)u(t), \tag{3.46b}$$

tracks the desired trajectory $\varphi_{\mathrm{d}}(t)$. Note that this system is linear time varying, even though $C(t)$, $D(t)$ and $\hat{\alpha}(t)$, $\hat{\beta}(t)$ will converge to constants as $e_{\mathrm{p}} \to 0$. If the matrices $C(t)$ and $D(t)$ vary slowly in time and converge to constants, the LQR controller can be applied at each frozen time t. However, when parameters change rapidly, this system is linear time varying and since the system parameters are not known ahead in time, it is not suitable to apply the LQR controller using the backward Riccati differential equation ([49]). In the following section, we will extend the controller for LTV systems using the Forward Differential Riccati equation (FDRE) developed in [49].

Let $e_2(t) \triangleq \varphi(t) - \varphi_{\mathrm{d}}(t)$, and define the filter of $e_2(t)$ as

$$\dot{x}_{\mathrm{I}}(t) = -\Lambda x_{\mathrm{I}}(t) + \Omega e_2(t), \quad x_{\mathrm{I}}(0) = x_{\mathrm{I}0},\ t \geq 0, \tag{3.47}$$

where $\Lambda \in \mathbb{R}^{p\times p},\ \Lambda \geq 0$ and $\Omega \in \mathbb{R}^{p\times p},\ \Omega \geq 0$. The dynamics (3.46) can be augmented to include (3.47) as follows

$$\begin{aligned}\dot{x}_{\mathrm{a}}(t) &= \begin{bmatrix} A_u & 0_{nm\times p} \\ \Omega C_u(t) & -\Lambda \end{bmatrix} \begin{bmatrix} \omega_u(t) \\ x_{\mathrm{I}}(t) \end{bmatrix} + \begin{bmatrix} B_u \\ \Omega D_u(t) \end{bmatrix} u(t) + \begin{bmatrix} 0_{nm} \\ -\Omega\varphi_{\mathrm{d}}(t) \end{bmatrix} \\ &= A_{\mathrm{a}}(t)x_{\mathrm{a}}(t) + B_{\mathrm{a}}(t)u(t) + \vartheta(t), \end{aligned} \tag{3.48}$$

where $x_{\mathrm{a}}(t) \triangleq \begin{bmatrix} \omega_u^{\mathrm{T}}(t) & x_{\mathrm{I}}^{\mathrm{T}}(t) \end{bmatrix}^{\mathrm{T}} \in \mathbb{R}^{n_{\mathrm{a}}}$, $n_{\mathrm{a}} \triangleq nm + p$, $\vartheta(t) = [0_{nm}^{\mathrm{T}} \quad -\varphi_{\mathrm{d}}^{\mathrm{T}}(t)]^{\mathrm{T}}$ and obvious definitions of $A_{\mathrm{a}}(t) \in \mathbb{R}^{n_{\mathrm{a}}\times n_{\mathrm{a}}}$ and $B_{\mathrm{a}}(t) \in \mathbb{R}^{n_{\mathrm{a}}\times m}$.

Proposition 3.4.1 *Let $R(t) : [t_0,\infty) \to \mathbb{R}^{m\times m},\ R(t) > 0$ and $Q(t) : [t_0,\infty) \to \mathbb{R}^{n_{\mathrm{a}}\times n_{\mathrm{a}}},\ Q(t) > 0$ be design bounded matrices. Assume that the system $(A_{\mathrm{a}}(t),\ B_{\mathrm{a}}(t))$ is uniformly controllable and the following state dependent Riccati differential equation*

$$\dot{P}(t) = P(t)(A_{\mathrm{a}}(t)+A_{\mathrm{b}}(t)) + (A_{\mathrm{a}}(t)+A_{\mathrm{b}}(t))^{\mathrm{T}}P(t) + Q(t) - \varepsilon(t)P(t)B_{\mathrm{a}}(t)R^{-1}(t)B_{\mathrm{a}}^{\mathrm{T}}(t)P(t), \tag{3.49}$$

with $P(t_0) = P_0 > 0$ admits solution $P(t) > 0$ over $[t_0,\infty)$, where

$$A_{\mathrm{b}}(t) = 2(x_{\mathrm{a}}^{\dagger\mathrm{T}}(t)\dot{x}_{\mathrm{a}}^{\mathrm{T}}(t) - \dot{x}_{\mathrm{a}}(t)x_{\mathrm{a}}^{\dagger}(t)). \tag{3.50}$$

If $Q(t)$, $R(t)$ and $\varepsilon(t) > 0$ satisfies

$$Q(t) + (2-\varepsilon(t))P(t)B_{\mathrm{a}}(t)R^{-1}(t)B_{\mathrm{a}}^{\mathrm{T}}(t)P(t) > \sigma I_{n_{\mathrm{a}}}, \tag{3.51}$$

where $\sigma > 0$, then the feedback control

$$u(t) = -K_{\mathrm{f}}(t)x_{\mathrm{a}}(t), \quad K_{\mathrm{f}}(t) = R^{-1}(t)B_{\mathrm{a}}^{\mathrm{T}}(t)P(t), \tag{3.52}$$

guarantees that the filtered tracking error $x_{\mathrm{I}}(t)$ is uniformly ultimately bounded.

Proof *First, consider the nominal system (3.48) without disturbance $\vartheta(t)$*

$$\dot{x}_{\mathrm{a}}(t) = A_{\mathrm{a}}(t)x_{\mathrm{a}}(t) + B_{\mathrm{a}}(t)u(t). \tag{3.53}$$

and the following transformation matrices

$$T(x_{\mathrm{a}}) \triangleq I_{n_{\mathrm{a}}} - 2x_{\mathrm{a}}(t)x_{\mathrm{a}}^{\dagger}(t) \in \mathbb{R}^{n_{\mathrm{a}}\times n_{\mathrm{a}}}, \qquad Q_T(x_{\mathrm{a}},t) \triangleq T(x_{\mathrm{a}})Q(t)T(x_{\mathrm{a}}) \in \mathbb{R}^{n_{\mathrm{a}}\times n_{\mathrm{a}}}, \tag{3.54}$$

$$A_T(x_{\mathrm{a}},t) \triangleq -T(x_{\mathrm{a}})A_{\mathrm{a}}(t)T(x_{\mathrm{a}}) \in \mathbb{R}^{n_{\mathrm{a}}\times n_{\mathrm{a}}}, \qquad B_T(x_{\mathrm{a}},t) \triangleq T(x_{\mathrm{a}})B_{\mathrm{a}}(t) \in \mathbb{R}^{n_{\mathrm{a}}\times m}. \tag{3.55}$$

Next, define the controller as

$$u(t) = R^{-1}(t)B_T^{\mathrm{T}}(x_{\mathrm{a}},t)P_{\mathrm{f}}(t)x_{\mathrm{a}}(t), \tag{3.56}$$

where $P_{\mathrm{f}}(t)$ is the solution of the FDRE

$$\dot{P}_{\mathrm{f}}(t) = -P_{\mathrm{f}}(t)A_T(x_{\mathrm{a}},t) - A_T^{\mathrm{T}}(x_{\mathrm{a}},t)P_{\mathrm{f}}(t) + Q_T(x_{\mathrm{a}},t) - \varepsilon(t)P_{\mathrm{f}}(t)B_T(x_{\mathrm{a}},t)R^{-1}(t)B_T^{\mathrm{T}}(x_{\mathrm{a}},t)P_{\mathrm{f}}(t), \tag{3.57}$$

with $P_{\mathrm{f}}(t_0) = P_{\mathrm{f}0} > 0$. Assume that (3.57) admits solution $P_{\mathrm{f}}(t) > 0$ over $[t_0,\infty)$, and $R(t)$, $Q(t),\sigma$ and $\varepsilon(t) > 0$ satisfies

$$Q_T(x_{\mathrm{a}},t) + (2-\varepsilon(t))P_{\mathrm{f}}(t)B_T(x_{\mathrm{a}},t)R^{-1}(t)B_T^{\mathrm{T}}(x_{\mathrm{a}},t)P_{\mathrm{f}}(t) > \sigma I_{n_{\mathrm{a}}}, \tag{3.58}$$

then, according to the Lemma 3.2.4, $x_{\mathrm{a}}(t)$ is exponentially stable.

Secondly, consider the closed loop system (3.48) with the feedback controller (3.56). Since we have proved that the nominal closed-loop system (3.53) with the feedback control (3.56)

$$\dot{x}_{\mathrm{a}}(t) = A_K(t)x_{\mathrm{a}}(t), \quad A_K(t) = A_{\mathrm{a}}(t) + B_{\mathrm{a}}(t)R^{-1}B_T(x_{\mathrm{a}},t)P_{\mathrm{f}}(t),$$

is globally exponentially stable, it follows from Lemma 3.2.3 that for $Q_{\mathrm{b}}(t) \geq c_1 I_{n_{\mathrm{a}}} > 0,\ t \geq 0$, *there exists* $P_{\mathrm{b}} > 0$, *such that* $0 < c_2 I_{n_{\mathrm{a}}} < P_{\mathrm{b}} < c_3 I_{n_{\mathrm{a}}}$ *and satisfies the Backward Differential Riccati equation*

$$-\dot{P}_{\mathrm{b}}(t) = A_K^{\mathrm{T}}(t) P_{\mathrm{b}}(t) + P_{\mathrm{b}}(t) A_K(t) + Q_{\mathrm{b}}(t). \tag{3.59}$$

Now, differentiating the Lyapunov function candidate

$$V(x_{\mathrm{a}}) = x_{\mathrm{a}}^{\mathrm{T}}(t) P_{\mathrm{b}}(t) x_{\mathrm{a}}(t), \tag{3.60}$$

along the trajectories defined by (3.48) and (3.59), yields

$$\dot{V}(x_{\mathrm{a}}) = -x_{\mathrm{a}}^{\mathrm{T}}(t) Q_{\mathrm{b}}(t) x_{\mathrm{a}}(t) + 2 x_{\mathrm{a}}^{\mathrm{T}}(t) P_{\mathrm{b}}(t) \vartheta(t). \tag{3.61}$$

Next, we introduce the following inequalities

$$x_{\mathrm{a}}^{\mathrm{T}}(t) Q_{\mathrm{b}}(t) x_{\mathrm{a}}(t) \geq \frac{\lambda_{\min}(Q_{\mathrm{b}}(t))}{\lambda_{\max}(P_{\mathrm{b}}(t))} V(x_{\mathrm{a}}), \tag{3.62}$$

and

$$\begin{aligned} 2 x_{\mathrm{a}}^{\mathrm{T}}(t) P_{\mathrm{b}}(t) \vartheta(t) &\leq \lambda_{\max}(P_{\mathrm{b}}(t)) \left(\frac{\|x_{\mathrm{a}}(t)\|^2}{\rho(t)} + \rho(t) \|\vartheta(t)\|^2 \right) \\ &\leq \frac{\lambda_{\max}(P_{\mathrm{b}}(t))}{\rho(t) \lambda_{\min}(P_{\mathrm{b}}(t))} V(x_{\mathrm{a}}) + \rho(t) \lambda_{\max}(P_{\mathrm{b}}(t)) \|\vartheta(t)\|^2, \end{aligned} \tag{3.63}$$

where $\rho(t) \in \mathscr{C}^0,\ \rho(t) > \lambda_{\max}^2(P_{\mathrm{b}}(t)) / (\lambda_{\min}(Q_{\mathrm{b}}(t)) \lambda_{\min}(P_{\mathrm{b}}(t)))$ *is a bounded function so that*

$$\Delta(t) \triangleq \frac{\lambda_{\min}(Q_{\mathrm{b}}(t))}{\lambda_{\max}(P_{\mathrm{b}}(t))} - \frac{\lambda_{\max}(P_{\mathrm{b}}(t))}{\rho(t) \lambda_{\min}(P_{\mathrm{b}}(t))} > 0.$$

Finally, substituting (3.62) and (3.63) into (3.61), we obtain

$$\dot{V}(x_{\mathrm{a}}) \leq -\Delta(t) V(x_{\mathrm{a}}) + d(t),$$

where $d(t) \triangleq \rho(t) \lambda_{\max}(P_{\mathrm{b}}(t)) \|\vartheta(t)\|^2$. *Hence, whenever*

$$V(x_{\mathrm{a}}) \geq \frac{d(t)}{\Delta(t)} = V_0(t),$$

then $\dot{V}(x_{\mathrm{a}}) \leq 0$. *Since all the signals* $\vartheta(t),\ P_{\mathrm{b}}(t),\ Q_{\mathrm{b}}(t)$ *are uniformly bounded,* $\|x_{\mathrm{a}}(t)\|$ *and thus*

$\|x_{\mathrm{I}}(t)\|$ *are uniformly ultimately bounded*

$$\|x_{\mathrm{I}}(t)\|^2 \le \frac{V_0(t)}{\lambda_{\min}(P_{\mathrm{b}})} - \|\omega_u(t)\|^2.$$

Next, we need to show that the controller given by (3.56) and (3.57) is equivalent to the controller defined by (3.52) and (3.49). Using the following property of the transform matrix defined in (3.54)

$$T(x_{\mathrm{a}})x_{\mathrm{a}}(t) = -x_{\mathrm{a}}(t), \quad T^{-1}(x_{\mathrm{a}}) = T(x_{\mathrm{a}}) = T^{\mathrm{T}}(x_{\mathrm{a}}), \tag{3.64}$$

and substituting (3.55) into (3.56), the controller in (3.56) can be rewritten as follow

$$u(t) = R^{-1}(t)B_{\mathrm{a}}^T(t)T(x_{\mathrm{a}})P_{\mathrm{f}}(t)\big(-T(x_{\mathrm{a}})x_{\mathrm{a}}(t)\big) = -R^{-1}(t)B_{\mathrm{a}}^T(t)P(t)x_{\mathrm{a}}(t), \tag{3.65}$$

where

$$P(t) \triangleq T(x_{\mathrm{a}})P_{\mathrm{f}}(t)T(x_{\mathrm{a}}). \tag{3.66}$$

Since the system is assumed to be controllable, it is well known that for the giving pair $(Q(t),\, R(t))$ *there exits an unique optimal LQR control*

$$u_{\mathrm{b}}(t) = -R^{-1}(t)B_{\mathrm{a}}^T(t)P_{\mathrm{b}}(t)x_{\mathrm{a}}(t), \tag{3.67}$$

where $P_{\mathrm{b}}(t)$ *is computed backward if* $A_{\mathrm{a}}(t), B_{\mathrm{a}}(t)$ *are known ahead in time. Comparing (3.65) and (3.67), if* $u_{\mathrm{b}}(t) \equiv u(t)$*, then* $P_{\mathrm{b}}(t) \equiv P(t)$*. Hence, the assumption that there exists a positive definite bounded matrix* $P(t)$ *that satisfies (3.49) is verified.*

Multiplying both sides of the condition (3.58) by $T(x_{\mathrm{a}})$ *yields*

$$T(x_{\mathrm{a}})(T(x_{\mathrm{a}})Q(t)T(x_{\mathrm{a}}) + (2-\varepsilon(t))P_{\mathrm{f}}(t)T(x_{\mathrm{a}})B_{\mathrm{a}}(t)R^{-1}(t)B_{\mathrm{a}}^{\mathrm{T}}(t)T(x_{\mathrm{a}})P_{\mathrm{f}})T(x_{\mathrm{a}}) > \sigma T(x_{\mathrm{a}})T(x_{\mathrm{a}}), \tag{3.68}$$

Substituting (3.55) and (3.58) into (3.68) to obtain

$$Q(t) + (2-\varepsilon(t))P(t)B_{\mathrm{a}}(t)R^{-1}(t)B_{\mathrm{a}}^{\mathrm{T}}(t)P(t) > \sigma I_{n_{\mathrm{a}}},$$

which is the condition (3.51) given in the Proposition 3.4.1. Furthermore, differentiating $P(t)$

yields

$$\dot{P}(t)=\dot{T}(x_{\rm a})P_{\rm f}(t)T(x_{\rm a})+T(x_{\rm a})\dot{P}_{\rm f}(t)T(x_{\rm a})+T(x_{\rm a})P_{\rm f}(t)\dot{T}(x_{\rm a}). \tag{3.69}$$

In the following, we will simplify the notation by not explicitly specifying all of the dependencies. It follows from (3.55), (3.64) and (3.57) that

$$\begin{aligned} T(x_{\rm a})\dot{P}_{\rm f}(t)T(x_{\rm a}) &= T(-P_{\rm f}(-TA_{\rm a}T)-(-TA_{\rm a}T)^{\rm T}P_{\rm f}+TQ_{\rm f}T-\varepsilon(t)P_{\rm f}(TB_{\rm a})R^{-1}(B_{\rm a}^{\rm T}T)P_{\rm f})T \\ &= P(t)A_{\rm a}(t)+A_{\rm a}^{\rm T}(t)P(t)+Q(t)-\varepsilon(t)P(t)B_{\rm a}(t)R^{-1}(t)B_{\rm a}^{\rm T}(t)P(t), \end{aligned} \tag{3.70}$$

Moreover, it follows from (3.64) that

$$\begin{aligned} T(x_{\rm a})P_{\rm f}(t)\dot{T}(x_{\rm a})+\dot{T}(x_{\rm a})P_{\rm f}(t)T(x_{\rm a}) &= T(x_{\rm a})P_{\rm f}(t)T(x_{\rm a})T(x_{\rm a})\dot{T}(x_{\rm a})+\dot{T}(x_{\rm a})T(x_{\rm a})T(x_{\rm a})P_{\rm f}(t)T(x_{\rm a}) \\ &= P(t)A_{\rm b}(t)+A_{\rm b}^{\rm T}(t)P(t), \end{aligned} \tag{3.71}$$

where $A_{\rm b}(t)\triangleq T(x_{\rm a})\dot{T}(x_{\rm a})=(\dot{T}(x_{\rm a})T(x_{\rm a}))^{\rm T}$*. It can be verified that*

$$A_{\rm b}(t)=2({x_{\rm a}^{\dagger}}^{\rm T}(t)\dot{x}_{\rm a}^{\rm T}(t)-\dot{x}_{\rm a}(t)x_{\rm a}^{\dagger}(t)). \tag{3.72}$$

Hence, substituting (3.70), (3.71), (3.72) into (3.69) to obtain the updated law of $P(t)$ *defined in (3.49)*

$$\dot{P}(t)=P(t)(A_{\rm a}(t)+A_{\rm b}(t))+(A_{\rm a}(t)+A_{\rm b}(t))^{\rm T}P(t)+Q(t)-\varepsilon(t)P(t)B_{\rm a}(t)R^{-1}(t)B_{\rm a}^{\rm T}(t)P(t),$$

where $Q(t),\ R(t)$ *and* $\varepsilon(t)$ *satisfy the condition (3.51), which concludes the proof.* □

Remark 3.4.1 *It follows from (3.44) and (3.47) that*

$$e_{\rm r}(s)=\frac{e_2(s)}{sI_p+k_{\rm p}I_p+K_{\rm r}}=\frac{sI_p+\Lambda}{sI_{\rm p}+k_{\rm p}I_p+K_{\rm r}}\Omega^{-1}x_{\rm I}(s)=H(s)\Omega^{-1}x_{\rm I}(s), \tag{3.73}$$

where $H(s)\triangleq(sI_p+\Lambda)/(sI_{\rm p}+k_{\rm p}I_p+K_{\rm r})$*. Since* $H(s)$ *is stable proper, it follows from lemma (3.2.1) that*

$$\|e_{\rm r}(t)\|_{\mathscr{L}_\infty}\leq\mathscr{L}_1H(s)\|\Omega^{-1}x_{\rm I}(t)\|_{\mathscr{L}_\infty}, \tag{3.74}$$

which proves that $e_{\mathrm{r}}(t)$ is uniformly ultimately bounded. If $K_{\mathrm{r}} = \mathrm{diag}([K_{\mathrm{r}1},...,K_{\mathrm{r}p}])$, $\Lambda = \mathrm{diag}([\Lambda_1,...,\Lambda_p])$, and $\Omega = \mathrm{diag}([\Omega_1,...,\Omega_p])$, it follows from (3.73) that

$$\|e_{\mathrm{r}i}(t)\|_{\mathscr{L}_\infty} \leq \Omega_i^{-1}\mathscr{L}_1 H_i(s)\|x_{\mathrm{I}i}(t)\|_{\mathscr{L}_\infty},\ H_i(s) = \frac{s+\Lambda_i}{s+k_{\mathrm{p}}+K_{\mathrm{r}i}}, \tag{3.75}$$

where $i = 1,\ldots,p$. When $\Lambda = k_{\mathrm{p}}I_p + K_{\mathrm{r}}$, then $e_{\mathrm{r}}(t) = \Omega^{-1}x_{\mathrm{I}}(t)$.

3.4.2 Actuator Amplitude and Rate Saturation constraints

In order to guarantee asymptotic stability of the closed-loop tracking error dynamics in the face of amplitude and rate saturation constraints, an approach to modify the reference signal based on [50] is provided in this section. Let $u_{\max} > 0$ be the maximum control magnitude, $\Delta u_{\max} > 0$ be the maximum change of $u(t)$ in a time interval Δt, and $u_{\mathrm{d}}(t)$ be the desired control signal obtained by (3.56). The saturation constraints $|u_i(t)| \leq u_{\max i}$ and $|u(t) - u(t-\Delta t)| \leq \Delta u_{\max}$ are guaranteed by

$$u(t) = \mathrm{Sat}(\hat{u}(t), u_{\max}), \tag{3.76a}$$

$$\hat{u}_i(t) = u_i(t-\Delta t) + \mathrm{Sat}(u_{\mathrm{d}i}(t) - u_i(t-\Delta t), \Delta u_{\max}), \tag{3.76b}$$

where $u_i(t)$ and $u_{\mathrm{d}i}(t)$ are the i^{th} component of $u(t)$ and $u_{\mathrm{d}}(t)$, $i = 1,\ldots,m$, respectively.

By partitioning the matrix $K_{\mathrm{f}}(t) = [K_{\omega_u}(t)\ \ K_{\mathrm{I}}(t)] \in \mathbb{R}^{m\times n_a}$, where $K_{\omega_u}(t) \in \mathbb{R}^{m\times nm}$ and $K_{\mathrm{I}}(t) \in \mathbb{R}^{m\times p}$, the desired control signal given in (3.52) can be rewritten as

$$u_{\mathrm{d}}(t) = K_{\mathrm{f}}(t)x_{\mathrm{a}}(t) = K_{\omega_u}(t)\omega_u(t) + K_{\mathrm{I}}(t)x_{\mathrm{I}}(t). \tag{3.77}$$

Eq.(3.77) indicates that when $u_{\mathrm{d}}(t)$ violates the saturation constrains, the error $x_{\mathrm{I}}(t)$ can be modified so that $u_{\mathrm{d}}(t)$ is no longer saturated. Using this approach, the control law needs not be altered and the saturation constraints can still be satisfied. It follows from (3.47) that the reference signal needs to be adjusted to modify $\varphi_{\mathrm{d}}(t)$ and $x_{\mathrm{I}}(t)$. For ease of presentation, 2 cases are considered

i) when all control inputs have relative degree 1 ($r_{ij} = 1$).

ii) when no control inputs have relative degree 1 ($r_{ij} \geq 2,\ i = 1,\ldots p,\ j = 1,\ldots,m$).

It is easy to combine both methods if the system has both types by separating the control indexes. For the following derivations, define the variables

$$P_{\mathrm{a}}(t) \triangleq P(t)A_{\mathrm{a}}(t) + A_{\mathrm{a}}^{\mathrm{T}}(t)P(t) - \varepsilon(t)P(t)B_{\mathrm{a}}(t)R^{-1}(t)B_{\mathrm{a}}^{\mathrm{T}}(t)P(t), \tag{3.78}$$

$$P_{\mathrm{b}}(t) \triangleq P(t)A_{\mathrm{b}}(t) + A_{\mathrm{b}}(t)^{\mathrm{T}}P(t). \tag{3.79}$$

It can be verified that

$$\dot{P}(t) = P_{\mathrm{a}}(t) + Q(t) + P_{\mathrm{b}}(t). \tag{3.80}$$

Theorem 3.4.1 *Consider the linear system (3.2), the predictor (3.21), the reference system (3.3), and the controller (3.56). For a given desired reference input $r_{\mathrm{d}}(t)$, consider the modified reference dynamics $\dot{y}_{\mathrm{m}}(t)$ along with the modified reference input $r(t)$*

$$\dot{y}_{\mathrm{m}}(t) = \bar{\varphi}_{\mathrm{d}}(t) + K_r e_r(t) + \eta^{\mathrm{T}}(t)\hat{\alpha}(t) - k_{\mathrm{p}}y_{\mathrm{m}}(t), \quad t \geq 0, \tag{3.81a}$$

$$r(t) = B_{\mathrm{m}}^{-1}(\dot{y}_{\mathrm{m}}(t) - A_{\mathrm{m}}(t)y_{\mathrm{m}}(t)), \tag{3.81b}$$

where $\bar{\varphi}_{\mathrm{d}}(t)$ is the modified signal of $\varphi_{\mathrm{d}}(t)$ due to the saturation of $u(t)$ defined in (3.76).
Case 1: *When all the relative degrees $r_{ij} = 1,\ i = 1, \dots p,\ j = 1, \dots, m$*

$$\bar{\varphi}_{\mathrm{d}}(t) = C_u(t)\omega_u(t) + D_u(t)u(t). \tag{3.82}$$

Case 2: *When all the relative degrees $r_{ij} \geq 2,\ i = 1, \dots p,\ j = 1, \dots, m$*

$$\bar{\varphi}_{\mathrm{d}}(t) = \varphi(t) - \Omega^{-1}(\dot{\bar{x}}_{\mathrm{I}}(t) + \Lambda\bar{x}_{\mathrm{I}}(t)), \tag{3.83}$$

$$\bar{x}_{\mathrm{I}}(t) = K_{\mathrm{I}}^{\dagger}(t)(u(t) - K_{\omega_u}(t)\omega_u(t)), \tag{3.84}$$

$$\dot{\bar{x}}_{\mathrm{I}}(t) = -S_{\mathrm{I}}^{\dagger}(t)(F(t) + S_{\omega_u}(t)\dot{\omega}_u(t)), \tag{3.85}$$

where $F(t) \in \mathbb{R}^m$ and $S(t) \triangleq [S_{\omega_u}\ S_I] \in \mathbb{R}^{m \times n_{\mathrm{a}}}$, $S_{\omega_u} \in \mathbb{R}^{m \times nm}$, $S_{\mathrm{I}} \in \mathbb{R}^{m \times p}$ are defined as

$$F(t) \triangleq \dot{R}^{-1}(t)B_{\mathrm{a}}^{\mathrm{T}}(t)P(t)x_{\mathrm{a}}(t) + R^{-1}(t)B_{\mathrm{a}}^{\mathrm{T}}(t)(P_{\mathrm{a}}(t) + Q(t))x_{\mathrm{a}}(t), \tag{3.86}$$

$$S(t) \triangleq R^{-1}(t)B_{\mathrm{a}}^{\mathrm{T}}(t)(2(P(t)x_{\mathrm{a}}(t)x_{\mathrm{a}}^{\dagger}(t) - x_{\mathrm{a}}(t)x_{\mathrm{a}}^{\dagger}(t)P(t)) - P(t) + 2x_{\mathrm{a}}^{\dagger}(t)P(t)x_{\mathrm{a}}(t)I_{n_{\mathrm{a}}}), \tag{3.87}$$

Then the control law (3.56) along with the saturation (3.76), based on the predictor (3.21), and the *reference system given by (3.3) and (3.81), guarantees that*

i) *The tracking error* $e(t) \triangleq y - y_{\mathrm{m}}(t)$ *are uniformly ultimately bounded.*

ii) $|u_i(t)| \leq u_{\max i}$ *and* $|u(t) - u(t-\Delta t)| \leq \Delta u_{\max},\ i = 1, \ldots, m.$

Proof *Statement i) is a direct consequence of Theorem 3.3.1 or Corollary 3.3.1 and Proposition 3.4.1 with* $r(t) = r_{\mathrm{d}}(t)$*, if the actuator amplitude and rate saturations constraints are not violated. To prove ii), for **Case 1**, it follows from (3.46b) and (3.47) by setting* $e_2(t) = 0$*, we obtain* $\dot{x}_{\mathrm{I}} = -\Lambda x_{\mathrm{I}}(t)$ *and*

$$\bar{\varphi}_{\mathrm{d}}(t) = \bar{\varphi}(t) = C_u(t)\omega_u(t) + D_u u(t),$$

which guarantees that $x_{\mathrm{I}}(t)$ *is exponentially stable until the control is no longer saturated.*
*For **Case 2**, note that when the control magnitude is saturated, the control rate* $\dot{u}(t) = 0$*. Therefore, it follows from (3.52) and (3.80) that*

$$\dot{u}(t) = -\dot{R}^{-1}(t)B_{\mathrm{a}}^{\mathrm{T}}P(t)x_{\mathrm{a}}(t) - R^{-1}(t)B_{\mathrm{a}}^{\mathrm{T}}((P_{\mathrm{a}}(t) + Q(t) + P_{\mathrm{b}}(t))x_{\mathrm{a}}(t) + P(t)\dot{x}_{\mathrm{a}}(t)) = 0. \tag{3.88}$$

where $P_{\mathrm{a}}(t)$ *and* $P_{\mathrm{b}}(t)$ *are defined in (3.78) and (3.79). In the following, we will simplify the notation by not explicitly specifying all of the dependencies. It follows from (3.50) and (3.79) that*

$$\begin{aligned} P_{\mathrm{b}}x_{\mathrm{a}} &= 2(P(x_{\mathrm{a}}^{\dagger\,\mathrm{T}}\dot{x}_{\mathrm{a}}^{\mathrm{T}} - \dot{x}_{\mathrm{a}}x_{\mathrm{a}}^{\dagger}) + (\dot{x}_{\mathrm{a}}x_{\mathrm{a}}^{\dagger} - x_{\mathrm{a}}^{\dagger\,\mathrm{T}}\dot{x}_{\mathrm{a}}^{\mathrm{T}})P)x_{\mathrm{a}} = 2(P(x_{\mathrm{a}}^{\dagger\,\mathrm{T}}x_{\mathrm{a}}^{\mathrm{T}}\dot{x}_{\mathrm{a}} - \dot{x}_{\mathrm{a}}) + \dot{x}_{\mathrm{a}}x_{\mathrm{a}}^{\dagger}Px_{\mathrm{a}} - x_{\mathrm{a}}^{\dagger\,\mathrm{T}}x_{\mathrm{a}}^{\mathrm{T}}P\dot{x}_{\mathrm{a}}) \\ &= (2(Px_{\mathrm{a}}^{\dagger\,\mathrm{T}}x_{\mathrm{a}}^{\mathrm{T}} - x_{\mathrm{a}}^{\dagger\,\mathrm{T}}x_{\mathrm{a}}^{\mathrm{T}}P) - 2P + 2x_{\mathrm{a}}^{\dagger}Px_{\mathrm{a}}I_{n_{\mathrm{a}}})\dot{x}_{\mathrm{a}} = (2(Px_{\mathrm{a}}x_{\mathrm{a}}^{\dagger} - x_{\mathrm{a}}x_{\mathrm{a}}^{\dagger}P) - 2P + 2x_{\mathrm{a}}^{\dagger}Px_{\mathrm{a}}I_{n_{\mathrm{a}}})\dot{x}_{\mathrm{a}}. \end{aligned} \tag{3.89}$$

Therefore, from (3.87) and (3.89) we obtain

$$R^{-1}(t)B_{\mathrm{a}}^{\mathrm{T}}(t)(P_{\mathrm{b}}(t)x_{\mathrm{a}}(t) + P(t)\dot{x}_{\mathrm{a}}(t)) = S(t)\dot{x}_{\mathrm{a}}(t) = S_u(t)\dot{\omega}_u(t) + S_I(t)\dot{\bar{x}}_I(t), \tag{3.90}$$

It follows from (3.86) and (3.90) that (3.88) can be rewritten as

$$F(t) + S_u(t)\dot{\omega}_u(t) + S_I(t)\dot{\bar{x}}_I(t) = 0. \tag{3.91}$$

Therefore, (3.85), (3.84) *and (3.83) are directly obtained from (3.91),* (3.77) *and (3.47) respectively. Finally, (3.81) is inferred from (3.47) and (3.45), which concludes the proof.* □

3.5 Implementation

Figure 3.1 presents the control framework, and the Fig 3.2 and the Fig 3.3 illustrate the predictor and the controller structures respectively. The adaptive laws in Theorem 3.3.1 and Corollary 3.3.1 can be rewritten in a general form as follow

$$\dot{\hat{\alpha}}(t) = P_\alpha\left(\eta_y(t)\Gamma^{\mathrm{T}} e_{\mathrm{p}}(t) + M_\alpha(t)\right), \tag{3.92a}$$

$$\dot{\hat{\beta}}(t) = P_\beta\left(\eta_u(t) e_{\mathrm{p}}^{\mathrm{T}}(t)\Gamma + M_\beta(t)\right), \tag{3.92b}$$

where $M_\alpha(t)$ and $M_\beta(t)$ are the modification terms given in Table 3.1

Table 3.1: Modification Terms of the Adaptive Laws in Theorem 3.3.1

Theorem 3.3.1	Corollary 3.3.1
$M_\alpha(t) = \sigma(t)\omega_y(t)\varepsilon(t)$,	$M_\alpha(t) = \int_{t-T}^{t} \sigma(t,\tau)\omega_y(\tau)\varepsilon(t,\tau)\mathrm{d}\tau$,
$M_\beta(t) = \sigma(t)\omega_u(t)\varepsilon^{\mathrm{T}}(t)$,	$M_\beta(t) = \int_{t-T}^{t} \sigma(t,\tau)\omega_u(\tau)\varepsilon^{\mathrm{T}}(t,\tau)\mathrm{d}\tau$,

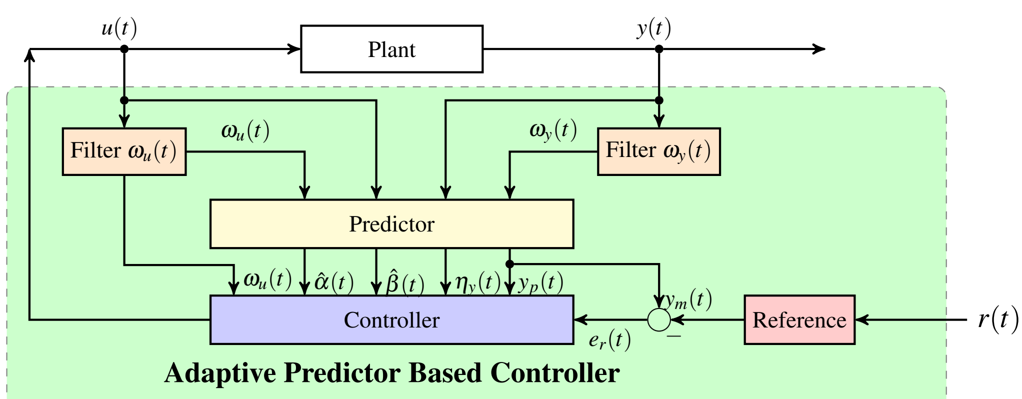

Figure 3.1: Adaptive Predictor based controller for linear systems block diagram

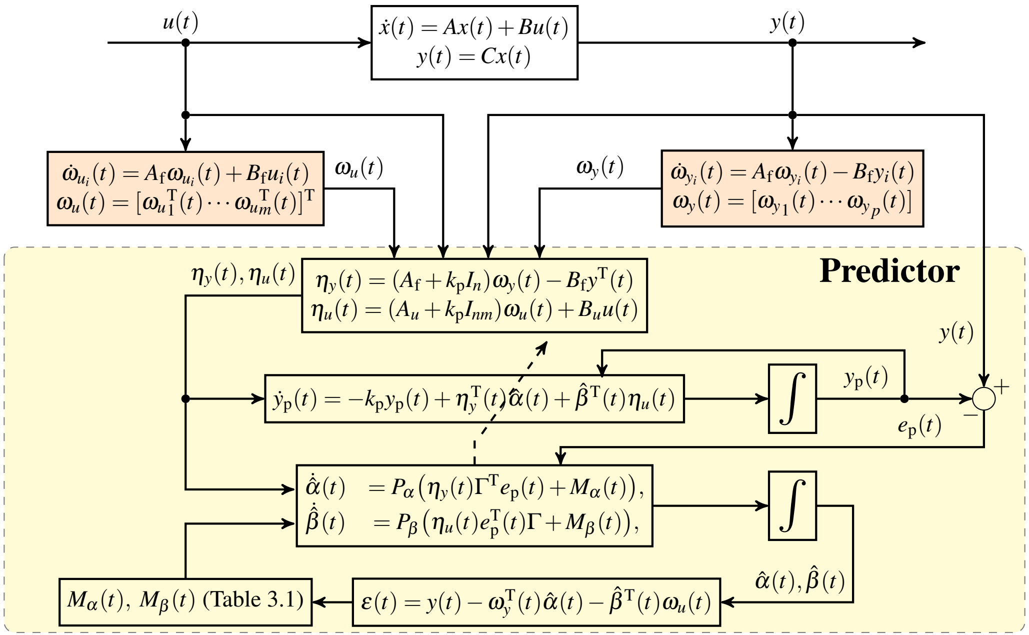

Figure 3.2: Predictor's structure for linear systems

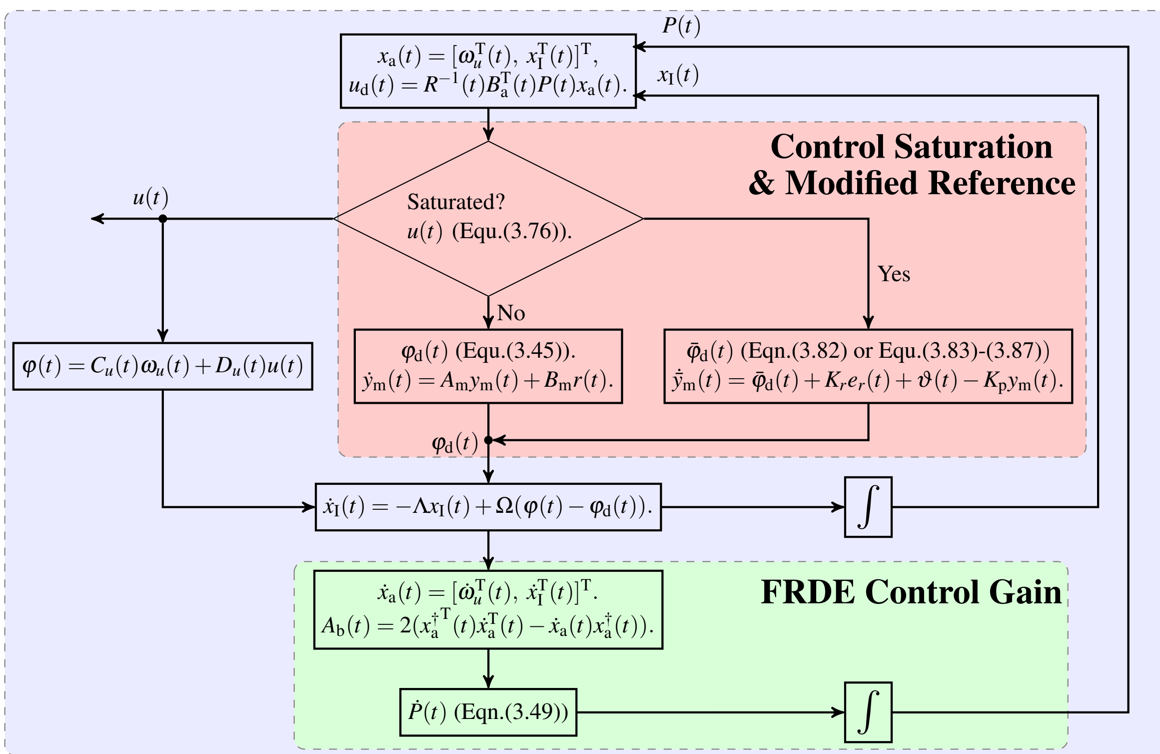

Figure 3.3: Controller's structure

3.6 Simulation

Example 3.6.1 *Consider designing a controller for the following LTI system with unknown parameters and unmeasured state*

$$\dot{x}(t) = \begin{bmatrix} -50 & 2 & 12 \\ -80 & -12 & 28 \\ -20 & -8 & 2 \end{bmatrix} x(t) + \begin{bmatrix} 0 & 0 \\ 0 & 2 \\ 2 & 3 \end{bmatrix} u(t), \quad x(0) = 0_3,$$
$$y(t) = \begin{bmatrix} 1 & 0 & 0 \\ 0 & 1 & 0 \end{bmatrix} x(t),$$

to track the reference system (3.3) with parameters $A_m = -2I_2,\ B_m = 2I_2$ *and* $r_{\mathrm{d}}(t) = [-5\sin(4t+\pi/4)\ \ 2\sin(3t)]^{\mathrm{T}}$. *We only know the relative degree* $r_{11} = r_{12} = 2;\ r_{21} = 2,\ r_{22} = 1$.

To design the predictor, we chose a 3^{nd} *order filter defined in (3.10) with parameters*

$$A_{\mathrm{f}} = \begin{bmatrix} 0 & 1 & 0 \\ 0 & 0 & 1 \\ -3375 & -675 & -45 \end{bmatrix}, \quad B_{\mathrm{f}} = \begin{bmatrix} 0 \\ 0 \\ 1 \end{bmatrix}.$$

The predictor parameters are $k_{\mathrm{p}} = 10,\ P_\alpha = 10^2 I_3,\ P_\beta = \mathrm{diag}([10^3 I_5,\ 0.5])$. *The delay time* $T = 1(s)$, $\sigma(\tau)$ *is given in (3.42) with* $\kappa_1 = 1, \kappa_2 = 0$. *The initial conditions are* $y(0) = y_{\mathrm{p}}(0) = 0_2,\ y_{\mathrm{m}}(0) = [0.5\ 0.2]^{\mathrm{T}},\ \omega_y(0) = \omega_u(0) = 0_6,\ \hat{\alpha}_{\mathrm{s}}(0) = [2400\ 500\ 12]^{\mathrm{T}},\ \hat{\beta}_{11}(0) = [380\ 30\ 0]^{\mathrm{T}},\ \hat{\beta}_{12}(0) = [450\ 50\ 0]^{\mathrm{T}},\ \hat{\beta}_{21}(0) = [900\ 60\ 0]^{\mathrm{T}},\ \hat{\beta}_{22}(0) = [1500\ 160\ 1.3]^{\mathrm{T}}$.

The augmented system has $\Lambda = 0_{2\times 2}$ *and* $\Omega = \mathrm{diag}([50,\ 80])$. *The FDRE controller parameters are* $K_{\mathrm{r}} = 10I_2,\ Q(t) = \mathrm{diag}([I_6,\ 200,\ 200]) - 2P(t),\ R = I_2,\ \varepsilon = 12$ *and* $P_0 = 10^{-5} I_8$. *The saturation parameters are* $u_{\max} = 100$ *and* $\Delta u_{\max} = 2$. *Figure (3.4) illustrates the tracking result and the control effort. Note that* $\hat{\alpha}_s^{\mathrm{T}}(t)\omega_y(t) + \hat{\beta}^{\mathrm{T}}(t)\omega_u(t) \to y(t)$ *and* $y(t),\ y_{\mathrm{p}}(t)$ *all converge to* $y_{\mathrm{m}}(t)$ *as* $t \to \infty$.

Example 3.6.2 *Consider the 3D Quanser helicopter, whose dynamics are described by ([65])*

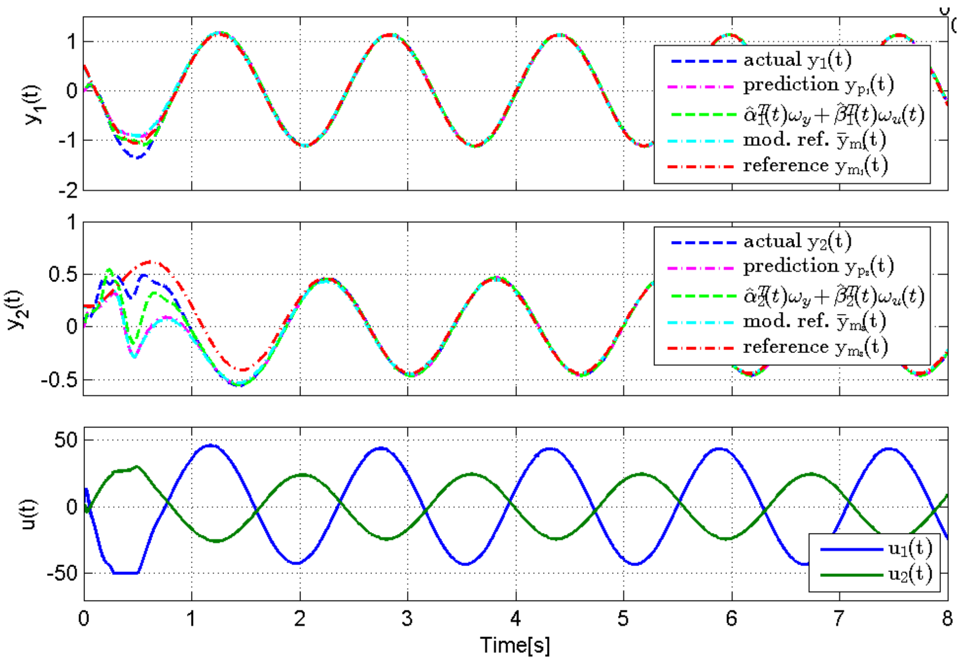

Figure 3.4: The system output, the predictor and the reference trajectories (top and middle) and the control effort (bottom) using the FDRE controller

$$\dot{\eta}(t) = J(\eta(t))\nu(t), \qquad \eta(0) = \eta_0, \quad t \geq 0 \tag{3.93}$$

$$\dot{\nu}(t) = \Theta_1 \varphi(\eta(t)) + \Theta_2 \tau(t), \qquad \nu(0) = \nu_0, \tag{3.94}$$

where $\eta(t) \triangleq [\phi(t) \;\; \theta(t) \;\; \psi(t)]^{\mathrm{T}} \in \mathbb{R}^3$ *is the measured output where* $\phi(t),\ \theta(t),\ \psi(t)$ *are the roll, elevation and the travel angles respectively,* $\nu(t) \in \mathbb{R}^3$ *are the unmeasured states, and* $\tau(t) \in \mathbb{R}^2$ *is the control input applied to the system, and*

$$J(\eta) \triangleq \begin{bmatrix} 1 & \tan(\theta)\sin(\phi) & \tan(\theta)\cos(\phi) \\ 0 & \cos(\phi) & -\sin(\phi) \\ 0 & \sin(\phi)/\cos(\theta) & \cos(\phi)/\cos(\theta) \end{bmatrix}, \qquad \phi(\eta) \triangleq \begin{bmatrix} \cos(\theta)\cos(\phi) \\ -\cos(\theta)\sin(\phi) \end{bmatrix},$$

$$\Theta_1 = \begin{bmatrix} -2.6828 & 3.2966 \\ -9.8298 & -9.9455 \\ 0 & -20 \end{bmatrix}, \qquad \Theta_2 = \frac{1}{2}\begin{bmatrix} 0.25 & -0.25 \\ 0.575 & 0.575 \\ 0 & 0 \end{bmatrix}$$

Note that system dynamics and parameters are only used to simulate the nonlinear plant. We only know the relative degree $r_{ij} = 2,\ i = 1,2,\ j = 1,2$. *When the control is set at* $\tau^* = [27.8265 \;\; 6.3641]^{\mathrm{T}}$, *the system stays at the equilibrium point* $x^* = [\eta^{\mathrm{T}}(t)\ \nu^{\mathrm{T}}(t)]^{\mathrm{T}} = 0_6$.

In order to apply the proposed controller, we ***assume*** *that the system dynamics can be approximated by a linear model in a small neighbor hood of* x^*

$$\begin{aligned}\dot{x}(t) &= Ax(t) + Bu(t), \quad x(0) = x_0, \quad t \geq 0,\\ y(t) &= Cx(t)\end{aligned}$$

where $A \in \mathbb{R}^{6\times 6}$, $B \in \mathbb{R}^{6\times 2}$ *and* $C \in \mathbb{R}^{3\times 6}$ *are unknown constant matrices, and* $u(t) = \tau(t) - \tau^* \in \mathbb{R}^2$ *is the control signal.*

The autoregressive vectors are constructed using a 6^{th} *order filter defined in (3.10) with parameters*

$$A_{\mathrm{f}} \triangleq \begin{bmatrix} 0_5 & & I_5 \\ -\lambda_5 & \dots & -\lambda_0 \end{bmatrix} \in \mathbb{R}^{6\times 6}, \quad B_{\mathrm{f}} \triangleq \begin{bmatrix} 0_5 \\ 1 \end{bmatrix} \in \mathbb{R}^{6},$$

where $\det(sI_n - A_{\mathrm{f}}) = s^n + \lambda_5 s^{n-1} + \dots + \lambda_1 s + \lambda_0 = (s+5)^6$. *The predictor parameters are* $k_{\mathrm{p}} = 10$, $P_\alpha = I_6, P_\beta = 10I_{12}$. *The delay time* $T = 1(s)$, $\sigma(\tau)$ *is given in (3.42) with* $\kappa_1 = 1, \kappa_2 = 0$. *The initial conditions are* $y_0 = \frac{\pi}{180}[2\ -27\ 0]^{\mathrm{T}}$, $y_p(0) = \frac{\pi}{180}[2\ -20\ 0]^{\mathrm{T}}$ *and*

$$\hat{\alpha}^{\mathrm{T}}(0) = [-\lambda_0 \dots - \lambda_5] = [-15625\ -18750\ -9375\ -2500\ -375\ -30],$$

$$\hat{\beta}^{\mathrm{T}}(0) = \begin{bmatrix} 0 & 0 & 0 & 0 & 0.2 & 0 & 0 & 0 & 0 & 0 & -0.2 & 0 \\ 0 & 0 & 2 & 0 & 0.2 & 0 & 0 & 0 & -0.2 & 0 & 0.2 & 0 \\ 0 & 0 & 2 & 0 & 0 & 0 & 0 & 0 & -2 & 0 & 0 & 0 \end{bmatrix}.$$

The projector operator boundary for $\hat{\alpha}(t)$ *and* $\hat{\beta}(t)$ *are setup at* $\hat{\alpha}_{\mathrm{max,min}} = \hat{\alpha}(0) \pm 0.2\hat{\alpha}(0)$ *and* $\hat{\beta}_{\mathrm{max,min}} = \hat{\beta}(0) \pm 0.5(\hat{\beta}(0) + 0.1I_{3\times 12}$.

First, we aim to control only the pitch and elevation angle $[\phi(t)\ \theta(t)]^{\mathrm{T}}$ *of the helicopter to track the output* $y_{\mathrm{m}} = [\phi_{\mathrm{d}}(t)\ \theta_{\mathrm{d}}(t)]^{\mathrm{T}}$ *of the reference system (3.3) with* $A_m = -I_2, B_m = I_2$ *and the reference signal* $r_{\mathrm{d}}(t) = \frac{\pi}{180}[10\sin(0.4\pi t)\ \ 15\sin(0.2\pi t)]^{\mathrm{T}}$.

The augmented system has $\Lambda = \mathrm{diag}([10,\ 10])$ *and* $\Omega = \mathrm{diag}([1000,\ 500])$. *The FDRE controller parameters are* $K_{\mathrm{r}} = -5I_2$, $Q(t) = \mathrm{diag}([I_{12},\ 50,\ 50]) - P(t)$, $R = 0.5I_2$, $\varepsilon = 20$ *and* $P_0 = I_{14}$.

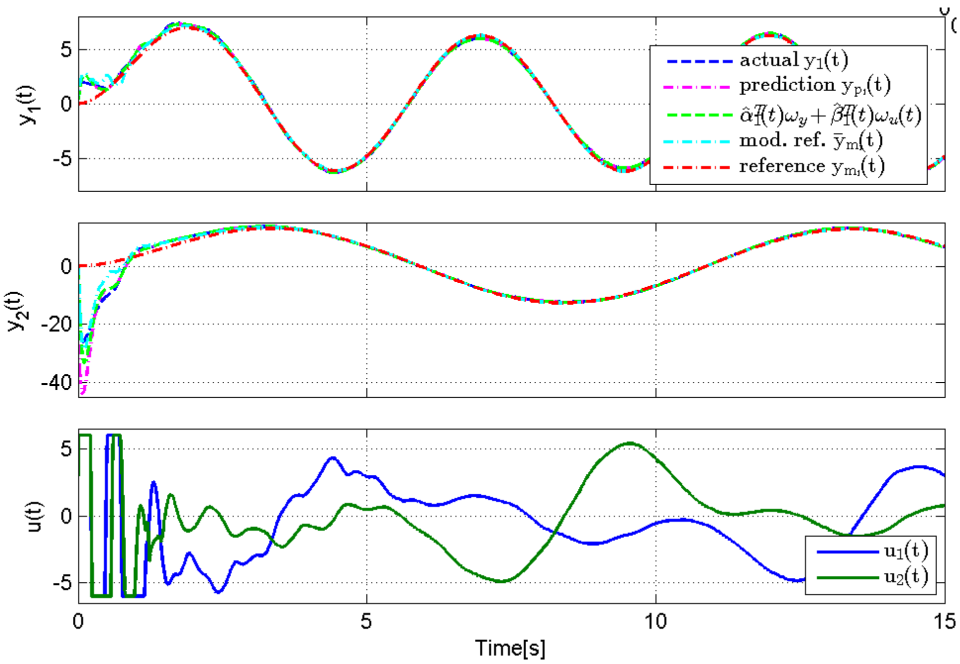

Figure 3.5: The system output $y(t)$,the predictor output $y_{\mathrm{p}}(t)$, the modified reference $\bar{y}_{\mathrm{m}}(t)$ and the reference signals $y_{\mathrm{m}}(t)$ (top and middle) and the control effort (bottom) using the FDRE controller

The saturation parameters are $u_{\max} = 6$ *and* $\Delta u_{\max} = 1$. *Figure (3.5) illustrates the tracking result and the control effort applied to the nonlinear model (3.93). In this example, we control two outputs by using two actuators; since the system is square, we can achieve the exact tracking result for both outputs simultaneously.*

Secondly, we attempt to control the system's output to track the desired trajectory $y_{\mathrm{m}} = [\phi_{\mathrm{d}}(t)\ \theta_{\mathrm{d}}(t)\ \psi_{\mathrm{d}}(t)]^{\mathrm{T}}$, *using the reference system (3.3) with* $A_m = -I_3, B_m = I_3$ *and*

$$r_{\mathrm{d}}(t) = \frac{\pi}{180}[0\ 10\sin(0.08\pi t)\ 90\sin(0.12\pi t)]^{\mathrm{T}}.$$

For this situation, we aim to control 3 outputs of the system simultaneously by using only two actuators, the system is an under-actuated, which implies that there is a constraint between 3 feasible outputs $[\phi_{\mathrm{d}}(t)\ \theta_{\mathrm{d}}(t)\ \psi_{\mathrm{d}}(t)]$. *Therefore, an arbitrary selection of the desired outputs is not necessarily achievable. In order to handle such constraint, different entries in the weight matrices* Ω *and* $Q(t)$ *are selected depending on each output's priority.*

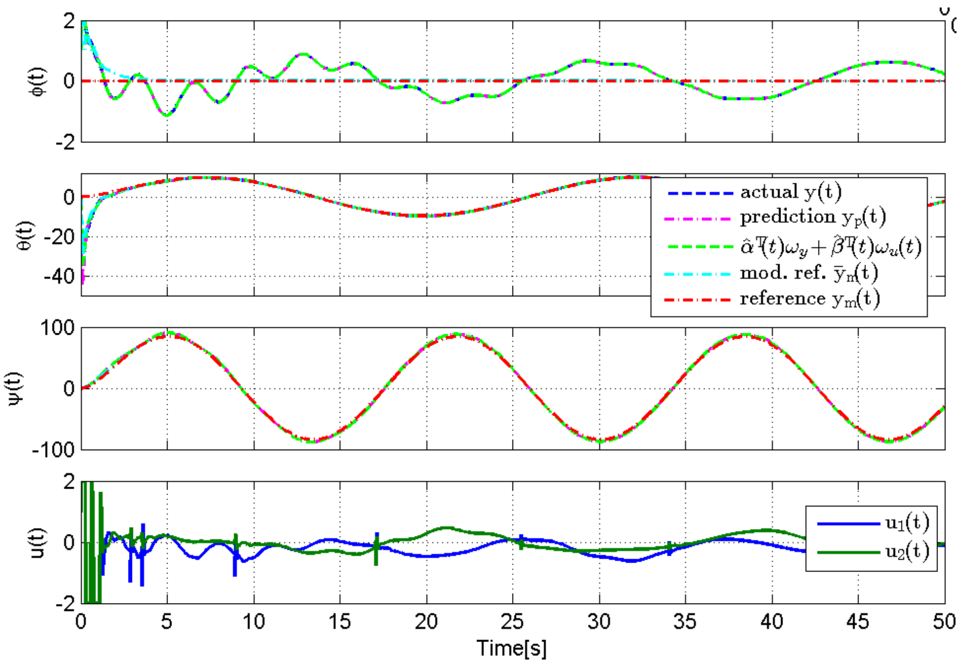

Figure 3.6: The system output $y(t)$, the predictor output $y_{\mathrm{p}}(t)$, the modified reference $\bar{y}_{\mathrm{m}}(t)$ and the reference signals $y_{\mathrm{m}}(t)$ (top and middle) and the control effort (bottom) using the FDRE controller.

The controller is designed by choosing the parameters as follow. The delay time $T = 0.05(s)$*,* $\sigma(\tau)$ *is given in (3.42) with* $\kappa_1 = 1, \kappa_2 = -5$*. The augmented system has* $\Lambda = \mathrm{diag}([10\ 10\ 18])$*. The FDRE controller parameters are* $K_{\mathrm{r}} = -5I_3$*,* $Q(t) = \mathrm{diag}([I_{12},\ 50,\ 50,\ 100]) - 15P(t)$*,* $R = I_2$*,* $\varepsilon = 12$ *and* $P_0 = I_{15}$*. The saturation parameters are* $u_{\max} = 2$ *and* $\Delta u_{\max} = 1$*. Figure 3.6 illustrates the tracking result and the control effort applied to the nonlinear system.*

Note that although the plant, the predictor and the reference started at different initial conditions, they all converge at the end. For the second case, worth noting is that the tracking performance of the pitch angle $\phi(t)$ *is not as good as that of the other states. This is due to our particular choice of weights in matrices* Ω *and* $Q(t)$*, which penalizes the tracking error of* $\theta(t)$ *and* $\psi(t)$ *more than the tracking error of* $\phi(t)$*. In the mean time, the tracking error of roll* $\phi_{\mathrm{d}}(t)$ *is small and bounded, with the maximum error is about* 1^o*.*

3.7 Experimental Setup and Result

The controller performance is further studied by real time implementation on the Quanser 3-DOF helicopter depicted in Fig 3.7.

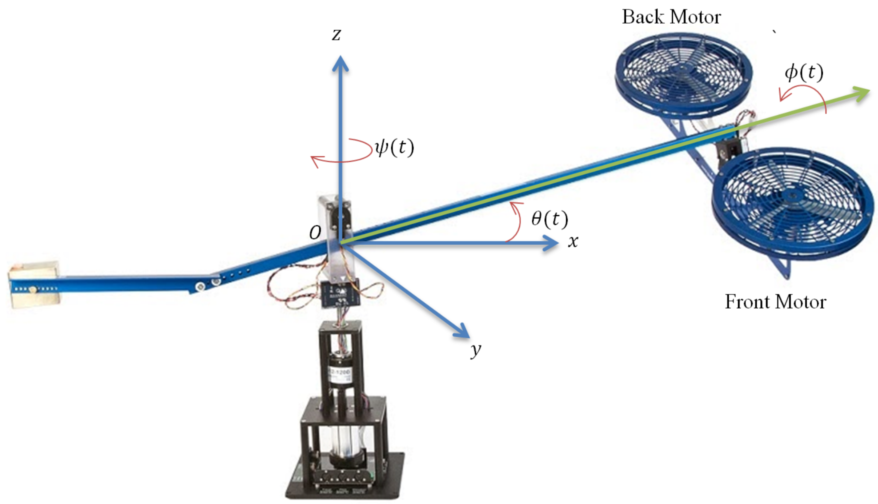

Figure 3.7: The 3D helicopter prototype

The helicopter body is mounted at the end of an arm and is free to rotate around the arm (pitch), and the arm is free to rotate around the y-axis (elevation) and z-axis (travel) at the pivot point O. Two DC motors with attached propellers generate driving forces for the helicopter. Hence, the system has 3 outputs, i.e. the pitch $\phi(t)$, the elevation $\theta(t)$, the travel $\psi(t)$ angles, all of which are measured via optical encoders, and has 2 control inputs $v(t) = [v_\mathrm{f}(t),\ v_\mathrm{b}(t)]^\mathrm{T}$ where $v_\mathrm{f},\ v_\mathrm{b}$ are the voltages applied to the front and the back motor respectively. The controller is implemented using Simulink running on a digital computer with a Pentium(R) D 3.4Ghz CPU, and the encoder sampling frequency is 1kHz.

The system model is unknown, but we assume that it has a minimal representation consisting of 6 states ($n = 6$), and relative degrees $r_{ij} = 2,\ i = 1,3,\ j = 1,2$. When the control is set at $v^* = [12.5\ 12.5](Vol)$, the system stays at the equilibrium point $x^* = 0_6$. We make the same assumptions and use the same filters as in Example 5.2.

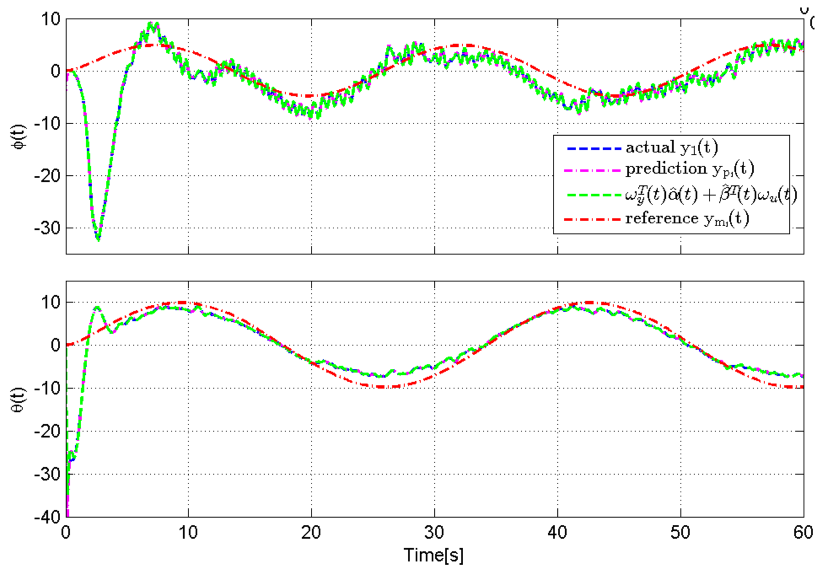

Figure 3.8: The time evolution of $y(t)$, $y_{\mathrm{p}}(t)$, and $y_{\mathrm{m}}(t)$ for the parameters described in Set 1

3.7.1 Tracking Pitch and Elevation

First, we aim to control only the pitch and elevation angle $[\phi(t)\ \theta(t)]^{\mathrm{T}}$ of the helicopter to track the output $y_{\mathrm{m}} = [\phi_{\mathrm{d}}(t)\ \theta_{\mathrm{d}}(t)]^{\mathrm{T}}$ of the reference system (3.3) with $A_m = -I_2, B_m = I_2$ and the reference signal

$$r_{\mathrm{d}}(t) = \frac{\pi}{180}[5\sin(0.08\pi t)\ \ 10\sin(0.06\pi t)].$$

Figure 3.8 demonstrates the controller's tracking performance with the initial conditions and control parameters selected as in Set (1)

Set 1: The predictor parameters are $k_{\mathrm{p}} = 10,\ P_\alpha = I_6, P_\beta = 10I_{12}$. The delay time $T = 0.01(s)$, $\sigma(\tau)$ is given in (3.42) with $\kappa_1 = 1, \kappa_2 = 0$. The initial conditions are $y_0 = \frac{\pi}{180}[2\ \ -27\ 0]^{\mathrm{T}}$, and $y_p(0) = \frac{\pi}{180}[-5\ \ -25\ 0]^{\mathrm{T}}$ and

$$\begin{aligned}
\hat{\alpha}^{\mathrm{T}}(0) &= [-\lambda_0 \ldots -\lambda_5] = [-15625\ \ -18750\ \ -9375\ \ -2500\ \ -375\ \ -30],\\
\hat{\beta}^{\mathrm{T}}(0) &= \begin{bmatrix} 0 & 0 & 0 & 0 & 0.07 & 0 & 0 & 0 & 0 & 0 & -0.07 & 0\\ 0 & 0 & 0 & 0 & 0.1 & 0 & 0 & 0 & 0 & 0 & 0.1 & 0\\ 0 & 0 & -1 & 0 & 0 & 0 & 0 & 0 & 1 & 0 & 0 & 0 \end{bmatrix}.
\end{aligned}$$

The projector operator boundary for $\hat{\alpha}(t)$ and $\hat{\beta}(t)$ are setup at $\hat{\alpha}_{\text{max,min}} = \hat{\alpha}(0) \pm 0.2\hat{\alpha}(0)$ and $\hat{\beta}_{\text{max,min}} = \hat{\beta}(0) \pm 0.5(\hat{\beta}(0) + 0.1I_{3\times 12}$.

The augmented system has $\Lambda = \text{diag}([30,\ 10])$ and $\Omega = \text{diag}([10^4,\ 10^4])$. The FDRE controller parameters are $K_{\text{r}} = \text{diag}([-2, 2])$, $Q(t) = \text{diag}([I_{12},\ 100,\ 100]) - 2P(t)$, $R = I_2$, $\varepsilon = 2$ and $P_0 = I_{14}$. Figure 3.8 shows that although the plant, the predictor and the reference started at different initial conditions, they all converge to each other.

3.7.2 Tracking 3 DOF

Secondly, we attempt to control the system's output to track the desired trajectory $y_{\text{m}} = [\phi_{\text{d}}(t)\ \theta_{\text{d}}(t)\ \psi_{\text{d}}(t)]^{\text{T}}$, using the reference system (3.3) with $A_m = -I_3, B_m = I_3$ and different reference inputs $r_{\text{d}}(t)$. Figure 3.9 to Fig 3.11 demonstrate the control's tracking performance using the predictor with parameters selected in Set (1), and different control gains for different reference inputs.

Figure 3.9 demonstrates the tracking performance for a reference input $r(t) = 0_3$, under an impulse disturbance generated by a random external force at time $t = 44(s)$, depicted by a vertical line, with the control gains $K_{\text{r}} = 2I_3$ and $\Lambda = \text{diag}([30,\ 16,\ 18])$, $\Omega = \text{diag}([2.5,\ 2,\ 2.7] \times 10^4)$, $Q(t) = \text{diag}([I_{12},\ 30,\ 30,\ 30])$, $R = I_2$, $\varepsilon = 1$ and $P_0 = I_{15}$. The saturation parameters are $u_{\text{max}} = [2\ 2]$.

Figure 3.10 illustrates the controller's tracking performance for the reference inputs

$$r(t) = \frac{\pi}{180}[0\ 0\ 20\sin(0.12\pi t)]^{\text{T}},$$

with the control gains $K_{\text{r}} = \text{diag}([2,\ 2,\ 4])$ and $\Lambda = \text{diag}([35,\ 16,\ 18])$, $\Omega = \text{diag}([12,\ 2.5,\ 16] \times 10^4)$, $Q(t) = \text{diag}([I_{12},\ 30,\ 50,\ 50])$, $R = I_2$, $\varepsilon = 1$ and $P_0 = I_{15}$. The saturation parameters are $u_{\text{max}} = [4\ 4]$.

Finally, Fig 3.11 depicts the experimental tracking results for the reference input

$$r(t) = \frac{\pi}{180}[0\ 10\sin(0.08\pi t)\ 30\sin(0.12\pi t)]^{\text{T}},$$

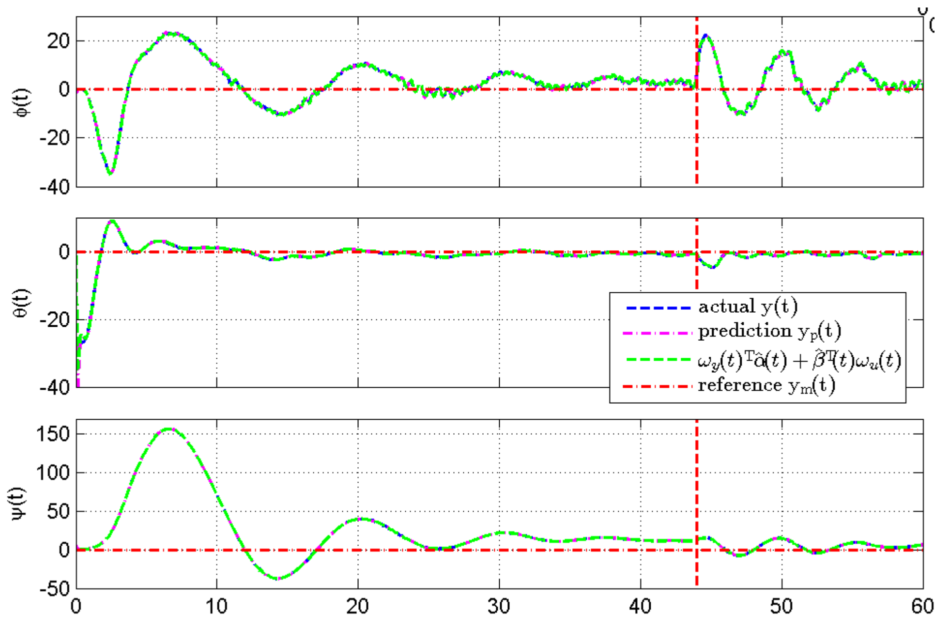

Figure 3.9: The time evolution of $y(t)$, $y_\mathrm{p}(t)$, and $y_\mathrm{m}(t)$ under a random impulse disturbance

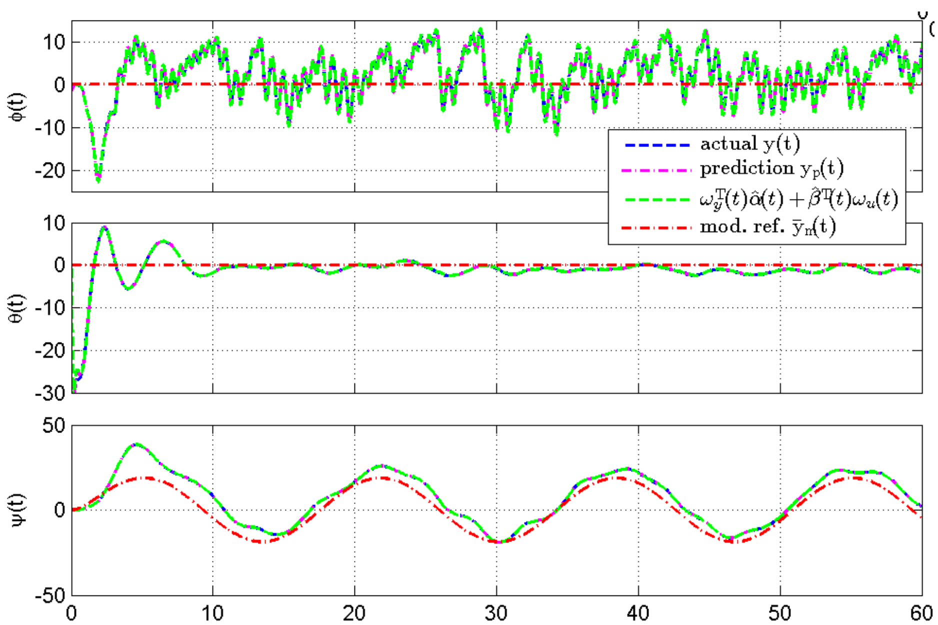

Figure 3.10: The time evolution of $y(t)$, $y_\mathrm{p}(t)$, and $y_\mathrm{m}(t)$ for $r(t) = \frac{\pi}{180}[0\ 0\ 20\sin(0.12\pi t)]^\mathrm{T}$

with the control gains $K_\mathrm{r} = \mathrm{diag}([2,\ 2,\ 4])$ and $\Lambda = \mathrm{diag}([35,\ 16,\ 18])$, $\Omega = \mathrm{diag}([10,\ 8,\ 20] \times 10^4)$, $Q(t) = \mathrm{diag}([I_{12},\ 30,\ 50,\ 50])$, $R = I_2$, $\varepsilon = 1$ and $P_0 = I_{15}$.

Worth noting is that the tracking performance of the pitch angle $\phi(t)$ is not as good as that of

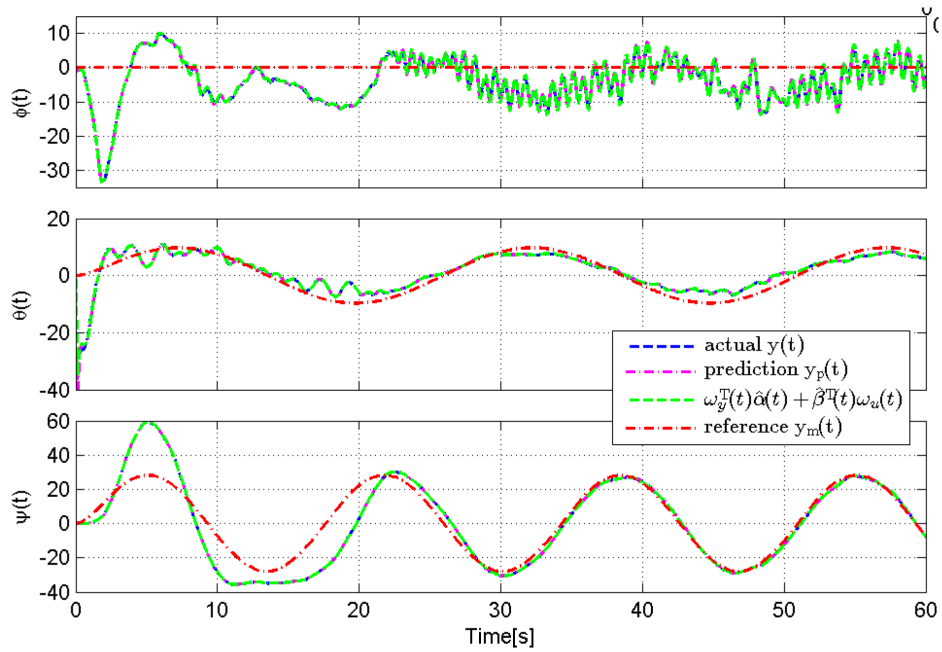

Figure 3.11: The time evolution of $y(t)$, $y_\mathrm{p}(t)$, and $y_\mathrm{m}(t)$ for the reference input $r(t) = \frac{\pi}{180}[0\ 10\sin(0.08\pi t)\ 30\sin(0.12\pi t)]^\mathrm{T}$.

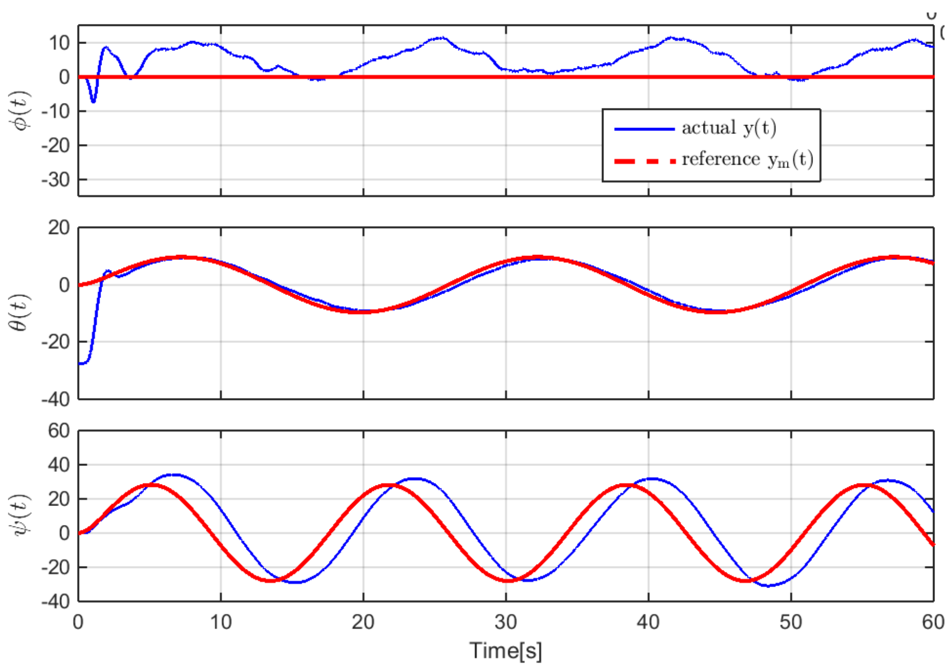

Figure 3.12: The time evolution of $y(t)$ and $y_\mathrm{m}(t)$ using the LQR controller

the other states. This is due to our particular choice of different entries in the matrix M, the gains

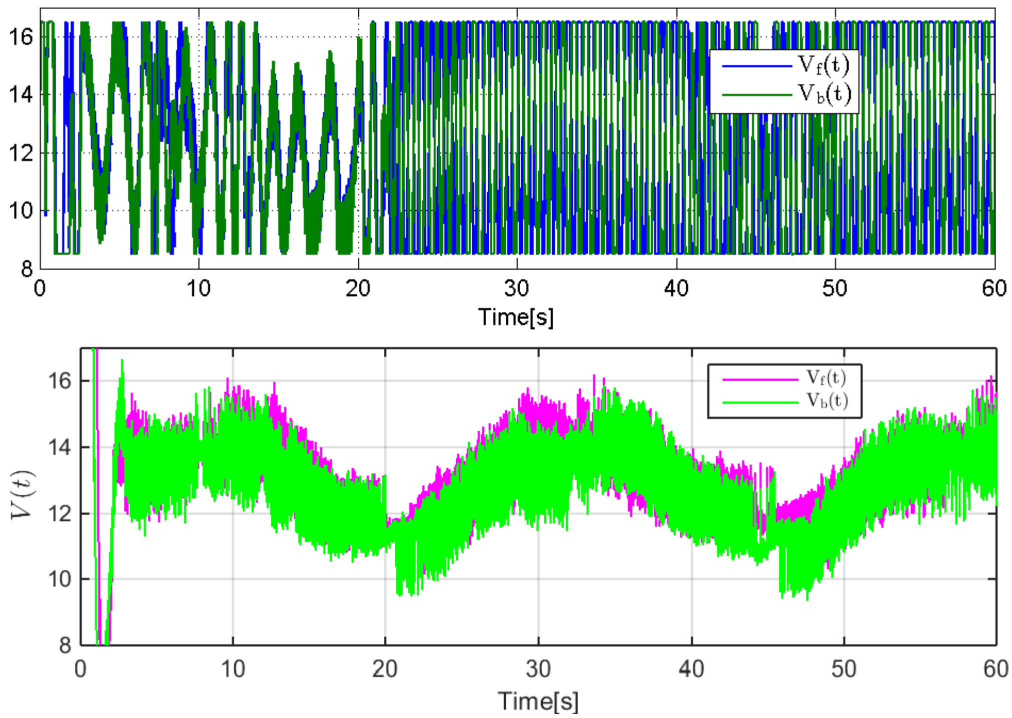

Figure 3.13: The time evolution of $u(t)$ using the proposed controller (upper) and the LQR controller (lower)

K_r and Q, R, which penalizes the tracking error of $\theta(t)$ and $\psi(t)$ more than the tracking error of $\phi(t)$.

We also compare the performance of the proposed adaptive controller with the LQR controller provided by the Quanser, with $u_{\text{LQR}}(t) = Kx(t)$, where

$$K = \begin{bmatrix} 13.21 & 37.67 & -11.50 & 4.77 & 20.95 & -16.10 & 10 & -1 \\ -13.21 & 37.67 & 11.50 & -4.77 & 20.95 & 16.10 & 10 & -1 \end{bmatrix},$$

$$x(t) = \left[\phi(t)\ \theta(t)\ \psi(t)\ \dot{\phi}(t)\ \dot{\theta}(t)\ \dot{\psi}(t)\ \int_0^t e_\theta(\tau)d\tau\ \int_0^t e_\psi(\tau)d\tau\right]^{\mathrm{T}}.$$

where $e_\theta(\tau) \triangleq \theta(\tau) - \theta_m(\tau)$ and $e_\psi(\tau) \triangleq \psi(\tau) - \psi_m(\tau)$.

Figure 3.12 depicts the tracking performance using such LQR controller for the same desired trajectory as in Fig 3.11. Figure 3.13 depicts the corresponding control input for the tracking task using the proposed controller and the control input obtained with the LQR controller.

Figure 3.11 and Fig 3.12 show that in general the proposed adaptive controller can yields better performance than the LQR controller. Furthermore, it can be seen from the Fig 3.13 that the control signal using LQR controller is very noisy due to the numerical derivatives to obtain $[\dot{\phi}(t)\ \dot{\theta}(t)\ \dot{\psi}(t)]$. The proposed control's input is less noisy but still chattering, which can be improved by further tuning. Nevertheless, the controller tracking performance is in general satisfying.

3.8 Conclusion

This chapter presents a novel output feedback control for a class of unknown linear systems. The algorithm relies on an adaptive predictor, which can predict the system output for any admissible input by using the output and input prior history. The only required knowledge about the system is the relative degree in order to ensure the topological equivalence between the predictor and the plant. The prediction error is proved to be exponentially stable using the Lyapunov direct method. From that, any available control algorithms that can drive the predictor to track the trajectories can be applied to the original system and simultaneously drive the plant output to also converge to the desired trajectories. We adopt the FRDE method for our tracking task. In addition, actuator amplitude and rate saturation constraints are enforced by using the modified reference trajectory method. The proposed controller was experimentally tested on the Quanser helicopter and yielded satisfying results. The next chapter will incorporate disturbances in the system and generalization to nonlinear systems.

Chapter 4

Adaptive Predictor-Based Output Feedback Control for a Class of Unknown MIMO Nonlinear Systems

The following result was presented at the American Control Conference 2015 ([66]) and object of an article submitted to Journal of Intelligent and Robotic Systems.

4.1 Introduction

In this chapter, the problem of characterizing adaptive output feedback control laws for a general class of unknown MIMO nonlinear systems is addressed. In particular, the control method for linear systems presented in the previous chapter is extended to the nonlinear case. Following the same design philosophy, we first construct an output predictor capable to predict the system output for all admissible input signals. Using this approach, the problem of controlling a nonlinear system with unknown dynamics and unmeasurable full-state reduces to design a controller for the predictor, which is a virtual system whose dynamics and state are all known. Similar to the previous chapter, it is then shown that the tracking task can be achieved by designing a tracking controller for a linear time varying system, and the same Forward Riccati Differential Equation controller can be implemented. Uniform ultimately boundedness of the prediction error and the tracking error are proved based on the Lyapunov's direct method.

This chapter is organized as follows. Section 4.2 establishes the mathematical background and the problem formulation. In Section 4.3, the output predictor for a class of MIMO nonlinear systems is derived. Design of the control algorithm for the predictor in the presence of actuator amplitude and rate saturation constraints is then presented in Section 4.4. Section 4.5 summarizes the framework to implement the algorithm. The control effectiveness is proved by simulation in Section 4.6. Section 4.7 further provides the experimental results in implementing the algorithm on a helicopter. Finally, Section 4.8 concludes the chapter.

4.2 Mathematical Preliminaries

In this section, we establish the control problem, notations and assumptions used later in the paper. Consider the following nonlinear MIMO system $\mathscr{G}$

$$\dot{x}(t) = f(x(t), u(t), t) \quad x(0) = x_0, \quad t \geq 0, \tag{4.1a}$$

$$y(t) = Cx(t), \tag{4.1b}$$

where $x(t) \in \mathbb{R}^n$ is the unmeasured state vector, $y(t) \in \mathbb{R}^p$ is the output, $u(t) \in \mathbb{R}^m$ is the control input, and $f : \mathbb{R}^n \times \mathbb{R}^m \times \mathbb{R}^+ \to \mathbb{R}^n$ is a $\mathscr{C}^0$ unknown, bounded nonlinear function, and $C = [c_1 \dots c_p]^{\mathrm{T}} \in \mathbb{R}^{p \times n}$ where $c_i \in \mathbb{R}^n,\ i = 1 \dots p$ are unknown vectors defined accordingly. r_{ij} is the known relative degree of the input $u_j(t)$ with respect to the output $y_i(t)$.

The control objective is to design an adaptive controller to ensure that, for a given bounded reference input $r(t) \in \mathbb{R}^p$, $y(t)$ tracks the output $y_{\mathrm{m}}(t)$ of the following desired system

$$\dot{y}_{\mathrm{m}}(t) = A_{\mathrm{m}} y_{\mathrm{m}}(t) + B_{\mathrm{m}} r(t), \quad t \geq 0. \tag{4.2}$$

where $A_\mathrm{m} \in \mathbb{R}^{p\times p}$ is a stable matrix, and B_m is a full rank matrix.

For a given compact operating domain $\mathscr{D}(x(t),u(t)) \subseteq \mathbb{R}^n \times \mathbb{R}^m$, the system $\mathscr{G}$ can be rewritten as

$$\dot{x}(t) = Ax(t) + B(u(t)-u_0) + h(x(t),u(t),t), \qquad x(0)=x_0,\ t\geq 0, \tag{4.3a}$$

$$y(t) = Cx(t), \tag{4.3b}$$

where $A \in \mathbb{R}^{n\times n}$, $B = [b_1 \dots b_m] \in \mathbb{R}^{n\times m}$, $b_j \in \mathbb{R}^n,\ j = 1\dots m$ are unknown matrices, $h(x,u,t) \triangleq f(x,u,t) - Ax(t) - B(u(t)-u_0)$ is the unknown nonlinear term, u_0 is a chosen constant input.

Assumption 4.2.1 *In the domain $\mathscr{D}(x(t),u(t))$, there exists a controllable matrix pair (A,B) such that $\|h(x,u,t)\| < \delta_1 < \infty$ and $\|h(x,u,t)\| < \delta_2 < \infty$ (i.e radically bounded). Furthermore, we know the relatives degree r_{ij} between each input $u_j,\ j=1\dots m$ to each output $y_i,\ i=1\dots p$ of the nominal system $\dot{x}(t) = Ax(t)+B(u(t)-u_0)$. For simplicity and without losing generality, we also assume $u_0 = 0$. In general, we can define $u_E(t) = u(t)-u_0$ and follow the same steps by replacing $u(t)$ with $u_E(t)$.*

Lemma 4.2.1 *The i^{th} output of the system $\mathscr{G}_\mathrm{L}$ can be represented in the Laplace domain by the following transfer function*

$$y_i(s) = G_i(s)u(s) + H_i(s)h(s) = \frac{\sum_{j=1}^m N_{ij}(s)u_j(s)}{D(s)} + \frac{Z_i(s)h(s)}{D(s)}, \tag{4.4}$$

where $s \in \mathbb{C}$ denotes the Laplace variable, $G_i(s) \triangleq c_i^\mathrm{T}(sI_n - A)^{-1}B$ is the transfer function of $u(t)$ relative to the output $y_i(t)$, and $H_i(s) \triangleq c_i^\mathrm{T}(sI_n-A)^{-1}$ is the transfer function of $h(x,t)$ relative to the output $y_i(t)$. Accordingly, $D(s) = s^n + \alpha_{n-1}s^{n-1} + \dots + \alpha_1 s + \alpha_0 = \det(sI_n - A)$ and $N_{ij}(s) = \beta_{ij_{n-r_{ij}}} s^{n-r_{ij}} + \dots + \beta_{ij_1}s + \beta_{ij_0} = c_i^\mathrm{T}A_\mathrm{a}(s)b_j$ represent the denominator and the numerator's component of the transfer function $G_i(s)$, respectively. Furthermore, $Z_i(s) \triangleq c_i^\mathrm{T}A_\mathrm{a}(s)$, where $A_\mathrm{a}(s)$ denotes the adjunct matrix of $(sI_n - A)$. Then, the system output can be obtained as follows

$$y(t) = \omega_y^\mathrm{T}(t)\alpha + \beta^\mathrm{T}\omega_u(t) + z(t), \quad t\geq 0, \tag{4.5}$$

where $\alpha \in \mathbb{R}^n$ *and* $\beta \in \mathbb{R}^{nm\times p}$ *are defined as*

$$\alpha \triangleq \begin{bmatrix} \alpha_0 - \lambda_0 & \dots & \alpha_{n-1} - \lambda_{n-1} \end{bmatrix}^{\mathrm{T}}, \tag{4.6a}$$

$$\beta \triangleq \begin{bmatrix} \beta_{11} & \cdots & \beta_{p1} \\ \vdots & \ddots & \vdots \\ \beta_{1m} & \cdots & \beta_{pm} \end{bmatrix}, \qquad \beta_{ij} \triangleq \begin{bmatrix} \beta_{ij}^{(0)} & \dots & \beta_{ij}^{(n-r_{ij})} & 0_{r_{ij}-1}^{\mathrm{T}} \end{bmatrix}^{\mathrm{T}} \in \mathbb{R}^n, \tag{4.6b}$$

and $\omega_y(t) \in \mathbb{R}^{n\times p}$ *and* $\omega_u(t) \in \mathbb{R}^{nm}$ *are defined as*

$$\omega_y(t) \triangleq [\omega_{y_1}(t) \cdots \omega_{y_p}(t)], \qquad \omega_u(t) \triangleq [\omega_{u1}^{\mathrm{T}}(t) \cdots \omega_{um}^{\mathrm{T}}(t)]^{\mathrm{T}}, \tag{4.7a}$$

where $\omega_{y_i} \in \mathbb{R}^n$, $\omega_{uj} \in \mathbb{R}^n$ *are the regression vectors obtained as follows*

$$\dot{\omega}_{y_i}(t) = A_{\mathrm{f}}\omega_{y_i}(t) - B_{\mathrm{f}}y_i(t), \qquad \omega_{y_i}(0) = \omega_{y_{i0}}, \;\; t \geq 0, \tag{4.8a}$$

$$\dot{\omega}_{u_j}(t) = A_{\mathrm{f}}\omega_{u_j}(t) + B_{\mathrm{f}}u_j(t), \qquad \omega_{u_j}(0) = \omega_{u_{i0}}, \;\; t \geq 0, \tag{4.8b}$$

where $i = 1,\dots,p$ *and* $j = 1,\dots,m$, *and*

$$A_{\mathrm{f}} \triangleq \begin{bmatrix} 0_{n-1} & & I_{(n-1)} \\ -\lambda_0 & \dots & -\lambda_{n-1} \end{bmatrix} \in \mathbb{R}^{n\times n}, \;\; B_{\mathrm{f}} \triangleq \begin{bmatrix} 0_{n-1} \\ 1 \end{bmatrix} \in \mathbb{R}^n, \tag{4.9}$$

such that $\Lambda(s) \triangleq \det(sI_n - A_{\mathrm{f}}) = s^n + \lambda_{n-1}s^{n-1} + \dots + \lambda_1 s + \lambda_0$ *is a* n^{th} *order, Hurwitz polynomial. Finally,* $z(t)$ *is the inverse Laplace transform of* $z(s) \triangleq [z_1(s)\dots z_p(s)]^{\mathrm{T}}$, $z_i(s) \triangleq Z_i(s)h(s)/\Lambda(s)$, $i = 1,\dots,p$, *such that* $z(t)$ *and* $\dot{z}(t)$ *are bounded.*

Proof *Consider the single output transfer function defined in (4.4), by multiplying both sides of (4.4) by* $D(s)/\Lambda(s)$, *it follows*

$$\frac{D(s)}{\Lambda(s)}y_i(s) = \frac{\sum_{j=1}^m N_{ij}(s)u_j(s)}{\Lambda(s)} + \frac{Z_i(s)h(s)}{\Lambda(s)}, \tag{4.10}$$

which implies

$$\begin{aligned} y_i(s) &= -\frac{D(s)-\Lambda(s)}{\Lambda(s)}y_i(s) + \frac{\sum_{j=1}^{m} N_{ij}(s)u_j(s)}{\Lambda(s)} + \frac{Z_i(s)h(s)}{\Lambda(s)} \\ &= \omega_{y_i}^{\mathrm{T}}(s)\alpha + \sum_{j=1}^{m} \beta_{ij}^{\mathrm{T}}\omega_{u_j}(s) + z_i(s), \end{aligned} \tag{4.11}$$

where α and β_{ij} are defined in (4.6), and

$$\omega_{y_i}(s) = -(sI_n - A_{\mathrm{f}})^{-1}B_{\mathrm{f}}y_i(s) = -\left[\frac{y_i(s)}{\Lambda(s)}, \cdots, \frac{s^{n-1}y_i(s)}{\Lambda(s)}\right]^{\mathrm{T}}, \tag{4.12a}$$

$$\omega_{u_j}(s) = (sI_n - A_{\mathrm{f}})^{-1}B_{\mathrm{f}}u_j(s) = \left[\frac{u_j(s)}{\Lambda(s)}, \cdots, \frac{s^{n-1}u_j(s)}{\Lambda(s)}\right]^{\mathrm{T}}, \tag{4.12b}$$

$$z_i(s) \triangleq \frac{Z_i(s)h(s)}{\Lambda(s)}, \tag{4.12c}$$

which are the Laplace transform of $\omega_{y_i}(t)$ and $\omega_{u_j}(t)$ defined in (4.8) and $z_i(t)$ respectively. Hence, it follows from (4.11) that the output of the system can be obtained by

$$y(t) = \begin{bmatrix} \omega_{y_1}^{\mathrm{T}}(t) \\ \vdots \\ \omega_{y_p}^{\mathrm{T}}(t) \end{bmatrix} \alpha + \begin{bmatrix} \beta_{11}^{\mathrm{T}} & \cdots & \beta_{1m}^{\mathrm{T}} \\ \vdots & \ddots & \vdots \\ \beta_{p1}^{\mathrm{T}} & \cdots & \beta_{pm}^{\mathrm{T}} \end{bmatrix} \begin{bmatrix} \omega_{u_1}(t) \\ \vdots \\ \omega_{u_m}(t) \end{bmatrix} + z(t), \tag{4.13}$$

which proves (4.5). Finally, since $Z_i(s)/\Lambda(s)$ is a strictly proper transfer function and $h(x,t)$ is bounded. Hence, it follows from (4.12c) and Lemma 3.2.1 that $z(t)$ and $\dot{z}(t)$ are bounded. □

Assumption 4.2.2 *In the domain $\mathscr{D}$, α, β, and $z(t)$ satisfy $\alpha \in \Theta_\alpha$, $\beta \in \Theta_\beta$, $z(t) \in \Theta_z$, where Θ_α, Θ_β, Θ_z are the known convex compact sets, and d_0, d_1, d_2 are the known constants such that*

$$\begin{aligned} \|z(t)\| &\leq \sqrt{n}\|_{\mathscr{L}_\infty}\| \leq \sqrt{n}\left\|\frac{Z(s)}{\Lambda(s)}\right\|\delta_1 \triangleq d_0 < \infty \\ \|\dot{z}(t)\| &\leq \sqrt{n}\left\|\frac{sZ(s)}{\Lambda(s)}\right\|\delta_1 \triangleq d_1 < \infty, \\ \|\ddot{z}(t)\| &\leq \sqrt{n}\left\|\frac{sZ(s)}{\Lambda(s)}\right\|\delta_2 \triangleq d_2 < \infty \end{aligned}$$

4.3 Predictor Design

Theorem 4.3.1 *Consider the system $\mathscr{G}_{\rm L}$ defined in (4.3) which has input $u(t) \in \mathbb{R}^m$, output $y(t) \in \mathbb{R}^p$, and the regression vectors $\omega_y(t)$, $\omega_u(t)$ defined in (4.7). Let $k_{\rm p} > 0$ and matrices $\Gamma \in \mathbb{R}^{p\times p}$, $P_\alpha \in \mathbb{R}^{n\times n}$, $P_\beta \in \mathbb{R}^{nm\times nm}$, $P_1 \in \mathbb{R}^{p\times p}$, $P_2 \in \mathbb{R}^{p\times p}$ are the positive definite matrices. Then, the output predictor*

$$\dot{y}_{\rm p}(t) = -k_{\rm p}y_{\rm p}(t) + \eta_y^{\rm T}(t)\hat{\alpha}(t) + \hat{\beta}^{\rm T}(t)\eta_u(t) + k_{\rm p}\hat{z}_1(t) + \hat{z}_2(t), \quad y_{\rm p}(0) = y_{\rm p_0},\ t \geq 0, \tag{4.14}$$

guarantees that the system defined by (4.14 - 4.15) is Lyapunov stable and the prediction error $e_{\rm p}(t) \triangleq y(t) - y_{\rm p}(t)$ is ultimately bounded, provided that $\hat{\alpha}(t) \in \mathbb{R}^n$, $\hat{\beta}(t) \in \mathbb{R}^{nm\times p}$, $\hat{z}_1(t) \in \mathbb{R}^p$ and $\hat{z}_2(t) \in \mathbb{R}^p$ are obtained from the adaptive law

$$\dot{\hat{\alpha}}(t) = P_\alpha\big(\eta_y(t)\Gamma^{\rm T}e_{\rm p}(t) + \Omega_y(t){\rm vec}(f(t))\big), \qquad \hat{\alpha}(0) = \hat{\alpha}_0, \tag{4.15a}$$

$$\dot{\hat{\beta}}(t) = P_\beta\big(\eta_u(t)e_{\rm p}^{\rm T}(t)\Gamma + \Omega_u(t)f^{\rm T}(t)\big), \qquad \hat{\beta}(0) = \hat{\beta}_0, \tag{4.15b}$$

$$\dot{\hat{z}}_1(t) = \hat{z}_2(t) + P_1\big(\Gamma^{\rm T}k_{\rm p}e_{\rm p}(t) + f_1(\varepsilon_1(t),t)\big), \qquad \hat{z}_1(0) = \hat{z}_{10}, \tag{4.15c}$$

$$\dot{\hat{z}}_2(t) = P_2\big(\Gamma^{\rm T}e_{\rm p}(t) + f_2(\varepsilon_2(t),t)\big), \qquad \hat{z}_1(0) = \hat{z}_{10}, \tag{4.15d}$$

where $\Omega_y(t) \triangleq [\omega_y(t)\ \dot{\omega}_y(t)] \in \mathbb{R}^{n\times 2p}$, $\Omega_u(t) \triangleq [\omega_u(t)\ \dot{\omega}_u(t)] \in \mathbb{R}^{nm\times 2}$, and $\varepsilon(t) \triangleq [\varepsilon_1^{\rm T}(t)\ \varepsilon_2^{\rm T}(t)]^{\rm T}$, $\varepsilon_1(t) \in \mathbb{R}^p$, $\varepsilon_2(t) \in \mathbb{R}^p$ are defined as

$$\varepsilon_1(t) \triangleq y(t) - \omega_y^{\rm T}(t)\hat{\alpha}(t) - \hat{\beta}^{\rm T}(t)\omega_u(t) - \hat{z}_1(t), \tag{4.16a}$$

$$\varepsilon_2(t) \triangleq \dot{y}(t) - \dot{\omega}_y^{\rm T}(t)\hat{\alpha}(t) - \hat{\beta}^{\rm T}(t)\dot{\omega}_u(t) - \hat{z}_2(t), \tag{4.16b}$$

and $f(t) \triangleq [f_1(\varepsilon_1,t)\ f_2(\varepsilon_2,t)] \in \mathbb{R}^{p\times 2}$, $f_i : \mathbb{R}^p \times \mathbb{R}^+ \to \mathbb{R}^p$ is the bounded function satisfying $f_i^{\rm T}(\varepsilon_i(t),t)\varepsilon_i(t) \geq 0$, $i = 1,2$.

Proof *It follows from Lemma (4.2.1) that any $n^{\rm th}$ order MIMO system can be represented by*

$$y(t) = \omega_y^{\rm T}(t)\alpha + \beta^{\rm T}\omega_u(t) + z(t), \tag{4.17}$$

Taking the time derivative of (4.17) yields

$$\begin{aligned}\dot{y}(t) &= \dot{\omega}_y^{\mathrm{T}}(t)\alpha + \beta^{\mathrm{T}}\dot{\omega}_u(t) + \dot{z}(t)\\ &= -k_{\mathrm{p}}y(t) + (\dot{\omega}_y(t) + k_{\mathrm{p}}\omega_y(t))^{\mathrm{T}}\alpha + \beta^{\mathrm{T}}(\dot{\omega}_u(t) + k_{\mathrm{p}}\omega_u(t)) + k_{\mathrm{p}}z(t) + \dot{z}(t)\\ &= -k_{\mathrm{p}}y(t) + \eta_y^{\mathrm{T}}(t)\alpha + \beta^{\mathrm{T}}\eta_u(t) + k_{\mathrm{p}}z(t) + \dot{z}(t),\end{aligned} \tag{4.18}$$

where $\eta_y(t)$ and $\eta_u(t)$ are defined in (3.19) and (3.20), respectively. It follows from (4.18) and (4.14) that the prediction error dynamics is obtained as

$$\dot{e}_{\mathrm{p}}(t) = -k_{\mathrm{p}}e_{\mathrm{p}}(t) + \eta_y^{\mathrm{T}}(t)\tilde{\alpha}(t) + \tilde{\beta}^{\mathrm{T}}(t)\eta_u(t) + k_{\mathrm{p}}\tilde{z}_1(t) + \tilde{z}_2(t), \quad e_{\mathrm{p}}(0) = e_{\mathrm{p}0},\ t \geq 0, \tag{4.19}$$

where $\tilde{\alpha}(t) \triangleq \alpha - \hat{\alpha}(t) \in \mathbb{R}^n$, $\tilde{\beta}(t) \triangleq \beta - \hat{\beta}(t) \in \mathbb{R}^{nm\times p}$, $\tilde{z}_1(t) \triangleq z(t) - \hat{z}_1(t) \in \mathbb{R}^p$ and $\tilde{z}_2(t) \triangleq \dot{z}(t) - \hat{z}_2(t) \in \mathbb{R}^p$. Now, differentiating the Lyapunov function candidate

$$\begin{aligned}V(e_{\mathrm{p}},\tilde{\alpha},\tilde{\beta},\tilde{z}_1,\tilde{z}_2) = \frac{1}{2}e_{\mathrm{p}}^{\mathrm{T}}(t)\Gamma e_{\mathrm{p}}(t) + \frac{1}{2}\tilde{\alpha}^{\mathrm{T}}(t)P_\alpha^{-1}\tilde{\alpha}(t) + \frac{1}{2}\mathrm{tr}[\tilde{\beta}^{\mathrm{T}}(t)P_\beta^{-1}\tilde{\beta}(t)]\\ + \frac{1}{2}\tilde{z}_1^{\mathrm{T}}(t)P_1^{-1}\tilde{z}_1(t) + \frac{1}{2}\tilde{z}_2^{\mathrm{T}}(t)P_2^{-1}\tilde{z}_2(t),\end{aligned} \tag{4.20}$$

along the error dynamics trajectories given by (4.19) and substituting the update law (4.15), yields

$$\begin{aligned}\dot{V}(t) &= -k_{\mathrm{p}}e_{\mathrm{p}}^{\mathrm{T}}(t)\Gamma e_{\mathrm{p}}(t) + e_{\mathrm{p}}^{\mathrm{T}}(t)\Gamma\eta_y^{\mathrm{T}}(t)\tilde{\alpha}(t) + e_{\mathrm{p}}^{\mathrm{T}}(t)\Gamma\tilde{\beta}^{\mathrm{T}}(t)\eta_u(t) + e_{\mathrm{p}}^{\mathrm{T}}(t)\Gamma k_{\mathrm{p}}\tilde{z}_1(t) + e_{\mathrm{p}}^{\mathrm{T}}(t)\Gamma\tilde{z}_2(t)\\ &\qquad - \tilde{\alpha}^{\mathrm{T}}(t)P_\alpha^{-1}\dot{\hat{\alpha}}(t) - \mathrm{tr}[\tilde{\beta}^{\mathrm{T}}(t)P_\beta^{-1}\dot{\hat{\beta}}(t)]\\ &\qquad + \tilde{z}_1^{\mathrm{T}}(t)P_1^{-1}(\dot{z}(t) - \hat{z}_2(t) + \hat{z}_2(t) - \dot{\hat{z}}_1(t)) + \tilde{z}_2^{\mathrm{T}}(t)P_2^{-1}(\ddot{z}(t) - \dot{\hat{z}}_2(t))\\ &= -k_{\mathrm{p}}e_{\mathrm{p}}^{\mathrm{T}}(t)\Gamma e_{\mathrm{p}}(t) + \tilde{\alpha}^{\mathrm{T}}(t)\big(\eta_y(t)\Gamma^{\mathrm{T}}e_{\mathrm{p}}(t) - P_\alpha^{-1}\dot{\hat{\alpha}}(t)\big) + \mathrm{tr}[\tilde{\beta}^{\mathrm{T}}(t)(\eta_u(t)e_{\mathrm{p}}^{\mathrm{T}}(t)\Gamma - P_\beta^{-1}\dot{\hat{\beta}}(t))]\\ &\qquad + \tilde{z}_1^{\mathrm{T}}(t)(\Gamma^{\mathrm{T}}k_{\mathrm{p}}e_{\mathrm{p}}(t) + P_1^{-1}(\hat{z}_2(t) - \dot{\hat{z}}_1(t)))\\ &\qquad + \tilde{z}_2^{\mathrm{T}}(t)(\Gamma^{\mathrm{T}}e_{\mathrm{p}}(t) - P_2^{-1}\dot{\hat{z}}_2(t)) + \tilde{z}_2^{\mathrm{T}}(t)(P_1^{-1}\tilde{z}_1 + P_2^{-1}\ddot{z}(t))\\ &= -k_{\mathrm{p}}e_{\mathrm{p}}^{\mathrm{T}}(t)\Gamma e_{\mathrm{p}}(t) - \tilde{\alpha}^{\mathrm{T}}(t)\Omega_y(t)\mathrm{vec}(f(t)) - \mathrm{tr}[\tilde{\beta}^{\mathrm{T}}(t)\Omega_u(t)f^{\mathrm{T}}(t)]\\ &\qquad - \tilde{z}_1^{\mathrm{T}}(t)f_1(\varepsilon_1(t),t) - \tilde{z}_2^{\mathrm{T}}(t)f_2(\varepsilon_2(t),t) + \tilde{z}_2^{\mathrm{T}}(t)(P_1^{-1}\tilde{z}_1 + P_2^{-1}\ddot{z}(t)).\end{aligned} \tag{4.21}$$

Using the property $x = x^{\mathrm{T}}$ *if* $x \in \mathbb{R}$ *yields*

$$\tilde{\alpha}^{\mathrm{T}}(t)\Omega_y(t)\mathrm{vec}(f(t)) = \mathrm{vec}(f(t))^{\mathrm{T}}\Omega_y^{\mathrm{T}}(t)\tilde{\alpha}(t) = f_1^{\mathrm{T}}(\varepsilon_1(t),t)\omega_y^{\mathrm{T}}(t)\tilde{\alpha}(t) + f_2^{\mathrm{T}}(\varepsilon_2(t),t)\dot{\omega}_y^{\mathrm{T}}(t)\tilde{\alpha}(t). \tag{4.22}$$

and the property $\mathrm{tr}[X^{\mathrm{T}}Y] = \mathrm{tr}[YX^{\mathrm{T}}] = YX^{\mathrm{T}}$ *if* $YX^{\mathrm{T}} \in \mathbb{R}$ *yields*

$$\begin{aligned}\mathrm{tr}[\tilde{\beta}^{\mathrm{T}}(t)\Omega_u(t)f^{\mathrm{T}}(t)] &= \mathrm{tr}[\tilde{\beta}^{\mathrm{T}}(t)\omega_u(t)f_1^{\mathrm{T}}(\varepsilon_1(t),t)] + \mathrm{tr}[\tilde{\beta}^{\mathrm{T}}(t)\dot{\omega}_u(t)f_2^{\mathrm{T}}(\varepsilon_2(t),t)] \\ &= f_1^{\mathrm{T}}(\varepsilon_1(t),t)\tilde{\beta}^{\mathrm{T}}(t)\omega_u(t) + f_2^{\mathrm{T}}(\varepsilon_2(t),t)\tilde{\beta}^{\mathrm{T}}(t)\dot{\omega}_u(t).\end{aligned} \tag{4.23}$$

Moreover, substituting (4.17) into (4.16) to rewrite $\varepsilon_1(t)$ *and* $\varepsilon_2(t)$ *as*

$$\varepsilon_1(t) = \omega_y^{\mathrm{T}}(t)\tilde{\alpha}(t) + \tilde{\beta}^{\mathrm{T}}(t)\omega_u(t) + \tilde{z}_1(t), \tag{4.24a}$$

$$\varepsilon_2(t) = \dot{\omega}_y^{\mathrm{T}}(t)\tilde{\alpha}(t) + \tilde{\beta}^{\mathrm{T}}(t)\dot{\omega}_u(t) + \tilde{z}_2(t), \tag{4.24b}$$

Finally, substituting (4.22), (4.23) and (4.24) into (4.21) to obtain

$$\begin{aligned}\dot{V}(t) &= -k_{\mathrm{p}}e_{\mathrm{p}}^{\mathrm{T}}(t)\Gamma e_{\mathrm{p}}(t) - f_1^{\mathrm{T}}(\varepsilon_1(t),t)\underbrace{(\omega_y^{\mathrm{T}}(t)\tilde{\alpha}(t) + \tilde{\beta}^{\mathrm{T}}(t)\omega_u(t) + \tilde{z}_1(t))}_{\varepsilon_1(t)} \\ &\quad - f_2^{\mathrm{T}}(\varepsilon_2(t),t)\underbrace{(\dot{\omega}_y^{\mathrm{T}}(t)\tilde{\alpha}(t) + \tilde{\beta}^{\mathrm{T}}(t)\omega_u(t) + \tilde{z}_2(t))}_{\varepsilon_2(t)} + \underbrace{\tilde{z}_2^{\mathrm{T}}(t)(P_1^{-1}\tilde{z}_1 + P_2^{-1}\ddot{z}(t))}_{d(t)} \\ &= -k_{\mathrm{p}}e_{\mathrm{p}}^{\mathrm{T}}(t)\Gamma e_{\mathrm{p}}(t) - f_1^{\mathrm{T}}(\varepsilon_1(t),t)\varepsilon_1(t) - f_2^{\mathrm{T}}(\varepsilon_2(t),t)\varepsilon_2(t) + d(t)\end{aligned} \tag{4.25}$$

where $d(t) \triangleq \tilde{z}_2^{\mathrm{T}}(t)(P_1^{-1}\tilde{z}_1 + P_2^{-1}\ddot{z}(t))$. *According to the Assumption 4.2.2, the projection operator keeps* $\tilde{\alpha}$, $\tilde{\beta}$, $\tilde{z}_1(t)$, $\tilde{z}_2(t)$ *bounded, so that*

$$\begin{aligned}&\frac{1}{2}\tilde{\alpha}^{\mathrm{T}}(t)P_\alpha^{-1}\tilde{\alpha}(t) + \frac{1}{2}\mathrm{tr}[\tilde{\beta}^{\mathrm{T}}(t)P_\beta^{-1}\tilde{\beta}(t)] + \frac{1}{2}\tilde{z}_1^{\mathrm{T}}(t)P_1^{-1}\tilde{z}_1(t) + \frac{1}{2}\tilde{z}_2^{\mathrm{T}}(t)P_2^{-1}\tilde{z}_2(t) \\ &\leq \frac{1}{2}\left(\frac{4}{\lambda_{\min}(P_\alpha)}\max_{\alpha\in\Theta_\alpha}\|\alpha\|^2 + \frac{4}{\lambda_{\min}(P_\beta)}\max_{\beta\in\Theta_\beta}\|\beta\|^2 + \frac{4}{\lambda_{\min}(P_1)}\max_{z(t)\in\Theta_z}\|z(t)\|^2 + \frac{4d_1^2}{\lambda_{\min}(P_2)}\right) \triangleq D_{\max},\end{aligned} \tag{4.26}$$

$$d(t) \leq 2d_1\left(\frac{2}{\lambda_{\min}(P_1)}\max_{z(t)\in\Theta_z}\|z(t)\| + \frac{d_2}{\lambda_{\min}(P_2)}\right) \triangleq d_{\max}. \tag{4.27}$$

Substituting (4.20), (4.27) and (4.26) into (4.25) to obtain

$$\dot{V}(t) \leq -2k_{\mathrm{p}}V(t) + 2k_{\mathrm{p}}D_{\max} + d_{\max} - f^{\mathrm{T}}(\varepsilon(t),t)\varepsilon(t). \tag{4.28}$$

Denote $\zeta \triangleq (e_{\mathrm{p}}, \tilde{\alpha}, \tilde{\beta}, \tilde{z}_1, \tilde{z}_2)$ *and* $V_{\max} \triangleq D_{\max} + \dfrac{d_{\max} - f^{\mathrm{T}}(\varepsilon(t),t)\varepsilon(t)}{2k_{\mathrm{p}}}$. *Note that*

$$-2k_{\mathrm{p}}V_{\max} + 2k_{\mathrm{p}}D_{\max} + d_{\max} - f^{\mathrm{T}}(\varepsilon(t),t)\varepsilon(t) = 0,$$

hence the set $\Omega_V \triangleq \{\zeta \in \mathbb{R}^p \times \Omega_\alpha \times \Omega_\beta \times \Omega_z \times \Omega_{\dot{z}} \mid V(\zeta) \leq V_{\max}\}$ *is such that* $\dot{V}(\zeta) \leq 0$ *for all* $\zeta \in \{\zeta \in \mathbb{R}^p \times \Omega_\alpha \times \Omega_\beta \times \Omega_z \times \Omega_{\dot{z}}\}\backslash\Omega_V$, *which according to Lyapunov theory (Theorem 4.1 in [31]) guarantees that* Ω_V *is a positive invariant set and all state trajectories enter and remain in* Ω_V *after an initial transience. Note that* $\varepsilon_1(t)$, $\varepsilon_1(t)$ *are the measurable signals, and* $f_i(\varepsilon_i(t),t)$ *are the designed bounded signals satisfying* $f_i^{\mathrm{T}}(\varepsilon_i(t),t)\varepsilon_i(t) > 0,\ i = 1,2$, *which reduce the maximum bound* $V_{\max}$. *Moreover, since* $\lambda_{\min}(\Gamma)\|e_{\mathrm{p}}\|^2 \leq e_{\mathrm{p}}^{\mathrm{T}}(t)\Gamma e_{\mathrm{p}}(t) \leq 2V(t)$, *then*

$$\|e_{\mathrm{p}}(t)\| \leq \sqrt{\frac{2V_{\max}}{\lambda_{\min}(\Gamma)}}. \tag{4.29}$$

Therefore, the dynamic system given by (4.19) and (4.15) is Lyapunov stable, and $e_{\mathrm{p}}(t)$ *is ultimately bounded, which concludes the proof.* □

Remark 4.3.1 *The projection operator should be applied to all adaptive laws (4.15), to ensure the boundedness of the estimated signals* $\hat{\alpha}(t)$, $\hat{\beta}(t)$, $z_1(t)$, $z_2(t)$. *Furthermore,* $\hat{\beta}_{ij}(t)$ *needs to satisfy the topological equivalence of the input* $u_j(t)$ *with respect to the output* $y_i(t)$, *such that*

$$\hat{\beta}_{ij}(t) \triangleq \begin{bmatrix} \hat{\beta}_{ij}^{(0)}(t) & \ldots & \hat{\beta}_{ij}^{(n-r)}(t) & 0_{r_{ij}-1}^{\mathrm{T}} \end{bmatrix}^{\mathrm{T}} \in \mathbb{R}^n. \tag{4.30}$$

Remark 4.3.2 *A simple choice of* $f_i(\varepsilon_i,t)$ *is*

$$f_i(\varepsilon_i,t) = \sigma_i(t)\frac{\varepsilon_i(t)}{\Delta_i(t)}, \quad \Delta_i(t) = \begin{cases} \|\omega_y(t)\|^2 + \|\omega_u(t)\|^2 + 1, \text{ if } i = 1 \\ \|\dot{\omega}_y(t)\|^2 + \|\dot{\omega}_u(t)\|^2 + 1, \text{ if } i = 2 \end{cases} \tag{4.31}$$

where $\sigma_i(t) > 0$ *is any scalar bounded function and* $\Delta(t)$ *is the normalizing term. It follows from (4.25) that* $\sigma(t)$ *can be conditionally adjusted to achieve small errors* $\|e_{\mathrm{p}}(t)\|$ *and* $\|\varepsilon(t)\|$.

4.4 Controller Design

It follows from (3.20) and (4.14) that the predictor dynamics can be obtained as

$$\begin{aligned}\dot{y}_{\mathrm{p}}(t) &= -k_{\mathrm{p}}y_{\mathrm{p}}(t) + \eta_y^{\mathrm{T}}(t)\hat{\alpha}(t) + \hat{\beta}^{\mathrm{T}}(t)(A_u + k_{\mathrm{p}}I_{nm})\omega_u(t) + \hat{\beta}^{\mathrm{T}}(t)B_u u(t) + k_{\mathrm{p}}\hat{z}_1(t) + \hat{z}_2(t) \\ &= -k_{\mathrm{p}}y_{\mathrm{p}}(t) + \upsilon(t) + C_u(t)\omega_u(t) + D_u(t)u(t), \end{aligned} \tag{4.32}$$

where

$$\upsilon(t) \triangleq \eta_y^{\mathrm{T}}(t)\hat{\alpha}(t) + k_{\mathrm{p}}\hat{z}_1(t) + \hat{z}_2(t), \tag{4.33}$$

$$C_u(t) \triangleq \hat{\beta}^{\mathrm{T}}(t)(A_u + k_{\mathrm{p}}I_{nm}) \in \mathbb{R}^{p\times nm}, \quad D_u(t) \triangleq \hat{\beta}^{\mathrm{T}}(t)B_u \in \mathbb{R}^{p\times m}. \tag{4.34}$$

Note that if the control inputs $u_j(t),\ j = 1,\dots,m$, have relative degree $r_{ij} \geq 2$ then $D_u(t) = 0_{p\times m}$. Now, consider the desired reference system defined in (4.2) and let $e_{\mathrm{r}}(t) \triangleq y_{\mathrm{p}}(t) - y_{\mathrm{m}}(t)$ be the tracking error between the predictor and the reference system. It follows from (4.2) and (4.32) that

$$\begin{aligned}\dot{e}_{\mathrm{r}}(t) &= -k_{\mathrm{p}}(y_{\mathrm{p}}(t) - y_{\mathrm{m}}(t)) + \upsilon(t) + C_u(t)\omega_u(t) + D_u(t)u(t) - (A_{\mathrm{m}} + k_{\mathrm{p}}I_p)y_{\mathrm{m}}(t) - B_{\mathrm{m}}r(t) \\ &= -(k_{\mathrm{p}}I_p + K_{\mathrm{r}})e_{\mathrm{r}}(t) + C_u(t)\omega_u(t) + D_u(t)u(t) - \varphi_{\mathrm{d}}(t), \end{aligned} \tag{4.35}$$

where $K_{\mathrm{r}} \in \mathbb{R}^{p\times p}, K_{\mathrm{r}} > 0$ and

$$\varphi_{\mathrm{d}}(t) \triangleq -K_{\mathrm{r}}e_{\mathrm{r}}(t) - \upsilon(t) + (A_{\mathrm{m}} + k_{\mathrm{p}}I_p)y_{\mathrm{m}}(t) + B_{\mathrm{m}}r(t). \tag{4.36}$$

The problem of driving $e_{\mathrm{r}}(t)$ to the origin therefore reduces to design a full state feedback controller such that the following linear system

$$\dot{\omega}_u(t) = A_u\omega_u(t) + B_u u(t), \tag{4.37a}$$

$$\varphi(t) = C_u(t)\omega_u(t) + D_u(t)u(t), \tag{4.37b}$$

tracks the desired trajectory $\varphi_{\mathrm{d}}(t)$. Hence, the problem can be solved by simply applying the FRDE controller given in the Proposition 3.4.1 and the saturation mechanism provided in Theorem 3.4.1.

4.5 Implementation

Figure 4.1 presents the control framework, and the Fig 4.2 and the Fig 4.3 illustrate the predictor and the controller structures respectively.

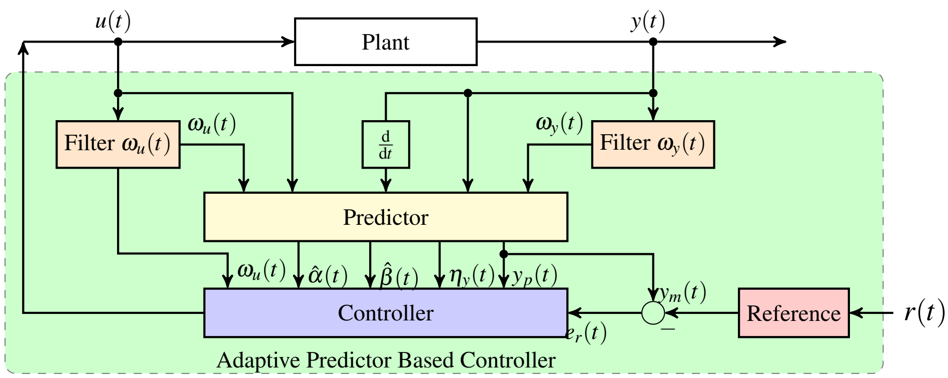

Figure 4.1: Adaptive Predictor based controller for nonlinear systems block diagram

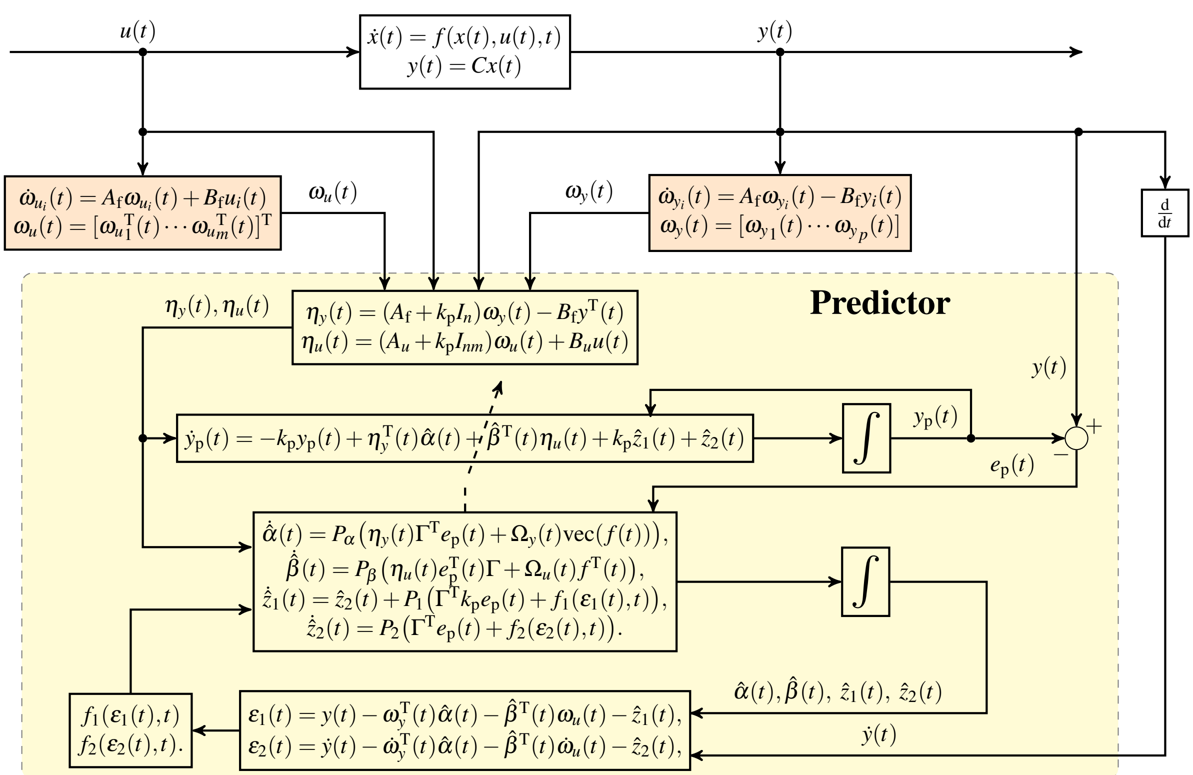

Figure 4.2: Predictor's structure for nonlinear systems

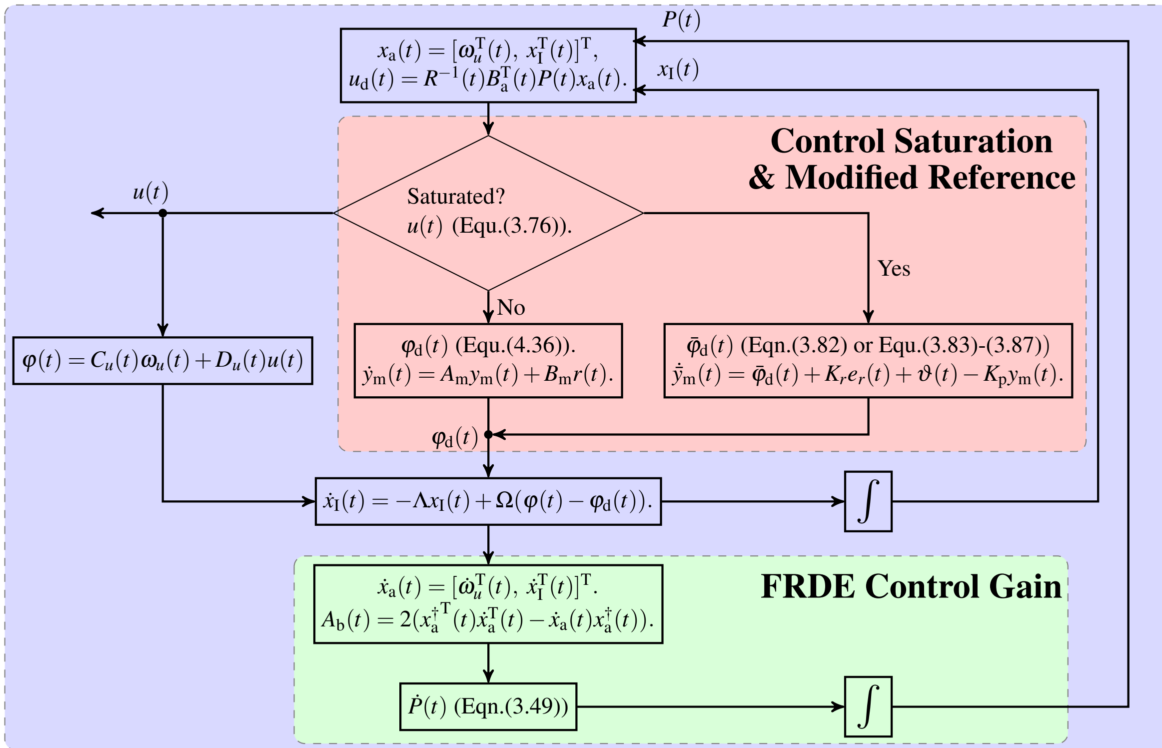

Figure 4.3: Controller's structure

4.6 Simulation

Example 4.6.1 *Consider designing a controller for the following nonlinear system*

$$\dot{x}(t) = \begin{bmatrix} -50 & 2 & 12 \\ -80 & -12 & 28 \\ -20 & -8 & 2 \end{bmatrix} x(t) + \begin{bmatrix} 0 & 0 \\ 0 & 2 \\ 2 & 3 \end{bmatrix} u(t) + \begin{bmatrix} \tanh(x_2(t)) + 2\sin(t) \\ 2\sin(3x_1(t)) \\ 3\sin(x_3(t))\cos(2x_1(t)x_2(t)) \end{bmatrix},$$

$$y(t) = \begin{bmatrix} 1 & 0 & 0 \\ 0 & 1 & 0 \end{bmatrix} x(t), \qquad x(0) = 0_3,$$

to track the reference system (3.3) with parameters $A_{\mathrm{m}} = -I_2,\ B_{\mathrm{m}} = I_2$ *and*

$$r_{\mathrm{d}}(t) = [-5\sin(4t + \pi/4)\ \ 2\sin(4t)]^{\mathrm{T}}.$$

The system dynamics is unknown and the vector state $x(t) \triangleq [x_1(t)\ x_2(t)\ x_3(t)]^{\mathrm{T}}$ *is not fully measurable. We only know the relative degrees* $r_{11} = r_{12} = 2;\ r_{21} = 2,\ r_{22} = 1.$

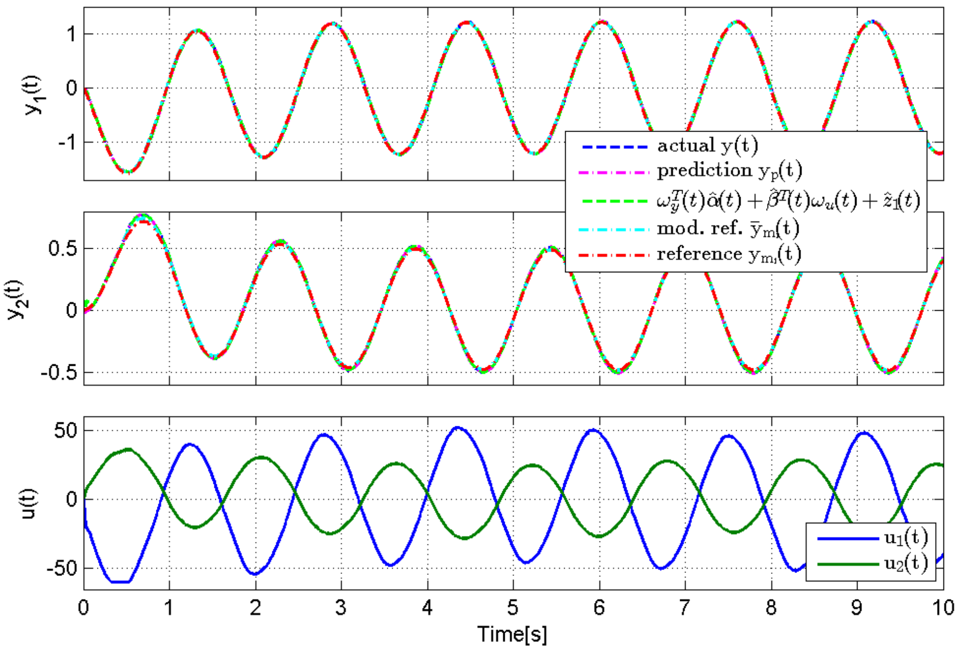

Figure 4.4: The system output, the predictor and the reference trajectories (top and middle) and the control effort (bottom) using the FDRE controller

To design the predictor, we chose a 3^{nd} *order filter defined in (3.10) with parameters*

$$A_{\mathrm{f}} = \begin{bmatrix} 0 & 1 & 0 \\ 0 & 0 & 1 \\ -3375 & -675 & -45 \end{bmatrix}, \quad B_{\mathrm{f}} = \begin{bmatrix} 0 \\ 0 \\ 1 \end{bmatrix}.$$

The predictor parameters are $k_{\mathrm{p}} = 5,\ P_\alpha = 10I_3,\ P_\beta = 10I_6,\ P_1 = 10^2 I_2$ *and* $P_2 = 5 \times 10^3 I_2$. $f_i(\varepsilon_1(t), t)$ *is chosen as in (4.31), with* $\sigma(\tau) = 1 + e_{\mathrm{p}}^{\mathrm{T}}(t) e_{\mathrm{p}}(t)$*. The initial conditions are* $y(0) = y_{\mathrm{p}}(0) = 0_2$, $y_{\mathrm{m}}(0) = 0_2$, $\omega_y(0) = \omega_u(0) = 0_6$, $\hat{\alpha}_{\mathrm{s}}(0) = [2400\ 500\ 12]^{\mathrm{T}}$, $\hat{\beta}_{11}(0) = [380\ 30\ 0]^{\mathrm{T}}$, $\hat{\beta}_{12}(0) = [450\ 50\ 0]^{\mathrm{T}}$, $\hat{\beta}_{21}(0) = [900\ 60\ 0]^{\mathrm{T}}$, $\hat{\beta}_{22}(0) = [1500\ 160\ 1.3]^{\mathrm{T}}$.

The augmented system has $\Lambda = \mathrm{diag}([2,4])$ *and* $\Omega = \mathrm{diag}([100,100])$*. The FDRE controller parameters are* $K_{\mathrm{r}} = \mathrm{diag}([20,40])$, $Q(t) = \mathrm{diag}([I_6,\ 100,\ 100]) - 2P(t)$, $R = I_2$, $\varepsilon = 10$ *and* $P_0 = 10^{-4} I_8$*. The saturation parameters are* $u_{\max} = 60$ *and* $\Delta u_{\max} = 1$*. Figure (4.4) illustrates the tracking result and the control effort. Note that* $\hat{\alpha}_s^{\mathrm{T}}(t)\omega_y(t) + \hat{\beta}^{\mathrm{T}}(t)\omega_u(t) + \hat{z}_1(t) \to y(t)$ *and*

$y(t),\ y_{\rm p}(t)$ *all converge to* $y_{\rm m}(t)$ *as* $t \to \infty$.

Example 4.6.2 *Consider the 3D Quanser helicopter, which has a dynamic system ([65])*

$$\dot{\eta}(t) = J(\eta(t))\nu(t), \qquad \eta(0) = \eta_0, \quad t \geq 0 \tag{4.38}$$

$$\dot{\nu}(t) = \Theta_1 \varphi(\eta(t)) + \Theta_2 \tau(t), \qquad \nu(0) = \nu_0, \tag{4.39}$$

where $\eta(t) \triangleq [\phi(t)\ \ \theta(t)\ \ \psi(t)]^{\rm T} \in \mathbb{R}^3$ *is the measured output where* $\phi(t),\ \theta(t),\ \psi(t)$ *are the roll, elevation and the travel angles respectively,* $\nu(t) \in \mathbb{R}^3$ *are the unmeasured states, and* $\tau(t) \in \mathbb{R}^2$ *is the control input applied to the system, and*

$$J(\eta) \triangleq \begin{bmatrix} 1 & \tan(\theta)\sin(\phi) & \tan(\theta)\cos(\phi) \\ 0 & \cos(\phi) & -\sin(\phi) \\ 0 & \sin(\phi)/\cos(\theta) & \cos(\phi)/\cos(\theta) \end{bmatrix}, \qquad \phi(\eta) \triangleq \begin{bmatrix} \cos(\theta)\cos(\phi) \\ -\cos(\theta)\sin(\phi) \end{bmatrix},$$

$$\Theta_1 = \begin{bmatrix} -2.6828 & 3.2966 \\ -9.8298 & -9.9455 \\ 0 & -20 \end{bmatrix}, \qquad \Theta_2 = \frac{1}{2}\begin{bmatrix} 0.25 & -0.25 \\ 0.575 & 0.575 \\ 0 & 0 \end{bmatrix}.$$

Note that system dynamics and parameters are only used to simulate the nonlinear plant, and we only know the relative degree $r_{ij} = 2,\ i = 1,2,\ j = 1,2.$

In order to apply the proposed controller, the system dynamics can be rewritten in the following nonlinear form

$$\dot{x}(t) = Ax(t) + Bu(t) + h(x(t), u(t), t), \quad x(0) = x_0, \quad t \geq 0, \tag{4.40a}$$

$$y(t) = Cx(t) \tag{4.40b}$$

where $A \in \mathbb{R}^{6\times 6}$, $B \in \mathbb{R}^{6\times 2}$ *and* $C \in \mathbb{R}^{3\times 6}$ *are unknown constant matrices,* $h(t)$ *is unknown nonlinear function, and* $u(t) = \tau(t) - \tau_0 \in \mathbb{R}^2$ *is the control signal, and* $\tau_0 = [25; 8]$ *is chosen arbitrarily.*

To implement the predictor, the autoregressive vectors are constructed using a $6^{\rm th}$ *order filter* *defined in (4.8) with parameters*

$$A_{\mathrm{f}} \triangleq \begin{bmatrix} 0_5 & & I_5 \\ -\lambda_5 & \dots & -\lambda_0 \end{bmatrix} \in \mathbb{R}^{6\times 6}, \quad B_{\mathrm{f}} \triangleq \begin{bmatrix} 0_5 \\ 1 \end{bmatrix} \in \mathbb{R}^6,$$

where $\det(sI_n - A_{\mathrm{f}}) = s^n + \lambda_5 s^{n-1} + \dots + \lambda_1 s + \lambda_0 = (s+5)^6$. *The predictor parameters are* $k_{\mathrm{p}} = 10$, $P_\alpha = 10I_6$, $P_\beta = 10I_{12}$, $P_1 = 10I_3$ *and* $P_2 = 10I_3$. $f_i(\varepsilon_i(t),t)$ *is chosen as in (4.31), with* $\sigma(\tau) = 1 + e_{\mathrm{p}}^{\mathrm{T}}(t)e_{\mathrm{p}}(t)$. *The initial conditions are* $y_0 = \frac{\pi}{180}[2\ -27\ 0]^{\mathrm{T}}$, $y_p(0) = \frac{\pi}{180}[2\ -20\ 0]^{\mathrm{T}}$ *and*

$$\hat{\alpha}_s^{\mathrm{T}}(0) = [-\lambda_0 \dots - \lambda_5] = [-15625\ -18750\ -9375\ -2500\ -375\ -30],$$

$$\hat{\beta}^{\mathrm{T}}(0) = \begin{bmatrix} 0 & 0 & 0 & 0 & 0.2 & 0 & 0 & 0 & 0 & 0 & -0.2 & 0 \\ 0 & 0 & 2 & 0 & 0.2 & 0 & 0 & 0 & -0.2 & 0 & 0.2 & 0 \\ 0 & 0 & 2 & 0 & 0 & 0 & 0 & 0 & -2 & 0 & 0 & 0 \end{bmatrix}.$$

The projector operator boundary for $\hat{\alpha}(t)$ *and* $\hat{\beta}(t)$ *are setup at* $\hat{\alpha}_{\max,\min} = \hat{\alpha}(0) \pm 0.2\hat{\alpha}(0)$ *and* $\hat{\beta}_{\max,\min} = \hat{\beta}(0) \pm 0.5(\hat{\beta}(0) + 0.1I_{3\times 12}$.

First, we aim to control only the pitch and elevation angle $[\phi(t)\ \theta(t)]^{\mathrm{T}}$ *of the helicopter to track the output* $y_{\mathrm{m}} = [\phi_{\mathrm{d}}(t)\ \theta_{\mathrm{d}}(t)]^{\mathrm{T}}$ *of the reference system (4.2) with* $A_m = -I_2, B_m = I_2$ *and the reference signal* $r_{\mathrm{d}}(t) = \frac{\pi}{180}[10\sin(0.4\pi t)\ \ 15\sin(0.2\pi t)]^{\mathrm{T}}$.

The augmented system has $\Lambda = \mathrm{diag}([10,\ 10])$ *and* $\Omega = \mathrm{diag}([1000,\ 500])$. *The FDRE controller parameters are* $K_{\mathrm{r}} = -5I_2$, $Q(t) = \mathrm{diag}([I_{12},\ 50,\ 50]) - P(t)$, $R = 0.5I_2$, $\varepsilon = 20$ *and* $P_0 = I_{14}$. *The saturation parameters are* $u_{\max} = 6$ *and* $\Delta u_{\max} = 1$. *Figure (4.5) illustrates the tracking result and the control effort. In this example, we control two outputs by using two actuators; since the system is square, we can achieve the exact tracking result for both outputs simultaneously.*

Secondly, we attempt to control the system's output to track the desired trajectory $y_{\mathrm{m}} = [\phi_{\mathrm{d}}(t)\ \theta_{\mathrm{d}}(t)\ \psi_{\mathrm{d}}(t)]^{\mathrm{T}}$, *using the reference system (3.3) with* $A_m = -I_3, B_m = I_3$ *and*

$$r_{\mathrm{d}}(t) = \frac{\pi}{180}[0\ 10\sin(0.08\pi t)\ 90\sin(0.12\pi t)]^{\mathrm{T}}.$$

For this situation, since we aim to control 3 outputs of the system simultaneously by using only

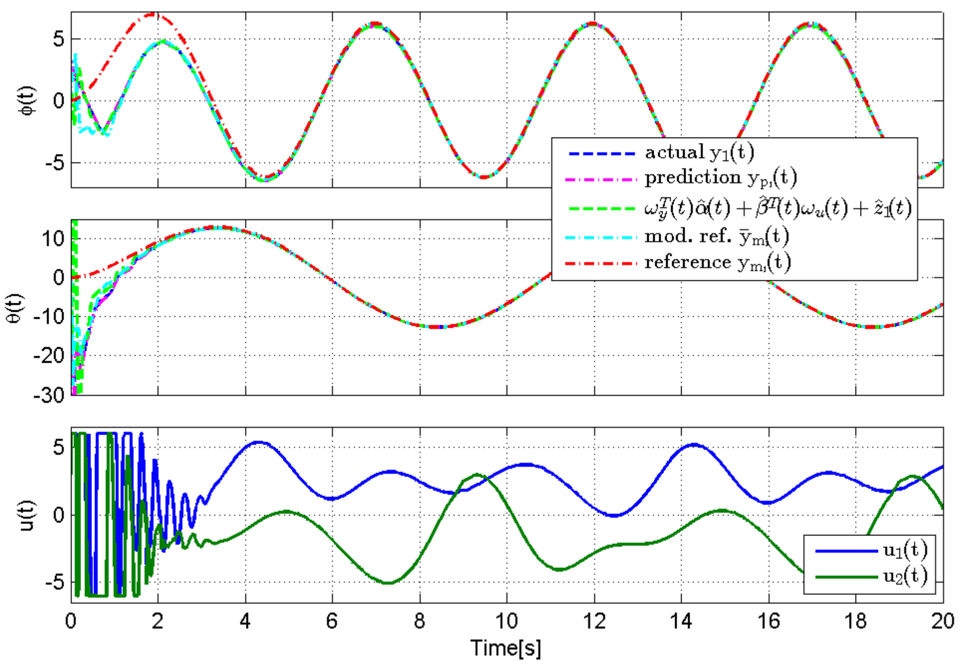

Figure 4.5: The system output $y(t)$, the predictor output $y_{\mathrm{p}}(t)$, the modified reference $\bar{y}_{\mathrm{m}}(t)$ and the reference signals $y_{\mathrm{m}}(t)$ (top and middle) and the control effort (bottom) using the FDRE controller

two actuators, the system is an under-actuated, which implies that there is a constraint between 3 feasible outputs $[\phi_{\mathrm{d}}(t)\ \theta_{\mathrm{d}}(t)\ \psi_{\mathrm{d}}(t)]$. *Therefore, an arbitrary selection of the desired outputs is not necessarily achievable. In order to handle such constraint, different entries in the matrices* Ω *and* $Q(t)$ *are selected depending on each output's priority.*

The augmented system has $\Lambda = \mathrm{diag}([10,\ 10,\ 20])$ *and* $\Omega = \mathrm{diag}([1,\ 1,\ 6] \times 10^3)$. *The FDRE controller parameters are* $K_{\mathrm{r}} = \mathrm{diag}([-2, -2, -4])$, $Q(t) = \mathrm{diag}([I_{12},\ 50,\ 50]) - 8P(t)$, $R = 10I_2$, $\varepsilon = 15$ *and* $P_0 = I_{14}$. *The saturation parameters are* $u_{\max} = 6$ *and* $\Delta u_{\max} = 1$. *Figure (4.6) illustrates the tracking result and the control effort.*

Note that although the plant, the predictor and the reference started at different initial conditions, they all converge at the end. For the second case, worth noting is that the tracking performance of the pitch angle $\phi(t)$ *is not as good as that of the other states. This is due to our particular choice of weights in matrices* Ω *and* $Q(t)$, *which penalizes the tracking error of* $\theta(t)$ *and* $\psi(t)$ *more than the tracking error of* $\phi(t)$. *Regardless, we note that the tracking error of* $\phi(t)$ *remains small*

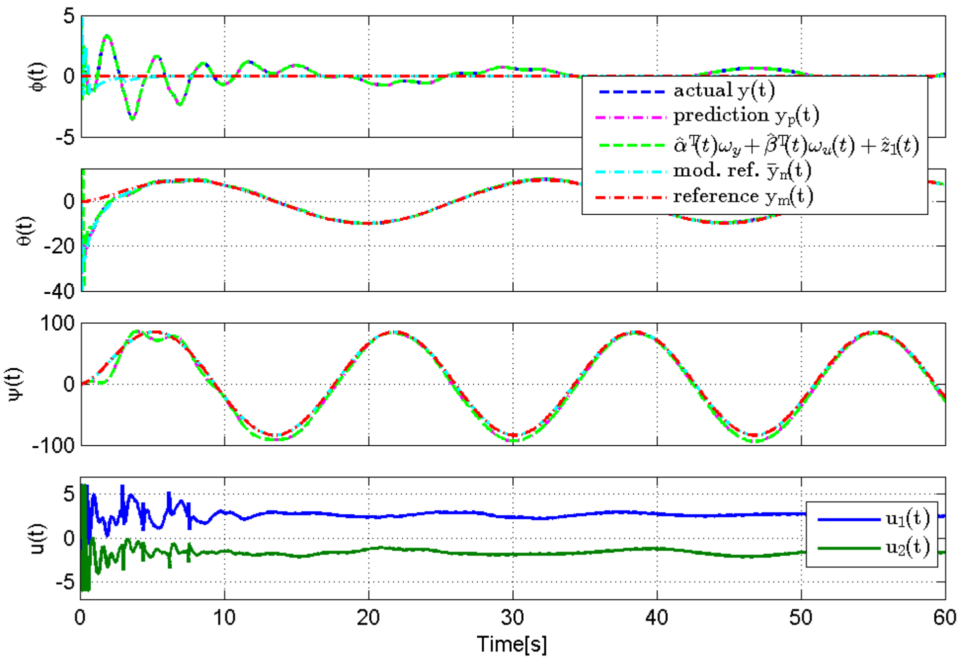

Figure 4.6: The system output $y(t)$, the predictor output $y_p(t)$, the modified reference $\bar{y}_m(t)$ and the reference signals $y_m(t)$ (top and middle) and the control effort (bottom) using the FDRE controller.

and bounded with the maximum error is about 1^o.

4.7 Experimental Setup and Result

The controller performance is further studied by considering the real time implementation on the Quanser 3-DOF helicopter with the same experiment setup described in Section 3.7.

The system model is unknown, but we assume that it has a minimal representation consisting of 6 states ($n = 6$), and relative degrees $r_{ij} = 2,\ i = 1,3,\ j = 1,2$. When the control is set at $v^* = [12.5\ \ 12.5](Vol)$, the system stays at the equilibrium point $x^* = 0_6$. We make the same assumption and use the same filters as in Example 4.6.2.

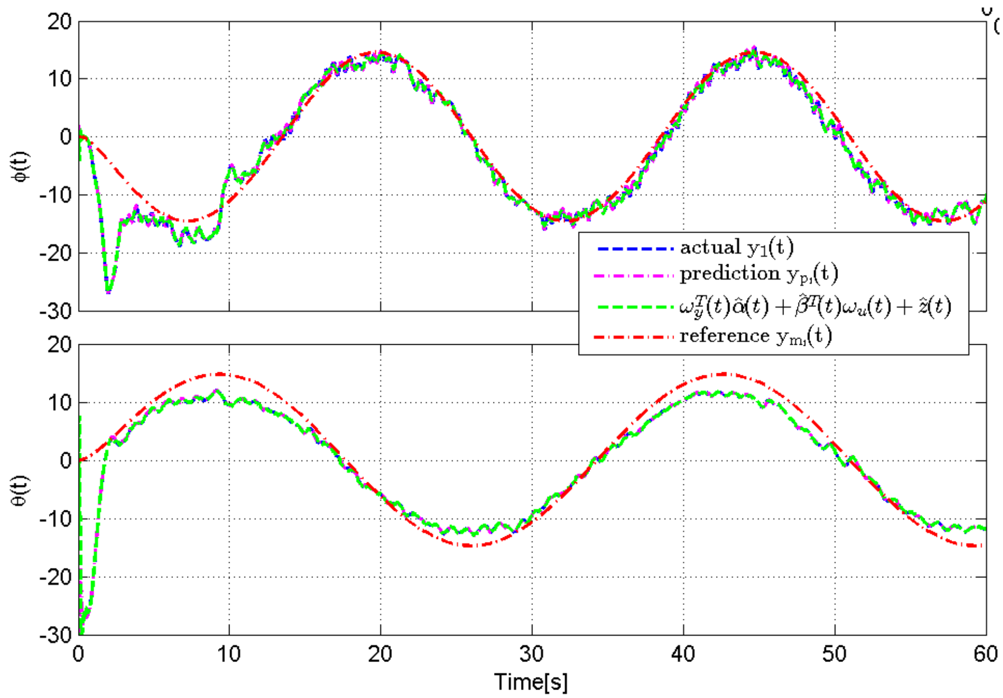

Figure 4.7: The time evolution of $y(t)$, $y_{\mathrm{p}}(t)$, and $y_{\mathrm{m}}(t)$ for the parameters described in Set 1

4.7.1 Tracking Pitch and Elevation

In this section, we aim to control only the pitch and elevation angle $[\phi(t)\ \ \theta(t)]^{\mathrm{T}}$ of the helicopter to track the output $y_{\mathrm{m}} = [\phi_{\mathrm{d}}(t)\ \ \theta_{\mathrm{d}}(t)]^{\mathrm{T}}$ of the reference system (4.2) with $A_m = -I_2, B_m = I_2$ and the reference signal

$$r_{\mathrm{d}}(t) = \frac{\pi}{180}[5\sin(0.08\pi t)\ \ 10\sin(0.06\pi t)].$$

Figure 4.7 demonstrates the controller's tracking performance with the initial conditions and control parameters selected as in Set (1)

Set 1: The predictor parameters are $k_{\mathrm{p}} = 10,\ P_\alpha = 10I_6, P_\beta = 10I_{12}, P_1 = P_2 = 100I_2$. $f_i(\varepsilon_i(t),t)$ is chosen as in (4.31), with $\sigma(\tau) = 1 + e_{\mathrm{p}}^{\mathrm{T}}(t)e_{\mathrm{p}}(t)$. The initial conditions are $y_0 = \frac{\pi}{180}[0\ -27\ 0]^{\mathrm{T}}$, and $y_p(0) = \frac{\pi}{180}[2\ -25\ 0]^{\mathrm{T}}$ and

$$\hat{\alpha}^{\mathrm{T}}(0) = [-\lambda_0 \ldots -\lambda_5] = [-15625\ -18750\ -9375\ -2500\ -375\ -30],$$

$$\hat{\beta}^{\mathrm{T}}(0) = \begin{bmatrix} 0 & 0 & 0 & 0 & 0.07 & 0 & 0 & 0 & 0 & 0 & -0.07 & 0 \\ 0 & 0 & 0 & 0 & 0.1 & 0 & 0 & 0 & 0 & 0 & 0.1 & 0 \\ 0 & 0 & -1 & 0 & 0 & 0 & 0 & 0 & 1 & 0 & 0 & 0 \end{bmatrix}.$$

The projector operator boundary for $\hat{\alpha}(t)$ and $\hat{\beta}(t)$ are setup at $\hat{\alpha}_{\text{max,min}} = \hat{\alpha}(0) \pm 0.2\hat{\alpha}(0)$ and $\hat{\beta}_{\text{max,min}} = \hat{\beta}(0) \pm 0.5(\hat{\beta}(0) + 0.1I_{3\times 12}$. The augmented system has $\Lambda = \text{diag}([35,\ 10])$ and $\Omega = \text{diag}([8,8] \times 10^3)$. The FDRE controller parameters are $K_{\mathrm{r}} = \text{diag}([2,2])$, $Q(t) = \text{diag}([I_{12},\ 50,\ 50]) - 5P(t)$, $R = I_2$, $\varepsilon = 10$ and $P_0 = I_{14}$. The saturation parameters are $u_{\max} = 3.75(Vol)$. Figure 4.7 shows that although the plant, the predictor and the reference started at different initial conditions, they all converge to each other.

4.7.2 Tracking 3 DOF

In this section, we aim to control the system to track the reference system (3.3) where $y_{\mathrm{m}} = [\phi_{\mathrm{d}}(t)\ \theta_{\mathrm{d}}(t)\ \psi_{\mathrm{d}}(t)]^{\mathrm{T}}$ is the desired trajectory, and $A_m = -I_3$, $B_m = I_3$ for different reference inputs. Figure 4.8 to Fig 4.10 demonstrate the control's tracking performance using the same predictor selected in Set (2), and different control gains for different reference inputs.

The predictor uses the same parameter as in Set 1. Figure 4.8 demonstrates the tracking performance for a step reference input $r(t) = \frac{\pi}{180}[0,0,20]$ with the control gains $K_{\mathrm{r}} = 2I_3$ and $\Lambda = \text{diag}([30,\ 16,\ 18])$, $\Omega = \text{diag}([2.5,\ 2,\ 2.7] \times 10^4)$, $Q(t) = \text{diag}([I_{12},\ 30,\ 30,\ 30])$, $R = I_2$, $\varepsilon = 1$ and $P_0 = I_{15}$. The saturation parameters are $u_{\max} = [2\ 2]$.

Figure 4.9 illustrates the controller's tracking performance for the reference inputs

$$r(t) = \frac{\pi}{180}[0\ \ 0\ \ 40\sin(0.12\pi t)]^{\mathrm{T}},$$

using the control gains $K_{\mathrm{r}} = \text{diag}([2,\ 2,\ 8])$ and $\Lambda = \text{diag}([30,\ 16,\ 18])$, $\Omega = \text{diag}([2.2,\ 1,\ 10] \times 10^4)$, $Q(t) = \text{diag}([I_{12},\ 60,\ 60,\ 60]) - 5P(t)$, $R = I_2$, $\varepsilon = 10$ and $P_0 = I_{15}$. The saturation parameters are $u_{\max} = [3.75\ 3.75]$.

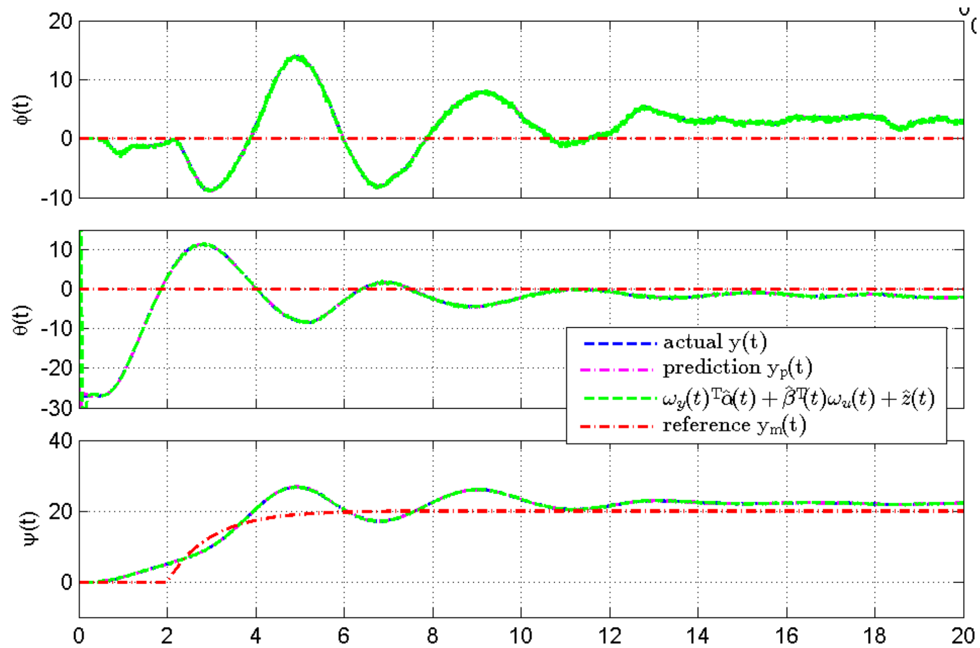

Figure 4.8: The time evolution of $y(t)$, $y_p(t)$, and $y_m(t)$ under a random impulse disturbance

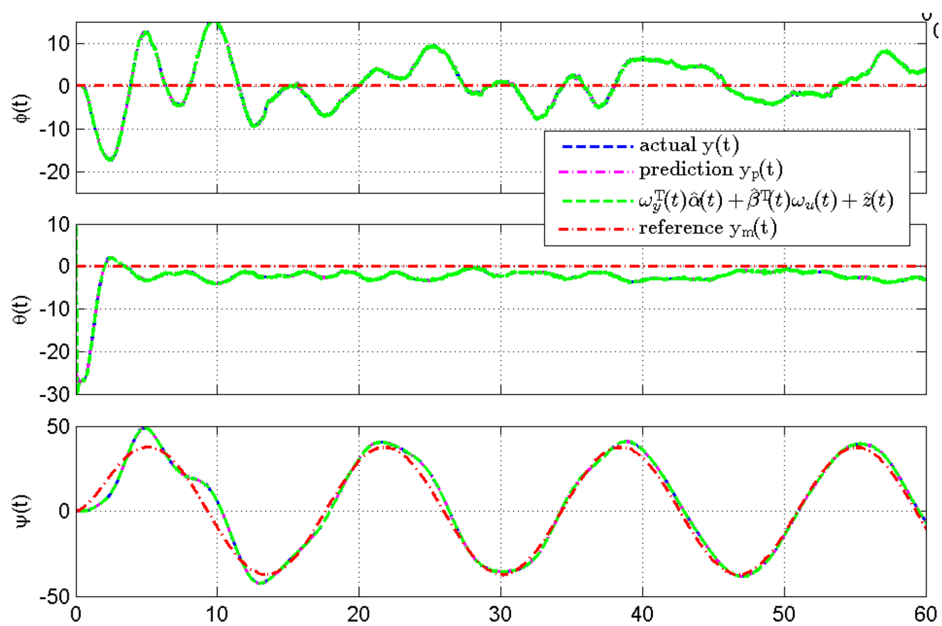

Figure 4.9: The time evolution of $y(t)$, $y_p(t)$, and $y_m(t)$ for $r(t) = \frac{\pi}{180}[0\ 0\ 40\sin(0.12\pi t)]^T$

Finally, Fig 4.10 depicts the experimental tracking results for the reference input

$$r(t) = \frac{\pi}{180}[0\ \ 15\sin(0.08\pi t)\ \ 30\sin(0.12\pi t)]^T,$$

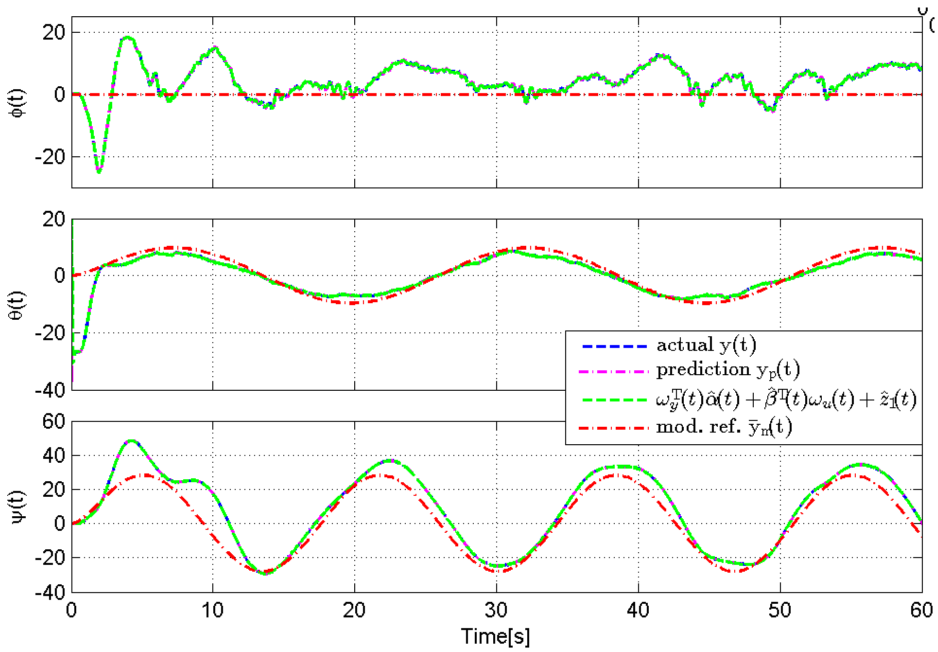

Figure 4.10: The time evolution of $y(t)$, $y_{\mathrm{p}}(t)$, and $y_{\mathrm{m}}(t)$ for the reference input $r(t) = \frac{\pi}{180}[0\ 10\sin(0.08\pi t)\ 30\sin(0.12\pi t)]^{\mathrm{T}}$.

using the control gains $K_{\mathrm{r}} = \mathrm{diag}([2,\ 2,\ 9])$ and $\Lambda = \mathrm{diag}([35,\ 16,\ 18])$, $\Omega = \mathrm{diag}([2.5,\ 1.8,\ 13] \times 10^4)$, $Q(t) = \mathrm{diag}([I_{12},\ 60,\ 60,\ 60]) - 5P(t)$, $R = I_2$, $\varepsilon = 10$ and $P_0 = I_{15}$. The saturation parameters are $u_{\max} = [3.75\ 3.75]$ and $\Delta u_{max} = 0.06$ between the sampling interval $\Delta t = 0.001$.

Figure 4.11 depicts the control voltage applied on the system for the tracking task shown in Fig 4.10. Worth noting is that the tracking performance of the pitch angle $\phi(t)$ is not as good as that

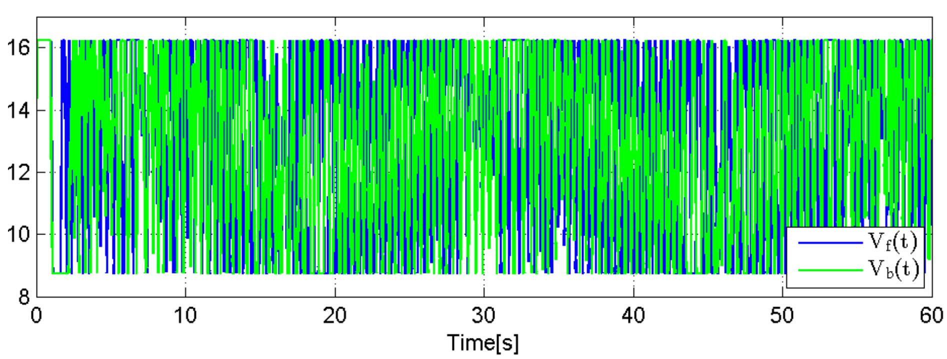

Figure 4.11: The time evolution of control input $u(t)$

of the other states. This is due to our particular choice of weights in matrices Ω and $Q(t)$, which penalizes the tracking error of $\theta(t)$ and $\psi(t)$ more than the tracking error of $\phi(t)$. Comparing the experimental results from Chapter 3 and Chapter 4, we can see that incorporating the adaptive nonlinear terms to the predictor proposed in Chapter 4 improved the tracking performance and the transience of control signal.

4.8 Conclusion

This section presents a novel output feedback control for a class of unknown nonlinear systems. Extending the control approach for linear systems presented in Chapter 3, the algorithm for nonlinear systems also has three main components, which are the adaptive predictor, the controller and the reference system. The only required knowledge about the system is its relative degree in order to ensure the topological equivalence between the predictor and the plant. The prediction error is proved to be uniform ultimately bounded based on the Lyapunov direct method. From that, any available control algorithms that can drive the predictor to track the desired trajectories can also simultaneously drive the plant output to converge to the desired trajectories. Particularly, the FRDE and the saturation mechanism established in Chapter 3 are reused in this chapter. The proposed controller performance is demonstrated by simulation. Furthermore, it is also experimentally tested on the Quanser helicopter. Experiments demonstrates the successfulness of the method for systems with unmodeled dynamics and unmeasured states in presence of control saturation constraints.

One problem with the approach presented in this chapter is that in the presence of time-varying uncertain parameters, the only option to reduce the bound of the prediction error is to increase the adaptive gain to a significantly large value. However, high gain adaptation will induce high frequencies in the adaptive parameters, which leads to a problem of noisy control signals. This is a well know trace-off problem of adaptive control when the uncertainties are time-varying. Furthermore, the FRDE is quite computationally expensive, especially for high order systems. These problems will be addressed in the next chapter.

Chapter 5

Adaptive Predictor-Based Output Feedback Control for a Class of High Relative Degree Uncertain Nonlinear Systems with Fast Adaptation and Simple Control Structure

The results featured in this chapter are the object of an article published in Journal of Dynamic Systems, Measurement and Control ([67]).

5.1 Introduction

One of the biggest challenges in designing adaptive controllers for an uncertain nonlinear system with high relative degree is that due to the cascade structure, the mismatched uncertainties appearing in the first level can not be directly cancelled by the control signal appearing in the lowest level. Instead, the control signal would need to know the high order derivatives of the uncertainties in order to indirectly compensate for these mismatches. The problem becomes even harder when the uncertainties are time-varying, hence their derivatives are unknown.

The most common approach to handling this problem is *adaptive backstepping control* ([15]) and its variations, such as *dynamic surface control* ([24, 26, 68–72]) or *command filtered backstepping* ([28, 73–75]). In general, for backstepping-like control techniques, the adaptive laws will be used to estimate the uncertainties at the first level. Then, the estimated terms will be differentiated as many times as the system relative degrees. In order to avoid numerical differentiation of the estimated terms, the original adaptive backstepping ([15]) proposes a systematic design approach, in which the adaptive laws are recursively designed to estimate at each level, so that the uncertainty's derivatives are available to feed to the lower level. The design process will require r step, where r is the system relative degrees, until the uncertainties's derivatives are available to cancel directly at the level of the control signal. However, this approach leads to an extremely complicated control structure, which is well known as the "explosion of terms" effect, that prevents its practical implementation for systems with the relative degree larger than 3. Giving up in implementing the analytical approach, the backstepping variations return to the original idea, in which the uncertainties are estimated once by adaptive laws at the first level. Then, the estimated terms are fed to the low pass filters before being differentiated to approximate their derivatives. Theoretically, it can be proved that the desired boundedness of the tracking error can be obtained by choosing sufficiently high gain for the low pass filters ([28, 73–75]). Therefore, the backstepping variations can yield simpler solutions, but the control signals suffer from high magnitude effects due to the approximation of the virtual control signals' differentiations. This effect is more serious if high adaptation gain is used. On the other hand, small adaptation gains lead to slow convergence and unsatisfied tracking results. This is a well known trade-off of backstepping-like adaptive controls, besides its complexity and the computational burden of building the cascade of low pass filters for high relative degree systems. Another idea to reduce the unmatched uncertainty to matched certainty is to estimate the high order derivatives of the outputs, which is in general equivalent to estimating the full state. The most common technique is *adaptive sliding mode control* (ASMC) ([5, 76–90]). However, despite many attempts to reduce the intrinsic chattering effect, estimating high order derivatives of the outputs in ASMC, especially in the presence of corrupting noise, is still not appealing to many practitioners. In short, the literature shows that for high relative degree systems, the exact backstepping approach can yield the best transient behavior but it is too complicated to apply. In contrast, approximating approaches are simpler but often require some sort of high-gain parameters; hence encountering the trade-off problems between the smoothness of control signals and acceptable tracking performances. In addition, the complexity of the controller increases as the systems relative degree increases.

Therefore, this chapter proposes an adaptive control for a class of unknown dynamics systems with unmatched uncertainty and high relative degrees. The proposed controller has three components: the predictor, the controller and the reference system, similar to that in Chapter 3 and Chapter 4. However, the proposed controller avoids the recursive step-by-step design of backstepping or the expensive computation of FRDE, and therefore is significantly simpler than the mentioned approaches. In order to guarantee the smoothness of the control signals and fast convergence, the feed-forward gain recently proposed in ([91, 92]) is incorporated into the predictor. It can be shown that by appropriately choosing the tuning parameters, the tracking error can be rendered as small as desired while the control signal is still smooth. The controller is then applied to control a musculoskeletal system to track a desired trajectory. Specifically, the model Arm26 provided in OpenSim ([54]) is selected to validate our proposed controller.

This chapter is organized as follows. Section 5.2 establishes the mathematical background and the problem formulation. Section 5.3 summarizes the main results and presents the controller structure. Analysis and assumptions about the systems are provided in Section 5.4. In Section 5.5, the output predictor using fast adaptation is derived. Design of the controller for the SISO case is then presented in Section 5.6. In addition, the transient behavior of the control signal and the tracking errors are analyzed in Section 5.7. Section 5.8 provides numerical simulations to illustrate the algorithm's efficacy. Section 5.9 presents simulations to control the musculotendon arm model. Section 5.10 presents a discussion to distinguish our work from literature and Section 5.11 concludes this chapter.

5.2 Mathematical Preliminaries

Lemma 5.2.1 *([92]) Consider the following SISO sytem*

$$\begin{bmatrix} \dot{z}_1(t) \\ \dot{z}_2(t) \end{bmatrix} = \begin{bmatrix} 0 & 1 \\ -\gamma h(t) & -2a \end{bmatrix} \begin{bmatrix} z_1(t) \\ z_2(t) \end{bmatrix} + \begin{bmatrix} b_1 \\ b_2 \end{bmatrix} f(t) \tag{5.1}$$

where $\gamma > 0$, $0 < h_1 \leq h(t) \leq h_2$ *and* $f(t) : \mathbb{R}^+ \to \mathbb{R}$ *is piecewise continuous and bounded function. Let* $h_0 \triangleq (h_1 + h_2)/2$, $h_3 \triangleq (h_2 - h_1)/2$, $\omega^2 \triangleq \gamma h_0$, *and* $a \triangleq \zeta\omega$. *If* $\zeta \geq 1$, *then the following bounds are hold*

$$|z_1(t)| \leq c_4 e^{-\nu t} + \left[\frac{c_1 |b_1| \sqrt{h_0}}{h_1 \sqrt{\gamma}} + \frac{|b_2|}{h_1 \gamma} \right] \|f(t)\|_{\mathscr{L}_\infty},$$
$$|z_2(t)| \leq c_4 e^{-\nu t} + \left[|b_1|(1 + \frac{h_3}{h_1} c_1 c_2) + \frac{c_2 |b_2| \sqrt{h_0}}{\sqrt{\gamma}} \right] \|f(t)\|_{\mathscr{L}_\infty}$$

where $c_4 \triangleq c_3 \|z(0)\|$, $c_3 > 0$, $\nu = \frac{\sqrt{\gamma}}{2}(\sqrt{\zeta h_0} - \sqrt{\zeta h_0 - h_1})$, $c_1 \geq 2$ *and* $\frac{2}{e} \geq c_2 > 0$.

Consider the following nonlinear MIMO system $\mathscr{G}$

$$\dot{\xi}(t) = f(\xi(t), u(t), t) \quad \xi(0) = \xi_0, \quad t \geq 0,$$
$$y(t) = C\xi(t),$$

where $\xi(t) \in \mathbb{R}^n$ is the unmeasured state vector, $y(t) \in \mathbb{R}^p$ is the output, $u(t) \in \mathbb{R}^m$ is the control input, $f : \mathbb{R}^n \times \mathbb{R}^m \times \mathbb{R}^+ \to \mathbb{R}^n$ is a $\mathscr{C}^0$ unknown nonlinear function, and $C = [c_1 \ldots c_p]^{\mathrm{T}} \in \mathbb{R}^{p \times n}$ where $c_i \in \mathbb{R}^n,\ i = 1 \ldots p$ are unknown vectors defined accordingly. The known relative degree of $u_j(t)$ with respect to $y_i(t)$ is denoted with r_{ij}. Since the solutions for systems with relative degree $r_{ij} = 1$ are well established in the literature (i.e [93]), we shall only consider the systems which have $r_{ij} \geq 2$.

The control objective is to design an adaptive controller to ensure that, for a given bounded reference input $r(t) \in \mathbb{R}^p$, $y(t)$ tracks the output $y_{\mathrm{m}}(t)$ of the following desired system

$$\dot{x}_{\mathrm{m}}(t) = A_{\mathrm{m}} x_{\mathrm{m}}(t) + B_{\mathrm{m}} k_g r(t), \quad x_{\mathrm{m}}(0) = x_0, \tag{5.2a}$$
$$y_{\mathrm{m}}(t) = C_{\mathrm{m}} x_{\mathrm{m}}(t), \tag{5.2b}$$

where A_{m} is stable, $k_g \triangleq -(C_{\mathrm{m}} A_{\mathrm{m}}^{-1} B_{\mathrm{m}})^{-1}$ and $A_{\mathrm{m}},\ B_{\mathrm{m}},\ C_{\mathrm{m}}$ are chosen appropriately as presented later.

In the following sections, parameters explicit time dependence (t) are used upon introduction, and then omitted thereafter except for emphasis.

5.3 Main results

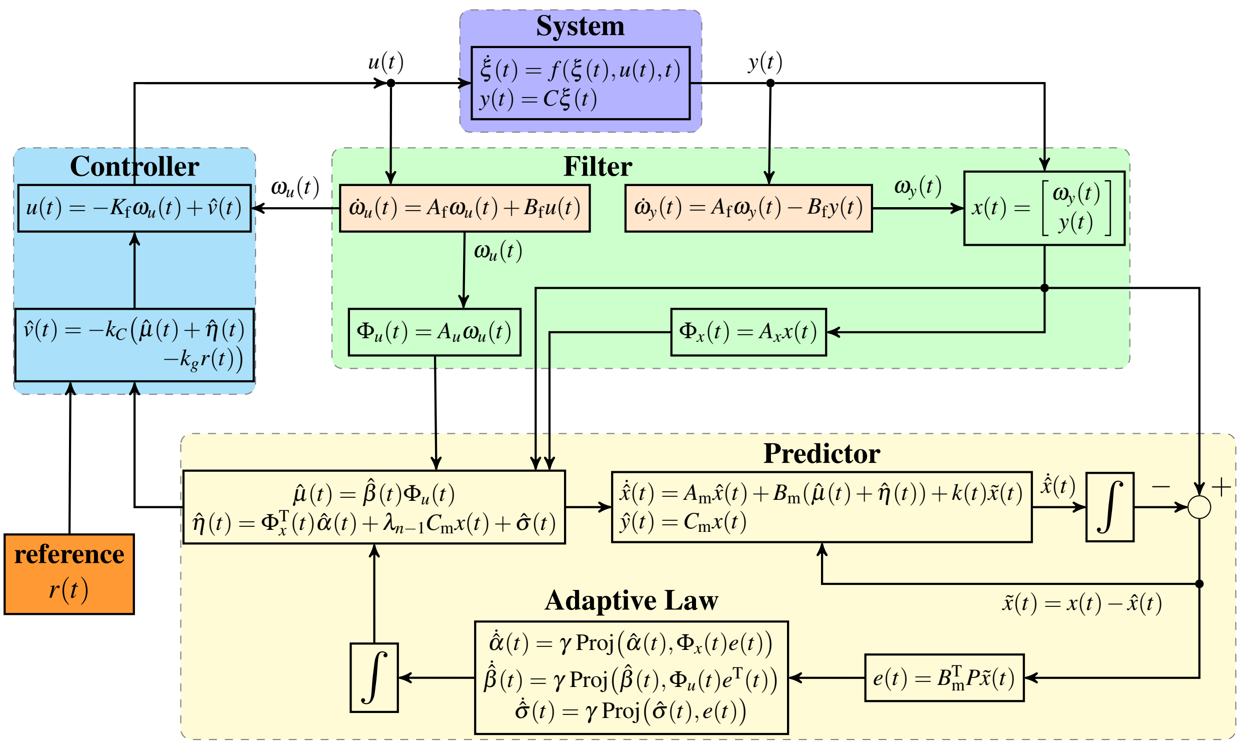

Figure 5.1: Controller structure for SISO systems

The chapter's main results are summarized as follow

- **System Analysis**: In this section, main assumptions are made to represent the system dynamics in an useful form for control and analysis. Furthermore, problems that are not easily solved by common control techniques are presented to promote our new controller structure.

- **Predictor with fast adaptation**: The fast adaptation technique is presented to address the problem of estimating time-varying parameters, and the prediction error is analyzed in this section. In contrast with classical adaptive control approaches, it will be shown that the prediction error can be specified as small as needed without damaging the control signal transient by increasing the adaptive gain.

- **Simple control structure** is then presented to address the problem of canceling the mismatched uncertainties of high relative degree systems. In addition, we also show how difficult is to solve this problem if common control techniques such as *backstepping* , *dynamics surface control* or *command filter backstepping* are used instead.

- **Transient Analysis**: Finally, all the prediction and control errors are proved to be bounded, and the bounds can be designed as small as needed by tuning appropriate parameters.

Figure 5.1 illustrates the controller structure for the SISO case.

5.4 System Analysis

In a given compact operating domain $\mathscr{D} \subset \mathbb{R}^n \times \mathbb{R}^m \times \mathbb{R}^+$, the system $\mathscr{G}$ can be rewritten as

$$\begin{aligned} \dot{\xi}(t) &= A\xi(t) + Bu(t) + h(\xi(t), u(t), t), \quad \xi(0) = \xi_0, \\ y(t) &= C\xi(t), \end{aligned}$$

where $A \in \mathbb{R}^{n\times n}$, $B = [b_1 \ldots b_m] \in \mathbb{R}^{n\times m}$, $b_j \in \mathbb{R}^n,\ j = 1\ldots m$ are unknown matrices, and

$$h(\xi,u,t) \triangleq f(\xi,u,t) - A\xi(t) - Bu(t)$$

is the unknown nonlinear term.

Assumption 5.4.1 *In the domain $\mathscr{D}$, there exists a pair (A,B) such that the linear system (A,B,C) is minimum phase, and $\|h(\xi,u,t)\|$ and $\|\dot{h}(\xi,u,t)\|$ are radically bounded, i.e. $\|h(\xi,u,t)\|_{\mathscr{L}_\infty} \leq$*

$\delta_0 < \infty$, $\|\dot{h}(\xi,u,t)\|_{\mathscr{L}_\infty} \leq \delta_1 < \infty$. *For instance, if* (ξ_e,u_e) *is an equilibrium point, one possible choice of* A *and* B *is*

$$A \triangleq \frac{\partial f}{\partial \xi}(\xi_\mathrm{e},u_\mathrm{e}),\ \ B \triangleq \frac{\partial f}{\partial u}(\xi_\mathrm{e},u_\mathrm{e}),\ \ (\xi_e,u_e) \in \mathscr{D}.$$

The Lemma 5.4.1 is restated as follow with the minor change of the definition of α to facilitate the proof in the next sections.

Lemma 5.4.1 *The* i^{th} *output of the system* $\mathscr{G}$ *can be represented in the Laplace domain by the following transfer function*

$$y_i(s) = G_i(s)u(s) + H_i(s)h(s) = \frac{\sum_{j=1}^{m} N_{ij}(s)u_j(s)}{D(s)} + \frac{Z_i(s)h(s)}{D(s)},$$

where $G_i(s) \triangleq c_i^{\mathrm{T}}(sI_n - A)^{-1}B$ *is the transfer function of* $u(t)$ *relative to the output* $y_i(t)$*, and* $H_i(s) \triangleq c_i^{\mathrm{T}}(sI_n - A)^{-1}$ *is the transfer function of* $h(t)$ *relative to the output* $y_i(t)$*. Let* $S(s) \triangleq [s^{n-1} \ldots s\ 1]^{\mathrm{T}} \in \mathbb{C}^n$*, then the denominator and the numerator's component of* $G_i(s)$ *are defined as*

$$D(s) \triangleq \det(sI_n - A) = s^n + \alpha^{\mathrm{T}} S(s), \qquad N_{ij}(s) \triangleq c_i^{\mathrm{T}} A_\mathrm{a}(s) b_j = \beta_{ij}^{\mathrm{T}} S(s),$$

where

$$\alpha \triangleq [\alpha_{n-1} \ldots \alpha_0]^{\mathrm{T}} \in \mathbb{R}^n, \qquad \beta_{ij} \triangleq [0_{r_{ij}-1}^{\mathrm{T}}\ \beta_m^{(ij)} \ldots \beta_0^{(ij)}]^{\mathrm{T}} \in \mathbb{R}^n.$$

Furthermore, $Z_i(s) \triangleq c_i^{\mathrm{T}} A_\mathrm{a}(s)$*, where* $A_\mathrm{a}(s)$ *denotes the adjunct matrix of* $(sI_n - A)$*. Then, the system output can be obtained as follows*

$$y(t) = \omega_y^{\mathrm{T}}(t)(\alpha - \lambda) + \beta^{\mathrm{T}} \omega_u(t) + z(t), \quad t \geq 0, \tag{5.3}$$

where $\lambda \in \mathbb{R}^n$ *and* $\beta \in \mathbb{R}^{nm \times p}$ *are defined as*

$$\lambda \triangleq \left[\begin{array}{ccc} \lambda_{n-1} & \ldots & \lambda_0 \end{array}\right]^{\mathrm{T}} \in \mathbb{R}^n, \qquad \beta \triangleq \left[\begin{array}{ccc} \beta_{11} & \cdots & \beta_{p1} \\ \vdots & \ddots & \vdots \\ \beta_{1m} & \cdots & \beta_{pm} \end{array}\right] \in \mathbb{R}^{nm \times p},$$

and $\omega_y(t) \in \mathbb{R}^{n\times p}$ *and* $\omega_u(t) \in \mathbb{R}^{nm}$ *are defined as*

$$\omega_y(t) \triangleq [\omega_{y_1}(t)\cdots\omega_{y_p}(t)], \quad \omega_u(t) \triangleq [\omega_{u1}^{\mathrm{T}}(t)\cdots\omega_{um}^{\mathrm{T}}(t)]^{\mathrm{T}},$$

where $\omega_{y_i} \in \mathbb{R}^n,\ i = 1,\ldots,p$, *and* $\omega_{uj} \in \mathbb{R}^n,\ j = 1,\ldots,m$, *are the regression vectors obtained as follows*

$$\dot{\omega}_{y_i}(t) = A_{\mathrm{f}}\omega_{y_i}(t) - B_{\mathrm{f}}y_i(t), \qquad \omega_{y_i}(0) = \omega_{y_{i0}}, \tag{5.4a}$$

$$\dot{\omega}_{u_j}(t) = A_{\mathrm{f}}\omega_{u_j}(t) + B_{\mathrm{f}}u_j(t), \qquad \omega_{u_j}(0) = \omega_{u_{j0}}, \tag{5.4b}$$

and

$$A_{\mathrm{f}} \triangleq \begin{bmatrix} -\lambda_{n-1} & \ldots & -\lambda_0 \\ I_{(n-1)} & & 0_{n-1} \end{bmatrix} \in \mathbb{R}^{n\times n},\ B_{\mathrm{f}} \triangleq \begin{bmatrix} 1 \\ 0_{n-1} \end{bmatrix} \in \mathbb{R}^n, \tag{5.5}$$

such that $\Delta(s) \triangleq \det(sI - A_{\mathrm{f}}) = s^n + \lambda^{\mathrm{T}}S(s)$ *is Hurwitz. Finally,* $z(t)$ *is the inverse Laplace transform of* $z(s) \triangleq [z_1(s)\ldots z_p(s)]^{\mathrm{T}},\ z_i(s) \triangleq Z_i(s)h(s)/\Delta(s),\ i = 1,\ldots,p.$ *It follows from Assumption 5.4.1 that* $z(t)$, $\dot{z}(t)$ *and* $\ddot{z}(t)$ *are bounded.*

Lemma 5.4.2 *It follows from Assumption 5.4.1 and Lemma 5.4.1 that the output of system* $\mathscr{G}$ *can be obtained by*

$$\dot{x}(t) = A_{\mathrm{m}}x(t) + B_{\mathrm{m}}\left(\mu(t) + \eta(t)\right), \quad x(0) \triangleq x_0, \tag{5.6a}$$

$$y(t) = C_{\mathrm{m}}x(t). \tag{5.6b}$$

where

$$\mu(t) = \beta^{\mathrm{T}}\Phi_u(t), \quad \eta(t) = \Phi_x^{\mathrm{T}}(t)\alpha + \lambda_{n-1}y(t) + \sigma(t), \tag{5.7}$$

and $x(t) \triangleq [\mathrm{vec}(\omega_y(t))^{\mathrm{T}}\ y^{\mathrm{T}}(t)]^{\mathrm{T}} \in \mathbb{R}^{n^*},\ n^* \triangleq np + p$, *is the augmented (measurable) state vector, and*

$$A_{\mathrm{m}} \triangleq \begin{bmatrix} \bar{A}_{\mathrm{f}} & -\bar{B}_{\mathrm{f}} \\ -\bar{\lambda}^{\mathrm{T}}\bar{A}_{\mathrm{p}} & -k_{\mathrm{p}}I_p \end{bmatrix} \in \mathbb{R}^{n^*\times n^*}, \quad k_{\mathrm{p}} > 0 \tag{5.8a}$$

$$B_{\mathrm{m}} \triangleq \begin{bmatrix} 0_{np\times p} \\ I_p \end{bmatrix} \in \mathbb{R}^{n^*\times p}, \quad C_{\mathrm{m}} \triangleq B_{\mathrm{m}}^{\mathrm{T}}. \tag{5.8b}$$

where $\bar{(\cdot)} \triangleq I_p \otimes (\cdot),\ (\cdot) = \{A_{\mathrm{f}},\ B_{\mathrm{f}},\ \lambda, A_{\mathrm{p}}\}$, $A_{\mathrm{p}} \triangleq A_{\mathrm{f}} + k_{\mathrm{p}} I_n$, *and*

$$\Phi_x(t) \triangleq A_x[\omega_y^{\mathrm{T}}(t)\ y(t)]^{\mathrm{T}} \in \mathbb{R}^{n\times p}, \qquad A_x \triangleq [A_{\mathrm{p}}\ \ -B_{\mathrm{f}}] \in \mathbb{R}^{n\times(n+1)},$$
$$\Phi_u(t) \triangleq A_u \omega_u(t) \in \mathbb{R}^{nm}, \qquad A_u \triangleq I_m \otimes A_{\mathrm{p}}.$$

Finally, α *and* β *are vectors of unknown parameters, and* $\sigma(t) \triangleq k_{\mathrm{p}} z(t) + \dot{z}(t) \in \mathbb{R}^p$ *is an unknown, bounded term.*

Proof *Differentiating (5.3) along the trajectories of (5.4), and subtracting and adding* $k_{\mathrm{p}} y(t)$ *yields*

$$\begin{aligned}\dot{y} &= \left(\omega_y^{\mathrm{T}} A_{\mathrm{f}}^{\mathrm{T}} - y B_{\mathrm{f}}^{\mathrm{T}}\right)(\alpha - \lambda) + \beta^{\mathrm{T}}(\bar{A}_{\mathrm{f}}\omega_u + \bar{B}_{\mathrm{f}} u) + \dot{z} \\ &= -k_{\mathrm{p}} y + \left(\omega_y^{\mathrm{T}}(A_{\mathrm{f}}^{\mathrm{T}} + k_{\mathrm{p}} I_n) - y B_{\mathrm{f}}^{\mathrm{T}}\right)(\alpha - \lambda) + \beta^{\mathrm{T}}\left((\bar{A}_f + k_{\mathrm{p}} I_{nm})\omega_u\right) + \dot{z} + k_{\mathrm{p}} z \\ &= -k_{\mathrm{p}} y + \Phi_x^{\mathrm{T}}(\alpha - \lambda) + \beta^{\mathrm{T}}\Phi_u + \sigma. \end{aligned} \tag{5.9}$$

where we use the fact that $\beta^{\mathrm{T}}\bar{B}_{\mathrm{f}} = 0$ *due to* $r_{ij} \geq 2$. *Finally, augmenting (5.9) with* $(5.4a)$ *we obtain (5.6). Since* $z(t)$, $\dot{z}(t)$ *and* $\ddot{z}(t)$ *are bounded by Lemma 5.4.1,* $\sigma(t)$ *and* $\dot{\sigma}(t)$ *are also bounded, which concludes the proof.* □

Assumption 5.4.2 *We assume that* $\alpha \in \Theta_\alpha \subset \mathbb{R}^n$, $\beta \in \Theta_\beta \subset \mathbb{R}^{nm\times p}$, $\sigma(t) \in \Theta_\sigma \subset \mathbb{R}^p$, *where* $\Theta_\alpha,\ \Theta_\beta,\ \Theta_\sigma$ *are known convex compact sets. In addition, denote*

$$\alpha_{\max} \triangleq \max_{\alpha\in\Theta_\alpha} \|\alpha\|, \qquad \beta_{\max} \triangleq \max_{\beta\in\Theta_\beta} \|\beta\|,$$
$$\sigma_{\max} \triangleq \max_{\sigma\in\Theta_\sigma} \|\sigma(t)\|, \qquad d_\sigma \triangleq \max_{\sigma\in\Theta_\sigma} \|\dot{\sigma}(t)\|.$$

Remark 5.4.1 *System (5.6) provides an useful form to develop a predictor to predict the system output* $y(t)$ *for an arbitrary admissible input* $u(t)$. *Hence, designing a tracking control for the unknown system* $\mathscr{G}$ *is equivalent to constructing a tracking control for the predictor, which is a virtual system whose dynamics and state are all known.*

One challenge of designing the predictor for (5.6) is the presence of the time-varying term $\sigma(t)$ *in (5.7). In classical adaptive control approaches,* $\dot{\sigma}(t)$ *will lead to a derivative of the Lyapunov function candidate of unknown sign, which cannot be used to guarantee a bounded prediction error. This problem often leads to a trade off between reducing the error by increasing the adaptive gains and sacrificing the robustness of control signals. This problem is addressed in the next section.*

5.5 Predictor Design

Lemma 5.5.1 *Consider the system defined in (5.6). Let* $\gamma > 0$ *be the adaptation gain,* $0 < k(t) \leq k_{\max}$*, and* $P = P^{\mathrm{T}} > 0$ *solve the algebraic Lyapunov equation* $A_{\mathrm{m}}^{\mathrm{T}}P + PA_{\mathrm{m}} = -Q$ *for an arbitrary symmetric positive definite Q. Then, the output predictor*

$$\dot{\hat{x}}(t) = A_{\mathrm{m}}\hat{x}(t) + B_{\mathrm{m}}\left(\hat{\mu}(t) + \hat{\eta}(t)\right) + k(t)\tilde{x}(t), \quad \hat{x}(0) = x_0, \tag{5.10a}$$

$$\hat{y}(t) = C_{\mathrm{m}}\hat{x}(t). \tag{5.10b}$$

where

$$\hat{\mu}(t) = \hat{\beta}^{\mathrm{T}}(t)\Phi_u(t), \; \hat{\eta}(t) = \Phi_x^{\mathrm{T}}(t)\hat{\alpha}(t) + \lambda_{n-1}y(t) + \hat{\sigma}(t), \tag{5.11}$$

with $\hat{\alpha}(t) \in \mathbb{R}^n$*,* $\hat{\beta}(t) \in \mathbb{R}^{nm\times p}$*, and* $\hat{\sigma}(t) \in \mathbb{R}^p$ *obtained from the adaptive law*

$$\dot{\hat{\alpha}}(t) = \gamma \operatorname{Proj}\big(\hat{\alpha}(t), \Phi_x(t)e(t)\big), \qquad \hat{\alpha}(0) = \hat{\alpha}_0, \tag{5.12a}$$

$$\dot{\hat{\beta}}(t) = \gamma \operatorname{Proj}\big(\hat{\beta}(t), \Phi_u(t)e^{\mathrm{T}}(t)\big), \qquad \hat{\beta}(0) = \hat{\beta}_0, \tag{5.12b}$$

$$\dot{\hat{\sigma}}(t) = \gamma \operatorname{Proj}\big(\hat{\sigma}(t), e(t)\big), \qquad \hat{\sigma}(0) = \hat{\sigma}_0, \tag{5.12c}$$

where $e(t) \triangleq (\tilde{x}^{\mathrm{T}}(t)PB_{\mathrm{m}})^{\mathrm{T}}$*, guarantees that the prediction error* $\tilde{x}(t) \triangleq x(t) - \hat{x}(t)$ *is uniformly ultimately bounded.*

Proof *It follows from (5.6) and (5.10) that*

$$\dot{\tilde{x}} = A_{\mathrm{m}}\tilde{x} + B_{\mathrm{m}}\left(\tilde{\beta}^{\mathrm{T}}\Phi_u + \Phi_x^{\mathrm{T}}\tilde{\alpha} + \tilde{\sigma}\right) - k\tilde{x}, \;\; \tilde{x}(0) = 0_{n^*}, \tag{5.13}$$

$$\tilde{y} = C_{\mathrm{m}}\tilde{x}. \tag{5.14}$$

where $\tilde{\beta}(t) \triangleq \beta - \hat{\beta}(t)$*,* $\tilde{\alpha}(t) \triangleq \alpha - \hat{\alpha}(t)$*, and* $\tilde{\sigma}(t) \triangleq \sigma(t) - \hat{\sigma}(t)$*. Differentiating the Lyapunov function*

$$V(\tilde{x}, \tilde{\alpha}, \tilde{\beta}, \tilde{\sigma}) = \tilde{x}^{\mathrm{T}} P \tilde{x} + \frac{1}{\gamma}(\tilde{\alpha}^{\mathrm{T}}\tilde{\alpha} + \tilde{\beta}^{\mathrm{T}}\tilde{\beta} + \tilde{\sigma}^{\mathrm{T}}\tilde{\sigma}),$$

along (5.13), and using the adaptive laws (5.12), we obtain

$$\begin{aligned}\dot{V} &= -\tilde{x}^{\mathrm{T}}(Q + 2kP)\tilde{x} + 2\mathrm{tr}[\tilde{\beta}^{\mathrm{T}}(\Phi_u e^{\mathrm{T}} - \gamma^{-1}\dot{\hat{\beta}})] + 2\tilde{\alpha}^{\mathrm{T}}(\Phi_x e - \gamma^{-1}\dot{\hat{\alpha}}) + 2\tilde{\sigma}^{\mathrm{T}}(e - \gamma^{-1}\dot{\hat{\sigma}}) + 2\gamma^{-1}\tilde{\sigma}\dot{\sigma} \\ &= -\tilde{x}^{\mathrm{T}}(Q + 2kP)\tilde{x} + 2\gamma^{-1}\tilde{\sigma}^{\mathrm{T}}\dot{\sigma}. \end{aligned} \tag{5.15}$$

The projection operator ensures that $\alpha(t) \in \Theta_\alpha$*,* $\beta(t) \in \Theta_\beta$*,* $\sigma(t) \in \Theta_\sigma$ *for all* $t \geq 0$*. Therefore, Assumption 5.4.2 leads to the following upper bound*

$$\tilde{\alpha}^{\mathrm{T}}\tilde{\alpha} + \mathrm{tr}[\tilde{\beta}^{\mathrm{T}}\tilde{\beta}] + \tilde{\sigma}^{\mathrm{T}}\tilde{\sigma} \leq 4(\alpha_{\max}^2 + \beta_{\max}^2 + \sigma_{\max}^2) \triangleq d_1,$$

Furthermore, it follows from Assumption 5.4.2 that $\|\dot{\sigma}(t)\| \leq d_\sigma$*. Hence, using the Cauchy Schwarz inequality yields*

$$2\tilde{\sigma}^{\mathrm{T}}(t)\dot{\sigma}(t) \leq 2\|\tilde{\sigma}(t)\|\|\dot{\sigma}(t)\| \leq 4\sigma_{\max} d_\sigma \triangleq d_2, \quad t \geq 0.$$

Moreover,

$$\tilde{x}^{\mathrm{T}} Q \tilde{x} \geq \tilde{x}^{\mathrm{T}} \lambda_{\min}(Q)\tilde{x} \geq \frac{\lambda_{\min}(Q)}{\lambda_{\max}(P)}\tilde{x}^{\mathrm{T}} P \tilde{x} = q_p \tilde{x}^{\mathrm{T}} P \tilde{x},$$

where $q_p \triangleq \lambda_{\min}(Q)/\lambda_{\max}(P)$*. Hence, substituting the above inequalities in (5.15) yields*

$$\dot{V} \leq -(q_p + 2k)V + \gamma^{-1}((q_p + 2k)d_1 + d_2).$$

Denote $\zeta \triangleq (\tilde{x},\ \tilde{\alpha},\ \tilde{\beta},\ \tilde{\sigma})$ *and* $V_{\max} \triangleq \frac{1}{\gamma}\left(d_1 + \frac{1}{q_p + 2k}\, d_2\right)$*. Note that* $-(q_p + 2k)V_{\max} + \gamma^{-1}((q_p + 2k)d_1 + d_2) = 0$*, hence the set* $\Omega_V \triangleq \{\zeta \in \mathbb{R}^{n^*} \times \Theta_\alpha \times \Theta_\beta \times \Theta_\sigma \mid V(\zeta) \leq V_{\max}\}$ *is such that* $\dot{V}(\zeta) \leq 0$ *for all* $\zeta \in \mathbb{R}^{n^*} \times \Theta_\alpha \times \Theta_\beta \times \Theta_\sigma \setminus \Omega_V$ *which according to Lyapunov theory (Theorem 4.1 in [31]) guarantees that* Ω_V *is a positively invariant set and all state trajectories enter and* *remain in Ω_V after an initial transient. Since $\lambda_{\min}(P)\tilde{x}^{\mathrm{T}}\tilde{x} \leq \tilde{x}^{\mathrm{T}}P\tilde{x} \leq V \leq V_{\max}$, then*

$$\|\tilde{x}(t)\|^2 \leq \frac{1}{\gamma\lambda_{\min}(P)}\left(d_1 + \frac{1}{q_p + 2k_{\min}}d_2\right) \triangleq \|\tilde{x}_{\max}\|^2, \tag{5.16}$$

where $k_{\min} \triangleq \min\limits_{t\geq 0}\{k(t)\}$, which concludes the proof. □

Notice that the prediction error $\|\tilde{x}(t)\|$ can be reduced by either increasing γ and $k_{\min}$. Tuning these adaptive parameters will be addressed in Section 5.7 to obtain both tracking's accuracy and smoothness of the control signal.

5.6 Controller Design

The next problem is to control the predictor (5.10) to track the reference system (5.2), where the reference's system matrices are chosen as in (5.8). In the following, we summarize the drawbacks of backstepping like techniques, which also motivate our simple controller structure. For ease of analysis, we first present the controller for the SISO case, and will extend the result to MIMO case.

5.6.1 Drawbacks of Backstepping-like techniques

Step 1: Let $e_1(t) \triangleq \hat{x}(t) - x_{\mathrm{m}}(t)$. It follows from (5.10) and (5.2), the error dynamics between the predictor and the reference system is

$$\dot{e}_1(t) = A_{\mathrm{m}}e_1(t) + B_{\mathrm{m}}(\hat{\mu}(t) + \hat{\eta}(t) - k_g r(t)) + k(t)\tilde{x}(t),$$

which leads to the desired virtual control signal

$$\hat{\mu}(t) = k_g r(t) - \hat{\eta}(t),$$

or, by substituing (5.11), we obtain

$$\hat{\beta}^{\mathrm{T}}(t)\Phi_u(t) = k_g r(t) - (\Phi_x^{\mathrm{T}}(t)\hat{\alpha}(t) + \lambda_{n-1}y(t) + \hat{\sigma}(t)). \tag{5.17}$$

Since the system relative degree $r_{ij} \geq 2$, $\Phi_u(t)$ can not be set directly as in (5.17) but through its derivative. Following the backstepping procedure, however, we will drop the crossing terms in the next levels for the purpose of simple explanation.

Step 2: Differentiate (5.17) yields

$$\hat{\beta}^{\mathrm{T}}(t)\dot{\Phi}_u(t) = k_g \dot{r}(t) - S_1(t), \tag{5.18}$$

where

$$S_1(t) \triangleq \dot{\Phi}_x^{\mathrm{T}}(t)\hat{\alpha}(t) + \Phi_x^{\mathrm{T}}(t)\dot{\hat{\alpha}}(t) + \lambda_{n-1}\dot{y}(t) + \dot{\hat{\sigma}}(t) + \dot{\hat{\beta}}(t)\Phi_u(t),$$

Note that, $\dot{\hat{\alpha}}(t)$, $\dot{\hat{\beta}}(t)$, $\dot{\hat{\sigma}}(t)$ in (5.18) are the adaptive laws, which contain $\tilde{x}(t)$. If $r_{ij} \geq 3$, then further derivatives of (5.18) are required until $u(t)$ appears explicitly.

Step 3: Differentiating (5.18) yields

$$\hat{\beta}^{\mathrm{T}}(t)\ddot{\Phi}_u(t) = k_g \ddot{r}(t) - S_2(t), \tag{5.19}$$

where

$$S_2(t) \triangleq \dot{S}_1(t) + \dot{\hat{\beta}}(t)\dot{\Phi}_u(t)$$

Note that, $\dot{S}_1(t)$, and hence $S_2(t)$, contain $\ddot{\hat{\alpha}}(t)$, $\ddot{\hat{\beta}}(t)$, $\ddot{\hat{\sigma}}(t)$, which involve $\dot{\tilde{x}}(t)$ or $\dot{y}(t)$. As seen from (5.18) and (5.19), higher backstepping levels require the measurements of $\frac{d^{(i)}y}{dt^{(i)}}, i = 1, \ldots, r_{ij} - 1$.

In many approaches, it is often assumed that output derivatives up to $(r_{ij} - 1)$ order are available. In fact, this assumption is equivalent to the full state measurement assumption. This case, however, is often unrealistic, especially in biological systems.

Hence, one approach to avoid the explicit need of output derivatives is *adaptive backstepping*, which requires redesigning the predictor recursively. However, for system with relative degree $r_{ij} \geq 3$, the adaptive terms will suffer the "explosion of complexity", which makes the predictor extremely complicated. Furthermore, without further assumptions, it is complicated to use the fast adaptation technique to reduce the prediction errors due to time-varying term $\sigma(t)$.

To overcome the mentioned complexity, other versions of adaptive backstepping, such as *dynamic surface* or *command filter backstepping*, address the problem by approximating the analytical derivative with a high-pass filter. For example, follow the steps 2 and 3, one would derive

$$S_2(t) \triangleq \dot{\bar{S}}_1(t) + \dot{\hat{\beta}}(t)\Phi_u(t), \tag{5.20}$$

$$\dot{\bar{S}}_1(t) = \frac{1}{\tau}(-\bar{S}_1(t) + S_1(t)). \tag{5.21}$$

Or, in the frequency domain, denoting with $S_3(t) \triangleq \dot{\bar{S}}_1(t)$, then

$$sS_1(s) \simeq S_3(s) = \frac{s}{1+\tau s} S_1(t). \tag{5.22}$$

In order to obtain an acceptable tracking error, one needs $\tau \to 0$ so that $S_3(s) \to sS_1(s)$. This condition, however, will lead to high gain dynamics caused by $\frac{1}{\tau}$ in (5.21).

The high gain effect is even more serious when the high-pass filters are cascaded, as the systems relative degree increases. Consequently, the large number of filters will lead to larger approximation error. A higher gain $\frac{1}{\tau}$ for each filter therefore is needed to reduce this accumulated error. As the result, the control signal suffers severe overshoot and oscillations, especially when high gain adaptation is simultaneously used.

Notice that the drawbacks of backstepping-like techniques are rooted from the intention of designing $u(t)$ so that $\hat{\mu}(t)$ exactly cancels the mismatch term $\hat{\eta}(t)$. However, this ends up with either too complicated analytical solution or high gain approximation approaches.

These mentioned analysis inspires our approach, where the tracking accuracy can be obtained without exact cancelling the mismatch term. Hence, the solution remains simple regardless of the system relative degree. The main idea is shown as follow. First, rewrite (5.10) as

$$\hat{x}(s) = H(s)(\hat{\mu}(s) + \hat{\eta}(s)) + (sI - A_{\mathrm{m}})^{-1}\chi(s) + \hat{x}_{\mathrm{in}}(s), \tag{5.23}$$

where $\hat{x}_{\mathrm{in}}(s)$ is the exponential decay term due to the initial condition, and

$$H(s) \triangleq (sI - A_{\mathrm{m}})^{-1} B_{\mathrm{m}}, \qquad \chi(t) \triangleq k(t)\tilde{x}(t). \tag{5.24}$$

Notice that $H(s)$ plays a role of a low-pass filter of $\hat{\eta}(s)$. Therefore, we only need to cancel the low-frequency components of $\hat{\eta}(s)$, since the high frequency components outside the bandwidth of $H(s)$ is already suppressed. Our control approach presented in the next section is designed with this purpose in mind.

5.6.2 Adaptive Controller

Lemma 5.6.1 *Consider the SISO system (5.6) and the following adaptive controller*

$$u(t) = -K_{\mathrm{f}}\omega_u(t) + \hat{v}(t), \tag{5.25a}$$

$$\hat{v}(t) = -k_C\left(\hat{\mu}(t) + \hat{\eta}(t) - k_g r(t)\right), \tag{5.25b}$$

All signals of the closed loop system in Fig 5.1 are bounded if K_{f} and k_C are chosen such that $L\|G(s)\|_{\mathscr{L}_1} < 1$ and $C(s)$ and $\Lambda(s)$ are stable, where $L \triangleq \max\limits_{\alpha\in\Theta_\alpha} \|\alpha^{\mathrm{T}}D + \lambda_{n-1}C_{\mathrm{m}}\|_1$, and

$$G(s) \triangleq H(s)(1 - C(s)), \qquad C(s) \triangleq \frac{k_C P(s)}{\Lambda(s) + k_C P(s)}, \tag{5.26}$$

$$P(s) \triangleq \beta^{\mathrm{T}} A_u S(s), \qquad \Lambda(s) \triangleq \det(sI - (A_{\mathrm{f}} - B_{\mathrm{f}}K_{\mathrm{f}})). \tag{5.27}$$

Proof *First, we will evaluate $\hat{\mu}(s)$ in the closed loop system. Substituting (5.25a) into (5.4b), we obtain*

$$\omega_u(s) = (sI - (A_{\mathrm{f}} - B_{\mathrm{f}}K_{\mathrm{f}}))^{-1}B_{\mathrm{f}}\hat{v}(s) = \frac{S(s)}{\Lambda(s)}\hat{v}(s) \tag{5.28}$$

where $S(s) \triangleq [s^{n^*-1} \ldots s\ 1]^{\mathrm{T}} \in \mathbb{C}^{n^*}$, and $\Lambda(s)$ is given in (5.27). Furthermore, (5.11) can be rewritten as

$$\hat{\mu}(t) = \beta^{\mathrm{T}} A_u \omega_u(t) - \tilde{\mu}(t), \tag{5.29}$$

where $\tilde{\mu}(t) = \tilde{\beta}^{\mathrm{T}}(t) A_u \omega_u(t)$. Hence, substituting (5.28) to (5.29), we obtain

$$\hat{\mu}(s) = \frac{\beta^{\mathrm{T}} A_u S(s)}{\Lambda(s)}\hat{v}(s) - \tilde{\mu}(s) = F(s)\hat{v}(s) - \tilde{\mu}(s), \tag{5.30}$$

where $F(s) \triangleq \frac{P(s)}{\Lambda(s)}$, and $P(s)$ is given in (5.27). Substituting (5.30) in (5.25b) yields

$$\hat{v}(s) = -k_C(F(s)\hat{v}(s) - \tilde{\mu}(s) + \hat{\eta}(s) - k_g r(s)).$$

and

$$\hat{v}(s) = -\frac{k_C}{1+k_C F(s)}(\hat{\eta}(s) - k_g r(s) - \tilde{\mu}(s)). \tag{5.31}$$

Substituting (5.31) in (5.30), we can rewrite $\hat{\mu}(s)$ as

$$\hat{\mu}(s) = -C(s)(\hat{\eta}(s) - k_g r(s)) - (1 - C(s))\tilde{\mu}(s), \tag{5.32}$$

where $C(s)$ is given in (5.27). Then, substituting (5.32) into (5.23) to obtain the closed loop system state provides

$$\hat{x}(s) = H(s)C(s)k_g r(s) + H(s)(1 - C(s))(\hat{\eta}(s) - \tilde{\mu}(s)) + (sI - A_{\mathrm{m}})^{-1}\chi(s) + \hat{x}_{\mathrm{in}}(s). \tag{5.33}$$

The next step will be to remove the unknown term $\tilde{\mu}(s)$ from (5.33). Let

$$\tilde{v}(t) \triangleq \tilde{\mu}(t) + \tilde{\eta}(t), \tag{5.34}$$

$$\tilde{\eta}(t) \triangleq \eta(t) - \hat{\eta}(t) = \Phi_x^{\mathrm{T}}(t)\tilde{\alpha}(t) + \tilde{\sigma}(t), \tag{5.35}$$

$$\Delta_{\hat{x}}(s) \triangleq H(s)(1 - C(s))\tilde{v}(s) - (sI - A_{\mathrm{m}})^{-1}\chi(s), \tag{5.36}$$

then (5.33) can be rewritten as

$$\hat{x}(s) = H(s)C(s)k_g r(s) + H(s)(1 - C(s))\eta(s) + \hat{x}_{\mathrm{in}}(s) - \Delta_{\hat{x}}(s). \tag{5.37}$$

Note that, $\Delta_{\hat{x}}(s)$ defined in (5.36) contains the estimation error. Hence, it can be rewritten in term of the prediction error $\tilde{x}(t)$. It follows from (5.34), (5.24) and (5.13) that

$$H(s)\tilde{v}(s) = \tilde{x}(s) + (sI - A_{\mathrm{m}})^{-1}\chi(s),$$

hence, (5.36) can rewritten as

$$\Delta_{\hat{x}}(s) = (1 - C(s))\tilde{x}(s) - C(s)(sI - A_{\mathrm{m}})^{-1}\chi(s).$$

Finally, we need to prove that all signals in the closed loop system, as seen in Fig 5.1, are bounded. Let

$$\Delta_x(s) \triangleq \tilde{x}(s) - \Delta_{\hat{x}}(s) = C(s)(\tilde{x}(s) + (sI - A_{\mathrm{m}})^{-1}\chi(s)),$$

it follows from (5.37) that

$$x(s) = \hat{x}(s) + \tilde{x}(s) = H(s)C(s)k_g r(s) + G(s)\eta(s) + \hat{x}_{\mathrm{in}}(s) + \Delta_x(s),$$

where $G(s)$ is defined in (5.26). It follows from the definition of $\eta(t)$ in (5.7), that

$$\|\eta\|_{\mathscr{L}_\infty} = \|(\alpha^{\mathrm{T}}D + \lambda_{n-1}C_{\mathrm{m}})x + \sigma\|_{\mathscr{L}_\infty} \leq L\|x\|_{\mathscr{L}_\infty} + \|\sigma\|_{\mathscr{L}_\infty},$$

which leads to

$$\|x\|_{\mathscr{L}_\infty} \leq \|H(s)C(s)\|_{\mathscr{L}_1}\|k_g r\|_{\mathscr{L}_\infty} + \|G(s)\|_{\mathscr{L}_1}L\|x\|_{\mathscr{L}_\infty} + \|G(s)\|_{\mathscr{L}_1}\|\sigma\|_{\mathscr{L}_\infty} + \|x_{\mathrm{in}}\|_{\mathscr{L}_\infty} + \|\Delta_x(s)\|_{\mathscr{L}_\infty}.$$

Since $\tilde{x}(t)$ is bounded by Lemma 5.5.1 and $C(s)$ and $(sI - A_{\mathrm{m}})^{-1}$ are strictly proper and stable transfer functions, $\Delta_x(s)$ is bounded. Furthermore, since $\sigma(t)$ and $r(t)$ are assumed to be bounded and $G(s)$ is designed to satisfy $\|G(s)\|_{\mathscr{L}_1}L < 1$, $x(t)$ is bounded by

$$\|x\|_{\mathscr{L}_\infty} \leq \frac{1}{1 - \|G(s)\|_{\mathscr{L}_1}L}(\|H(s)C(s)\|_{\mathscr{L}_1}\|k_g r\|_{\mathscr{L}_\infty} + \|G(s)\|_{\mathscr{L}_1}\|\sigma\|_{\mathscr{L}_\infty} + \|x_{\mathrm{in}}\|_{\mathscr{L}_\infty} + \|\Delta_x(s)\|_{\mathscr{L}_\infty}) \triangleq x_{\mathrm{b}}.$$

Hence, as $\tilde{x}(t)$ is bounded by Lemma 5.5.1, $\hat{x}(t)$ is also bounded. Furthermore, since $x(t)$ is bounded and $\hat{\alpha}(t)$, $\hat{\sigma}(t)$ are bounded by the projection operator, it follows from (5.11) that $\hat{\eta}(t)$ is also bounded. Because $C(s)$ is stable and $\hat{x}(t)$ is bounded, it follows from (5.33) that $\tilde{\mu}(t)$ is bounded, and, it is inferred from (5.31) and (5.32) that $\hat{v}(t)$ and $\hat{\mu}(t)$ are also bounded. Consequently, since $\hat{\mu}(t)$ is bounded, it follows from (5.11) that $\omega_u(t)$ is bounded. Finally, it is inferred from (5.25a) that $u(t)$ is bounded because $\omega_u(t)$ and $\hat{v}(t)$ are bounded. Hence, all signals of the adaptive closed loop system are bounded, which concludes the proof. □

Lemma 5.6.1 provides the conditions to ensure all the closed loop signals remain bounded. For tracking performance, as seen from (5.32), the controller is designed so that $\hat{\mu}(s)$ cancels the low frequency components of $\hat{\eta}(s)$ filtered by $C(s)$. Furthermore, it follows from (5.26) that increasing k_C will increase the bandwidth of $C(s)$. Hence, k_C needs to be large enough so that the bandwidth of $C(s)$ covers the bandwidth of $H(s)$. In the next section, the tracking error and transient behavior will be analyzed to give the guidance of choosing the parameters.

5.7 Transient Behavior

Theorem 5.7.1 *Consider the SISO system (5.6) and the adaptive control (5.25). If the damping $k(t)$ in (5.10) is chosen such that*

$$2\sqrt{\gamma h_0} + B_{\mathrm{m}}^{\mathrm{T}} P A_{\mathrm{m}} (B_{\mathrm{m}}^{\mathrm{T}} P)^{\dagger} + \max\left(0, \frac{\dot{\rho}(t)}{\rho(t)}\right) \leq k(t) \leq k_{\max}, \tag{5.38}$$

where $h_0 \triangleq \frac{\rho_{\min}+\rho_{\max}}{2} l_0$, $l_0 \triangleq B_{\mathrm{m}}^{\mathrm{T}} P B_{\mathrm{m}}$, $k_{\max} > 0$ is a chosen upper bound , and

$$\rho(t) \triangleq \Phi_x^{\mathrm{T}}(t)\Phi_x(t) + \Phi_u^{\mathrm{T}}(t)\Phi_u(t) + 1, \tag{5.39}$$

then the following bounds hold

$$|\tilde{v}(t)| < c_4 e^{-\nu t} + \frac{\tilde{u}_{\max}}{\sqrt{\gamma}}, \tag{5.40}$$

$$\|\Delta_x(t)\|_{\mathscr{L}_\infty} \leq \|H(s)C(s)\|_{\mathscr{L}_1} \|\tilde{v}(t)\|_{\mathscr{L}_\infty}, \tag{5.41}$$

$$\|y(t) - y_{\mathrm{m}}(t)\|_{\mathscr{L}_\infty} \leq \frac{\|T(s)\|_{\mathscr{L}_1}}{k_C} (\|\eta(t)\|_{\mathscr{L}_\infty} + k_g \|r(t)\|_{\mathscr{L}_\infty}) + \|e_{\mathrm{in}}\|_{\mathscr{L}_\infty} + \|C_m \Delta_x(t)\|_{\mathscr{L}_\infty}, \tag{5.42}$$

where $T(s) \triangleq C_{\mathrm{m}} H(s) \frac{1}{k_C^{-1} + F(s)}$, $e_{\mathrm{in}}(s) \triangleq C_{\mathrm{m}}(sI - A_{\mathrm{m}})^{-1}(x_0 - x_{\mathrm{m}0})$, and $\tilde{u}_{\max}$ is a constant defined in (5.49).

Proof *The proof follows the same lines of the proof in [92]. Differentiating (5.34) and substituting the adaptive laws (5.12) we obtain*

$$\dot{\tilde{v}}(t) = -\gamma \rho(t) e(t) + z_1(t),$$

where $\rho(t)$ is defined in (5.39), and

$$z_1(t) \triangleq \tilde{\beta}^{\mathrm{T}}(t)\dot{\Phi}_u(t) + \dot{\Phi}_x^{\mathrm{T}}(t)\tilde{\alpha}(t) + \dot{\sigma}(t).$$

Consider the change of variable $p(t) \triangleq [p_1(t)\ p_2(t)]^{\mathrm{T}}$, *where*

$$p_1(t) \triangleq \tilde{v}(t), \qquad p_2(t) \triangleq \dot{\tilde{v}}(t) - z_1(t) = -\gamma\rho(t)B_{\mathrm{m}}^{\mathrm{T}}P\tilde{x}(t).$$

Differentiating $p_2(t)$ *and substituting (5.13) to obtain*

$$\dot{p}_2(t) = -\gamma\dot{\rho}(t)B_{\mathrm{m}}^{\mathrm{T}}P\tilde{x}(t) - \gamma\rho(t)B_{\mathrm{m}}^{\mathrm{T}}P\left(A_{\mathrm{m}}\tilde{x}(t) - k(t)\tilde{x}(t) + B_{\mathrm{m}}\tilde{v}(t)\right). \tag{5.43}$$

Define $H \triangleq I - (B_{\mathrm{m}}^{\mathrm{T}}P)^{\dagger}(B_{\mathrm{m}}^{\mathrm{T}}P)$ *to rewrite*

$$B_{\mathrm{m}}^{\mathrm{T}}PA_{\mathrm{m}}\tilde{x}(t) = B_{\mathrm{m}}^{\mathrm{T}}PA_{\mathrm{m}}\left[H + (B_{\mathrm{m}}^{\mathrm{T}}P)^{\dagger}(B_{\mathrm{m}}^{\mathrm{T}}P)\right]\tilde{x}(t),$$

then (5.43) can be rewritten as

$$\begin{aligned}
\dot{p}_2(t) &= -\gamma\dot{\rho}(t)B_{\mathrm{m}}^{\mathrm{T}}P\tilde{x}(t) - \gamma\rho(t)B_{\mathrm{m}}^{\mathrm{T}}PA_{\mathrm{m}}H\tilde{x}(t) - \gamma\rho(t)B_{\mathrm{m}}^{\mathrm{T}}PA_{\mathrm{m}}(B_{\mathrm{m}}^{\mathrm{T}}P)^{\dagger}(B_{\mathrm{m}}^{\mathrm{T}}P)\tilde{x}(t)\\
&\quad + \gamma\rho(t)B_{\mathrm{m}}^{\mathrm{T}}Pk(t)\tilde{x}(t) - \gamma\rho(t)B_{\mathrm{m}}^{\mathrm{T}}PB_{\mathrm{m}}\tilde{v}(t)\\
&= -\gamma\rho(t)\left(\frac{\dot{\rho}(t)}{\rho(t)} + B_{\mathrm{m}}^{\mathrm{T}}PA_{\mathrm{m}}(B_{\mathrm{m}}^{\mathrm{T}}P)^{\dagger} - k(t)\right)B_{\mathrm{m}}^{\mathrm{T}}P\tilde{x}(t) - \gamma\rho(t)B_{\mathrm{m}}^{\mathrm{T}}PB_{\mathrm{m}}\tilde{v}(t) - \gamma\rho(t)B_{\mathrm{m}}^{\mathrm{T}}PA_{\mathrm{m}}H\tilde{x}(t)\\
&= -2a(t)p_2(t) - \gamma\rho(t)l_0p_1(t) - \gamma z_2(t).
\end{aligned}$$

where $l_0 \triangleq B_{\mathrm{m}}^{\mathrm{T}}PB_{\mathrm{m}}$, *and*

$$a(t) \triangleq \frac{1}{2}\left(k(t) - B_{\mathrm{m}}^{\mathrm{T}}PA_{\mathrm{m}}(B_{\mathrm{m}}^{\mathrm{T}}P)^{\dagger} - \frac{\dot{\rho}(t)}{\rho(t)}\right), \tag{5.44}$$

$$z_2(t) \triangleq \rho(t)B_{\mathrm{m}}^{\mathrm{T}}PA_{\mathrm{m}}H\tilde{x}(t). \tag{5.45}$$

Then, the dynamics of $p(t)$ *can be written as*

$$\begin{bmatrix}\dot{p}_1\\ \dot{p}_2\end{bmatrix} = \begin{bmatrix}0 & 1\\ -\gamma\rho(t)l_0 & -2a(t)\end{bmatrix}\begin{bmatrix}p_1\\ p_2\end{bmatrix} + \begin{bmatrix}1\\ 0\end{bmatrix}z_1 + \begin{bmatrix}0\\ -\gamma\end{bmatrix}z_2, \tag{5.46}$$

According to Lemma 5.6.1, all the signals in the closed loop are bounded. Hence, $z_1(t)$, $z_2(t)$ *are bounded and* $0 < h_1 \leq h(t) \triangleq \rho(t)l_0 \leq h_2 < \infty$. *Furthermore, it follows from (5.38) that* $a(t) \geq \sqrt{\gamma h_0}$, *where* $h_0 = (h_1 + h_2)/2$. *Applying Lemma 5.2.1 with extension to the two inputs case, we* *obtain the following bound*

$$|\tilde{v}(t)| = |p_1(t)| \leq c_4 e^{-\nu t} + \frac{c_1\sqrt{h_0}}{h_1\sqrt{\gamma}}\|z_1(t)\|_{\mathscr{L}_\infty} + \frac{1}{h_1}\|z_2(t)\|_{\mathscr{L}_\infty}, \tag{5.47}$$

where $c_1 \geq 2$. The term $c_4 e^{-\nu t}$ represents the error due to the initial condition $p(0)$, which decays exponentially with rate proportional to $\sqrt{\gamma}$. Furthermore, it follows from (5.45) and (5.16) that

$$\|z_2(t)\|_{\mathscr{L}_\infty} \leq \max_{t\geq 0}\{\|\rho(t)B_{\mathrm{m}}^{\mathrm{T}}PA_{\mathrm{m}}H\tilde{x}(t)\|\} \leq \max_{t\geq 0}\{\|\rho(t)B_{\mathrm{m}}^{\mathrm{T}}PA_{\mathrm{m}}H\|\|\tilde{x}(t)\|\} \leq \frac{w_z}{\sqrt{\gamma}}, \tag{5.48}$$

where

$$w_z \triangleq \|h_2L^{-1}B_{\mathrm{m}}^{\mathrm{T}}PA_{\mathrm{m}}H\|\sqrt{\frac{1}{\lambda_{\min}(P)}\left(d_1 + \frac{1}{q_p + 2k_{\min}}d_2\right)},$$

Finally, (5.40) follows from (5.47) and (5.48), and (5.41) follows from (5.36) with $\tilde{u}_{\max}$ defined as

$$\tilde{u}_{\max} \triangleq \frac{c_1\sqrt{h_0}}{h_1}\|z_1(t)\|_{\mathscr{L}_\infty} + \frac{1}{h_1}w_z. \tag{5.49}$$

Eq. (5.42) follows directly from (5.6b), (5.33) and (5.41), which concludes the proof. □

Remark 5.7.1 *According to Theorem 5.7.1, for a chosen γ, (5.42) clearly shows that the tracking error can be reduced by increasing k_C. For a chosen k_C, $|\tilde{v}(t)|$ and hence $\|\Delta_x\|$ and $\|y(t) - y_{\mathrm{m}}(t)\|$ can be reduced as much as needed by increasing the adaptive gain γ, which is limited only by the computer processor. Furthermore, $k(t)$ plays a vital role, as it needs to be larger than a minimum value. However, a large $k(t)$ will also increase c_1 in (5.49), which leads to the larger upper bound $\tilde{u}_{\max}$ and hence affects all other errors.*

To guarantee closed-loop stability during the input saturation phase, we implement the approach described in [50] to modify the reference signal. When the control signal is saturated, the system is trying to track the desired trajectory, which is out of reach. In this case, the reference trajectory is modified by appropriately choosing the reference input in order to bring the reference trajectory within reach. In this way, we can still guarantee uniform boundedness of the tracking error in the face of the saturation constraint.

Theorem 5.7.2 *Consider the SISO system (5.6) and the adaptive control (5.25). For a given de-*

sired reference input $r_{\mathrm{d}}(t)$, consider the modified reference input $r(t)$

$$r(t) = \frac{v_{\mathrm{s}}(t) + k_C(\hat{\mu}(t) + \hat{\eta}(t))}{k_C k_g}, \tag{5.50a}$$

$$v_{\mathrm{s}}(t) = u_{\mathrm{s}} + K_f \omega_u(t), \tag{5.50b}$$

where $u_{\mathrm{s}} = \mathrm{Sat}(u(t), u_{\max})$ is the saturated control signal. Then the control law (5.25) along with the modified reference (5.50) guarantees that the tracking error $|y(t) - y_{\mathrm{m}}(t)|$ is uniformly bounded by (5.42), and $|u(t)| \leq u_{\max}$.

Proof *If the input is not saturated, $|y(t) - y_{\mathrm{m}}(t)|$ is uniformly bounded by (5.42) as consequence of Theorem 5.7.1. Otherwise, (5.50) is directly inferred from (5.25). When the control input is saturated, the closed-loop stability and boundedness of the tracking error* (5.42) *are guaranteed by modifying the reference signal $r(t)$, which is treated as a virtual control signal. Details of the stability proof can be found in ([50]).* □

5.8 Illustrative Numerical Examples

Example 5.8.1 *Consider the following SISO system*

$$\begin{aligned}\dot{\xi}(t) &= A\xi(t) + Bu(t) + h(\xi(t), t),\\ y(t) &= C\xi(t),\end{aligned}$$

where $\xi(t) \triangleq [\xi_1(t) \cdots \xi_4(t)]^{\mathrm{T}} \in \mathbb{R}^4$ is the state vector; $u(t) \in \mathbb{R}$ is the control inputs; matrices A, B, C are the realization of the following transfer function

$$G(s) \triangleq C(sI - A)^{-1}B = \frac{5s + 4}{(s - 0.2)(s - 0.3)(s - 0.4)(s + 6)},$$

and $h(\xi, t) = [\cos(2t) + \tanh(\xi_2) \;\; 1 + 0.5\sin(3t) \;\; 0.2\cos(0.2\xi_1) \;\; 0.3\sin(\xi_3)\cos(0.2\xi_1\xi_4)]^{\mathrm{T}} \in \mathbb{R}^4$. $G(s)$ and $h(\xi, t)$ are unknown and $\xi(t)$ is unmeasurable. It can be seen that $G(s)$ is unstable and has relative degree $r = 3$. Furthermore, the uncertainties $h(\xi, t)$ are nonlinear, time varying and *contain mismatched terms in respect to the control signal.*

To implement the proposed controller, the autoregressive vectors are constructed by using the low-pass filters defined in (5.4) with $\Delta(s) = s^n + \lambda^{\mathrm{T}} S(s) = (s+1)^4$, *so that* $\lambda \triangleq [-4\ -6\ -4\ -1]$. *Hence, the reference system defined in (5.2) with the chosen* $k_{\mathrm{p}} = 1$ *takes the following realization*

$$A_{\mathrm{m}} = \begin{bmatrix} A_{\mathrm{f}} & -B_{\mathrm{f}} \\ -\lambda^{\mathrm{T}} A_{\mathrm{p}} & -k_{\mathrm{p}} \end{bmatrix} = \begin{bmatrix} -4 & -6 & -1 & -1 & -1 \\ 1 & 0 & 0 & 0 & 0 \\ 0 & 1 & 0 & 0 & 0 \\ 0 & 0 & 1 & 0 & 0 \\ 6 & 14 & 11 & 3 & -1 \end{bmatrix}, \quad B_{\mathrm{m}} = \begin{bmatrix} 0 \\ 0 \\ 0 \\ 0 \\ 1 \end{bmatrix}, C_{\mathrm{m}} = B_{\mathrm{m}}^{\mathrm{T}}.$$

The following parameters are used to implement the controller: $P = I_5$, *adaptation gain* $\gamma = 10^4$; $k(t)$ *defined in (5.38) with* $h_0 = 35$ *and* $\dot{\rho}(t)$ *is approximated by* $\frac{s}{0.01s+1}\rho(s)$; $k_C \triangleq 150$ *and* $\Lambda(s) \triangleq s(s+0.8)(s+1)(s+1.2)$ *so that* $K_f = [-1 - 3.04 - 3.04 - 1]$.

For the adaptation law, we set the following projection bounds and the initial values are chosen randomly inside the projection bounds.

$$\begin{aligned} &\Omega_\alpha = \alpha_c \pm 0.8|\alpha_c|, && \alpha_c = [5\ -5\ 2\ -0.2]^{\mathrm{T}}, && \hat{\alpha}_0 = [3.2\ -3.5\ 2\ -0.15]^{\mathrm{T}}, \\ &\Omega_\beta = \beta_c \pm 0.8|\beta_c|, && \beta_c = [0\ 0\ 6\ 2]^{\mathrm{T}}, && \hat{\beta}_0 = [0\ 0\ 4\ 1.5]^{\mathrm{T}}, \\ &\Omega_\sigma = [-20\ 20], && && \hat{\sigma}_0 = 0. \end{aligned}$$

The tracking performance and the control effort for the reference signal $r(t) = 3\sin(2t)$ *are illustrated in Fig 5.2 and Fig 5.3 respectively. The reference signal* $r(t)$ *is passed through a low pass filter* $\frac{1}{(s+1)^2}$ *before entering the reference system. The control signal is saturated to avoid the initial overshoot effect. The time evolving adaptive parameters* $\hat{\alpha}(t), \hat{\beta}(t)$ *and* $\hat{\sigma}(t)$ *are illustrated in Figures 5.4, 5.5, 5.6, respectively.*

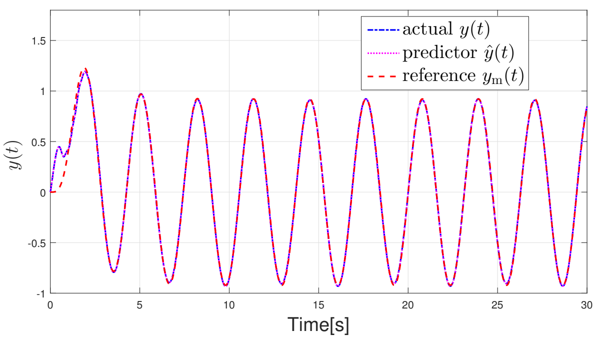

Figure 5.2: System trajectories.

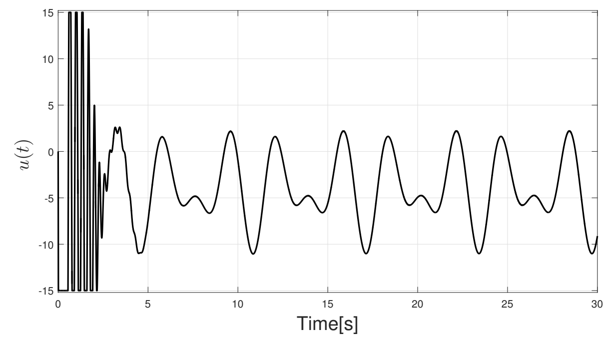

Figure 5.3: Control signal.

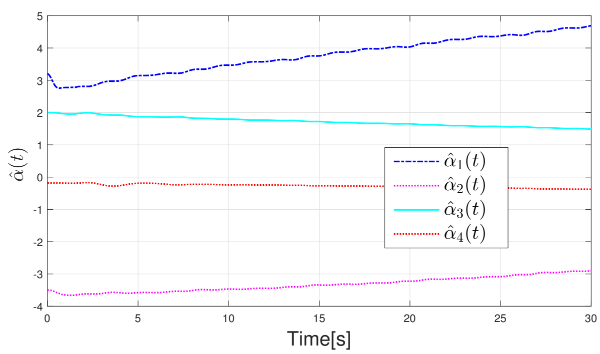

Figure 5.4: Evolution of $\hat{\alpha}(t)$ over time.

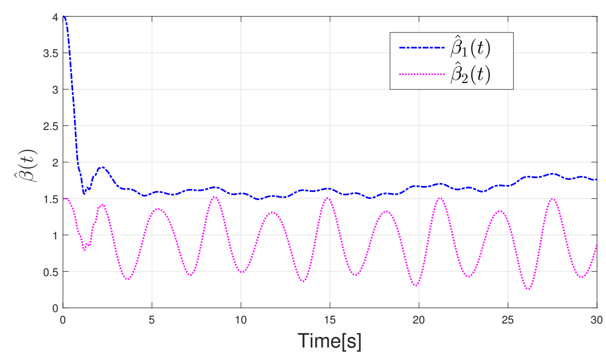

Figure 5.5: Evolution of $\hat{\beta}(t)$ over time.

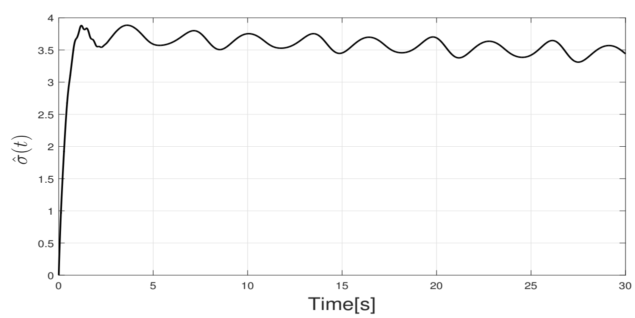

Figure 5.6: Evolution of $\hat{\sigma}(t)$ over time.

We can see that the tracking performance is satisfied. All adaptive parameters are inside the bounded area. Although the control signal is saturated at beginning due to the adaptation process as $\sigma(t)$ *and* $\beta(t)$ *change rapidly, the control signal is smooth after 3s. Furthermore, comparing to the adaptive backstepping algorithms, the proposed controller structure is significantly simpler and does not require numerically high order derivatives of the output signals.*

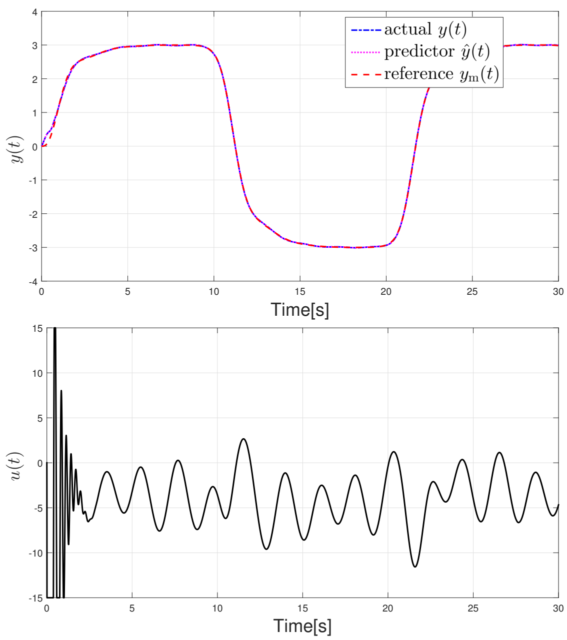

Figure 5.7: $k_C = 100$ and $h_0 = 3$.

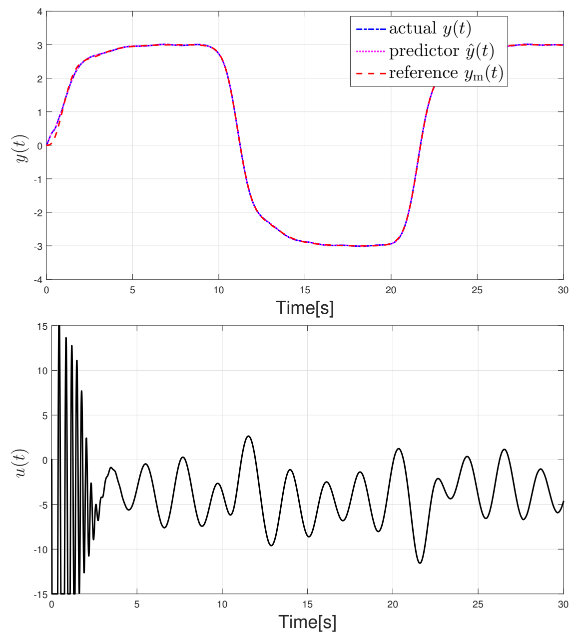

Figure 5.8: $k_C = 100$ and $h_0 = 20$.

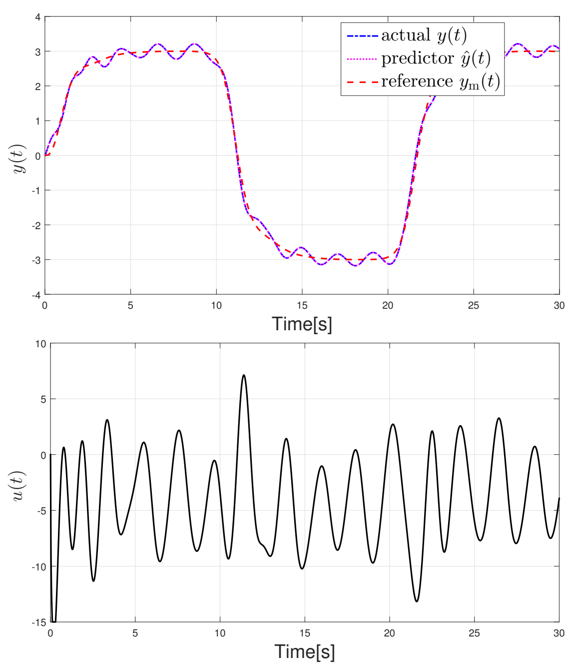

Figure 5.9: $k_C = 10$ and $h_0 = 3$.

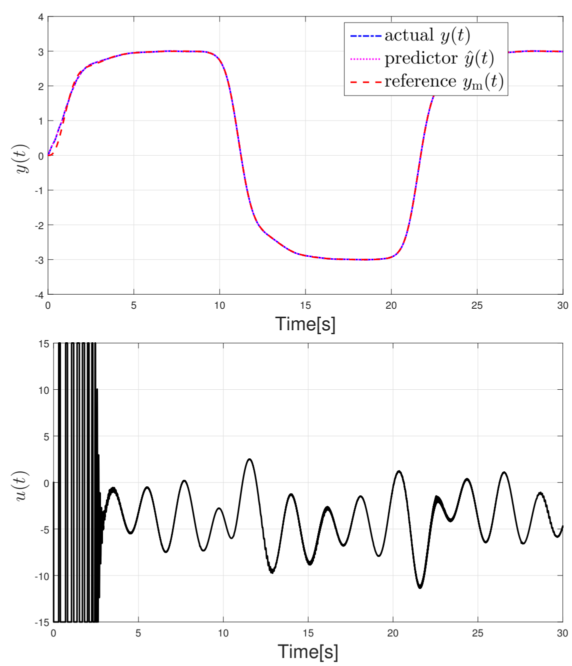

Figure 5.10: $k_C = 1000$ and $h_0 = 200$.

Another advantage of the proposed controller is that **there are only 2 parameters that need to be tuned:** h_0 and k_C, which are proportional to the frequency of the reference signal $r(t)$, while

γ is chosen as large as needed. To illustrate the effect of k_C and h_0, we consider the reference $r(t) = 3\tanh(5sin(0.3t))$. The reference signal $r(t)$ is passed through a low pass filter $\frac{1}{(s+1)^2}$ before entering the reference system. Figures (5.7 - 5.10) present the tracking results and the control signals for different values of k_C and h_0. The results confirm our theoretical analysis. Figure 5.7 and Figure 5.9 show that a larger k_C can yield better tracking results while a small k_C yields poorer tracking results but smoother control signal. However, as seen from Figure 5.8 and Figure 5.10, if k_C is chosen too large without appropriate tuning value of h_0, the control signals suffer the chattering effect.

As seen in Example 5.8.1, k_C and h_0 play a vital role to obtain the control signal's smoothness in the presence of fast adaptation. In the next example, we will increase the order and the relative degree of the system to obtain comparable results without hard effort of tuning the parameters.

Example 5.8.2 *Consider the following system*

$$\begin{aligned}\dot{\xi}(t) &= A\xi(t) + Bu(t) + h(\xi(t),t),\\ y &= C\xi(t),\end{aligned}$$

where $\xi(t) \triangleq [\xi_1(t)\cdots\xi_3(t)]^{\mathrm{T}} \in \mathbb{R}^3$ *is the state vector;* $u(t) \in \mathbb{R}$ *is the control inputs; matrices* A, B, C *are the realization of the following transfer function*

$$G(s) \triangleq C(sI - A)^{-1}B = \frac{6s+2}{(s-0.5)(s-0.6)(s-0.7)},$$

and $h(\xi,t) = [\cos(t)\tan(\xi_3)\;\; 2+\sin(1.5t)\;\; 0.2\cos(\xi_2)]^{\mathrm{T}} \in \mathbb{R}^3$. $G(s)$ *and* $h(\xi,t)$ *are unknown and* $\xi(t)$ *is unmeasurable. It can be seen that* $G(s)$ *is unstable and has relative degree* $r = 2$.

Now, let consider the following control signal

$$u(s) = Q(s)\bar{u}(s) = \frac{1}{s+15}\bar{u}(s),$$

which leads $G(s)Q(s)$ *to be a system of order* $n = 4$ *and relative degree* $\bar{r} = 3$ *in respect of the control input* $\bar{u}(t)$*. Hence, we can apply the same controller from example 1.*

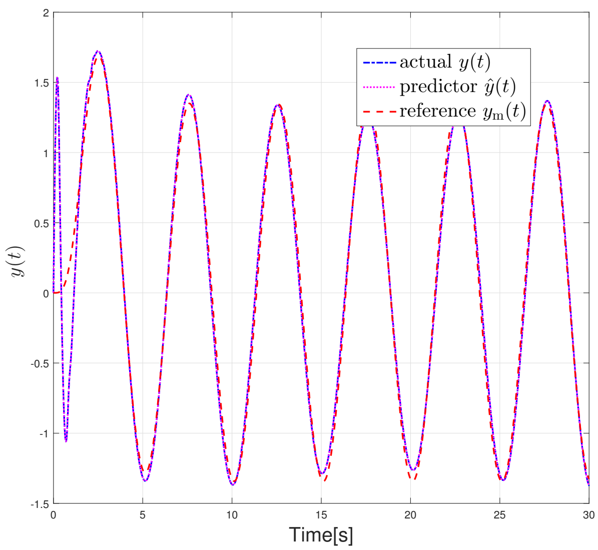

Figure 5.11: System trajectories.

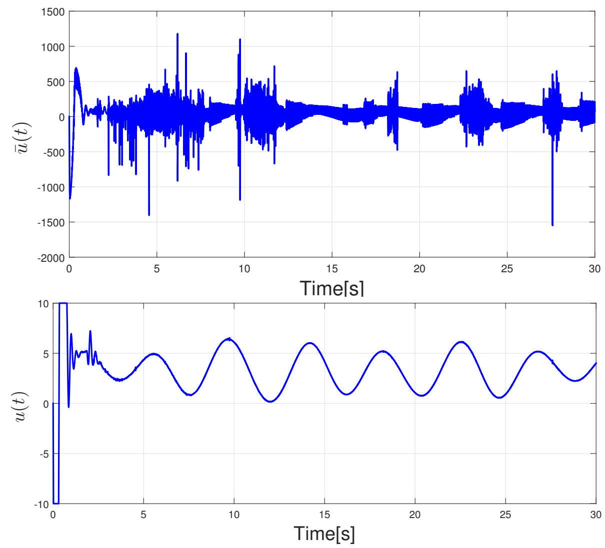

Figure 5.12: Control signal $\bar{u}(t)$ and $u(t)$.

To illustrate the simplicity and advantage of the proposed controller, we use the same parameters of example 1, except with bad tuning adaptation parameters: $\gamma = 5 \times 10^4$ *and* $h_0 = 1$. *Fig 5.11 and Fig 5.12 show the tracking performance, the virtual control* $\bar{u}(t)$ *and the control* $u(t)$*, respectively. It can be seen that although the virtual control signal* $\bar{u}(t)$ *is heavily chattering, the true control signal* $u(t)$ *is smooth.*

Notice that, different than the $\mathscr{L}_1$ *adaptive control, when incorporating the filter to smooth the control signal, we do increase the order and the relative degree of the system. However, in our approach, increasing the system order and relative degree still does not complicate the controller structure. In contrast, the idea of passing a control signal through a low-pass filter in order to keep it in a desired bandwidth can not be handled easily by using adaptive backstepping. This is because of doing so will increase the relative degree, hence requiring an extra design step and complicating the control structure. In fact, any* 4^{th} *order systems that satisfy our assumptions can be controlled by using the exact control structure given in Example 5.8.1 and choosing the projection bounds for the adaptive parameters intuitively. In the next section, we will apply the controller to control motion of the musculotendon arm model.*

5.9 Control the arm motion

The algorithm is implemented on the Arm26 model provided in OpenSim ([54]) to control the elbow flexion angle. The system dynamics can be summarized as follow.

$$\ddot{\theta}(t) = f(\theta(t), \dot{\theta}(t)) + g(\theta(t), \dot{\theta}(t))M(t), \tag{5.51a}$$

$$M(t) = \sum_{i=1}^{3} F_i(l_i(t))r_i(\theta), \tag{5.51b}$$

$$\dot{l}_i^{\mathrm{M}}(t) = \Psi_1({l^{\mathrm{M}}}_i(t), a_i(t)), \tag{5.51c}$$

$$\dot{a}_i(t) = \Psi_2(a_i(t), e_i(t)), \qquad i = 1, 2, 3, \tag{5.51d}$$

where in (5.51a), θ is the elbow flexion, and M is the elbow moment as illustrated in Fig 5.13. In (5.51b), three segments of muscles are considered to contribute to the elbow moment M: lateral and medial heads of triceps (TRIlat and TRImed), and brachialis (BRA). Each muscle creates a moment, which is a product of muscle force F_i with a corresponding moment arm r_i. Each muscle force F_i is a nonlinear function of its muscle length $l^{\mathrm{M}}(t)$. Eq. (5.51c) describes the muscle contraction dynamics driven by the muscle activation $a_i(t)$. Finally, (5.51d) presents the dynamics of the muscle activation, which is controlled by the excitation signal $e_i(t)$.

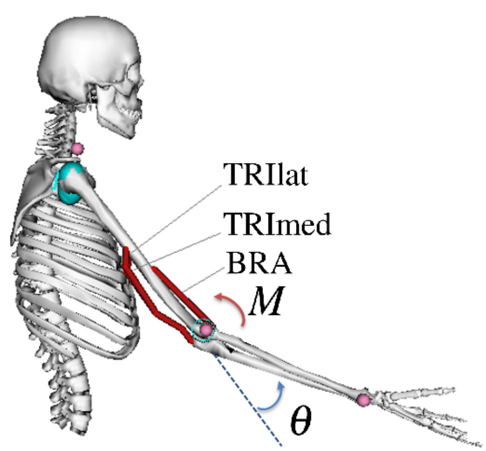

Figure 5.13: The Arm26 model with 3 active muscles:TRIlat, TRImed, BRA

The system dynamics (i.e. functions $f, g, F_i, r_i, \Psi_1, \Psi_2$) are unknown, and only the output $\theta(t)$ and the control input $e_i(t)$ generated by the FES system are measured. Details of the mathematics model (*used only for the simulation purpose*) can be found in ([5, 58]). It can be seen that system (5.51) has one output $\theta(t)$ and three inputs $e_i(t)$. Furthermore, due to the properties of human body, the considered system satisfies all our assumptions.

The simulation is conducted by using the default parameters given from OpenSim Arm26 Model, which include the following maximum isometric forces $F_{\mathrm{o}}^{\mathrm{M}}$, optimal fiber length $l_{\mathrm{o}}^{\mathrm{M}}$ and slack tendon lengths $l_{\mathrm{s}}^{\mathrm{T}}$

Muscles	TRIlat	TRimed	BRA
$F_0^{\mathrm{M}}(N)$	624.3	624.3	987.26
$l_0^{\mathrm{M}}(m)$	0.1138	0.1138	0.0858
$l_0^{\mathrm{M}}(m)$	0.0908	0.0908	0.0535

Since the excitation inputs are bounded by $0 \le e_i(t) \le 1$ and have the same relative degree $r = 4$, these inputs can be merged into one virtual control $u(t)$, in which the antagonist muscles TRIlat, Trimed provide $u(t) < 0$ and the agonist muscle BRA provides $u(t) > 0$. Hence, the controller can be implemented by considering the system as a SISO system with the order $n = 4$ and a virtual control signal $u(t) \in [-1\ 1]$.

The autoregressive vectors are constructed by using the low pass filter (5.4) with $\Delta(s) = s^4 + \lambda^{\mathrm{T}} S(s) = (s+10)^4$, so that the reference system defined in (5.2) is

$$A_{\mathrm{m}} = \begin{bmatrix} -40 & -600 & -4000 & -10^4 & -1 \\ 1 & 0 & 0 & 0 & 0 \\ 0 & 1 & 0 & 0 & 0 \\ 0 & 0 & 1 & 0 & 0 \\ 960 & 19400 & 146000 & 39\times 10^4 & -1 \end{bmatrix}, \quad B_{\mathrm{m}} = \begin{bmatrix} 0 \\ 0 \\ 0 \\ 0 \\ 1 \end{bmatrix}, \quad C_{\mathrm{m}} = B_{\mathrm{m}}^{\mathrm{T}}.$$

The following parameters are used to implement the controller: $P = I_5$, adaptation gain $\gamma = 5\times 10^5$; $k(t)$ is defined in (5.38); $k_C \triangleq 100$ and $\Lambda(s) \triangleq s(s+1.2)(s+1.3)(s+1.5)$ so that $K_f =$

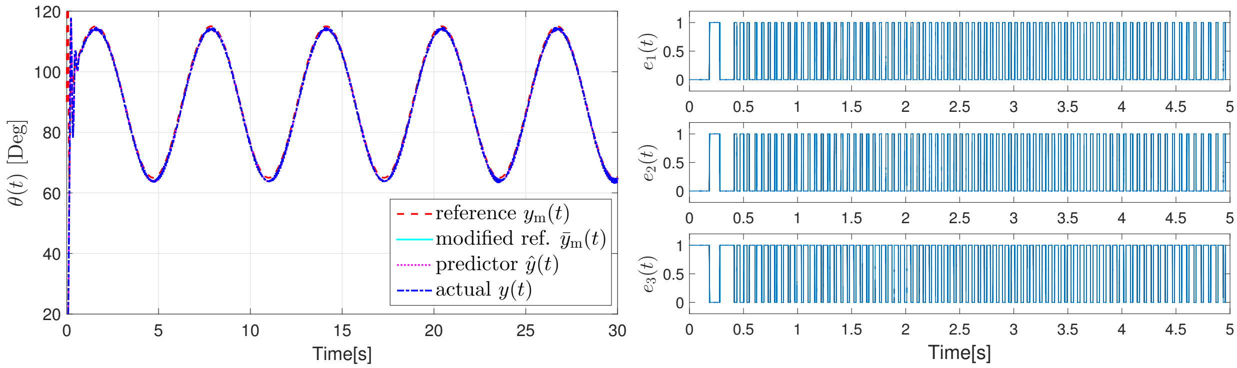

Figure 5.14: The time evolution of outputs $y_{\mathrm{m}}(t)$, $\bar{y}_{\mathrm{m}}(t)$, $\hat{y}(t)$, and $y(t)$ and the excitation signals $e_i(t)$ for $r(t) = \frac{\pi}{180}(25\sin(t)+90)$.

$[-36\ \ -595\ \ -3998\ \ -10^4]$.

For the adaptation law, we set the following projection bounds and the initial values as

$$
\begin{aligned}
\Omega_\alpha &= \pm[100\ 100\ 100\ 100]^{\mathrm{T}}, & \hat{\alpha}_0 &= [-4\ 6\ -4\ 1]^{\mathrm{T}},\\
\Omega_\beta &= \pm[0\ 0\ 0\ 100]^{\mathrm{T}}, & \hat{\beta}_0 &= [0\ 0\ 0\ 1]^{\mathrm{T}},\\
\Omega_\sigma &= [-30\ 30], & \hat{\sigma}_0 &= 0.
\end{aligned}
$$

The virtual control signal $u(t)$ is obtained by (5.25) and saturated in $[-1\ \ 1]$, and the excitation signals are derived as

$$
\begin{aligned}
e_1(t) &= e_2(t) = -u(t),\ \ e_3(t) = 0, && \text{if } \ u(t) < 0,\\
e_1(t) &= e_2(t) = 0,\ \ e_3(t) = u(t), && \text{if } \ u(t) > 0,
\end{aligned}
$$

OpenSim can be simulated in MATLAB by using MATLAB scripts ([94]) or Simulink ([95, 96]). In this implementation, the simulation is conducted on OpenSim 3.2 API and MATLAB 2014b by following the MATLAB Scripts tutorial in [94]. MATLAB ODE15s solver is used for integration.

The system responses and the control efforts for different reference signals $r(t)$ are illustrated

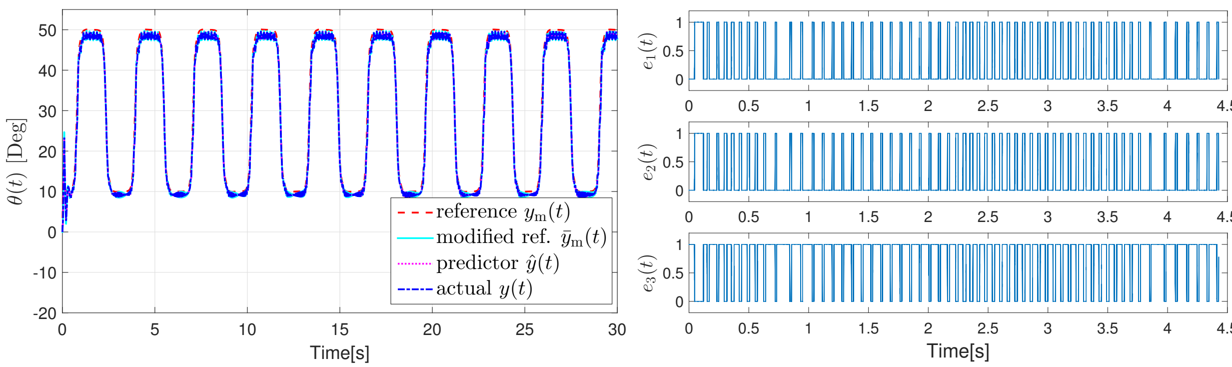

Figure 5.15: The time evolution of outputs $y_{\rm m}(t)$, $\bar{y}_{\rm m}(t)$, $\hat{y}(t)$, and $y(t)$ and the excitation signals $e_i(t)$ for $r(t) = \frac{\pi}{180}(-20\tanh(4\cos(2t)+30)$.

in Fig 5.14 and Fig 5.15, respectively. The reference input is chosen in order to obtain the desired trajectory with different ranges of motion. As seen from Fig 5.14 and Fig 5.15, the settling time for the system output $y(t)$, predictor output $\hat{y}(t)$, and the reference output $y_m(t)$ to converge to each other is less than $0.5s$. *Without retuning*, the tracking performance in both case are satisfied in a large range of motion, and confirm the theoretical analysis. The control signals have a bang-bang effect due to the saturation of control input. In practice, this is how muscles are activated, which helps reducing the muscle fatigue.

To avoid distortion of the reference output $y_{\rm m}(t)$, when increasing the frequency of the reference signal $r(t)$, we need to increase the cut-off frequencies of the reference system (5.2) and the low-pass filter (5.4). As suggested in literature ([97–100]), a limb motion with frequency less than $1Hz$ is commonly used, so that the low-pass filter bandwidth selected as $\Delta(s) = (s+10)^4$ is suitable for most applications. To further prove the numerical stability, Fig 5.16 shows the tracking results for the reference $r(t) = \frac{\pi}{180}(15\tanh(3\sin(5t))+70)$ over a period of 300s. As seen in Fig 5.16, for a constant k_C, increasing the reference frequency will induce a larger tracking error. This effect is predictable by our theoretical analysis, in particular, (5.32) and (5.37) show that increasing the frequency of $r(s)$ will increase the frequency of $\eta(s)$. However, $\mu(s)$ can only cancel the low frequency components of $\eta(s)$ filtered by $C(s)$. Therefore, to obtain a smaller tracking errors, increasing frequency of $r(t)$ will require increase k_C to increase the bandwidth of $C(s)$. Nevertheless, without retuning, the tracking performance is satisfied, with the error mean and the standard

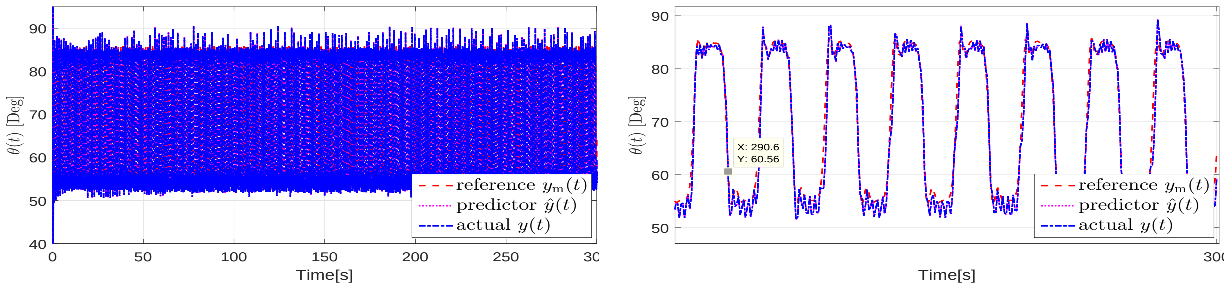

Figure 5.16: The time evolution of output $y_{\mathrm{m}}(t)$, $\hat{y}(t)$, and $y(t)$ and its closed-look in the time period [290 300(s)] for $r(t) = \frac{\pi}{180}(15\tanh(3\sin(5t))+70)$

deviation of the error $|y_m(t) - y(t)|$ given by $(M_{\mathrm{err}}, \sigma_{\mathrm{err}}) = (1.81°, 2.48°)$.

To further prove the robustness of the proposed controller to unstructured uncertainties, the Millard musculotendon model ([101]) is used to replace the default Thelen musculotendon model ([57]) in Arm26 model. The force-velocity curve, the fiber force-length curve, and the tendon force-length curve are set to the Millard model default values. Moreover, the maximum isometric forces F_0^{M}, optimal fiber length $l_{\mathrm{o}}^{\mathrm{M}}$ and slack tendon lengths $l_{\mathrm{s}}^{\mathrm{T}}$ are modified as

Muscles	TRIlat	TRimed	BRA
$F_0^{\mathrm{M}}(N)$	500	500	1100
$l_{\mathrm{s}}^{T}(m)$	0.1	0.1	0.09
$l_0^{\mathrm{M}}(m)$	0.08	0.08	0.05

These modifications of the model represent the uncertainties both in the system dynamics and the physical parameters. Note that although the two models are different, they have same level of complexity and the same high relative degrees. *The same control parameters are used again* to conduct the simulation study. The system response and a time window over the first 7 seconds are illustrated in Fig 5.17. As seen from Fig 5.17, although there is a little overshoot in the first second during the adaptation, the tracking result is satisfied despite of the changes in model and parameters. These simulations confirm our theoretical analysis about the controller properties of fast tracking and robustness to uncertainties.

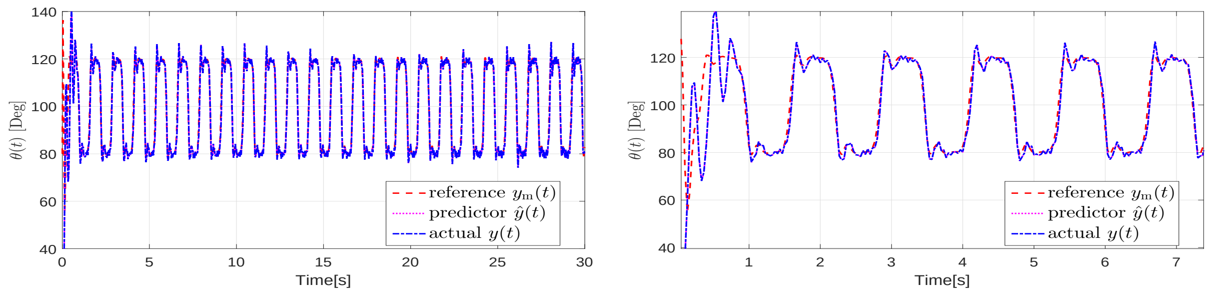

Figure 5.17: The time evolution of output $y_{\mathrm{m}}(t)$, $\hat{y}(t)$, and $y(t)$ conducted with Millard Model and its closed-look in the time period [0 7(s)] for $r(t) = \frac{\pi}{180}(-20\tanh(3\sin(5t)) + 100)$.

5.10 Discussion

The most valuable advantage of our proposed approach is that it is based on an output feedback control as opposed to open-loop and feed-forward controllers commonly used for FES systems. Furthermore, it can deal with complex nonlinearities, large uncertainties of the musculoskeletal system without the need of system dynamics and full state measurements, such as individual muscle forces, muscle lengths and activations. For example, in [100, 102, 103], the authors proposes open-loop and feed-forward controllers to stabilize the arm motion based on an optimization process to control joints' stiffness. These approaches assumes that muscle force is linearly proportional to the activation (i.e. Equ. (3) in [103])

$$f^{\mathrm{m}}(\alpha, q) = \alpha f_0^{\mathrm{m}}(q)$$

where $f^{\mathrm{m}}(\alpha, q)$ is the muscle force, α is the vector of muscle activation, and $f_0^{\mathrm{m}}(q)$ is the posture dependent maximum achievable muscle forces. This assumption has several drawbacks. First, it ignores the intrinsic nonlinearity of the muscle contraction dynamics and the delay of the muscle activation, which significantly simplify the problem that we attempt to solve. Furthermore, it requires a time-consuming calibration to obtain the functions $f_0^{\mathrm{m}}(q)$. In [98], a Dynamic Surface control is proposed to compensate for the nonlinearity of the contraction dynamics and the delay of the neuromuscular activation dynamics. However, the approach would require a full-state measurement, such as the angular velocity and the activation. In practice, muscle activation is not measurable and designing an observer to estimate the activation is very challenging because

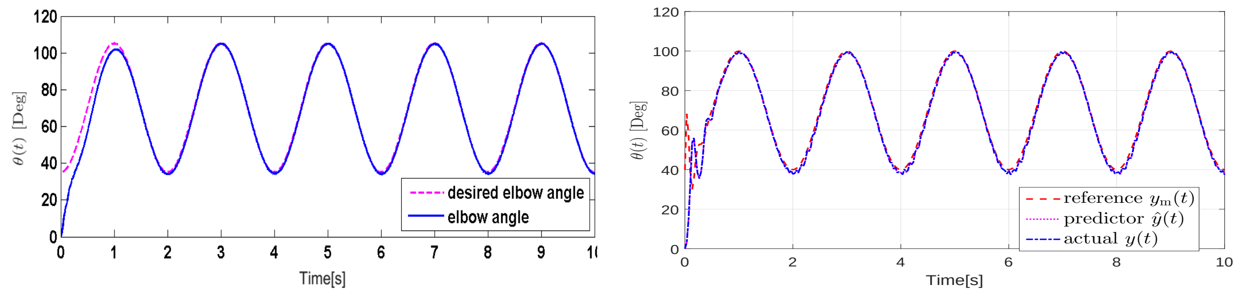

Figure 5.18: The tracking performance using the sliding mode control (Fig. 5 [5]) and the proposed controller for $r(t) = \frac{\pi}{180}(-35\cos(\pi t)) + 70)$.

the muscle contraction dynamics is highly nonlinear and unknown. Furthermore, the controller does not consider the case of agonist-antagonist muscles group. In [5], although the controller uses the adaptive sliding mode to deal with the dynamics uncertainties, it still relies heavily on the system dynamics through the back-stepping control process and full state measurements. Since the simulation study in [5] is conducted using the same model Arm26, the corresponding tracking results are shown in Fig 5.18 to compare the performance between our proposed controller and that presented in [5].

Note that, without retuning, without the need of model dynamics as in [5], and without model identification procedures as in [100], the new proposed controller can obtain faster tracking than the controller proposed in [5]. Furthermore, no output derivatives are required to implement the controller, as opposed to [98]. Only output measurement, such as the elbow angle, and the excitation signals simulated by FES are used to construct the predictor. To our best knowledge, this is the first output feedback FES controller that can theoretically prove stability when applied to the complete Hill-type musculostendon models, such as Thelen and Millard model ([57, 101]). This advantage provides more practical approach for closed-loop control of FES application.

5.11 Conclusion

This chapter presents an output feedback control for a class of unknown dynamics systems with unmatched uncertainties and high relative degree. The algorithm relies on an adaptive predictor, which can predict the system output for any admissible input. The prediction error is proved to be ultimately bounded using the Lyapunov direct method. Then, the control law is derived to cancel the unmatched uncertainty estimation. This control law avoids the recursive step-by-step design of backstepping and therefore remains simple regardless of the system relative degree. Theoretical analysis shows that fast convergence, accurate tracking and a smooth control signal can be obtained simultaneously. Simulation results of controlling the elbow flexion angle conducted in OpenSim validate the performance of the proposed control algorithm. Further implementation and experimental results will be presented in the next section to verify the control performance for MIMO systems.

Chapter 6

Adaptive Predictor-Based Output Feedback Control for a Class of High Relative Degree Uncertain Nonlinear Systems with Fast Adaptation and Simple Control Structure: Experimental Results for MIMO Systems

The following results will be submitted for consideration to the International Journal of Robust and Nonlinear Control.

6.1 Introduction

The results for SISO systems from Chapter 5 are extended for MIMO systems in this chapter. Specifically, the predictor remains similar to that of the SISO case. The MIMO predictor will then be decoupled into independent SISO systems for which the results from Chapter 5 can be applied to obtain the virtual control signals. Consequently, these virtual control signals are transformed back to the real control signals applied to the physical MIMO system. Simulation and experimental results are reported to verify the controller performance for MIMO systems.

This chapter is organized as follows. Section 6.2 summarizes the main results and presents the controller structure for MIMO systems. Section 6.3 provides simulation demos in Gazebo environment and experimental results to control a robotics arm to illustrate the algorithm's efficacy. Section 6.4 presents the experimental results for the Quanser helicopter and Section 6.5 concludes this chapter.

6.2 Adaptive Predictor-based Control for MIMO Systems

The result obtained for the SISO case can be easily extended to the MIMO case by making the following assumption

Assumption 6.2.1 *The system is at least square, i.e. $m \geq p$. For each output, all inputs have the same relative degree, i.e $r_{ij} = r_i,\ i = 1,\ldots,p,\ j = 1,\ldots,m$.*

Lemma 6.2.1 *Consider the MIMO system (5.6), and the following adaptive control*

$$u(t) = -\bar{K}_{\mathrm{f}}\omega_u(t) + \hat{v}(t),\ \ \hat{v}(t) = F^{-1}(t)(\tau(t) - \varsigma(t)), \tag{6.1a}$$

$$\hat{\tau}(t) = -K_c(\hat{\mu}(t) + \hat{\eta}(t) - k_g r(t)), \tag{6.1b}$$

$$\varsigma(t) = \left[\begin{array}{ccc} \sum\limits_{j=2}^{m} \varsigma_{1j}(t) & \cdots & \sum\limits_{j=2}^{m} \varsigma_{pj}(t) \end{array}\right]^{\mathrm{T}} \in \mathbb{R}^p, \tag{6.1c}$$

where $\bar{K}_{\mathrm{f}} \triangleq 1_m \otimes K_{\mathrm{f}} \in \mathbb{R}^{m\times nm}$, $K_c \triangleq \mathrm{diag}([k_{c1}\ \cdots\ k_{cp}]) \in \mathbb{R}^{p\times p}$, and $F(t) \in \mathbb{R}^{p\times m}$ is defined as

$$F(t) \triangleq \left[\begin{array}{cccc} 1 & \bar{\hat{p}}_{12}(t) & \cdots & \bar{\hat{p}}_{1m}(t) \\ \vdots & \vdots & \vdots & \vdots \\ 1 & \bar{\hat{p}}_{p2}(t) & \cdots & \bar{\hat{p}}_{pm}(t) \end{array}\right], \qquad \bar{\hat{p}}_{ij}(t) \triangleq \frac{\hat{p}_{ij}(t)}{\hat{p}_{i1}(t)}, \tag{6.2a}$$

$$\hat{P}_{ij}(s,t) \triangleq \hat{\beta}_{ij}^{\mathrm{T}}(t) A_{\mathrm{p}} S(s) \triangleq \hat{p}_{ij}(t)\bar{\hat{P}}_{ij}(s), \qquad S(s) \triangleq [s^{n-1}\ldots s\ 1]^{\mathrm{T}} \in \mathbb{C}^n, \tag{6.2b}$$

$$\bar{\hat{P}}_{ij}(s,t) \triangleq s^{l_i} + \hat{p}_{ij}^{(l_i-1)}(t)s^{l_i-1} + \cdots + \hat{p}_{ij}^{(1)}(t)s + \hat{p}_{ij}^{(0)}(t), \tag{6.2c}$$

where $A_{\mathrm{p}} \triangleq A_{\mathrm{f}} + k_{\mathrm{p}} I_n$, $l_i \triangleq n - r_i$, *and* $\varsigma_{ij}(t)$ *is the output of the system*

$$\dot{\vartheta}_{ij}(t) = A_i(t)\vartheta_{ij}(t) + B_i v_j(t), \quad \vartheta_{ij}(0) = \vartheta_{ij_0}, \tag{6.3a}$$

$$\varsigma_{ij}(t) = C_{ij}(t)\vartheta_{ij}(t), \tag{6.3b}$$

where $A_i(t), B_i, C_{ij}(t)$ *are the state-space realization of the transfer function*

$$V_{ij}(s,t) = \bar{\hat{p}}_{ij}(t) W_{ij}(s,t), \quad W_{ij}(s,t) \triangleq \frac{\bar{\hat{P}}_{ij}(s,t) - \bar{\hat{P}}_{i1}(s,t)}{\bar{\hat{P}}_{i1}(s,t)}. \tag{6.4}$$

All signals of the closed loop system remain bounded if K_{f} *and* K_C *are chosen such that* $C(s)$ *is stable and* $\|G(s)\|_{\mathscr{L}_1} L < 1$.

Proof *Similar to (5.30) for the SISO case,* $\mu(s)$ *has the form*

$$\mu(s) \triangleq \begin{bmatrix} \mu_1(s) \\ \vdots \\ \mu_p(s) \end{bmatrix} = \begin{bmatrix} F_{11}(s) & \cdots & F_{1m}(s) \\ \vdots & \ddots & \vdots \\ F_{p1}(s) & \cdots & F_{pm}(s) \end{bmatrix} \begin{bmatrix} v_1(s) \\ \vdots \\ v_m(s) \end{bmatrix}, \tag{6.5}$$

where $F_{ij}(s) = \frac{P_{ij}(s)}{\Lambda(s)}$ *is a minimum phase transfer function, and* $\Lambda(s) \triangleq \det(sI - (A_{\mathrm{f}} - B_{\mathrm{f}} K_{\mathrm{f}}))$ *is Hurwitz. Without loosing generality, by defining*

$$\tau_i(s) \triangleq v_1(s) + \sum_{j=2}^{m} \frac{F_{ij}(s)}{F_{i1}(s)} v_j(s), \tag{6.6}$$

(6.5) takes the form $\mu_i(s) = F_{i1}(s)\tau_i(s)$. *Therefore, the MIMO system is decoupled into p independent SISO systems, each of which has a control input* $\tau_i(t)$. *Hence, the results from Lemma 5.6.1 and Theorem 5.7.1 are hold for each single system, which proves (6.1b).*

It follows from Assumption 6.2.1 that $P_{ij}(s)$ *has the same order for all* $j = 1, \ldots, m$, *i.e.*

$$P_{ij}(s) = p_{ij}\bar{P}_{ij}(s), \quad \bar{P}_{ij}(s) \triangleq s^{l_i} + p_{ij}^{(l_i-1)} s^{l_i-1} + \cdots + p_{ij}^{(1)} s + p_{ij}^{(0)},$$

so that

$$\frac{F_{ij}(s)}{F_{i1}(s)} = \frac{p_{ij}}{p_{i1}}(1 + W_{ij}(s)),$$

where

$$W_{ij}(s) \triangleq \frac{\bar{P}_{ij}(s) - \bar{P}_{i1}(s)}{\bar{P}_{i1}(s)} = \frac{w_{ij}^{(l_i-1)} s^{l_i-1} + \cdots + w_{ij}^{(1)} s + w_{ij}^{(0)}}{s^{l_i} + p_{ij}^{(l_i-1)} s^{l_i-1} + \cdots + p_{i1}^{(1)} s + p_{i1}^{(0)}},$$

and $w_{ij}^{(q)} \triangleq p_{ij}^{(q)} - p_{i1}^{(q)}$, $q = 1, \ldots, (l_i - 1)$. *Note that* $W_{ij}(s)$ *are strictly proper stable transfer function. Let* $\bar{p}_{ij} \triangleq \frac{p_{ij}}{p_{i1}}$ *and* $\varsigma_{ij}(s) \triangleq \bar{p}_{ij} W_{ij}(s) v_j(s)$*, then*

$$\frac{F_{ij}(s)}{F_{i1}(s)} v_j(s) = \bar{p}_{ij} v_j(s) + \varsigma_{ij}(s), \tag{6.7}$$

where $\varsigma_{ij}(t)$ *can be obtained by the state-space realization (6.3), where* $A_i \in \mathbb{R}^{(l_i-1)\times(l_i-1)}$, $B_i \in \mathbb{R}^{(l_i-1)}$ *and* $C_{ij} \in \mathbb{R}^{1\times(l_i-1)}$ *are defined as*

$$A_i \triangleq \begin{bmatrix} -p_{i1}^{(l_i-1)} & \ldots & -p_{i1}^{(0)} \\ I_{l_i-1} & & 0_{l_i-1} \end{bmatrix}, \quad B_i \triangleq \begin{bmatrix} 1 \\ 0_{l_i-1} \end{bmatrix},$$

$$C_{ij} \triangleq \bar{p}_{ij} \begin{bmatrix} w_{ij}^{(l_i-1)} \cdots w_{ij}^{(0)} \end{bmatrix}. \tag{6.8}$$

The realization (6.3) holds for both ideal case in which A_i, C_{ij} *are assumed to be known constants and for adaptive case in which entries of matrices* A_i, C_{ij} *are time-varying and obtained from (6.2).*

To derive the control $\hat{v}(t)$*, it follows from (6.6) and (6.7) that*

$$\begin{bmatrix} 1 & \hat{\bar{p}}_{12} & \cdots & \hat{\bar{p}}_{1m} \\ \vdots & \vdots & \vdots & \vdots \\ 1 & \hat{\bar{p}}_{p2} & \cdots & \hat{\bar{p}}_{pm} \end{bmatrix} \begin{bmatrix} v_1 \\ \vdots \\ v_m \end{bmatrix} + \begin{bmatrix} \sum_{j=2}^{m} \varsigma_{1j} \\ \vdots \\ \sum_{j=2}^{m} \varsigma_{pj} \end{bmatrix} = \begin{bmatrix} \tau_1 \\ \vdots \\ \tau_p \end{bmatrix},$$

which prove (6.1) and conclude the proof. □

The control structure for MIMO systems are illustrated in Fig 6.1 and Fig 6.2.

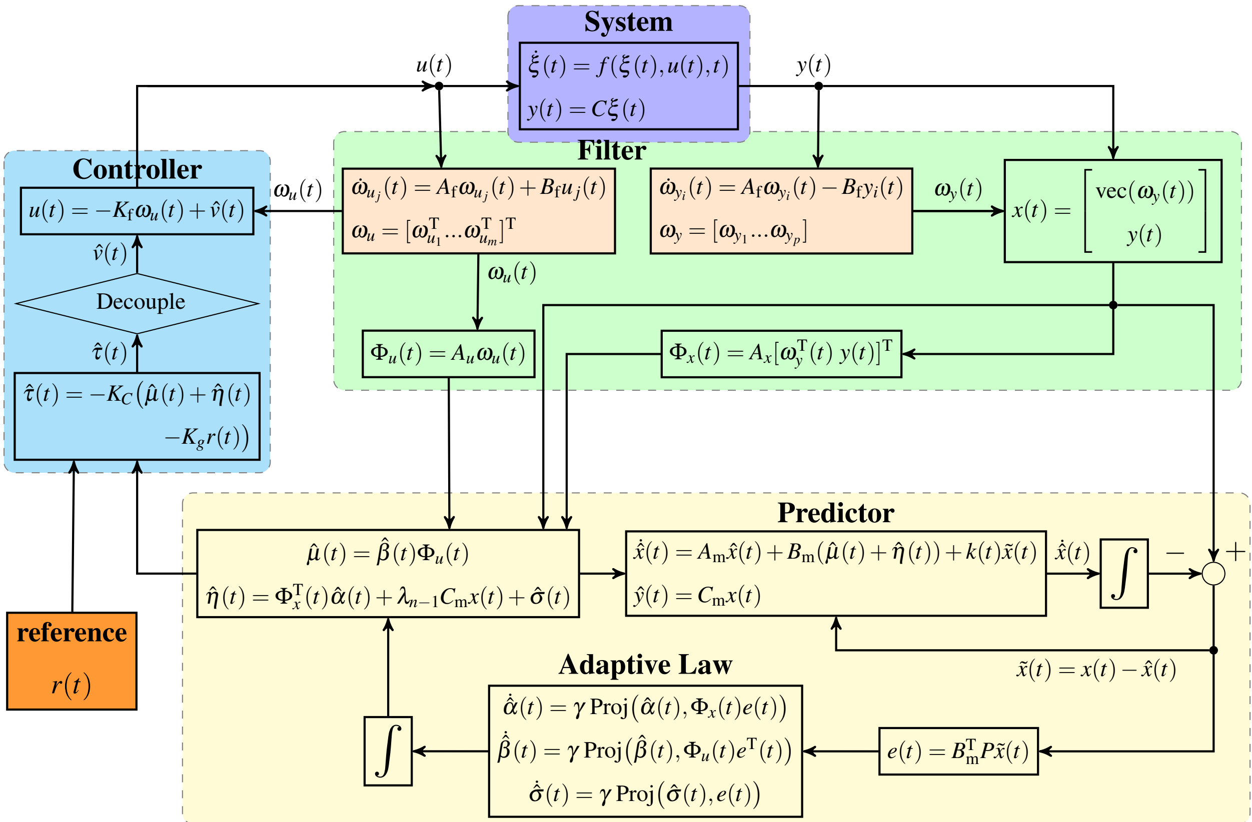

Figure 6.1: Controller structure for MIMO systems

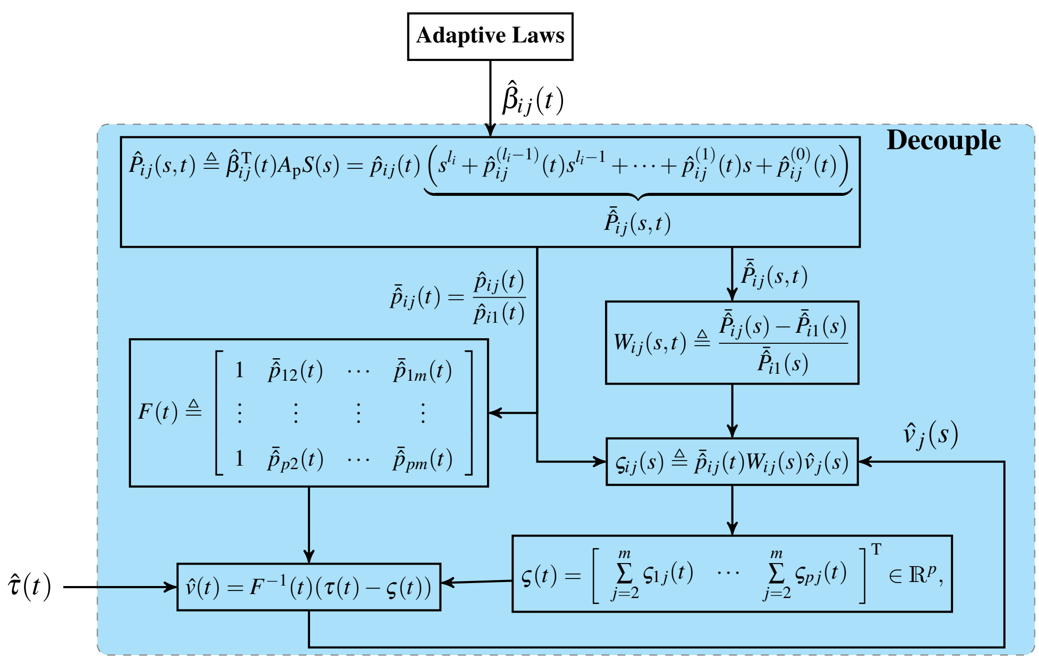

Figure 6.2: Decouple control signals for MIMO systems

6.3 Control Robotics Arm

The algorithm performance is studied by implementation in order to control the motion of the Fetch Robotics Arm. The robotics arm has 7 joints, as illustrated in Fig 6.3. Each joint can receive commanded torque as a control input signal. The default rate for the commands streaming from the robot computer to the joint and the sampling rate of the angular positions are 200Hz. The simulation is conducted in Gazebo environment ([104]) and Robotic Operating System (ROS) Indigo version ([105]). For this demonstration, we will select the torque generated at the shoulder lift joint and the elbow flex joint as the control input signals. The system output can be either the joints angles or the end-effector position. Hence, the system is a MIMO system with 2 inputs and 2 outputs. In this implementation, the integration is obtained by using the simplest form $x(t+\Delta t) = x(t) + \dot{x}(t)\Delta t$, where $\Delta t = 1/200 = 0.05(s)$.

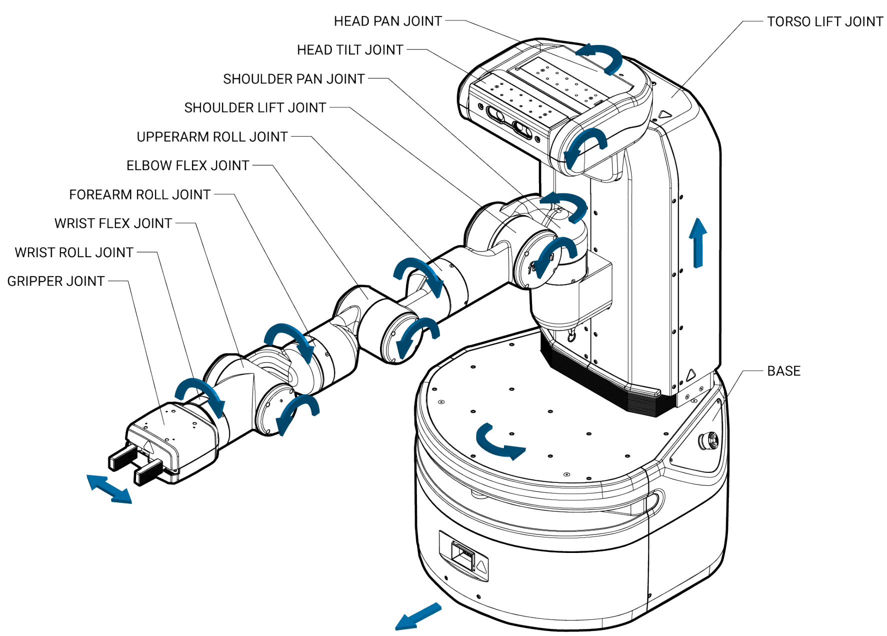

Figure 6.3: Fetch Robotics Arm (picture is adopted from [6])

6.3.1 Control Joint Angles

In this experiment, we attempt to simultaneously control two outputs: the shoulder lift joint angle $\phi_1(t)$ and the elbow flex joint angle $\phi_2(t)$. The MIMO system dynamics is unknown, but we assume that each elementary SISO system is a 2$^{\text{rd}}$ order system ($n = 2$) with relative degrees $r_{ij} = 2,\ i = 1,2,\ j = 1,2.$

To design the predictor, we chose a 2$^{\text{rd}}$ order autoregressive filter defined in (5.4) with parameters $\Delta(s) = s^2 + \lambda_T S(s) = (s+6)^2$, so that $\lambda = [12\ \ 36]$ and

$$A_{\mathrm{f}} = \begin{bmatrix} -12 & -36 \\ 1 & 0 \end{bmatrix} \in \mathbb{R}^{2\times 2}, \quad B_{\mathrm{f}} = \begin{bmatrix} 1 \\ 0 \end{bmatrix} \in \mathbb{R}^2.$$

Hence, the reference system is defined according to (5.2), with $k_{\mathrm{p}} = 1$ so that

$$A_{\mathrm{m}} = \begin{bmatrix} -12 & -36 & 0 & 0 & -1 & 0 \\ 1 & 0 & 0 & 0 & 0 & 0 \\ 0 & 0 & -12 & -36 & 0 & -1 \\ 0 & 0 & 1 & 0 & 0 & 0 \\ 96 & 396 & 0 & 0 & -1 & 0 \\ 0 & 0 & 96 & 396 & 0 & -1 \end{bmatrix}, \qquad B_{\mathrm{m}} = \begin{bmatrix} 0 & 0 \\ 0 & 0 \\ 0 & 0 \\ 0 & 0 \\ 1 & 0 \\ 0 & 1 \end{bmatrix},$$

$$C_{\mathrm{m}} = B_{\mathrm{m}}^{\mathrm{T}}, \quad k_g = 12 I_2,$$

and

$$A_x = \begin{bmatrix} -11 & -36 & -1 \\ 1 & 1 & 0 \end{bmatrix}, \quad A_u = \begin{bmatrix} -11 & -36 & 0 & 0 \\ 1 & 1 & 0 & 0 \\ 0 & 0 & -11 & -36 \\ 0 & 0 & 1 & 1 \end{bmatrix},$$

For the adaptation law, we set the following projection bounds and the initial values

$$\Omega_\alpha = \alpha_c \pm 5|\alpha_c|, \qquad \alpha_c = \hat{\alpha}_0 = [-48.0\ \ -6]^{\mathrm{T}},$$

$$\Omega_\beta = \beta_c \pm 0.6|\beta_c|, \qquad \beta_c = \hat{\beta}_0 = \begin{bmatrix} 0 & 1.6 & 0 & 12 \\ 0 & 0.3 & 0 & 5 \end{bmatrix}^{\mathrm{T}},$$

$$\Omega_\sigma = \pm[0.7\ 0.5], \qquad \hat{\sigma}_0 = 0_2.$$

The control law (6.1a) is implemented with the following parameters: $P = I$, adaptation gain $\gamma = 3000$, and $k(t)$ defined in (5.38). The control signal is saturated in $[120\ \ 80]$ (N.m).

We will follow the decouple process described in Fig 6.2 to implement the controller. For this simple case, since the system is assumed to be a second order system, we obtain

$$\hat{P}_{ij}(s,t) \triangleq \hat{\beta}_{ij}^{\mathrm{T}}(t) A_{\mathrm{p}} S(s) = \begin{bmatrix} 0 & \hat{\beta}_{ij}^{(0)}(t) \end{bmatrix} \begin{bmatrix} -11 & -36 \\ 1 & 1 \end{bmatrix} \begin{bmatrix} s \\ 1 \end{bmatrix} = \hat{\beta}_{ij}^{(0)}(t)(s+1)$$

Hence, $\hat{p}_{ij}(t) = \hat{\beta}_{ij}^{(0)}(t)$ and $\bar{\hat{P}}_{ij}(s) = s+1$, which yields

$$F(t) = \begin{bmatrix} 1 & \bar{\hat{p}}_{12}(t) \\ \bar{\hat{p}}_{21}(t) & 1 \end{bmatrix}, \quad \bar{\hat{p}}_{12}(t) = \frac{\hat{\beta}_{12}^{(0)}(t)}{\hat{\beta}_{11}^{(0)}(t)}, \ \ \bar{\hat{p}}_{21}(t) = \frac{\hat{\beta}_{21}^{(0)}(t)}{\hat{\beta}_{22}^{(0)}(t)},$$

$$W_{ij}(s) = \frac{\bar{\hat{P}}_{ij}(s) - \bar{\hat{P}}_{i1}(s)}{\bar{\hat{P}}_{i1}(s)} = 0 \qquad \Rightarrow \varsigma_{ij}(t) = 0.$$

The control signal is then obtained by

$$u(t) = -\bar{K}_{\mathrm{f}} \omega_u(t) + \hat{v}(t), \ \ \hat{v}(t) = F^{-1}(t)\tau(t),$$

$$\hat{\tau}(t) = -K_c(\hat{\mu}(t) + \hat{\eta}(t) - k_g r(t)),$$

In this experiment, the following values are used $K_C = 40I_2$, $h_0 = 2$, $\Lambda(s) = s(s+6)$ so that $K_f = [-6\ \ -36]$ and

$$\bar{K}_f = 1_2 \otimes K_{\mathrm{f}} = \begin{bmatrix} -6 & -36 & -6 & -36 \\ -6 & -36 & -6 & -36 \end{bmatrix}.$$

Fig 6.4 and Fig 6.6 show the tracking results and the control effort for the reference trajectory $r(t) = \frac{\pi}{180}[25\sin(t), 35\sin(0.5t)]^{\mathrm{T}}$ and $r(t) = \frac{\pi}{180}[35\sin(1.2t), 30\tanh(3\sin(0.4t)]^{\mathrm{T}}$, respectively.

Fig 6.5 and Fig 6.7 show the time evolving adaptive parameters for the corresponding case.

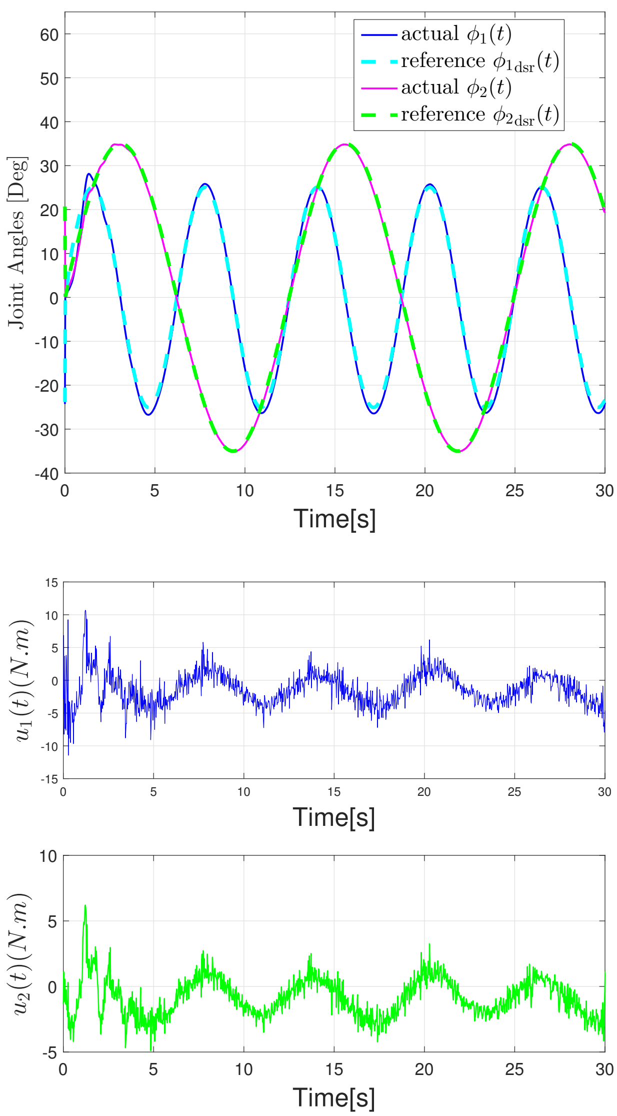

Figure 6.4: System trajectories and control effort for $r(t) = \dfrac{\pi}{180}[25\sin(t), 35\sin(0.5t)]^{\mathrm{T}}$.

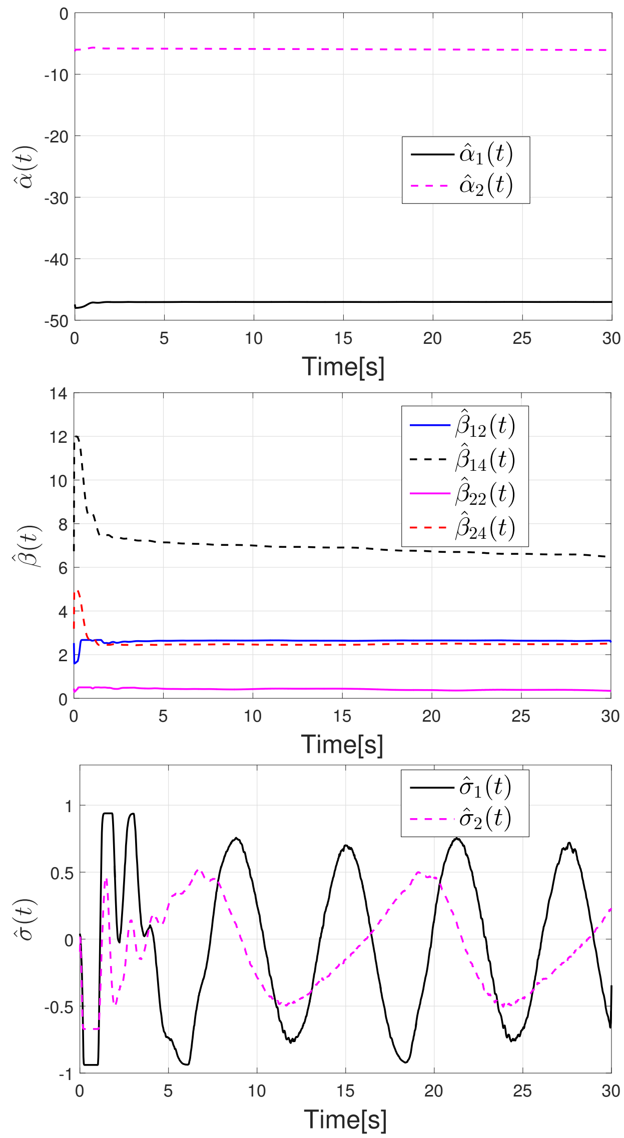

Figure 6.5: Time evolving of the adaptive parameters for $r(t) = \dfrac{\pi}{180}[25\sin(t), 35\sin(0.5t)]^{\mathrm{T}}$.

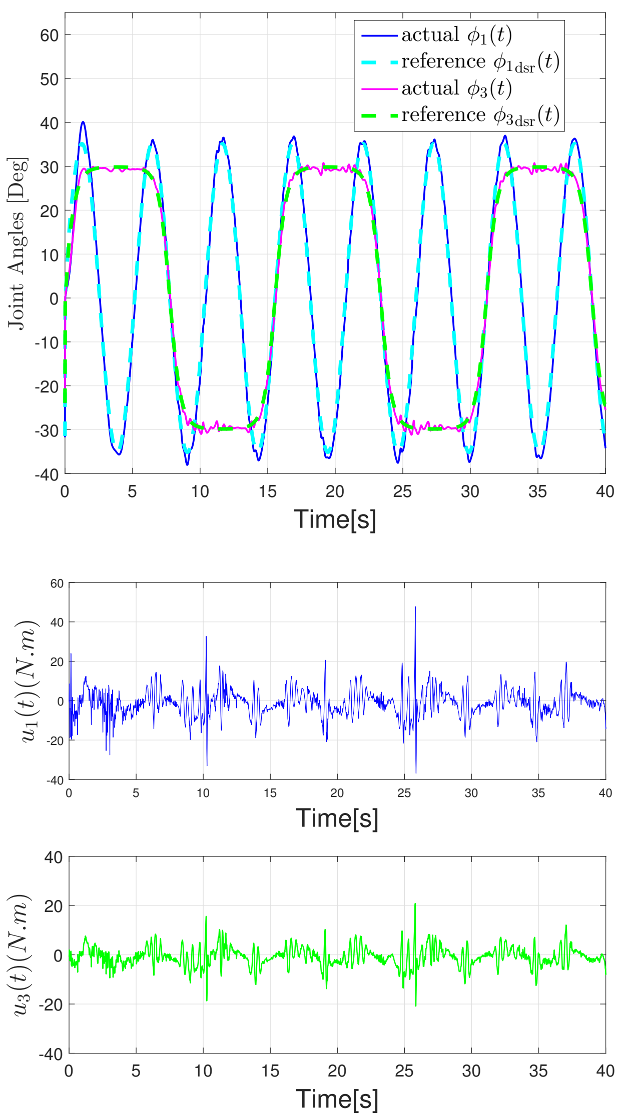

Figure 6.6: System trajectories and control effort for $r(t) = \frac{\pi}{180}[35\sin(1.2t), 30\tanh(3\sin(0.4t))]^{\mathrm{T}}$.

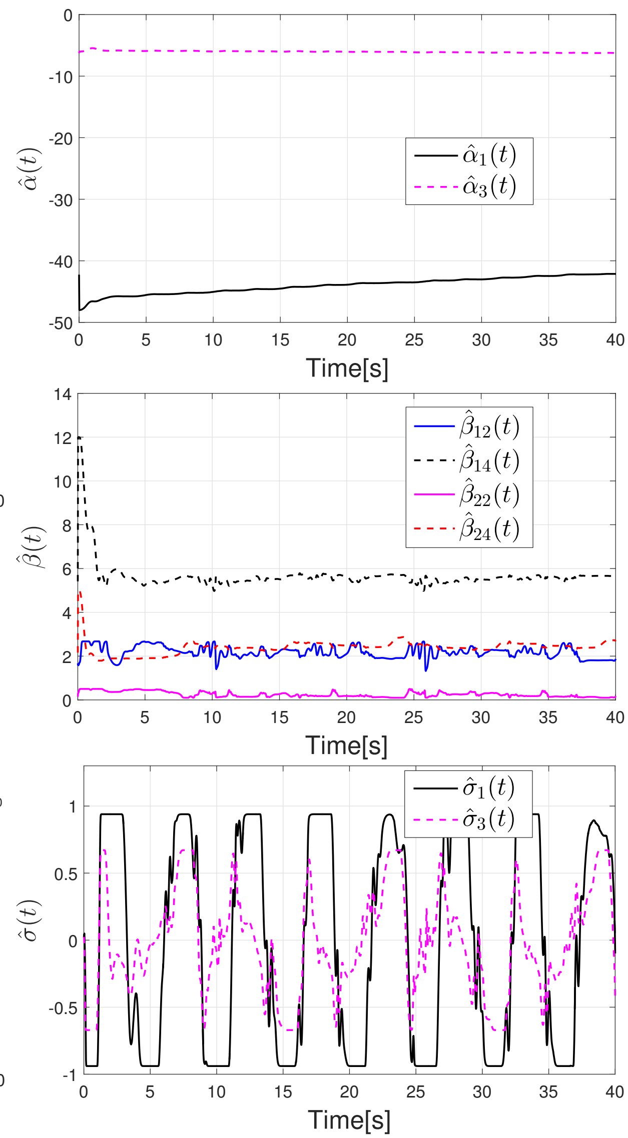

Figure 6.7: Time evolving of the adaptive parameters for $r(t) = \frac{\pi}{180}[35\sin(1.2t), 30\tanh(3\sin(0.4t))]^{\mathrm{T}}$.

As seen from the Fig 6.5 - Fig 6.7, the adaptive parameters are well bounded, and contain only low-frequency components. The adaptive terms $\hat{\sigma}(t)$ are able to capture the nonlinear time varying uncertainties of the dynamics. The control signal is not very smooth but still lies inside the allowed bandwidth, as illustrated in Fig 6.8 and Fig 6.9, and yields good tracking results.

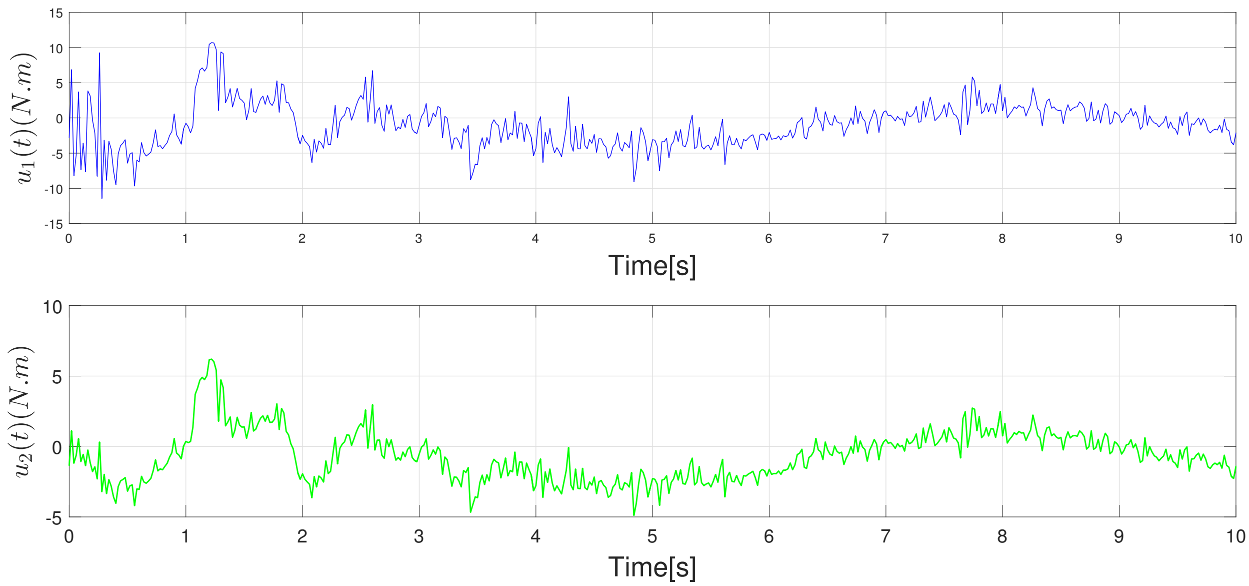

Figure 6.8: A closer look of control signals showed in Fig 6.4 in the time window $t = [0\ 10](s)$.

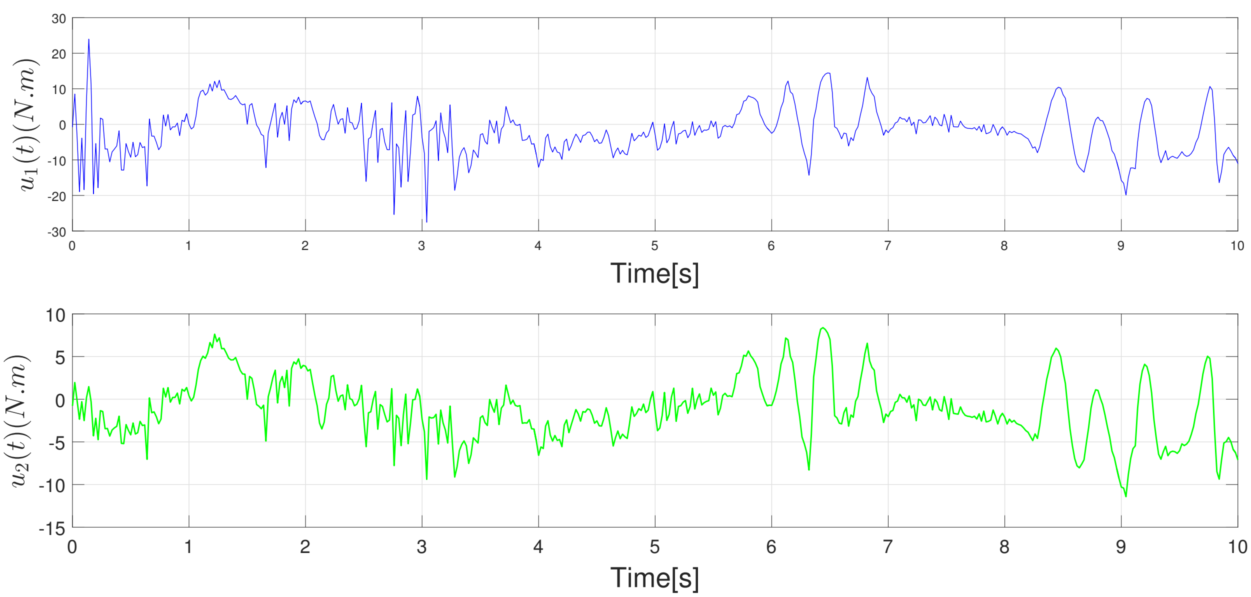

Figure 6.9: A closer look of control signals showed in Fig 6.6 in the time window $t = [0\ 10](s)$.

6.3.2 Control End-Effector position

In this experiment, we attempt to control the horizontal x and the vertical z positions of the robot arm end-effector using the joint torques as control inputs. Since we don't have any sensors to directly measure the tip position, we rely on the arm forward kinematics to obtain (x,z) from the measurement of the joint's angles. We emphasize that the forward kinematics serve as an indirect sensor, and we still assume the dynamics of the robot arm are unknown. Therefore, the controller do not use inverse kinematics to obtains the desired joint angles from the desired tip position.

Since we only change the output of the system from joints angle to the end-effector position, the considered system still remains as a 2 inputs and 2 outputs MIMO system. Therefore, the controller structure with the same parameters presented in Section 6.3.1 can be used. We select the adaptation gains $\gamma = 1000$, $h_0 = 20$, and the control gain $K_c = 60I_2$, and change the projection boundary of the adaptive parameters as follow

$$\Omega_\alpha = \alpha_c \pm 5|\alpha_c|, \qquad \alpha_c = \hat{\alpha}_0 = [-48.0 \ \ -6]^{\mathrm{T}},$$

$$\Omega_\beta = \beta_c \pm R_\beta, \qquad \beta_c = \hat{\beta}_0 = \begin{bmatrix} 0 & 1.6 & 0 & 12 \\ 0 & 0.35 & 0 & 5 \end{bmatrix}^{\mathrm{T}}, \quad R_\beta = \begin{bmatrix} 0 & 1.2 & 0 & 4 \\ 0 & 0.3 & 0 & 1 \end{bmatrix}^{\mathrm{T}},$$

$$\Omega_\sigma = \pm[0.04\ 0.06], \qquad \hat{\sigma}_0 = 0_2.$$

Fig 6.10 shows the tracking result and the control effort for the reference trajectory $r(t) = [0.1\cos(0.5t) + 0.95, 0.1\sin(0.5t)]^{\mathrm{T}}$. Fig 6.11 shows the time evolving of the adaptive parameters for the corresponding case. Fig 6.12 and Fig 6.13 shows the joint's angles trajectory and the end-effector position trajectory, respectively.

As seen from the figures, the tracking performance is satisfied. All adaptive parameters are bounded and the joint's angles also lie within their limits B_{ϕ_i}. Although all adaptive parameters and output measurement are smooth, the control signal is not very smooth. This effect is similar to the previous example, as illustrated in Fig 6.8 and Fig 6.9. Redoing this example using MATLAB/Simulink and ODE45 yields similar tracking performance but smooth control signals.

This can be attributed to the fact that the algorithm is implemented in a discrete manner, in which the integration takes the simplest form $x(t+\Delta t) = x(t) + \dot{x}(t)\Delta t$ with $\Delta t = 1/200 = 0.05(s)$. Nevertheless, the control signal still lies inside the allowed bandwidth, and yields good tracking results.

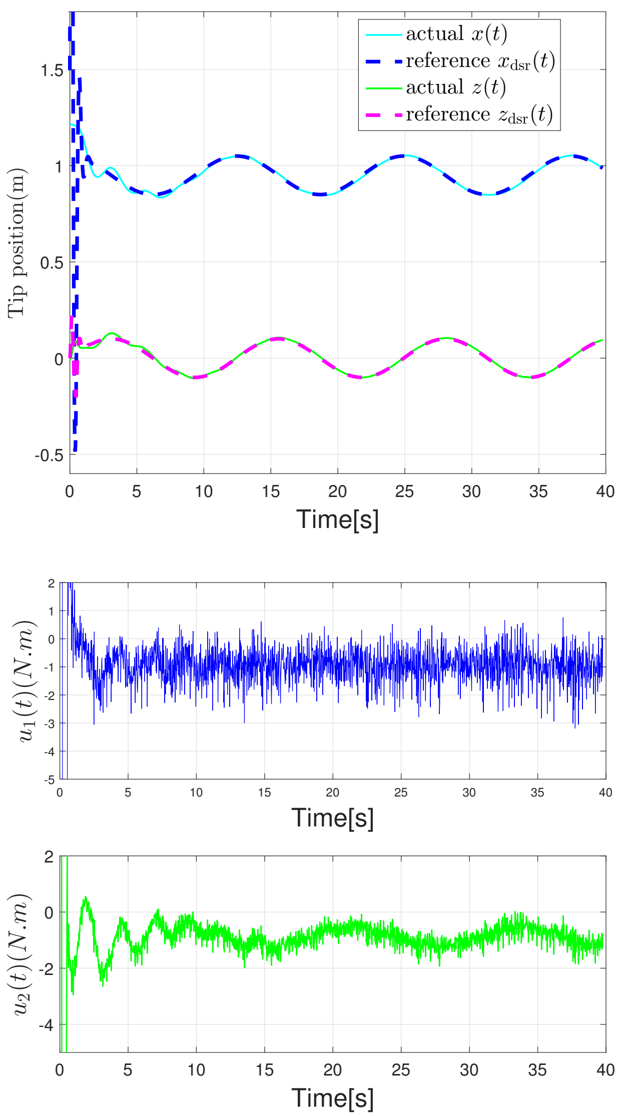

Figure 6.10: System trajectories and control effort for $r(t) = [0.1\cos(0.5t) + 0.95, 0.1\sin(0.5t)]^{\mathrm{T}}$.

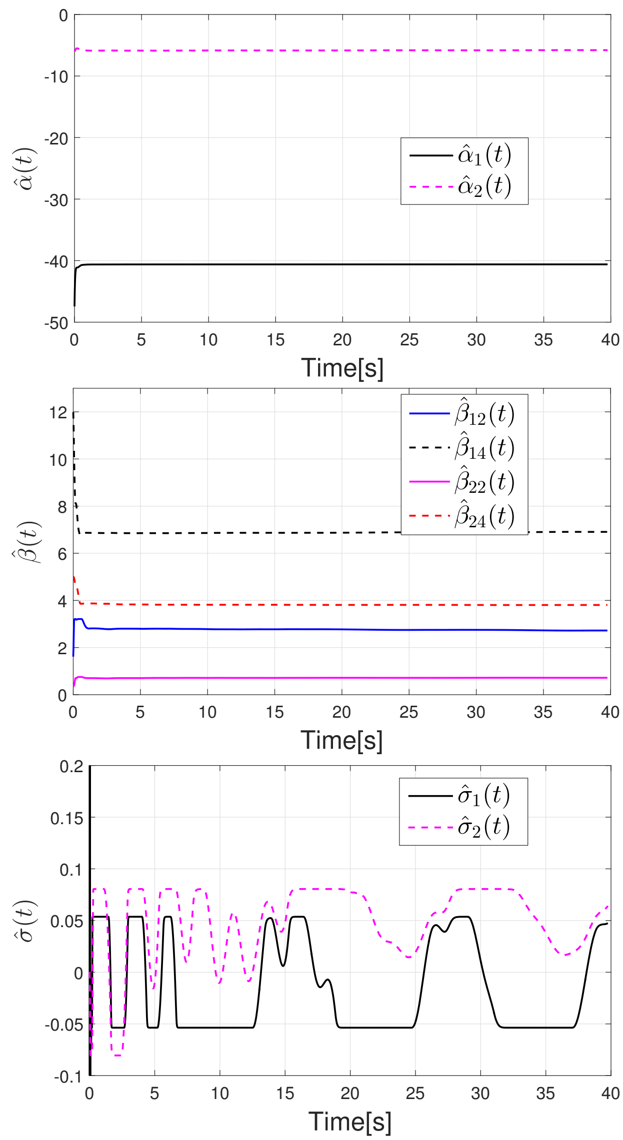

Figure 6.11: Time evolving of the adaptive parameters for $r(t) = [0.1\cos(0.5t) + 0.95, 0.1\sin(0.5t)]^{\mathrm{T}}$.

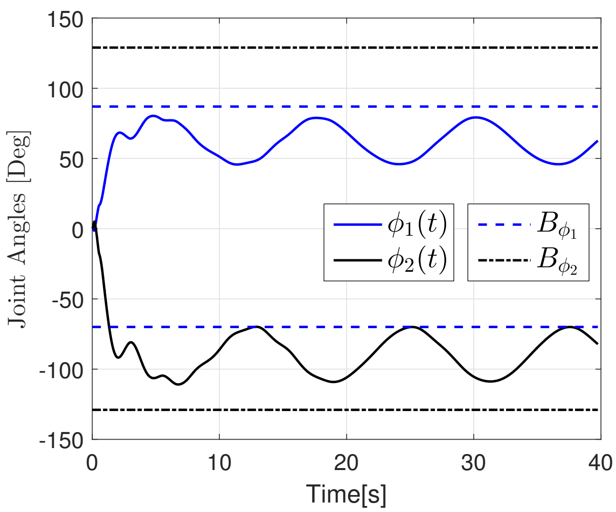

Figure 6.12: Joint Angles Trajectory.

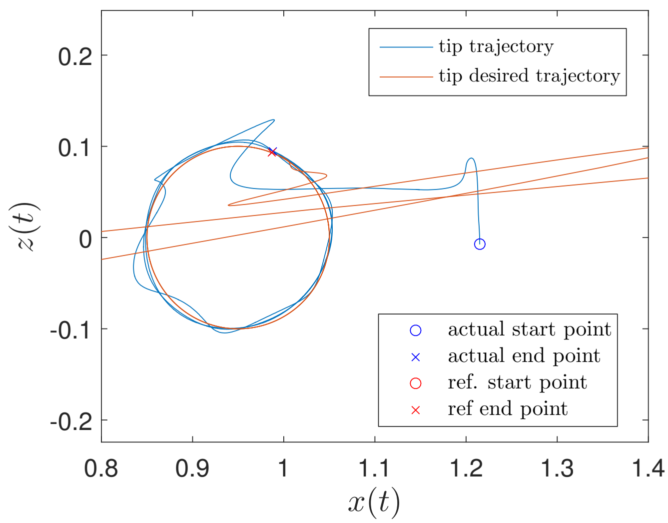

Figure 6.13: End-effector trajectory.

6.3.3 Experimental Results

The predictor-based controller presented in Section 6.3.1 and Section 6.3.2 is implemented on the physical robot to further verify its performance. However, there are several practical implementation issues.

The first problem is that the joints of the real robot possess nonneglected static friction, thus the actuators suffer a dead-zone effect ([106]). Specifically, the shoulder pan joint or the elbow flex joint can not move if the magnitude of the commanded torques to the joints are less than δ_f, where δ_f is a random value in the range $[8 \ \ 12](Nm)$.

Second, when a joint is moving freely in space, the joint's motor can not produce a torque equal to a commanded torque value set by the user. This is because each joint of the Fetch robot's arm has a micro controller board (MCB) that controls the motor torque in an effort to track the commanded torque. However, the MCB can only track the commanded torque accurately if the joint is statically held by a reacted force. When the joint moves freely, there is no reacted force feedback to the MCB. Thus, for a freely moving joint, the relationship between the actual torque output by MCB and the commanded torque is unknown.

The input-output map of the joints induced by these nonlinear effects are illustrated in Fig

6.14. As seen from Fig 6.14, there are a certain range of joint torque values that can not be set directly. Instead, the desired motor's torque can be achieved by imposing the bang-bang effect on the commanded torque. This rapidly changes the sign of the commanded torque, which makes the joint move forward and backward continuously, and consequently generates reacted force feedback to the MCU.

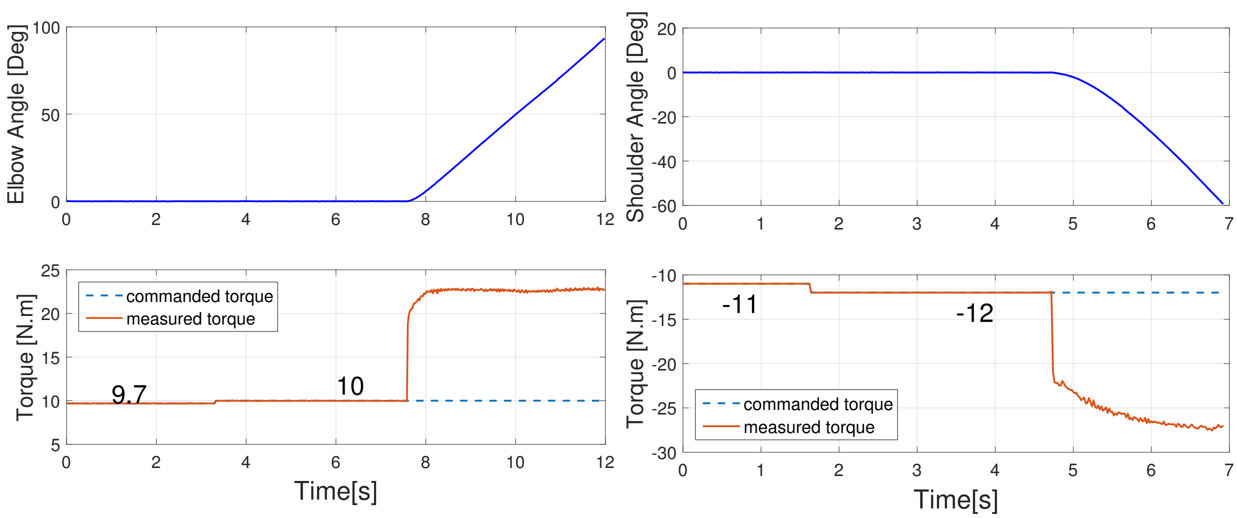

(a) Elbow Joint

(b) Shoulder Joint

Figure 6.14: Illustration of Nonlinear Actuator Effect.

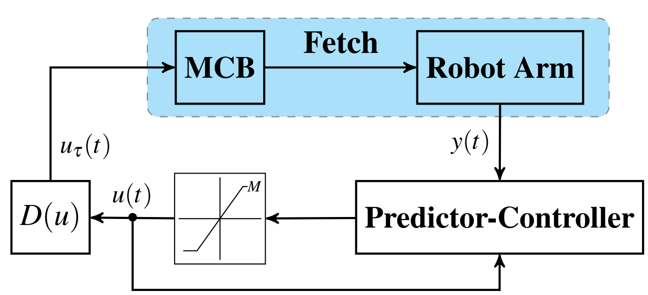

Figure 6.15: Implementation of the Predictor-Based controller on the Fetch robot.

In order to handle these problems, the control signal is saturated to create the bang-bang effect. Furthermore, we add the following dead-zone compensator to the controller:

$$u_\tau = D(u) \triangleq u + \text{sgn}(u)\delta_f, \quad \delta_f = 13;$$

Implementation of the controller on the physical robot is illustrated in Fig 6.15. The predictor-based controller uses the same parameters presented in Section 6.3.1 and Section 6.3.2.

Control Joint Angles

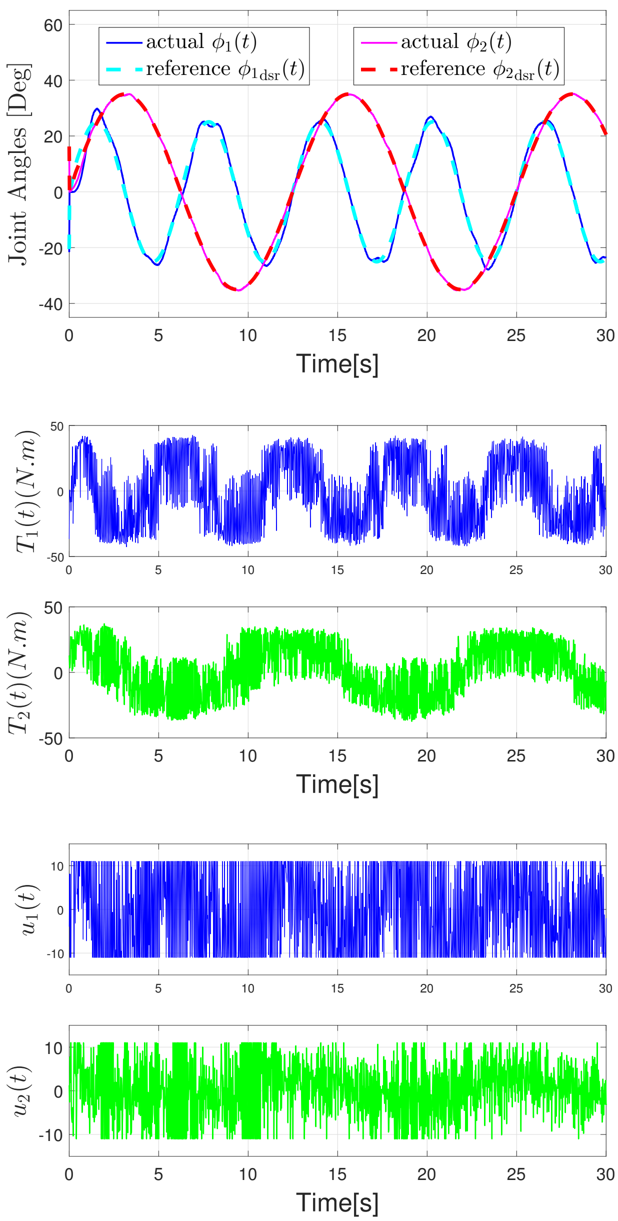

Figure 6.16: System trajectories and control effort for $r(t) = \frac{\pi}{180}[25\sin(t), 35\sin(0.5t)]^{\mathrm{T}}$.

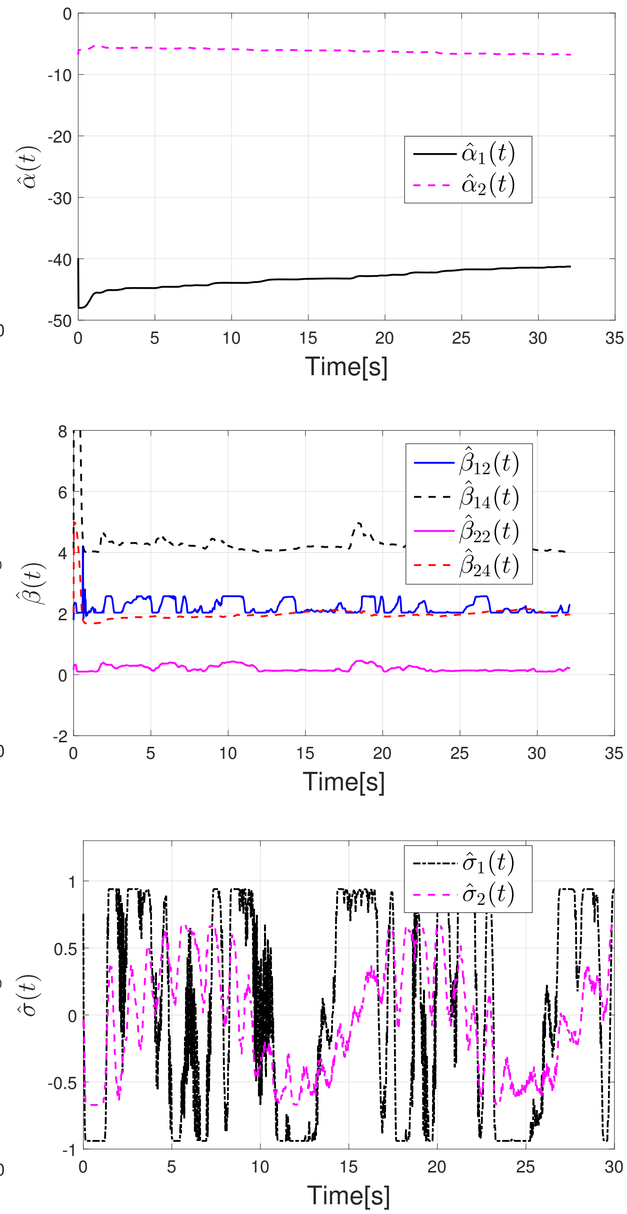

Figure 6.17: Time evolving of the adaptive parameters for $r(t) = \frac{\pi}{180}[25\sin(t), 35\sin(0.5t)]^{\mathrm{T}}$.

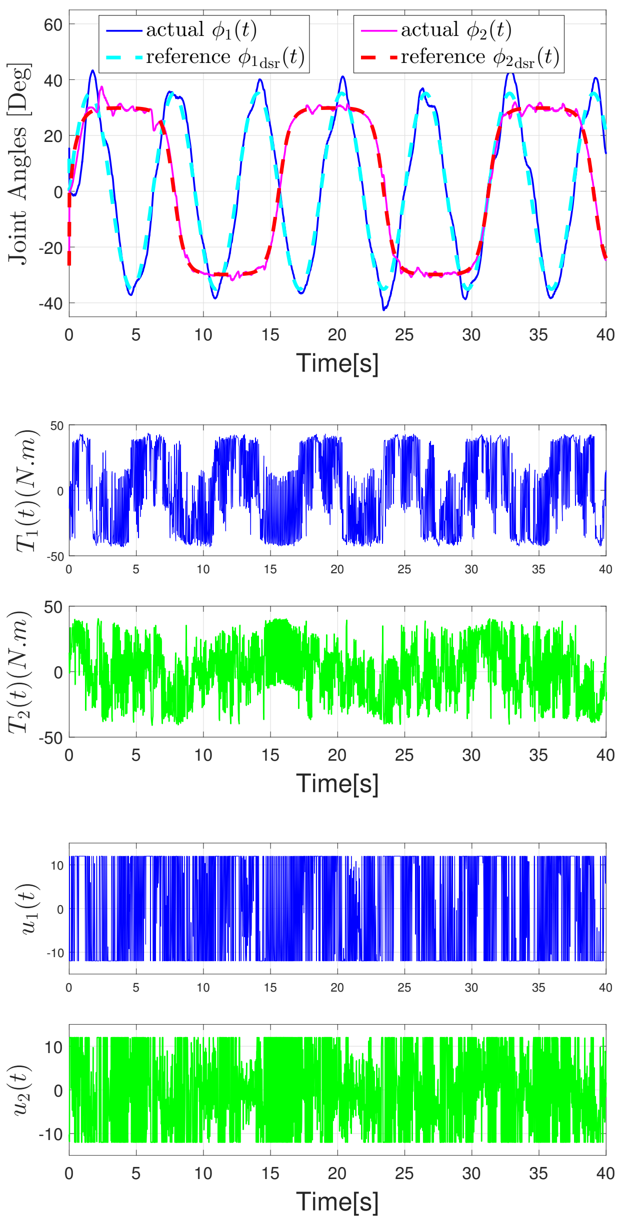

Figure 6.18: System trajectories and control effort for $r(t) = \frac{\pi}{180}[35\sin(t), 30\tanh(3\sin(0.4t)]^{\mathrm{T}}$.

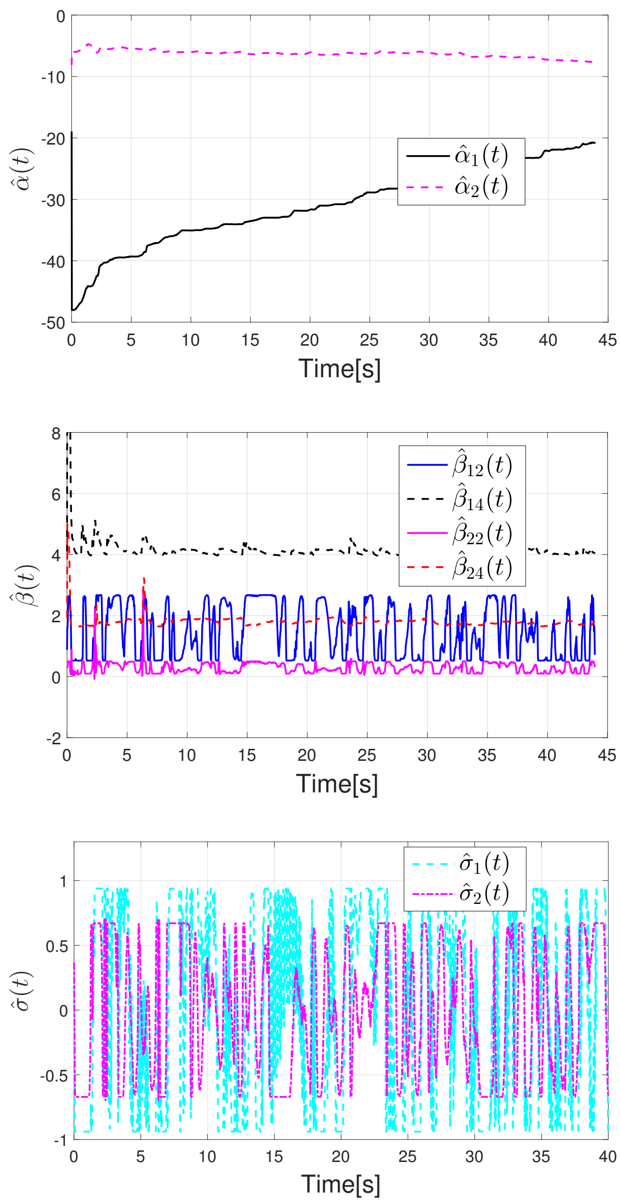

Figure 6.19: Time evolving of the adaptive parameters for $r(t) = \frac{\pi}{180}[35\sin(t), 30\tanh(3\sin(0.4t)]^{\mathrm{T}}$.

As seen from Fig 6.16 to Fig 6.19, although the bang-bang effect in the control signal is necessary to create desired the motor's torque, it also introduces more vibration on the joints, which affects the prediction error $e_{\mathrm{p}}(t)$. Consequently, the vibration leads to chattering $\hat{\sigma}(t)$ and worsens the tracking performance. However, we can see that the controller can still handle the unknown nonlinear mapping of the actuators, and the tracking performance is satisfied.

To reduce the vibration caused by the bang-bang effect, we set $\hat{\sigma}(t) = 0$ and rerun the experiments with the same setup parameters. The results are illustrated in Fig 6.20 - Fig 6.23.

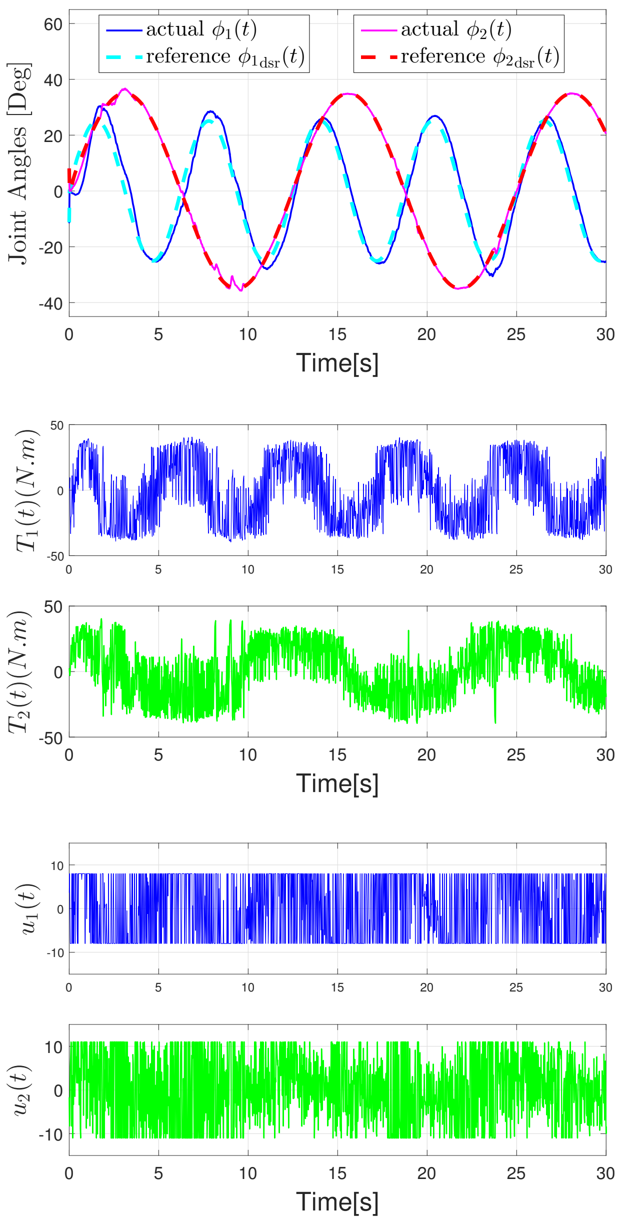

Figure 6.20: System trajectories and control effort for $r(t) = \dfrac{\pi}{180}[25\sin(t), 35\sin(0.5t)]^{\mathrm{T}}$.

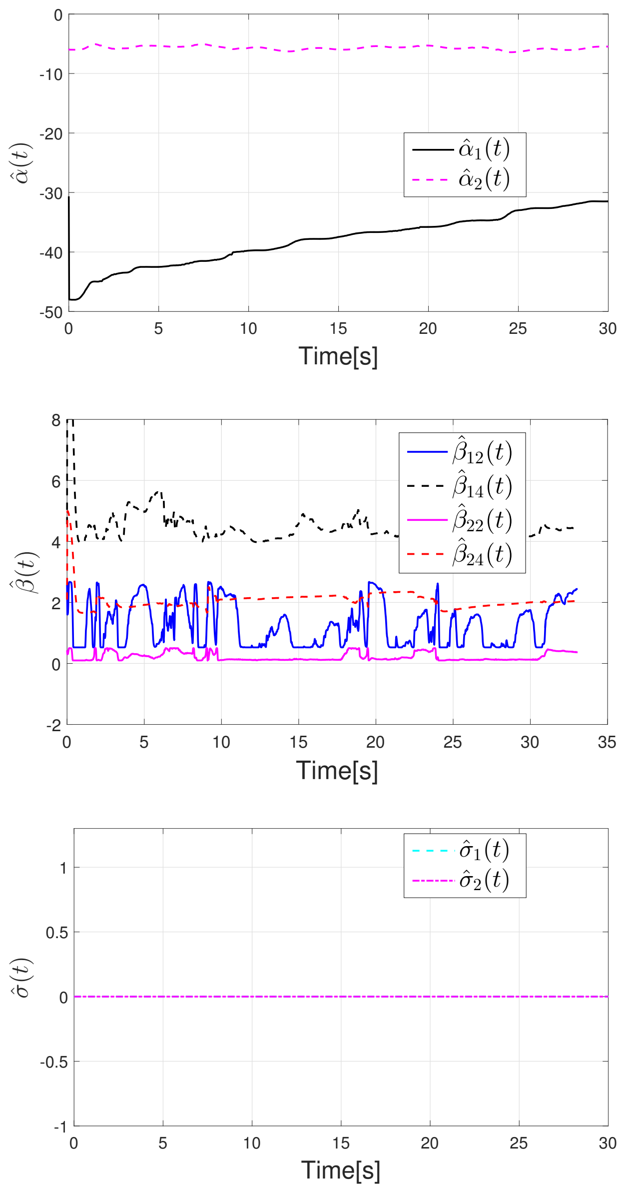

Figure 6.21: Time evolving of the adaptive parameters for $r(t) = \dfrac{\pi}{180}[25\sin(t), 35\sin(0.5t)]^{\mathrm{T}}$.

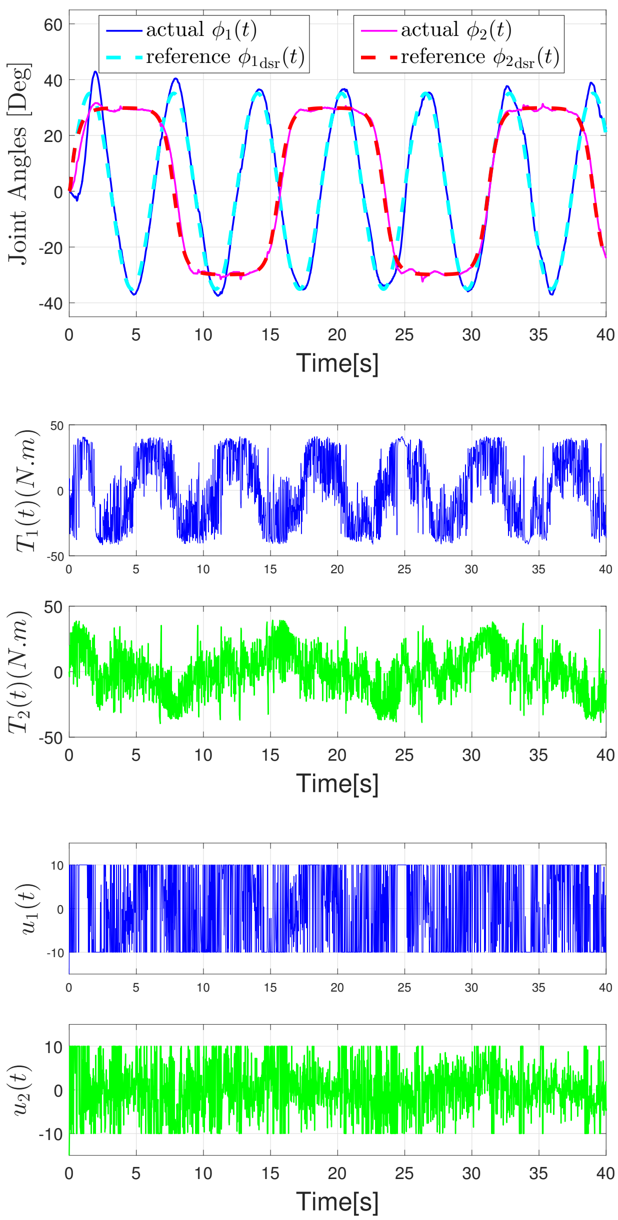

Figure 6.22: System trajectories and control effort for $r(t) = \frac{\pi}{180}[35\sin(t), 30\tanh(3\sin(0.4t)]^{\mathrm{T}}$.

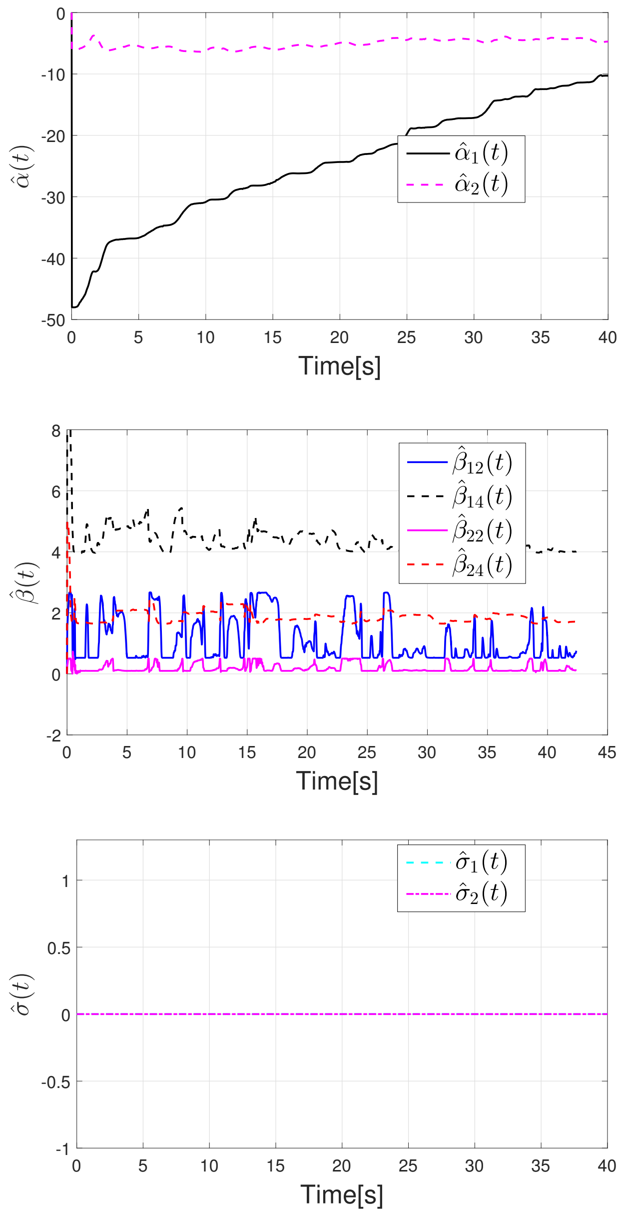

Figure 6.23: Time evolving of the adaptive parameters for $r(t) = \frac{\pi}{180}[35\sin(1.2t), 30\tanh(3\sin(0.4t))]^{\mathrm{T}}$.

It can be seen from Fig 6.20 and Fig 6.23, although it takes longer for the tracking error to converge to 0, the control signal has less chattering, which thus reduces vibration and the steady tracking error.

Control Tip Position

This experiment is conducted by controlling the end-effector as it draws circles in the horizontal plane. The controller structure with the same parameters presented in Section 6.3.3 is used. We select the adaptation gains $\gamma = 1000$, $h_0 = 1.25$, and the control gain $K_c = 40I_2$. The projection boundary of the adaptive parameters given in Section 6.3.2 is used, except we set $\hat{\sigma}(t) = 0$. Fig 6.24 shows that the experiment's tracking performance is satisfied. All adaptive parameters are bounded and the joint's angles also lie within their limits B_{ϕ_i}.

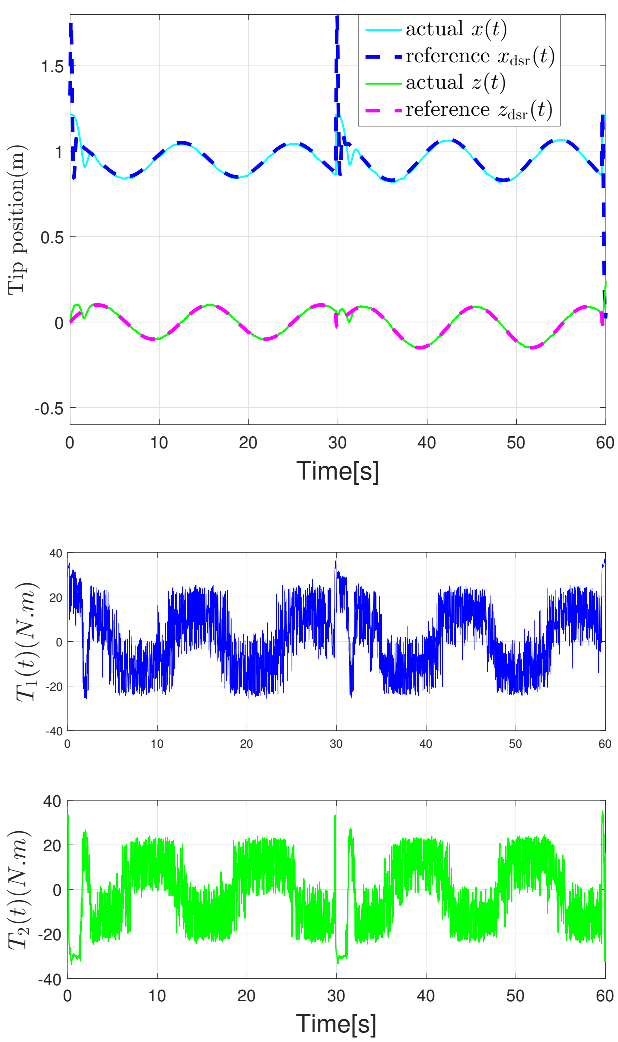

Figure 6.24: System trajectories and control torque.

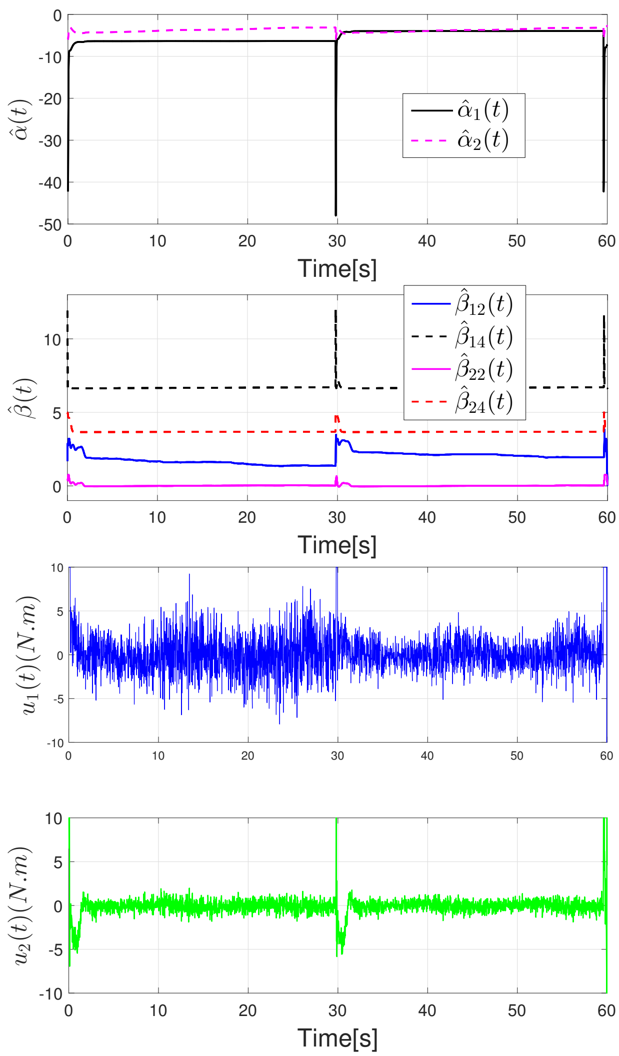

Figure 6.25: Time evolving of the adaptive parameters $\hat{\alpha}(t)$ and $\hat{\beta}(t)$ and control input $u(t)$.

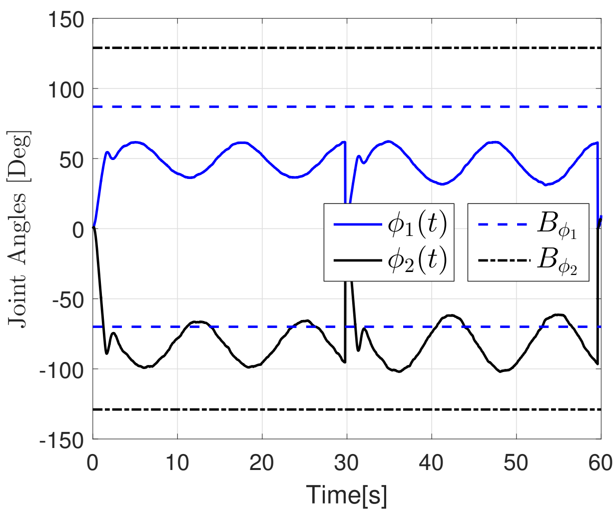

Figure 6.26: Joint Angles Trajectory.

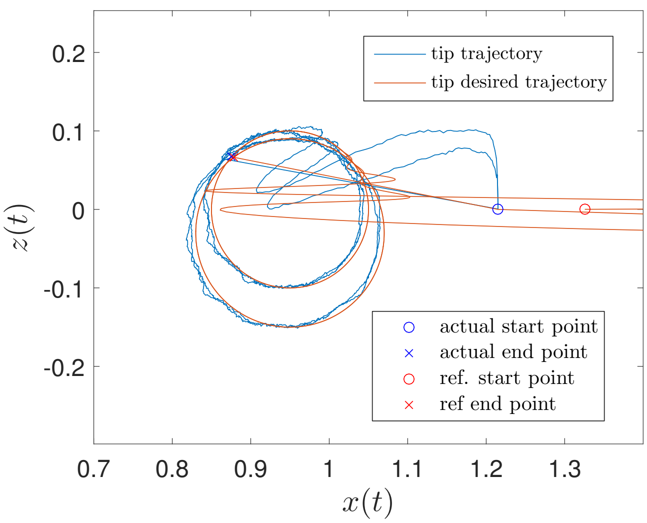

Figure 6.27: End-effector trajectory.

6.4 Control Quanser Helicopter

The controller performance is studied by considering the real time implementation on the Quanser 3-DOF helicopter depicted in Fig 6.28. The helicopter body is mounted at the end of an arm and is free to rotate around the arm (pitch). The arm is free to rotate around the y-axis (elevation) and z-axis (travel) at the pivot point O. Two DC motors with attached propellers generate driving forces for the helicopter. Hence, the system has 3 outputs, i.e. the pitch $\phi(t)$, the elevation $\theta(t)$, the travel $\psi(t)$ angles, all of which are measured via optical encoders, and has 2 control signals $v(t) = [v_f(t),\ v_b(t)]^T$ where v_f, v_b are the voltages applied to the front and the back motor respectively. The controller is implemented using Simulink running on a digital computer with a Pentium(R) D 3.4Ghz CPU, and the encoder sampling frequency is 1kHz.

6.4.1 Implementation using Second Order System

In this experiment, we attempt to simultaneously control two outputs: the pitch $\phi(t)$, the elevation $\theta(t)$. The MIMO system dynamics is unknown, but we assume that each elementary SISO system is a 2$^{\text{rd}}$ order system ($n = 2$) with relative degrees $r_{ij} = 2,\ i = 1,2,\ j = 1,2$. Furthermore, we assume that when the $v(t)$ is set at $v^* = [12\ \ 12](Vol)$, the system stays near the equilibrium point $x^* = 0$, and define $u(t) \triangleq v(t) - v^*$.

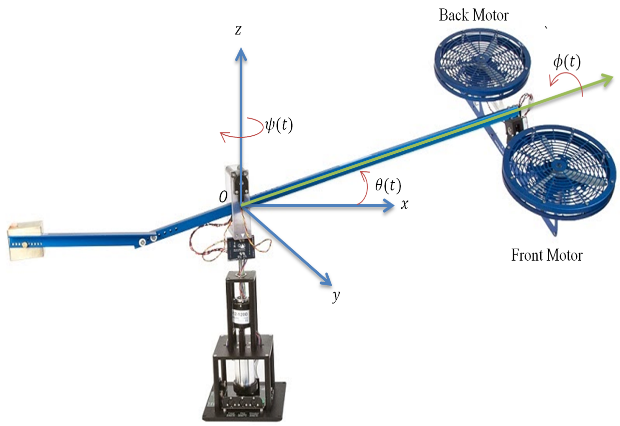

Figure 6.28: The 3D helicopter prototype

To design the predictor, we chose a 2$^{\text{rd}}$ order autoregressive filter defined in (5.4) with parameters $\Delta(s) = s^2 + \lambda^{\mathrm{T}} S(s) = (s+1)^2$, so that $\lambda = [2\ \ 1]$ and

$$A_{\mathrm{f}} = \begin{bmatrix} -2 & -1 \\ 1 & 0 \end{bmatrix} \in \mathbb{R}^{2\times 2}, \quad B_{\mathrm{f}} = \begin{bmatrix} 1 \\ 0 \end{bmatrix} \in \mathbb{R}^2.$$

Hence, the reference system is defined according to (5.2), with $k_{\mathrm{p}} = 1$ so that

$$A_{\mathrm{m}} = \begin{bmatrix} -2 & -1 & 0 & 0 & -1 & 0 \\ 1 & 0 & 0 & 0 & 0 & 0 \\ 0 & 0 & -2 & -1 & 0 & -1 \\ 0 & 0 & 1 & 0 & 0 & 0 \\ 1 & 1 & 0 & 0 & -1 & 0 \\ 0 & 0 & 1 & 1 & 0 & -1 \end{bmatrix} \in \mathbb{R}^{6\times 6},\ B_{\mathrm{m}} = \begin{bmatrix} 0 & 0 \\ 0 & 0 \\ 0 & 0 \\ 0 & 0 \\ 1 & 0 \\ 0 & 1 \end{bmatrix} \in \mathbb{R}^6,$$

$$C_{\mathrm{m}} = B_{\mathrm{m}}^{\mathrm{T}}.$$

For the adaptation law, we set the following projection bounds and the initial values

$$\Omega_\alpha = \alpha_c \pm 0.8|\alpha_c|, \qquad \alpha_c = \hat{\alpha}_0 = [-0.3\ \ \ 0.02]^{\mathrm{T}},$$

$$\Omega_\beta = \beta_c \pm 0.6|\beta_c|, \qquad \beta_c = \hat{\beta}_0 = \begin{bmatrix} 0 & 0.15 & 0 & 0.15 \\ 0 & 0.6 & 0 & -0.6 \end{bmatrix}^{\mathrm{T}},$$

$$\Omega_\sigma = [[-1\ 1];\ [-1\ 1]], \qquad \hat{\sigma}_0 = 0_2.$$

The control law (6.1a) is implemented with the following parameters: $P = I$, adaptation gain $\gamma = 1000$, and $k(t)$ defined in (5.38). The reference signal $r(t)$ is passed through a low pass filter $\frac{1}{(s+1)^2}$ before entering the reference system. The control signal is saturated in $[-3.5\ \ 3.5]$ (Vol).

We will follow the decouple process described in Fig 6.2 to implement the controller. For this simple case, since the system is assumed to be a second order system, we obtain

$$\hat{P}_{ij}(s,t) \triangleq \hat{\beta}_{ij}^{\mathrm{T}}(t) A_{\mathrm{p}} S(s) = \begin{bmatrix} 0 & \hat{\beta}_{ij}^{(0)}(t) \end{bmatrix} \begin{bmatrix} -1 & -1 \\ 1 & 1 \end{bmatrix} \begin{bmatrix} s \\ 1 \end{bmatrix} = \hat{\beta}_{ij}^{(0)}(t)(s+1)$$

Hence, $\hat{p}_{ij}(t) = \hat{\beta}_{ij}^{(0)}(t)$ and $\bar{\hat{P}}_{ij}(s) = s+1$, which yields

$$F(t) = \begin{bmatrix} 1 & \bar{\hat{p}}_{12}(t) \\ \bar{\hat{p}}_{21}(t) & 1 \end{bmatrix}, \quad \bar{\hat{p}}_{12}(t) = \frac{\hat{\beta}_{12}^{(0)}(t)}{\hat{\beta}_{11}^{(0)}(t)}, \ \ \bar{\hat{p}}_{21}(t) = \frac{\hat{\beta}_{21}^{(0)}(t)}{\hat{\beta}_{22}^{(0)}(t)},$$

$$W_{ij}(s) = \frac{\bar{\hat{P}}_{ij}(s) - \bar{\hat{P}}_{i1}(s)}{\bar{\hat{P}}_{i1}(s)} = 0 \qquad \Rightarrow \varsigma_{ij}(t) = 0.$$

The control signal is then obtained by

$$u(t) = -\bar{K}_{\mathrm{f}} \omega_u(t) + \hat{v}(t), \ \ \hat{v}(t) = F^{-1}(t)\tau(t),$$
$$\hat{\tau}(t) = -K_c(\hat{\mu}(t) + \hat{\eta}(t) - k_g r(t)),$$

Fig 6.29 and Fig 6.30 shows the tracking results and the control effort for the reference trajectory $r(t) = [10\sin(0.1\pi t), 0]^{\mathrm{T}}$ and $r(t) = [10\mathrm{square}(0.06\pi t) 0]^{\mathrm{T}}$, respectively. In this experiment, the following values are used $K_C = \mathrm{diag}([120, 60])$, $h_0 = 400$, $\Lambda(s) = s(s+2)$ so that $K_f = [0 \ \ -1]$ and $\bar{K}_f = 1_2 \otimes K_{\mathrm{f}}$.

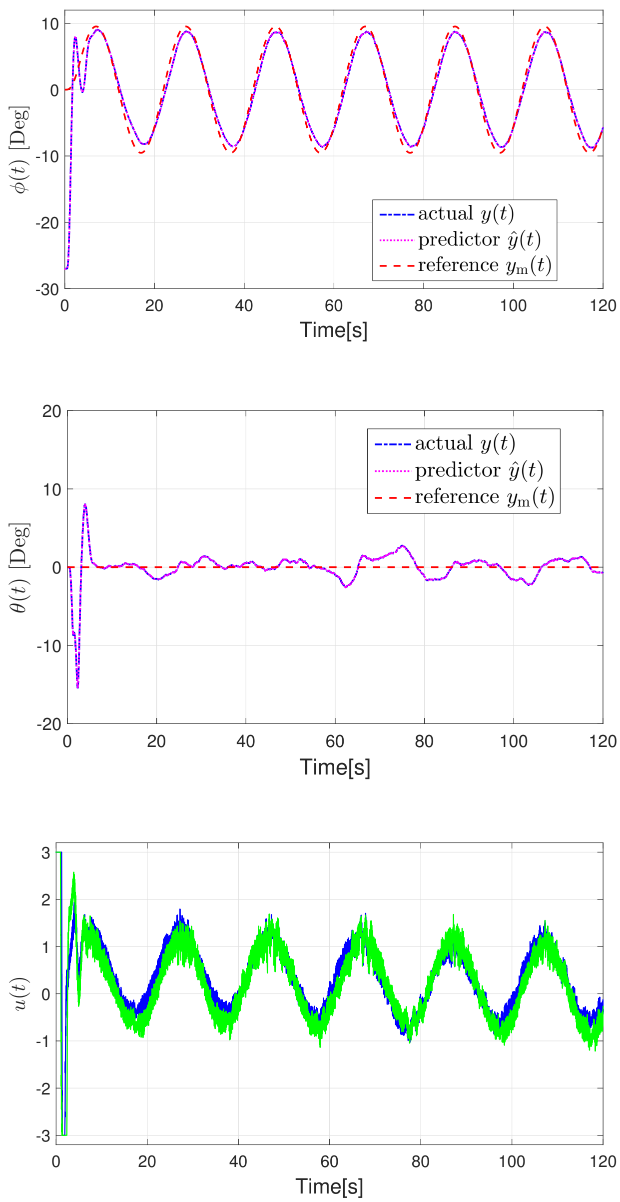

Figure 6.29: System trajectories and control effort for $r(t) = [10\sin(0.1\pi t), 0]^{\mathrm{T}}$.

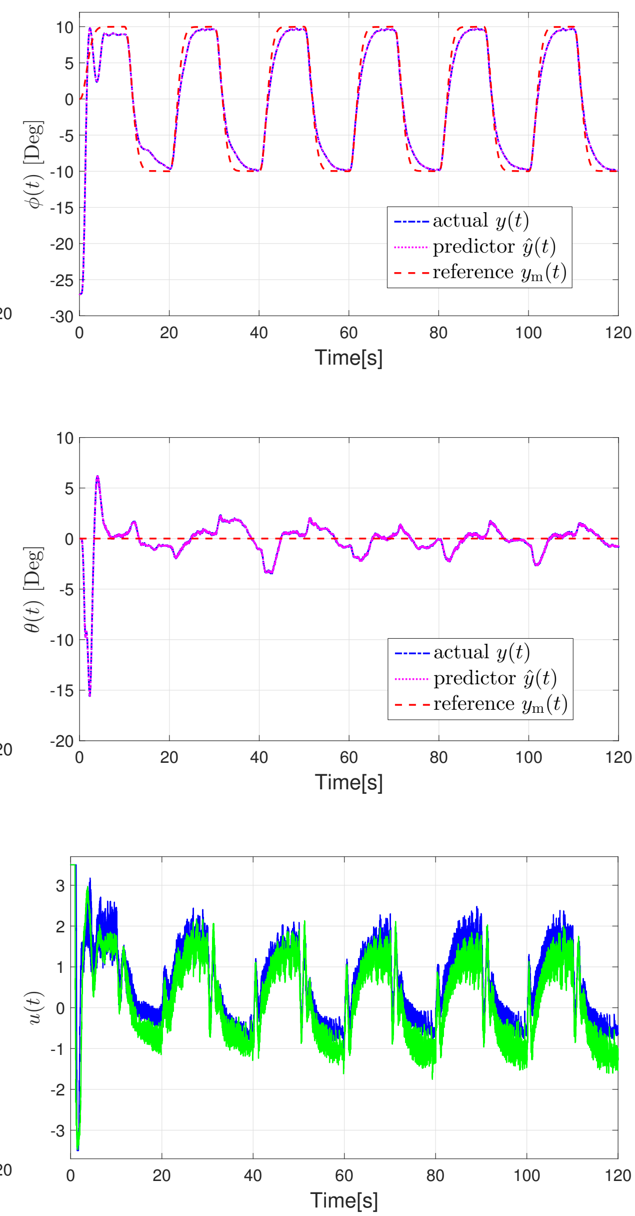

Figure 6.30: System trajectories and control effort for $r(t) = [10\text{square}0.1\pi t), 0]^{\mathrm{T}}$.

As seen from the Fig 6.29 and Fig 6.30, since we choose values of $k_{C1} = 120 > k_{C1} = 60$, the tracking performance of the output $y_1(t)$ is better than the output $y_2(t)$ in both cases. Nevertheless, the maximum error of $y_2(t)$ is 3.5^o, which happens only when $y_1(t)$ abruptly changes.

Fig 6.31 and Fig 6.32 show the tracking performance and the control effort for the same ref-

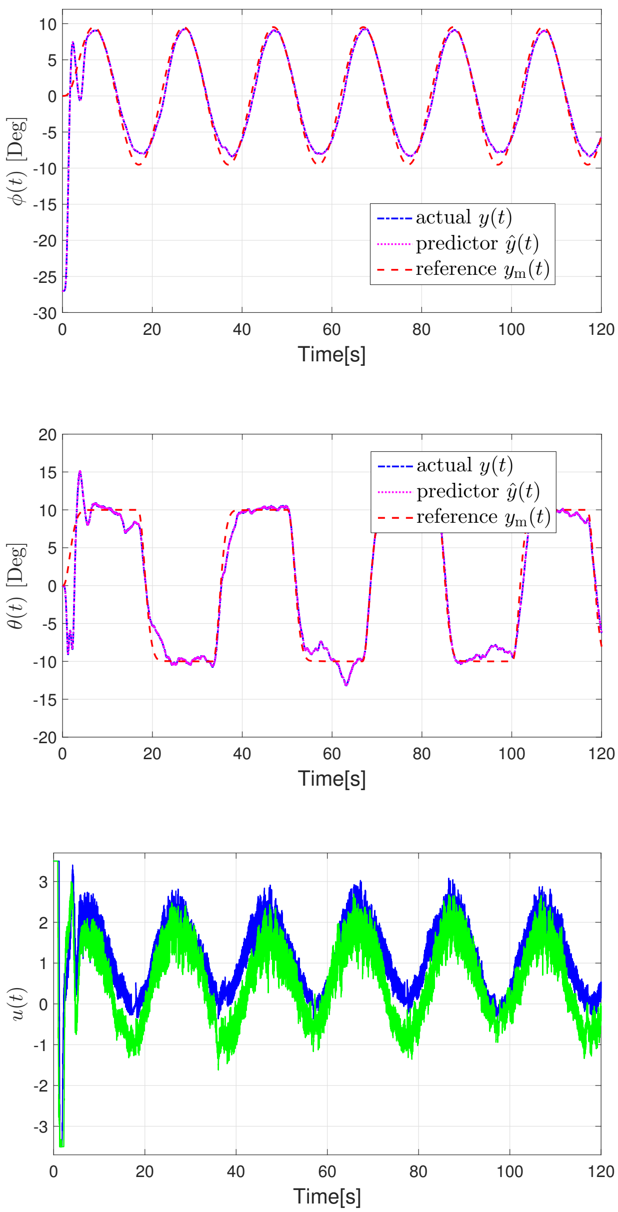

Figure 6.31: System trajectories and control effort using $K_C = \mathrm{diag}([120\ 60])$ and $h_0 = 400$.

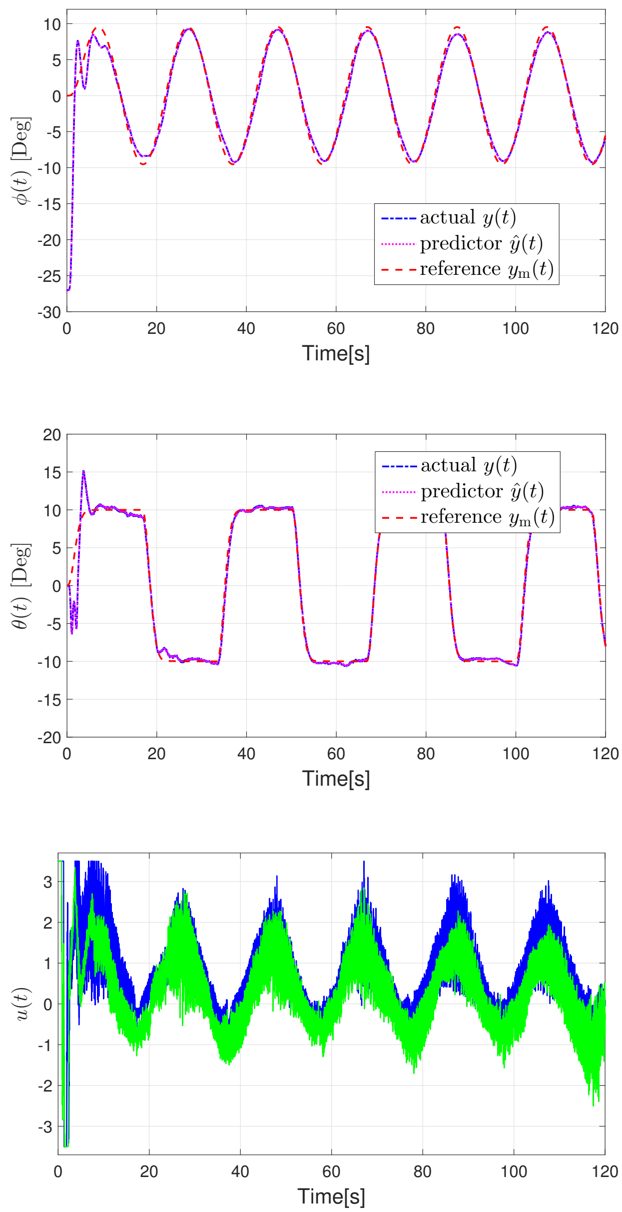

Figure 6.32: System trajectories and control effort using $K_C = \mathrm{diag}([120\ 120])$ and $h_0 = 20$.

erence trajectory $r(t) = [10sin(0.1\pi t), 10sw(0.06\pi t)]$ using different values of K_C and h_0, respectively. The tracking performance in both case are satisfied and confirm the theoretical analysis. The experimental results from both cases shows that increasing K_c can lead to better tracking performance; however, this also increases the chattering in the control signal. Choosing an exact value of h_0 to obtain a truly smooth signal in practice is challenging, due to the unpredicted disturbance, noisy measurements, and the hidden dynamics of the system. Nevertheless, we still can select an acceptable h_0 to obtain good tracking result and the control signal frequency is still in the actuator bandwidth.

6.4.2 Implementation using low-pass filtered control signals

To illustrate the high order implementation of the proposed controller, similar to Example 5.8.2, we consider the controller in the form of

Hence, the closed loop system converts to a system of order $\bar{n} = 4$ and the relative degree $\bar{r}_{ij} = 3$ in respect of the control input $\bar{u}(t)$.

In this implementation, the autoregressive filters are chosen as in (5.4) with $\Delta(s) = (s+1.25)^4$, so that $\lambda = [5 \;\; 9.375 \;\; 7.8125 \;\; 2.4411]$ and

$$A_{\mathrm{f}} = \begin{bmatrix} -5 & 9.375 & 7.8125 & 2.4411 \\ 1 & 0 & 0 & 0 \\ 0 & 1 & 0 & 0 \\ 0 & 0 & 1 & 0 \end{bmatrix}, \quad B_{\mathrm{f}} = \begin{bmatrix} 1 \\ 0 \\ 0 \\ 0 \end{bmatrix},$$

$$\bar{A}_{\mathrm{f}} = I_2 \otimes A_{\mathrm{f}} \in \mathbb{R}^{8\times 8}, \quad \bar{B}_{\mathrm{f}} = I_2 \otimes B_{\mathrm{f}} \in \mathbb{R}^{8\times 2},$$

Hence, the reference system is defined according to (5.2), with $k_{\mathrm{p}} = 1$ so that

$$A_{\mathrm{m}} \triangleq \begin{bmatrix} \bar{A}_{\mathrm{f}} & -\bar{B}_{\mathrm{f}} \\ -\bar{\lambda}^{\mathrm{T}}\bar{A}_{\mathrm{p}} & -k_{\mathrm{p}} I_p \end{bmatrix} \in \mathbb{R}^{10\times 10}, \quad B_{\mathrm{m}} \triangleq \begin{bmatrix} 0_{8\times 2} \\ I_2 \end{bmatrix} \in \mathbb{R}^{10\times 2}, \quad C_{\mathrm{m}} \triangleq B_{\mathrm{m}}^{\mathrm{T}}.$$

For the adaptation law, we set the following projection bounds and the initial values

$$\Omega_\alpha = \alpha_c \pm 0.8|\alpha_c|, \qquad \alpha_c = \hat{\alpha}_0 = [1.7 \;\; 0.42 \;\; -0.26 \;\; 0.02]^{\mathrm{T}},$$

$$\Omega_\beta = \beta_c \pm 0.3|\beta_c|, \qquad \beta_c = \hat{\beta}_0 = \begin{bmatrix} 0 & 0 & 0.3 & 0.1 & 0 & 0 & 0.3 & 0.1 \\ 0 & 0 & 2.4 & 0.8 & 0 & 0 & -2.4 & -0.8 \end{bmatrix}^{\mathrm{T}},$$

$$\Omega_\sigma = [[-1 \; 1]; \; [-1 \; 1]], \qquad \hat{\sigma}_0 = 0_2.$$

We will follow the decouple process described in Fig 6.2 to implement the controller. Since the system is assumed to be a 4^{th} order system, we obtain

$$\hat{P}_{ij}(s,t) = \hat{\beta}_{ij}^{\mathrm{T}}(t)A_{\mathrm{p}}S(s) = \begin{bmatrix} 0 & 0 & \hat{\beta}_{ij}^{(1)}(t) & \hat{\beta}_{ij}^{(0)}(t) \end{bmatrix} \begin{bmatrix} -4 & 9.375 & 7.8125 & 2.4411 \\ 1 & 1 & 0 & 0 \\ 0 & 1 & 1 & 0 \\ 0 & 0 & 1 & 1 \end{bmatrix} \begin{bmatrix} s^3 \\ s^2 \\ s \\ 1 \end{bmatrix}$$

$$= \hat{\beta}_{ij}^{(1)}(t)\left(s^2 + (1 + \frac{\hat{\beta}_{ij}^{(0)}(t)}{\hat{\beta}_{ij}^{(1)}(t)})s + \frac{\hat{\beta}_{ij}^{(0)}(t)}{\hat{\beta}_{ij}^{(1)}(t)}\right)$$

Hence, $\hat{p}_{ij}(t) = \hat{\beta}_{ij}^{(1)}(t)$ and $\bar{\hat{P}}_{ij}(s) = s^2 + \hat{p}_{ij}^{(1)}(t)s + \hat{p}_{ij}^{(0)}(t)$, where $\hat{p}_{ij}^{(1)}(t) = 1 + \hat{p}_{ij}^{(0)}(t)$ and $\hat{p}_{ij}^{(0)}(t) \triangleq \frac{\hat{\beta}_{ij}^{(0)}(t)}{\hat{\beta}_{ij}^{(1)}(t)}$. Therefore, it follows from (6.2) that

$$F(t) = \begin{bmatrix} 1 & \bar{p}_{12}(t) \\ \bar{p}_{21}(t) & 1 \end{bmatrix}, \quad \bar{p}_{12}(t) = \frac{\hat{\beta}_{12}^{(0)}(t)}{\hat{\beta}_{11}^{(0)}(t)}, \;\; \bar{p}_{21}(t) = \frac{\hat{\beta}_{21}^{(0)}(t)}{\hat{\beta}_{22}^{(0)}(t)},$$

$$W_{ij}(s) = \frac{\bar{\hat{P}}_{ij}(s) - \bar{\hat{P}}_{i1}(s)}{\bar{\hat{P}}_{i1}(s)} = (\hat{p}_{i2}^{(0)}(t) - \hat{p}_{i1}^{(0)}(t))\frac{1}{s + p_{i1}^{(0)}(t)}.$$

Hence, it follows from (6.3) that $\varsigma(t) = [\varsigma_1(t) \quad \varsigma_2(t)]^{\mathrm{T}}$, which has elements obtained from the following state space realization

$$\dot{\vartheta}_i(t) = -p_{i1}^{(0)}(t)\vartheta_i(t) + \hat{v}_j(t), \qquad \vartheta_{ij}(0) = \vartheta_{i0},$$
$$\varsigma_i(t) = c_i(t)\vartheta_i(t), \qquad c_i(t) \triangleq \bar{p}_{i2}(t)(\hat{p}_{i2}^{(0)} - \hat{p}_{i1}^{(0)}),$$

Finally, the control signals $u(t)$ can be obtained by the block diagram illustrated in Fig 6.33.

Fig 6.34 shows the tracking results and the control effort for the reference trajectory $r(t) = [10\sin(0.1\pi t), 0]^{\mathrm{T}}$. In this experiment, the following values are used $\gamma = 2000$, $K_C = 1000I_2$, $h_0 = 500$, $\Lambda(s) = s(s+1.5)(s+2)(s+2.2)$ so that $K_f = [0.8200 \;\; 1.7696 \;\; -0.6634 \;\; -2.2153]$ and $\bar{K}_f = 1_2 \otimes K_{\mathrm{f}}$.

As seen from the Fig 6.34, since the parameters K_C and h_0 are not well tuned, the virtual control signal $\bar{u}(t)$ is very noisy. However, the true control signal $u(t)$ to the physical system is significantly

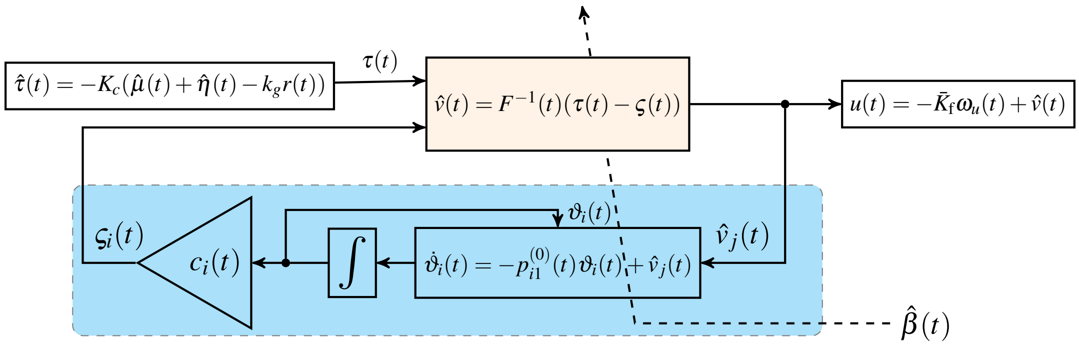

Figure 6.33: Decouple control signals for 4th order MIMO systems

smooth, since its bandwidth is limited by the low-pass filter $L_p(s)$.

In order to compare the performances between the 2rd and the 4th controllers, we tuned the parameters for the 4th controller as follow:

$$u_i(s) = L_p(s)\bar{u}_i(s) = \frac{3s+1}{(s+1)^2}\bar{u}_i(s)$$

and $\gamma = 1000$, $K_C = 1200I_2$, $h_0 = 500$, $\Lambda(s) = s(s+1)(s+1.3)(s+1.5)$ so that $K_f = [-1.2 \quad -4.6250 \quad -5.8625 \quad -2.4414]$ and $\bar{K}_f = I_2 \otimes K_{\mathrm{f}}$.

Fig 6.35 and Fig 6.36 compares the tracking performances using the 2rd order controller (with the same parameters as in Fig 6.29) and the 4th controller respectively. The figures show that the two controllers yield comparable tracking performance, while the 4th order controller yields significantly smoother control signal.

In our best knowledge, comparing with the other experimental results found in the literatures ([61, 66, 107–111]), the proposed adaptive non-modeled based output feedback controller yields the most competitive performance in the respect of the combination of control signal smoothness, fast convergence and tracking accuracy.

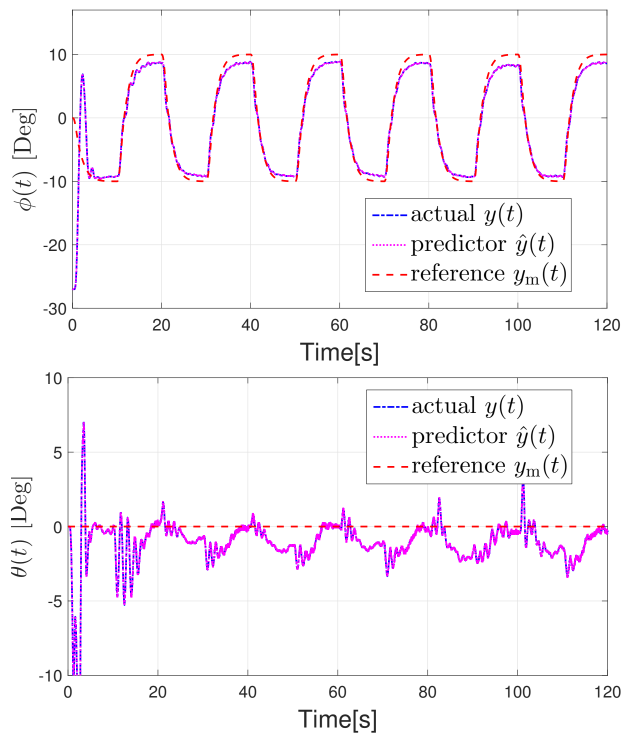

(a) System trajectories.

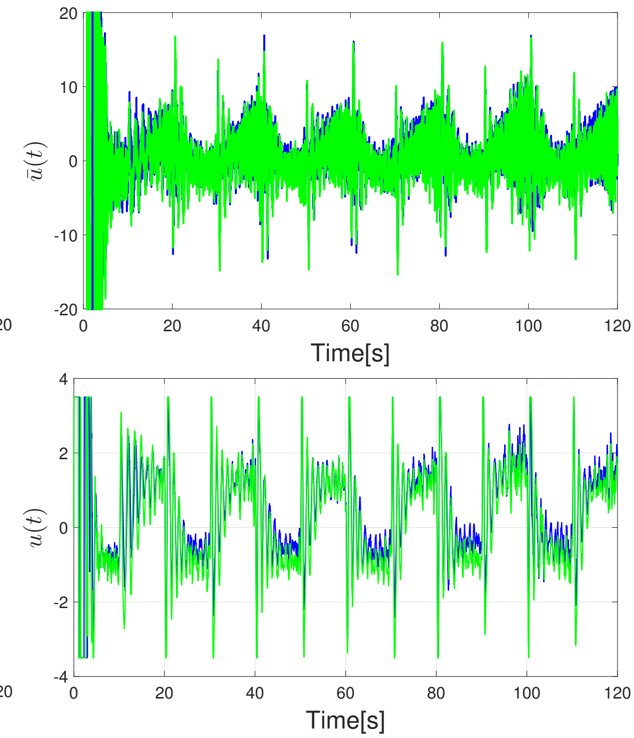

(b) Control signals $\bar{u}(t)$ and $u(t)$.

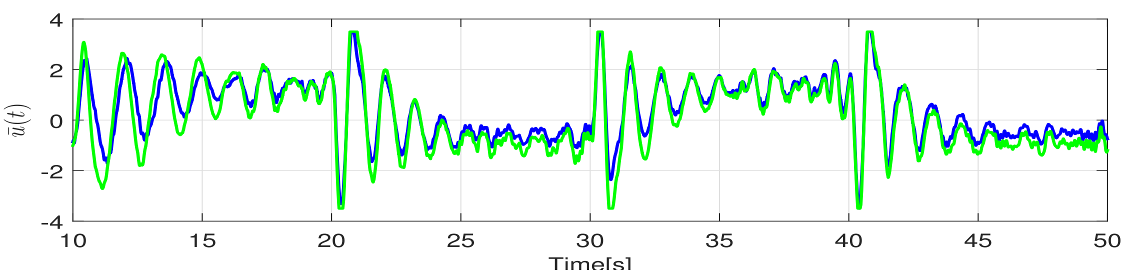

(c) Control signal $u(t)$ in the time window $t = [10 \ \ 50](s)$.

Figure 6.34: Tracking performance using the low-passed filtered control signal.

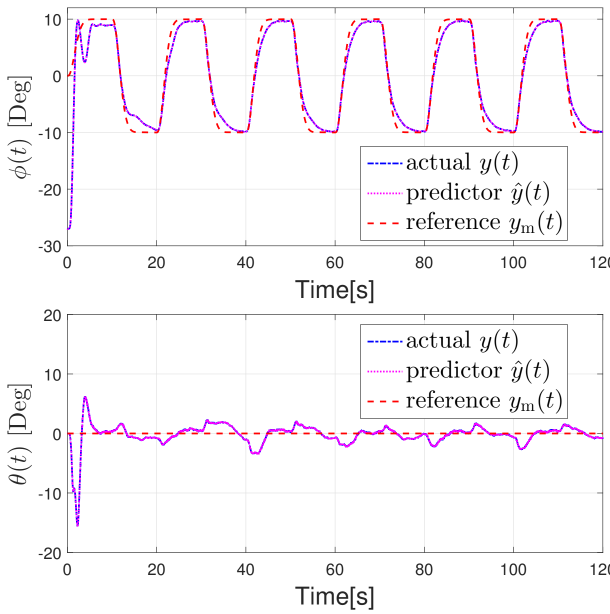

(a) System trajectories.

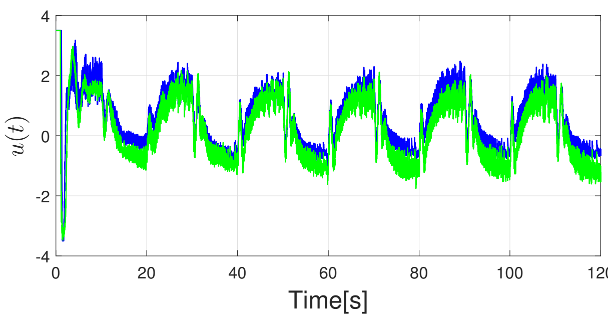

(b) Control signals.

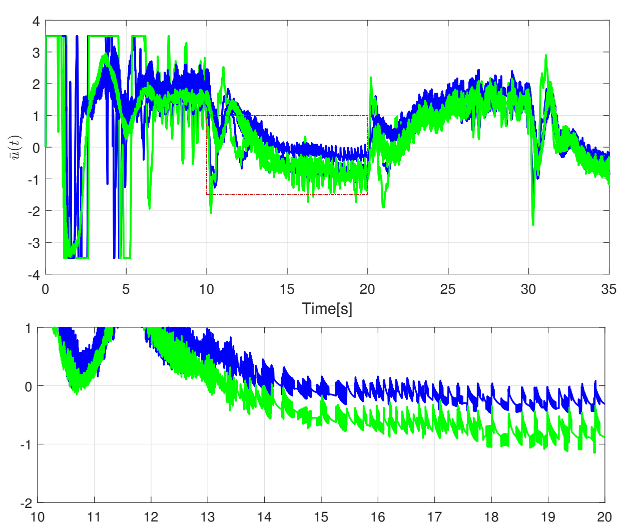

(c) Control signal in $t = [0 \;\; 35]$.

Figure 6.35: System trajectories and control effort using the 2[rd] order controller.

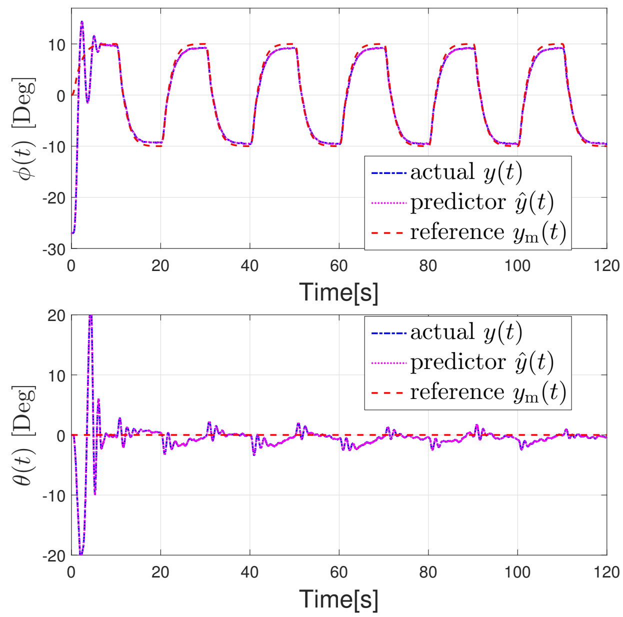

(a) System trajectories.

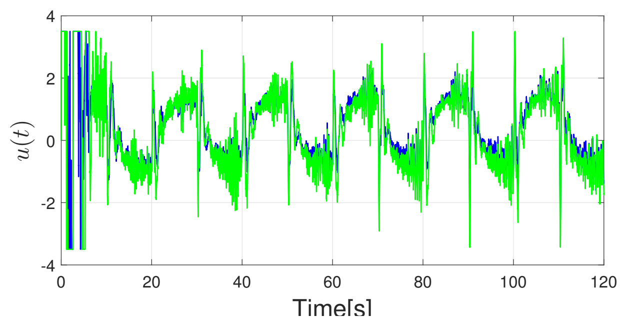

(b) Control signals.

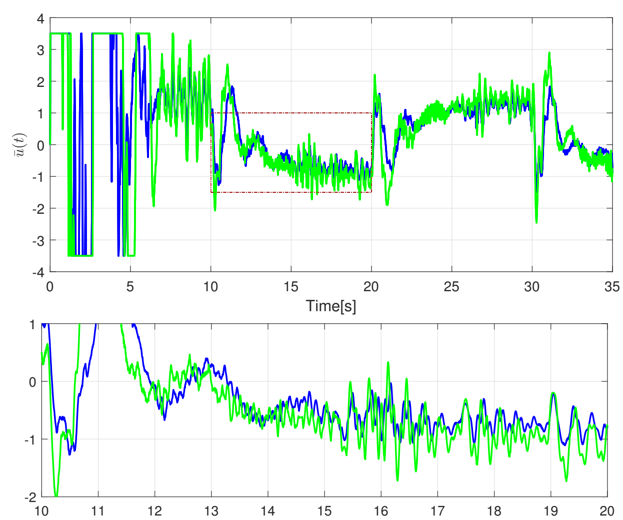

(c) Control signal in $t = [0 \;\; 35]$.

Figure 6.36: System trajectories and control effort using the 4[th] order controller.

6.5 Conclusion

This chapter extends the results for SISO systems from Chapter 5 to the MIMO systems. Specifically, the controller for the MIMO case still has three components: the predictor, the controller, and the reference system. The predictor structure remains similar to the SISO case. Next, the predictor is decoupled into independent SISO systems for which the results from Chapter 5 can be applied to obtain the virtual control signals. In consequence, these virtual control signals are then transformed to the real control signals applied to the MIMO system.

The algorithm performance is first validated by controlling motion of the Fetch Robotics Arm in Gazebo. The simulation shows good tracking results, and all parameters are well bounded. Furthermore, because the controller does not rely on the system dynamics, switching the desired output from the joint's angles to the end-effector position takes minimum effort to adjust the controller. The controller is then implemented on the physical robot to verify its performance. The experiments demonstrate its good tracking performance in the presence of the actuator's unknown nonlinearities. Furthermore, experimental results conducted on the Quanser Helicopter are also reported and confirm our theoretical analysis. Good tracking performances are obtained while the control signals remain smooth. Low order and high order structure implementation of the controller are also compared to illustrate the efficiency and flexibility of the proposed algorithm.

Chapter 7

Conclusions and Future Research

This dissertation presents a number of results pertaining to the control of unknown Multi-Input Multi-Output systems using output feedback with a focus on biomedical applications. In Chapter 2, an adaptive sliding mode control combined with backstepping framework was introduced to control the motion of a human arm model by using muscle excitations as control signals. Although the control algorithm is capable of handling the bounded uncertainties, it requires the knowledge of the system's dynamics and fully measurable state. In practice, accurate model of complex biosystems such as a human arm is almost unable to be obtained. Furthermore, there are no available sensors that can measure the dynamic state of the considered biosystems *in vivo*.

Hence, these drawbacks inspired the set of adaptive predictor-based output feedback control algorithms developed from Chapter 3 to Chapter 6. The novel idea is that the predictor is designed to predict the system output for any admissible inputs. Hence, the controller can be derived independently and applied to control the predictor. Therefore, the problem of controlling systems with unknown dynamics using only output feedback can be reduced to controlling the predictor, which has well known dynamics and full state feedback. In Chapter 3, the adaptive predictor based, output feedback controller was developed for a class of MIMO linear systems. The results were extended to handle MIMO nonlinear systems in Chapter 4. In Chapter 3 and Chapter 4, the Forward Riccati Differential Equation (FRDE) was adopted to control the predictor in order to avoid the complexity of adaptive backstepping recursive design. However, FRDE is computationally expensive and unsuitable for high order systems. Chapter 5 addressed this problem by proposing a simple control structure for high relative degrees, unknown dynamics nonlinear SISO systems. A strategy to handle the adaptation problem for time varying nonlinear terms proposed by [91] were also adopted in this chapter. The results were extended to handle MIMO nonlinear systems in Chapter 6. Simulation and experimental results were reported in each chapter to verify the proposed approaches.

Future Research

The output feedback adaptive control presented in Chapter 5 and Chapter 6 requires the gain K_C be appropriately tuned to obtain satisfactory tracking results. A larger K_C yields small tracking error. However, too large K_C can lead to unnecessary high magnitude control signals at the transient state, which leads to overshoot problems and may violate the assumption about the bound of the adaptive parameters. This problem was handled by the saturation mechanism and altering the reference signal in this work. However, the transient performance of the controller can also be improved by making K_C adaptive. Specifically, the gain K should be adjusted depending on the current tracking error and the frequency of the reference signals.

As illustrated from Example 5.8.2, the simple control structure allows us to increase the system's orders and relative degrees by adding low pass filters in front of control signals. Hence, we can obtain smooth control signal without complicating the controller structure. This advantage suggests to improve the controller performance by replacing the adaptive term $\hat{\sigma}(t)$ with a switching function $\sigma_{\max}\text{sgn}(e)$ to suppress the time varying uncertainties $\sigma(t)$. Hence, this will simplify the predictor structure and we can obtain the asymptotically stable condition instead of uniformly ultimately bounded error as seen from the current approach. The final control signal is guaranteed to be smooth due to the low pass filter. Another extension is to make the adaptive gain be time varying to obtain better adaptation.

For MIMO systems presented in Chapter 6, we are currently limitted to the assumption that the number of inputs must be equal or greater than the number of outputs. We suggest an extension to use optimal control to handle the problem of under-actuated systems. Another aspect is that the proposed controllers do not account for actuator nonlinear effects, such dead-zone, backslash effect or delay. In practice, dead-zone effect often happens when the systems have significant static friction, and delay is found in the muscle activation process. Incorporating an adaptive inverse nonlinear compensation to the predictor can extend the application to a larger class of systems. Most importantly, we would like to implement the controller on the FES systems and evaluate the performance as the main motivation of the research.

Chapter 8

Bibliography

[1] E. Rocon, J. M. Belda-Lois, A. F. Ruiz, M. Manto, J. C. Moreno, and J. L. Pons, "Design and validation of a rehabilitation robotic exoskeleton for tremor assessment and suppression," *Neural Systems and Rehabilitation Engineering, IEEE Transactions on*, vol. 15, no. 3, pp. 367–378, 2007.

[2] K. Kiguchi, Y. Hayashi, and T. Asami, "An upper-limb power-assist robot with tremor suppression control," in *Rehabilitation Robotics (ICORR), 2011 IEEE International Conference on*, pp. 1–4.

[3] L. P. Maneski, N. Jorgovanović, V. Ilić, S. Došen, *et al.*, "Electrical stimulation for the suppression of pathological tremor," *Medical & biological engineering & computing*, vol. 49, no. 10, pp. 1187–1193, 2011.

[4] J. A. Gallego, Rocon, *et al.*, "A soft wearable robot for tremor assessment and suppression," in *Robotics and Automation (ICRA), 2011 IEEE International Conference on*, pp. 2249–2254, IEEE, 2011.

[5] C. H. Nguyen and A. Leonessa, "Control motion of a human arm: A simulation study," in *International Conference of Control, Dynamic Systems, and Robotics*, no. 98, May 15 2014.

[6] F. R. Inc, “Fetch robot manual.” Website, 2015. `http://docs.fetchrobotics.com/robot_hardware.html`.

[7] G. K. Wenning, S. Kiechl, K. Seppi, J. Müller, B. Högl, M. Saletu, G. Rungger, A. Gasperi, J. Willeit, and W. Poewe, “Prevalence of movement disorders in men and women aged 50–89 years (bruneck study cohort): a population-based study,” *The lancet neurology*, vol. 4, no. 12, pp. 815–820, 2005.

[8] C. W. Olanow and J. A. Obeso, “Preventing levodopa-induced dyskinesias.,” *Annals of neurology*, vol. 47, no. 4 Suppl 1, pp. S167–76, 2000.

[9] F. Widjaja, S. Cheng Yap, P. Poignet, and A. Wei Tech, “Fes artifact suppression for real-time tremor compensation,” in *Rehabilitation Robotics, 2009. ICORR 2009. IEEE International Conference on*, pp. 53–58.

[10] E. Rocon, J. A. Gallego, L. Barrios, A. R. Victoria, J. Ibanez, D. Farina, F. Negro, J. L. Dideriksen, S. Conforto, T. D’Alessio, G. Severini, J. M. Belda-Lois, L. Z. Popovic, G. Grimaldi, M. Manto, and J. L. Pons, “Multimodal bci-mediated fes suppression of pathological tremor,” in *Engineering in Medicine and Biology Society (EMBC), 2010 Annual International Conference of the IEEE*, pp. 3337–3340.

[11] G. Grimaldi, S. Camut, and M. Manto, “Functional electrical stimulation effect on upper limb tremor,” *International Journal of Bioelectromagnetism*, vol. 13, pp. 123–124, 2011.

[12] F. Widjaja, C. Y. Shee, D. Zhang, W. T. Ang, P. Poignet, A. Bo, D. Guiraud, *et al.*, “Current progress on pathological tremor modeling and active compensation using functional electrical stimulation,” in *ISG’08: The 6th Conference of the International Society for Gerontechnology*, pp. 001–006, 2008.

[13] Z. Dingguo and A. Wei Tech, “Tremor suppression of elbow joint via functional electrical stimulation: A simulation study,” in *Automation Science and Engineering, 2006. CASE ’06. IEEE International Conference on*, pp. 182–187.

[14] N. Shariati, A. Maleki, and A. Fallah, "Genetic-pid control of elbow joint angle for functional electrical stimulation: A simulation study," in *Control, Instrumentation and Automation (ICCIA), 2011 2nd International Conference on*, pp. 150–155, 2011.

[15] M. Krstic, I. Kanellakopoulos, and P. V. Kokotovic, *Nonlinear and adaptive control design*. Wiley, 1995.

[16] S. S. Ge, C. C. Hang, T. H. Lee, and T. Zhang, *Stable adaptive neural network control*, vol. 13. Springer Science & Business Media, 2013.

[17] S. G. Shuzhi and I. Postlethwaite, "Adaptive neural network controller design for flexible joint robots using singular perturbation technique," *Transactions of the Institute of Measurement and Control*, vol. 17, no. 3, pp. 120–131, 1995.

[18] S. S. Ge and C. Wang, "Adaptive neural control of uncertain mimo nonlinear systems," *Neural Networks, IEEE Transactions on*, vol. 15, no. 3, pp. 674–692, 2004.

[19] T.-P. Zhang and S. Ge, "Adaptive dynamic surface control of nonlinear systems with unknown dead zone in pure feedback form," *Automatica*, vol. 44, no. 7, pp. 1895–1903, 2008.

[20] T. Shaocheng, L. Changying, and L. Yongming, "Fuzzy adaptive observer backstepping control for mimo nonlinear systems," *Fuzzy Sets and Systems*, vol. 160, no. 19, pp. 2755–2775, 2009.

[21] S. Tong, Y. Li, Y. Li, and Y. Liu, "Observer-based adaptive fuzzy backstepping control for a class of stochastic nonlinear strict-feedback systems," *Systems, Man, and Cybernetics, Part B: Cybernetics, IEEE Transactions on*, vol. 41, no. 6, pp. 1693–1704, 2011.

[22] S.-C. Tong, Y.-M. Li, G. Feng, and T.-S. Li, "Observer-based adaptive fuzzy backstepping dynamic surface control for a class of mimo nonlinear systems," *Systems, Man, and Cybernetics, Part B: Cybernetics, IEEE Transactions on*, vol. 41, no. 4, pp. 1124–1135, 2011.

[23] Y.-J. Liu, S.-C. Tong, and T.-S. Li, "Observer-based adaptive fuzzy tracking control for a class of uncertain nonlinear mimo systems," *Fuzzy Sets and Systems*, vol. 164, no. 1, pp. 25–44, 2011.

[24] W. Chenliang and L. Yan, "Adaptive dynamic surface control for linear multivariable systems," *Automatica*, vol. 46, no. 10, pp. 1703–1711, 2010.

[25] D. Swaroop, J. K. Hedrick, P. P. Yip, and J. C. Gerdes, "Dynamic surface control for a class of nonlinear systems," *Automatic Control, IEEE Transactions on*, vol. 45, no. 10, pp. 1893–1899, 2000.

[26] P. P. Yip and J. K. Hedrick, "Adaptive dynamic surface control: a simplified algorithm for adaptive backstepping control of nonlinear systems," *International Journal of Control*, vol. 71, no. 5, pp. 959–979, 1998.

[27] D. Wang and J. Huang, "Neural network-based adaptive dynamic surface control for a class of uncertain nonlinear systems in strict-feedback form," *Neural Networks, IEEE Transactions on*, vol. 16, no. 1, pp. 195–202, 2005.

[28] W. Dong, J. A. Farrell, M. M. Polycarpou, V. Djapic, and M. Sharma, "Command filtered adaptive backstepping," *Control Systems Technology, IEEE Transactions on*, vol. 20, no. 3, pp. 566–580, 2012.

[29] B. Xu, Z. Shi, C. Yang, and F. Sun, "Composite neural dynamic surface control of a class of uncertain nonlinear systems in strict-feedback form," *Cybernetics, IEEE Transactions on*, vol. 44, no. 12, pp. 2626–2634, 2014.

[30] Y.-J. Liu and S. Tong, "Adaptive fuzzy control for a class of unknown nonlinear dynamical systems," *Fuzzy Sets and Systems*, vol. 263, pp. 49–70, 2015.

[31] H. K. Khalil, *Nonlinear systems*, vol. 3. Prentice hall Upper Saddle River, 2002.

[32] A. J. Krener and W. Respondek, "Nonlinear observers with linearizable error dynamics," *SIAM Journal on Control and Optimization*, vol. 23, no. 2, pp. 197–216, 1985.

[33] A. Atassi and H. Khalil, “A separation principle for the stabilization of a class of nonlinear systems,” *Automatic Control, IEEE Transactions on*, vol. 44, pp. 1672–1687, Sep 1999.

[34] S. Drakunov and V. Utkin, “Sliding mode observers. tutorial,” in *Decision and Control, 1995., Proceedings of the 34th IEEE Conference on*, vol. 4, pp. 3376–3378, IEEE, 1995.

[35] S. Oh and H. K. Khalil, “Nonlinear output-feedback tracking using high-gain observer and variable structure control,” *Automatica*, vol. 33, no. 10, pp. 1845–1856, 1997.

[36] D. Karagiannis and A. Astolfi, “Nonlinear observer design using invariant manifolds and applications,” in *Decision and Control, 2005 and 2005 European Control Conference. CDC-ECC’05. 44th IEEE Conference on*, pp. 7775–7780, IEEE, 2005.

[37] J. Chen, A. Behal, and D. M. Dawson, “Robust feedback control for a class of uncertain MIMO nonlinear systems,” *Automatic Control, IEEE Transactions on*, vol. 53, no. 2, pp. 591–596, 2008.

[38] Z. Wang, J. Chen, and A. Behal, “Robust adaptive control design for a class of uncertain MIMO nonlinear systems,” in *Intelligent Control (ISIC), 2010 IEEE International Symposium on*, pp. 2284–2289, IEEE, 2010.

[39] T. Shaocheng, L. Changying, and L. Yongming, “Fuzzy adaptive observer backstepping control for {MIMO} nonlinear systems,” *Fuzzy Sets and Systems*, vol. 160, no. 19, pp. 2755 – 2775, 2009. Theme: Control.

[40] C. Cao and N. Hovakimyan, “$\mathscr{L}_1$ adaptive output feedback controller for systems with time-varying unknown parameters and bounded disturbances,” in *Proc. of American Control Conference*, pp. 486–491, 2007.

[41] C. Cao and N. Hovakimyan, “$\mathscr{L}_1$ adaptive output feedback controller to systems of unknown dimension,” in *American Control Conference, 2007. ACC ’07*, pp. 1191–1196, July 2007.

[42] C. Cao and N. Hovakimyan, "$\mathscr{L}_1$ adaptive output feedback controller for non-strictly positive real reference systems with applications to aerospace examples," in *AIAA Guidance, Navigation, and Control Conference and Exhibit*, 2008.

[43] E. Kharisov and N. Hovakimyan, "$\mathscr{L}_1$ adaptive output feedback controller for minimum phase systems," in *American Control Conference (ACC), 2011*, pp. 1182–1187, IEEE, 2011.

[44] H. Lee, V. Cichella, and N. Hovakimyan, "L1 adaptive output feedback augmentation of model reference control," in *American Control Conference (ACC), 2014*, pp. 697–702, June 2014.

[45] P. Ioannou and J. Sun, *Robust Adaptive Control*. No. v. 1 in Control theory, PTR Prentice-Hall, 1996.

[46] C. Cao and N. Hovakimyan, "$\mathscr{L}_1$ adaptive output feedback controller for non strictly positive real multi-input multi-output systems in the presence of unknown nonlinearities," in *American Control Conference, 2009. ACC '09.*, pp. 5138–5143, June 2009.

[47] Y. Morel and A. Leonessa, "Nonlinear predictor-based output feedback control for a class of uncertain nonlinear systems," in *ASME 2010 Dynamic Systems and Control Conference*, pp. 939–946, American Society of Mechanical Engineers, 2010.

[48] J. Liu and X. Wang, *Advanced sliding mode control for mechanical systems*. Springer, 2012.

[49] M.-S. Chen and C.-Y. Kao, "Control of linear time-varying systems using forward riccati equation," *Journal of dynamic systems, measurement, and control*, vol. 119, no. 3, pp. 536–540, 1997.

[50] A. Leonessa, W. M. Haddad, T. Hayakawa, and Y. Morel, "Adaptive control for nonlinear uncertain systems with actuator amplitude and rate saturation constraints," *International Journal of Adaptive Control and Signal Processing*, vol. 23, no. 1, pp. 73–96, 2009.

[51] J. Yang, S. Li, J. Su, and X. Yu, "Continuous nonsingular terminal sliding mode control for systems with mismatched disturbances," *Automatica*, vol. 49, no. 7, pp. 2287 – 2291, 2013.

[52] M. Rubagotti, A. Estrada, F. Castanos, A. Ferrara, and L. Fridman, "Integral sliding mode control for nonlinear systems with matched and unmatched perturbations," *IEEE Transactions on Automatic Control*, vol. 56, pp. 2699–2704, Nov 2011.

[53] C. H. Nguyen and A. Leonessa, "Control motion of a human arm: A simulation study," in *Linear and Non-Linear Control, International Conference of Control, Dynamic Systems, and Robotics*, pp. 981–989, International ASET Inc., 2014.

[54] S. H. A. H. Jeff Reinbolt, Ajay Seth, "Arm26 models." Website, July 2008. `http://simtk-confluence.stanford.edu:8080/display/OpenSim/Musculoskeletal+Models`.

[55] Y.-J. Huang, T.-C. Kuo, *et al.*, "Adaptive sliding-mode control for nonlinearsystems with uncertain parameters," *Systems, Man, and Cybernetics, Part B: Cybernetics, IEEE Transactions on*, vol. 38, pp. 534 –539, april 2008.

[56] L. S. Lasdon, R. L. Fox, and M. W. Ratner, "Nonlinear optimization using the generalized reduced gradient method," *Revue française d'automatique, d'informatique et de recherche opérationnelle. Recherche opérationnelle*, vol. 8, no. 3, pp. 73–103, 1974.

[57] D. G. Thelen *et al.*, "Adjustment of muscle mechanics model parameters to simulate dynamic contractions in older adults," *Transactions-American Society Of Mechanical Engineers Journal Of Biomechanical Engineering*, vol. 125, no. 1, pp. 70–77, 2003.

[58] C. John, "Complete description of the thelen muscle model." Website, Oct 28 2011. `http://simtk-confluence.stanford.edu:8080/display/OpenSim24/Muscle+Model+Theory+and+Publications`.

[59] M. Mansouri and J. A. Reinbolt, "A platform for dynamic simulation and control of movement based on opensim and matlab," *Journal of Biomechanics*, vol. 45, no. 8, pp. 1517–1521, 2012.

[60] C. H. Nguyen and A. Leonessa, "Adaptive predictor-based output feedback control for a class of unknown MIMO linear systems," in *ASME 2014 Dynamic Systems and Control Conference*, American Society of Mechanical Engineers, 2014.

[61] C. H. Nguyen and A. Leonessa, "Adaptive predictor-based output feedback control for a class of unknown MIMO linear systems: Experimental results," in *ASME 2014 Dynamic Systems and Control Conference*, American Society of Mechanical Engineers, 2014.

[62] N. Hovakimyan and C. Cao, *L1 adaptive control theory: Guaranteed robustness with fast adaptation*, vol. 21. Siam, 2010.

[63] R. Penrose, "A generalized inverse for matrices," in *Proc. Cambridge Philos. Soc*, vol. 51, pp. 406–413, Cambridge Univ Press, 1955.

[64] R. D. Schafer, *An introduction to nonassociative algebras*, vol. 22. Courier Corporation, 1966.

[65] Y. Morel and A. Leonessa, "Direct adaptive tracking control of quadrotor aerial vehicles," in *ASME 2006 International Mechanical Engineering Congress and Exposition*, pp. 155–161, American Society of Mechanical Engineers, 2006.

[66] C. H. Nguyen and A. Leonessa, "Adaptive predictor-based output feedback control for a class of unknown MIMO systems: Experimental results," in *American Control Conference*, 2015.

[67] C. H. Nguyen and A. Leonessa, "Predictor-based adaptive output feedback control: Application to functional electrical stimulation of a human arm models," *ASME Journal of Dynamic Systems, Measurement and Control*, 2016. revision under review.

[68] M. Song and Y. Lin, "A robust adaptive dynamic surface control for linear systems," *International Journal of Control*, vol. 85, no. 7, pp. 950–963, 2012.

[69] M. Song and Y. Lin, "A robust output-feedback adaptive dynamic surface control for linear systems with input disturbance," *Journal of Control Theory and Applications*, vol. 11, no. 2, pp. 261–267, 2013.

[70] Z.-J. Yang, T. Nagai, S. Kanae, and K. Wada, "Dynamic surface control approach to adaptive robust control of nonlinear systems in semi-strict feedback form," *International Journal of Systems Science*, vol. 38, no. 9, pp. 709–724, 2007.

[71] L. Yi and L. Liu, "Adaptive dynamic surface control for a class of time-varying uncertain nonlinear systems and application," in *Intelligent Control and Automation (WCICA), 2010 8th World Congress on*, pp. 2523–2526, IEEE.

[72] T. P. Zhang and S. S. Ge, "Adaptive dynamic surface control of nonlinear systems with unknown dead zone in pure feedback form," *Automatica*, vol. 44, no. 7, pp. 1895–1903, 2008.

[73] J. A. Farrell, M. Polycarpou, M. Sharma, and D. Wenjie, "Command filtered backstepping," *Automatic Control, IEEE Transactions on*, vol. 54, no. 6, pp. 1391–1395, 2009.

[74] V. Stepanyan and K. Krishnakumar, "Certainty equivalence m-mrac for systems with unmatched uncertainties,"

[75] V. Stepanyan, K. Krishnakumar, and N. Nhan, "Transient performance and asymptotic tracking with filtering robust adaptive control," in *Aerospace conference, 2009 IEEE*, pp. 1–9.

[76] F. Castanos and L. Fridman, "Analysis and design of integral sliding manifolds for systems with unmatched perturbations," *Automatic Control, IEEE Transactions on*, vol. 51, no. 5, pp. 853–858, 2006.

[77] M.-S. Chen, C.-H. Chen, and F.-Y. Yang, "An ltr-observer-based dynamic sliding mode control for chattering reduction," *Automatica*, vol. 43, no. 6, pp. 1111–1116, 2007.

[78] X. Han, E. Fridman, and S. K. Spurgeon, “Sliding-mode control of uncertain systems in the presence of unmatched disturbances with applications,” *International Journal of Control*, vol. 83, no. 12, pp. 2413–2426, 2010.

[79] L. Hsu, “Smooth sliding control of uncertain systems based on a prediction error,” *International Journal of Robust and Nonlinear Control*, vol. 7, no. 4, pp. 353–372, 1997.

[80] Q. Khan, “Dynamic sliding mode control based on integral manifold for MIMO,” *Journal of Control Engineering and Applied Informatics*, vol. 16, no. 4, pp. 107–117, 2014.

[81] Q. Khan, A. I. Bhatti, S. Iqbal, and M. Iqbal, “Dynamic integral sliding mode for MIMO uncertain nonlinear systems,” *International Journal of Control, Automation and Systems*, vol. 9, no. 1, pp. 151–160, 2011.

[82] S. Laghrouche, F. Plestan, and A. Glumineau, “Higher order sliding mode control based on integral sliding mode,” *Automatica*, vol. 43, no. 3, pp. 531–537, 2007.

[83] X. Yu and O. Kaynak, “Sliding-mode control with soft computing: A survey,” *Industrial Electronics, IEEE Transactions on*, vol. 56, no. 9, pp. 3275–3285, 2009.

[84] H. Liu, “Variable structure model-reference adaptive control (vs-mrac) using only input and output measurements: the general case,” *Automatic Control, IEEE Transactions on*, vol. 35, no. 11, pp. 1238–1243, 1990.

[85] K. S. Narendra and J. D. Boskovic, “A combined direct, indirect, and variable structure method for robust adaptive control,” *Automatic Control, IEEE Transactions on*, vol. 37, no. 2, pp. 262–268, 1992.

[86] Y. V. Orlov, “Sliding mode observer-based synthesis of state derivative-free model reference adaptive control of distributed parameter systems,” *Journal of Dynamic Systems, Measurement, and Control*, vol. 122, no. 4, pp. 725–731, 2000.

[87] M. Rubagotti, A. Estrada, F. Castanos, A. Ferrara, and L. Fridman, "Integral sliding mode control for nonlinear systems with matched and unmatched perturbations," *Automatic Control, IEEE Transactions on*, vol. 56, no. 11, pp. 2699–2704, 2011.

[88] L. R. L. Teixeira, J. B. Oliveira, and A. D. Araujo, "Smooth indirect adaptive sliding mode control," *International Journal of Robust and Nonlinear Control*, pp. n/a–n/a, 2013.

[89] J. Yang, S. Li, and X. Yu, "Sliding-mode control for systems with mismatched uncertainties via a disturbance observer," *Industrial Electronics, IEEE Transactions on*, vol. 60, no. 1, pp. 160–169, 2013.

[90] J. Davila, "Exact tracking using backstepping control design and high-order sliding modes," *Automatic Control, IEEE Transactions on*, vol. 58, no. 8, pp. 2077–2081, 2013.

[91] V. Stepanyan and K. Krishnakumar, "Indirect M-MRAC for systems with time varying parameters and bounded disturbances," in *Intelligent Control (ISIC), 2012 IEEE International Symposium on*, pp. 1232–1237, IEEE.

[92] V. Stepanyan and K. Krishnakumar, "Modified Reference Model MRAC (M-MRAC): An application to a generic transport model," in *Advances in Intelligent and Autonomous Aerospace Systems*, vol. 241, 2012. Edited by J. Valasek, AIAA series.

[93] P. A. Ioannou and J. Sun, *Robust adaptive control*. Courier Corporation, 2012.

[94] J. D. Jennifer Hicks, "Scripting with matlab." Website, Sep 2014. `http://simtk-confluence.stanford.edu:8080/display/OpenSim/Scripting+with+Matlab`.

[95] M. Mansouri and J. A. Reinbolt, "A platform for dynamic simulation and control of movement based on opensim and matlab," *Journal of biomechanics*, vol. 45, no. 8, pp. 1517–1521, 2012.

[96] M. Mansouri, A. E. Clark, A. Seth, and J. A. Reinbolt, "Rectus femoris transfer surgery affects balance recovery in children with cerebral palsy: A computer simulation study," *Gait & Posture*, vol. 43, pp. 24–30, 2016.

[97] T. Kitamura, S. Sakaino, and T. Tsuji, "Bilateral control using functional electrical stimulation," in *Industrial Electronics Society, IECON 2015-41st Annual Conference of the IEEE*, pp. 002336–002341, IEEE, 2015.

[98] N. Alibeji, N. Kirsch, and N. Sharma, "Dynamic surface control of neuromuscular electrical stimulation of a musculoskeletal system with activation dynamics and an input delay," in *American Control Conference (ACC), 2015*, pp. 631–636, IEEE, 2015.

[99] S. Jezernik, R. G. Wassink, and T. Keller, "Sliding mode closed-loop control of fes controlling the shank movement," *Biomedical Engineering, IEEE Transactions on*, vol. 51, no. 2, pp. 263–272, 2004.

[100] E. M. Schearer, Y.-W. Liao, E. J. Perreault, M. C. Tresch, W. D. Memberg, R. F. Kirsch, and K. M. Lynch, "Multi-muscle fes force control of the human arm for arbitrary goals," *Neural Systems and Rehabilitation Engineering, IEEE Transactions on*, vol. 22, no. 3, pp. 654–663, 2014.

[101] M. Millard, T. Uchida, A. Seth, and S. L. Delp, "Flexing computational muscle: modeling and simulation of musculotendon dynamics," *Journal of biomechanical engineering*, vol. 135, no. 2, p. 021005, 2013.

[102] Y.-W. Liao, E. M. Schearer, X. Hu, E. J. Perreault, M. C. Tresch, and K. M. Lynch, "Modeling open-loop stability of a human arm driven by a functional electrical stimulation neuroprosthesis," in *Engineering in Medicine and Biology Society (EMBC), 2013 35th Annual International Conference of the IEEE*, pp. 3598–3601, IEEE, 2013.

[103] Y.-W. Liao, E. M. Schearer, E. J. Perreault, M. C. Tresch, and K. M. Lynch, "Multi-muscle fes control of the human arm for interaction tasksstabilizing with muscle co-contraction and

postural adjustment: A simulation study," in *Intelligent Robots and Systems (IROS 2014), 2014 IEEE/RSJ International Conference on*, pp. 2134–2139, IEEE, 2014.

[104] N. Koenig and A. Howard, "Design and use paradigms for gazebo, an open-source multi-robot simulator," in *Intelligent Robots and Systems, 2004.(IROS 2004). Proceedings. 2004 IEEE/RSJ International Conference on*, vol. 3, pp. 2149–2154, IEEE.

[105] M. Quigley, K. Conley, B. P. Gerkey, J. Faust, T. Foote, J. Leibs, R. Wheeler, and A. Y. Ng, "Ros: an open-source robot operating system," in *ICRA Workshop on Open Source Software*, 2009.

[106] G. Tao and P. V. Kokotovic, *Adaptive control of systems with actuator and sensor nonlinearities*. John Wiley & Sons, Inc., 1996.

[107] A. Boubakir, S. Labiod, F. Boudjema, and F. Plestan, "Design and experimentation of a self-tuning PIDcontrol applied to the 3dof helicopter," *Archives of Control Sciences*, vol. 23, no. 3, pp. 311–331, 2013.

[108] A. L. Fradkov, B. Andrievsky, and D. Peaucelle, "Adaptive control design and experiments for laas helicopter benchmark," *European Journal of Control*, vol. 14, no. 4, pp. 329–339, 2008.

[109] A. T. Kutay, A. J. Calise, M. Idan, and N. Hovakimyan, "Experimental results on adaptive output feedback control using a laboratory model helicopter," *Control Systems Technology, IEEE Transactions on*, vol. 13, no. 2, pp. 196–202, 2005.

[110] H. Liu, Y. Yu, and Y. Zhong, "Robust trajectory tracking control for a laboratory helicopter," *Nonlinear Dynamics*, vol. 77, no. 3, pp. 621–634, 2014.

[111] Ri, x, H. os, A. Rosales, A. Ferreira, Da, x, and A. vilay, "Robust regulation for a 3-dof helicopter via sliding-modes control and observation techniques," in *American Control Conference (ACC), 2010*, pp. 4427–4432.